

University of Bath



**PHD**

**Influence of excipients on stabilisation of amorphous cefuroxime axetil under process conditions of compression and coating**

Ghazal, Nadia Abder Rahman Ali

*Award date:*  
2005

*Awarding institution:*  
University of Bath

[Link to publication](#)

**General rights**

Copyright and moral rights for the publications made accessible in the public portal are retained by the authors and/or other copyright owners and it is a condition of accessing publications that users recognise and abide by the legal requirements associated with these rights.

- Users may download and print one copy of any publication from the public portal for the purpose of private study or research.
- You may not further distribute the material or use it for any profit-making activity or commercial gain
- You may freely distribute the URL identifying the publication in the public portal ?

**Take down policy**

If you believe that this document breaches copyright please contact us providing details, and we will remove access to the work immediately and investigate your claim.

**INFLUENCE OF EXCIPIENTS ON STABILISATION  
OF AMORPHOUS CEFUROXIME AXETIL  
UNDER PROCESS CONDITIONS OF  
COMPRESSION AND COATING**

**Nadia Abder Rahman Ali Ghazal**

**A thesis submitted for the degree of Doctor of Philosophy**

**University of Bath**

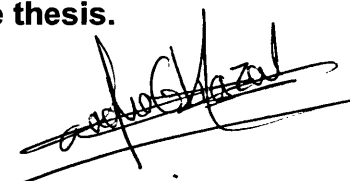
**Department of Pharmacy and Pharmacology**

**February 2005**

**COPYRIGHT**

Attention is drawn to the fact that copyright of this thesis rests with its author. This copy of the thesis has been supplied on condition that anyone who consults it is understood to recognise that its copyright rests with its author and that no quotation from the thesis and no information derived from it may be published with out the prior written consent of the author.

**This thesis may not be consulted, photocopied or lent to other libraries with out the permission of the author, for 3 years from the date of acceptance of the thesis.**



UMI Number: U601590

All rights reserved

INFORMATION TO ALL USERS

The quality of this reproduction is dependent upon the quality of the copy submitted.

In the unlikely event that the author did not send a complete manuscript and there are missing pages, these will be noted. Also, if material had to be removed, a note will indicate the deletion.



UMI U601590

Published by ProQuest LLC 2013. Copyright in the Dissertation held by the Author.  
Microform Edition © ProQuest LLC.

All rights reserved. This work is protected against  
unauthorized copying under Title 17, United States Code.



ProQuest LLC  
789 East Eisenhower Parkway  
P.O. Box 1346  
Ann Arbor, MI 48106-1346

UNIVERSITY OF BATH  
LIBRARY  
40 16 JUN 2005  
Ph.D.



## ACKNOWLEDGMENT

*First of all, I would like to send you millions of thanks father for always giving me the love and energizing me with the power of faith and success in all what I do.*

*This is just to let you know that what you did to me never goes unnoticed although was not spoken , and it is really appreciated. **Thank you DAD....***

*Then, I would like to express my gratitude to my supervisor **Dr. Rob Price** , whose encouragement , enthusiasm, and time given to discuss my work have made this thesis possible.*

*Next, I would like to thank **Prof. Antony Smith** , and **Prof. Duncan Craig** for the valuable knowledge I learned from them during my thesis discussion.*

*I would like also to take this opportunity to very much thank my manager **Dr. Rakan Rshaidat** , and my friends at “**Advanced Pharmaceuticals Industries**” for greatly motivating me , and continuously providing me with the proper research environment. *All thanks to all of them..**

*Special thanks to every member in my family, my mother **Yusra**, my son **Odai**, my brothers **Ali** and **Nabeel**, my sisters **Salwa** and **Laila** for all the love and care given to me to successfully finish this work. *Thank you very much...**

*Last but not least, for all my friends who really cared for me and always have been so helpful, I am saying **Thank You All.***

# TABLE OF CONTENTS

	Page
<b>INDEX</b> .....	1
<b>TABLE OF ABBREVIATIONS</b> .....	8
<b>TABLE OF FIGURES</b> .....	9
<b>TABLE OF TABLE S</b> .....	.13
<b>ABSTRACT</b> .....	.15
<b>CHAPTER 1: INTRODUCTION</b>	
<b>1.1 Polymorphism</b> .....	17
1.1.1 Screening of polymorphs .....	18
1.1.1.1 Solvent recrystallisation .....	18
1.1.1.2 Recrystallisation from the melt .....	19
1.1.1.3 Antisolvent addition .....	19
1.1.1.4 Vapor diffusion .....	19
1.1.1.5 Solution slurry .....	20
1.1.1.6 Annealing .....	20
1.1.2 Characterisation of a polymorph .....	20
1.1.3 Phase transitions .....	22
1.1.4 Crystallisation controlling the polymorphic form .....	22
1.1.5 Amorphous materials .....	24
1.1.5.1 Thermal history effects.....	26
1.1.5.2 Glass transition temperature .....	26
1.1.5.3 Relaxation phenomena .....	33
1.1.5.4 Plasticization of amorphous materials.....	33
1.1.5.5 Amorphous drugs and dissolution.....	34
1.1.5.6 Crystallisation of an amorphous material .....	36
1.1.5.7 Characterisation of the amorphous state .....	37
1.1.5.8 Physico-chemical factors which influence amorphous systems .....	50
<b>1.2 Cefuroxime axetil</b> .....	52
1.2.1 Activity.....	52
1.2.2 Bioavailability .....	52
1.2.3 Physical forms.....	56
1.2.4 Stability .....	57
1.2.5 Pharmaceutical formulations.....	58
<b>1.3 Formulation of Taste Masked Particles</b> .....	59
1.3.1 Taste masking approaches .....	59
1.3.2 Evaluation of taste masked API particles .....	69

<b>1.4 Enhancing Dissolution and Bioavailability of Poorly Soluble Drugs .....</b>	<b>71</b>
1.4.1 Approaches .....	71
1.4.1.1 Size reduction .....	72
1.4.1.2 Using solid carriers.....	74
1.4.1.3 Salt formation.....	74
1.4.1.4 Prodrug formation .....	74
1.4.1.5 Stabilisation of the amorphous form of a drug.....	74
1.4.1.6 Lipid matrix systems.....	77
1.4.1.7 Inclusion complex formation.....	78
1.4.1.8 Solid dispersions.....	78
1.4.2 Bioavailability enhancers.....	79
<b>1.5 Objectives.....</b>	<b>81</b>
 <b>CHAPTER 2: GENERAL MATERIALS AND METHODS</b>	
<b>2.1 Differential Scanning Calorimetry (DSC) .....</b>	<b>82</b>
2.1.1 Introduction .....	82
2.1.1.1 Glass transition temperature .....	84
2.1.1.2 Crystallisation.....	85
2.1.1.3 Melting .....	85
2.1.2 Materials and methods.....	86
 <b>2.2 Modulated Temperature DSC .....</b>	 <b>87</b>
2.2.1 Introduction .....	87
2.2.1.1 History.....	87
2.2.1.2 Choice of MTDSC parameters .....	90
2.2.1.3 Heat capacity calibration and measurement .....	91
2.2.2 Materials and methods.....	92
 <b>2.3 Laser Particle Size Analyses.....</b>	 <b>93</b>
2.3.1 Introduction .....	93
2.3.1.1 Ensemble techniques.....	93
2.3.1.2 Counting techniques .....	95
2.3.1.3 Separation techniques.....	96
2.3.2 Materials and methods.....	98
 <b>2.4 X-RAY POWDER DIFFRACTION .....</b>	 <b>98</b>
2.4.1 Introduction .....	98
2.4.1.1 X-ray generation and properties.....	99
2.4.1.2 Lattice planes and Bragg's law .....	100
2.4.2 Materials and methods.....	102
 <b>2.5 DYNAMIC VAPOUR SORPTION .....</b>	 <b>102</b>
2.5.1 Introduction .....	102
2.5.2 Materials and methods.....	103

<b>2.6 Scanning Electron Microscopy</b> .....	103
2.6.1 Introduction .....	103
2.6.1.1 Scanning process .....	105
2.6.1.2 Detection of secondary electrons .....	106
2.6.2 Materials and methods.....	106
<b>2.7 Dissolution</b> .....	107
2.7.1 Introduction .....	107
2.7.2 Materials and methods.....	109
2.7.2.1 Intrinsic dissolution .....	109
2.7.2.2 Dissolution using apparatus II .....	110
<b>2.8 Rat Intestinal Absorption Measurement</b> .....	111
2.8.1 Introduction .....	111
2.8.1.1 <i>In vivo</i> models .....	113
2.8.1.2 <i>In situ</i> models.....	114
2.8.1.3 <i>In vitro</i> models.....	116
2.8.2 Materials and methods.....	120
2.8.2.1 <i>In situ</i> perfusion test .....	120
2.8.2.2 <i>In vitro</i> gut absorption test.....	123
<b>2.9 HPLC Assay Methods</b> .....	125
2.9.1 Introduction .....	125
2.9.2 Materials and methods.....	126
2.9.2.1 HPLC assay method for testing content and homogeneity of cefuroxime axetil in the mixtures .....	126
2.9.2.2 HPLC assay method for testing cefuroxime axetil and cefuroxime sodium content in the <i>in situ</i> perfusion test .....	127
2.9.2.3 HPLC assay method for testing cefuroxime axetil and cefuroxime sodium content in the <i>in vitro</i> gut absorption tests.....	130
2.9.3 Validation of the HPLC methods .....	131
2.9.3.1 Validation of <i>in situ</i> perfusion HPLC method.....	131
2.9.3.2 Validation of <i>in vitro</i> gut testing HPLC method.....	134
<b>2.10 Karl Fisher (Water Content) Determination</b> .....	137
2.10.1 Introduction .....	137
2.10.2 Materials and methods.....	138

**CHAPTER 3: PHYSICAL PROPERTIES OF THE CEFUROXIME AXETIL  
AMORPHOUS POWDER (CAA) AND COMPRESSED  
(CAAC) AND THE POWDER CEFUROXIME AXETIL  
CRYSTALLINE (CAC)**

<b>3.1 Introduction</b> .....	139
-------------------------------	-----

<b>3.2 Materials and Methods</b> .....	143
3.2.1 Methods of testing CAA, CAC and CAAC.....	144
<b>3.3 Results and Discussions</b> .....	145
3.3.1 Particle size distribution .....	145
3.3.1.1 Particle size distribution of CAA .....	145
3.3.1.2 Particle size distribution of CAC .....	146
3.3.1.3 Particle size distribution of CAAC .....	147
3.3.2 Regular and modulated temperature DSC .....	147
3.3.3 Water content determination .....	156
3.3.4 X-Ray powder diffraction (X-RPD) .....	157
3.3.5 Dynamic vapour sorption (DVS).....	159
3.3.6 Intrinsic dissolution .....	161
3.3.6.1 Intrinsic dissolution of CAA .....	161
3.3.6.2 Intrinsic dissolution of CAC .....	162
3.3.7 Dissolution using apparatus II .....	164
3.3.8 <i>In situ</i> perfusion test.....	165
3.3.9 <i>In vitro</i> gut absorption test.....	170
3.3.9.1 <i>In vitro</i> gut absorption of CAA .....	170
3.3.9.2 <i>In vitro</i> gut absorption of CAC .....	172
3.3.9.3 <i>In vitro</i> gut absorption of CAAC .....	173
<b>3.4 Conclusions</b> .....	175

**CHAPTER 4: EFFECT OF SOME EXCIPIENTS ON THE PHYSICAL  
PROPERTIES OF CEFUROXIME AXETIL CRYSTALLINE  
(CAC) AND CEFUROXIME AXETIL AMORPHOUS (CAA)  
AS POWDER BLENDS AND COMPRESSED MIXTURES**

<b>4.1 Introduction</b> .....	177
<b>4.2 Materials and Methods</b> .....	179
4.2.1 Preparation of mixtures .....	179
4.2.1.1 Powder blends preparation .....	179
4.2.1.2 Compressed mixtures preparation .....	180
4.2.2 Powder blends and compressed mixtures prepared .....	180
4.2.2.1 Mixtures of CAA with Ac-Di-Sol.....	180
4.2.2.2 Mixtures of CAA with Starch 1500.....	181
4.2.2.3 Mixtures of CAA with Aerosil 200 .....	181
4.2.2.4 Mixtures of CAA with SLS .....	181
4.2.2.5 Blends of CAA and CAC with Ac-Di-Sol, Starch 1500 and Aerosil 200 .....	182
4.2.3 Mixtures testing.....	182
4.2.3.1 HPLC assay method for analyses of mixtures .....	182
4.2.3.2 DSC testing of mixtures .....	182
4.2.3.3 Modulated temperature DSC testing of mixtures .....	182
4.2.3.4 Dissolution testing of mixtures .....	183
4.2.3.5 <i>In vitro</i> gut absorption tests of mixtures.....	183

<b>4.3 Results and Discussion</b> .....	183
4.3.1 Mixtures of CAA with Ac-Di-Sol.....	183
4.3.1.1 Homogeneity measurements .....	183
4.3.1.2 DSC measurements.....	183
4.3.1.3 Dissolution testing.....	183
4.3.1.4 <i>In vitro</i> gut absorption testing .....	185
4.3.2 Mixtures of CAA with Starch 1500 .....	187
4.3.2.1 Homogeneity measurements .....	187
4.3.2.2 DSC measurements.....	187
4.3.2.3 Dissolution testing.....	187
4.3.2.4 <i>In vitro</i> gut absorption testing .....	189
4.3.3 Mixtures of CAA with Aerosil 200.....	190
4.3.3.1 Homogeneity measurements .....	190
4.3.3.2 DSC measurements.....	191
4.3.3.3 Dissolution testing.....	191
4.3.3.4 <i>In vitro</i> gut absorption testing .....	192
4.3.4 Mixtures of CAA with SLS .....	194
4.3.4.1 Homogeneity measurements .....	194
4.3.4.2 DSC measurements.....	194
4.3.4.3 Dissolution testing.....	195
4.3.4.4 <i>In vitro</i> gut absorption testing .....	196
4.3.5 Mixtures <i>in vitro</i> absorption summary results .....	197
4.3.6 Mixtures of CAA and CAC with all tested excipients .....	198
4.3.6.1 Homogeneity measurements .....	198
4.3.6.2 DSC measurements.....	198
4.3.6.3 Dissolution testing.....	203
4.3.6.4 <i>In vitro</i> gut absorption.....	205
<b>4.4 Conclusions</b> .....	206

**CHAPTER 5: EFFECT OF WAX COATING ON CEFUROXIME AXETIL IN  
THE PURE AMORPHOUS FORM (CAA) AND AS  
COMPRESSED MIXTURE WITH EXCIPIENTS (CADC)**

<b>5.1 Introduction</b> .....	208
<b>5.2 Wax Mixtures Prepared</b> .....	215
5.2.1 Materials and methods.....	215
5.2.1.1 Wax mixtures preparation .....	216
5.2.1.2 Melting point testing of wax mixtures .....	216
5.2.2 Results and discussions.....	216
<b>5.3 Mixtures of CAA and CADC with Waxes</b> .....	217
5.3.1 Materials and methods.....	217
5.3.1.1 Wax mixtures prepared.....	217
5.3.1.2 Method of preparation.....	217

5.3.1.3 Testing of mixtures.....	218
5.3.2 Results and discussions.....	218
5.3.2.1 HPLC analyses .....	218
5.3.2.2 DSC measurements.....	218
<b>5.4 Coated CAA with SA.....</b>	<b>219</b>
5.4.1 Materials and methods.....	219
5.4.1.1 Method of coating.....	219
5.4.1.2 HPLC analyses of wax coated particles .....	219
5.4.1.3 Laser particle size analyses of wax coated particles.....	219
5.4.1.4 DSC testing of wax coated particles.....	220
5.4.1.5 <i>In vitro</i> gut absorption testing of wax coated particles.....	220
5.4.2 Results and discussions.....	220
5.4.2.1 HPLC analyses .....	220
5.4.2.2 Particle size analyses.....	220
5.4.2.3 Dissolution testing.....	221
5.4.2.4 DSC measurement.....	221
5.4.2.5 <i>In vitro</i> gut absorption testing .....	222
<b>5.5 Coated CAA with Stearic Acid and Gelucire.....</b>	<b>224</b>
5.5.1 Materials and methods.....	224
5.5.1.1 Method of coating.....	224
5.5.1.2 HPLC analyses of coated particles .....	224
5.5.1.3 Particle size distribution of coated particles .....	224
5.5.1.4 DSC of coated particles .....	224
5.5.1.5 <i>In vitro</i> gut absorption testing of coated particles .....	225
5.5.2 Results and discussions.....	225
5.5.2.1 HPLC analyses .....	225
5.5.2.2 Particle size analyses.....	225
5.5.2.3 DSC measurement.....	226
5.5.2.4 <i>In vitro</i> gut absorption testing .....	227
<b>5.6 Coated CADC with Wax .....</b>	<b>229</b>
5.6.1 Materials and methods.....	229
5.6.1.1 Method of coating.....	229
5.6.1.2 HPLC analyses of coated particles .....	229
5.6.1.3 Particle size distribution of coated particles .....	229
5.6.1.4 DSC testing of coated particles.....	229
5.6.1.5 Electron microscopy testing of coated particles .....	230
5.6.1.6 <i>In vitro</i> gut absorption testing of coated particles .....	230
5.6.2 Results and discussions.....	230
5.6.2.1 HPLC analyses .....	230
5.6.2.2 Particle size analyses.....	230
5.6.2.3 DSC measurements.....	231
5.6.2.4 <i>In vitro</i> gut absorption testing .....	233
5.6.2.5 Electron microscopy testing of coated particles .....	235

<b>5.7 Coated cefuroxime axetil Mixture with Excipients</b> .....	237
5.7.1 Materials and methods.....	237
5.7.1.1 Mixtures preparation .....	237
5.7.1.2 HPLC testing .....	237
5.7.1.3 <i>In vitro</i> gut absorption testing .....	237
5.7.2 Results and discussions.....	238
5.7.2.1 HPLC analyses .....	238
5.7.2.2 <i>In vitro</i> gut absorption testing .....	238
<b>5.8 Conclusions</b> .....	239

**CHAPTER 6: COMPARISON BETWEEN WAX COATED COMPRESSED  
CEFUROXIME AXETIL MIXTURES WITH EXCIPIENTS  
(CADC) AND COMMERCIALY AVAILABLE WAX COATED  
CEFUROXIME AXETIL POWDER FOR SUSPENSION**

<b>6.1 Introduction</b> .....	240
<b>6.2 Materials and Methods</b> .....	240
6.2.1 Preparation of coated CADC dry suspension.....	241
6.2.2 Comparison tests .....	241
6.2.2.1 DSC testing.....	241
6.2.2.2 <i>In vitro</i> gut absorption testing .....	241
6.2.2.3 Pilot bioequivalence study .....	242
<b>6.3 Results and Discussions</b> .....	242
6.3.1 DSC measurements.....	242
6.3.2 <i>In vitro</i> gut absorption testing .....	243
6.3.3 Pilot bioequivalence study.....	245
<b>6.4 Conclusions</b> .....	248

**CHAPTER 7:SUMMARY,GENERAL CONCLUSIONS AND FUTURE  
WORK**

<b>7.1 Summary</b> .....	249
<b>7.2 General Conclusions</b> .....	253
<b>7.3 Future Work</b> .....	253
<b>REFERENCES</b> .....	254



## TABLE OF ABBREVIATIONS

C	: Cefuroxime sodium
CA	: Cefuroxime axetil
CAA	: Cefuroxime axetil amorphous
CAAc	: Cefuroxime axetil amorphous compressed
CAAh	: Cefuroxime axetil amorphous exposed to humid conditions
CAAD	: Cefuroxime axetil amorphous exposed to humid conditions then dried
CAC	: Cefuroxime axetil crystalline
Caco2	: Human colon adeno carcinoma cells
CADC	: Cefuroxime axetil compressed mixture with excipients
DSC	: Differential scanning calorimetry
G	: Gelucire 39/01
GIT	: Gastro intestinal tract
Min	: Minute
$P_{\text{eff}}$	: Effective intestinal permeability
R	: Reagent grade
RS	: Reference standard
SA	: Stearic acid
SLS	: Sodium lauryl sulphate
USP	: United states pharmacopeia
WS	: Working standard
m/m	: mass/mass
$T_g$	: Glass transition temperature
$T_m$	: Melting temperature
XRPD	: X-Ray powder diffraction
DVS	: Dynamic vapour sorption

## TABLE OF FIGURES

	Page
Figure 1.1 Schematic depiction of the variation of enthalpy (or volume) with temperature. ....	27
Figure 1.2 Structural formula of cefuroxime axetil. ....	53
Figure 2.1 Differential scanning calorimeter device parts. ....	84
Figure 2.2 A DSC thermogram of an amorphous substance. ....	86
Figure 2.3 Scheme of an X-ray powder diffractometer .....	100
Figure 2.4 Bragg's Law .....	101
Figure 2.5 Electron microscopy instrumentation. ....	105
Figure 2.6 Electrons and X-rays ejected from electron beam hitting the samples. ....	106
Figure 2.7 The apparatus for intrinsic dissolution testing. ....	109
Figure 2.8 Routes and mechanisms of transport of molecules across the intestinal epithelium. ....	112
Figure 2.9 Linearity of C using the BP 2000 HPLC method of CA analyses. ....	132
Figure 2.10 Linearity of C using the <i>in vitro</i> gut HPLC method of analyses. ....	136
Figure 2.11 A typical chromatogram for a standard solution of the <i>in vitro</i> gut HPLC method of analyses. ....	137
Figure 3.1 Log-normal particle size distribution of CAA. ....	145
Figure 3.2 Log-normal particle size distribution of CAC. ....	146
Figure 3.3 Log-normal particle size distribution of CAAC. ....	147
Figure 3.4 DSC thermograms of CAA, CAC and CAAC, at heating rate 25°C/min. ....	148
Figure 3.5 MTDSC heat flow thermograms of CAA, at heating rate 1°C/min, amplitude 0.5°C / 48 seconds. ....	149
Figure 3.6 Cp complex of CAA, at heating rate 1°C/min, amplitude 0.5°C/48 seconds. ....	149
Figure 3.7 MTDSC heat flow thermograms of CAC, at heating rate 1°C/min, amplitude 0.5°C / 48 seconds. ....	150

Figure 3.8	MTDSC heat flow thermograms of CAAc, at heating rate 1°C/min, amplitude 0.5°C / 48 seconds. ....	150
Figure 3.9	Cp complex of CAAc, at heating rate 1°C/min, amplitude 0.5°C/48 seconds. ....	151
Figure 3.10	Enthalpy / concentration curve of the mixtures of CAA with CAC.....	152
Figure 3.11	DSC thermograms of CAAd and CAAh after storage under 95%RH humidity for different time intervals, at heating flow 25°C/min. ....	154
Figure 3.12	DSC thermogram of CACH after storage for one week at 95%RH humidity, at heating rate 25°C/min.....	156
Figure 3.13	X-Ray powder diffraction for CAA(a), CAC(b), CAAc(c). ....	158
Figure 3.14	Dynamic vapour sorption isotherms of (CAA).....	160
Figure 3.15	Dynamic vapour sorption isotherms of (CAC).....	160
Figure 3.16	Dynamic vapour sorption isotherms of (CAAc). ....	161
Figure 3.17	Intrinsic dissolution profile of CA from CAA. ....	162
Figure 3.18	Intrinsic dissolution profile of CA from CAC. ....	163
Figure 3.19	Dissolution profile of CAAc using BP 2003 method. ....	165
Figure 3.20	Concentration of CA remained in the media after <i>in situ</i> perfusion test. ....	167
Figure 3.21	<i>In situ</i> perfusion HPLC chromatograms of CAA, at zero and 70 minutes.....	167
Figure 3.22	<i>In vitro</i> gut release of C from CAA to the media. ....	171
Figure 3.23	<i>In vitro</i> gut release of C from CAC to the media. ....	172
Figure 3.24	<i>In vitro</i> gut release of C from CAAc to the media.....	173
Figure 4.1	Dissolution % CA release from CAA mixtures with Ac-Di-Sol.....	184
Figure 4.2	<i>In vitro</i> gut release of C from compressed and uncompressed CAA mixtures with Ac-Di-Sol. ....	186
Figure 4.3	Dissolution %CA release from CAA mixtures with Starch 1500.....	188
Figure 4.4	<i>In vitro</i> gut release of C from compressed and uncompressed CAA mixtures with Starch 1500. ....	189
Figure 4.5	Dissolution %CA release from CAA mixtures with Aerosil 200. ....	191

Figure 4.6	<i>In vitro</i> gut release of C from compressed and uncompressed CAA mixtures with Aerosil 200. ....	193
Figure 4.7	Dissolution %CA release from CAA mixtures with SLS. ....	195
Figure 4.8	<i>In vitro</i> gut release of C from compressed and uncompressed CAA mixtures with SLS.....	196
Figure 4.9	DSC thermograms of CADC compared to CAAC, at heating rate 25°C/min. ....	199
Figure 4.10	MTDSC heat flow thermograms of CADC, at heating rate 1°C/min, amplitude 0.5°C / 48 second.....	199
Figure 4.11	Cp complex of CADC, at heating rate 1°C/min, amplitude 0.5°C/48 seconds. ....	200
Figure 4.12	DSC thermograms of CAA, heating–cooling–heating cycle, at rate of 10°C/min. ....	201
Figure 4.13	DSC thermograms of CAAC,heating–cooling–heating cycle, at rate of 10°C/min. ....	201
Figure 4.14	DSC thermograms of CADC,heating–cooling–heating cycle, at rate of 10°C/min. ....	202
Figure 4.15	Dissolution %CA release from CADC, CAA and CAC mixtures with all tested excipients. ....	204
Figure 4.16	<i>In vitro</i> gut release of C from CADC, CAA and CAC mixtures with all tested excipients. ....	205
Figure 5.1	Log-normal particle size distribution of CAA coated with SA. ....	220
Figure 5.2	DSC thermogram of CAA coated with SA, at heating rate 25°C/min. ....	222
Figure 5.3	<i>In vitro</i> gut release of C from CAA coated with SA. ....	223
Figure 5.4	Log-normal particle size distribution of coated CAA with SA and G. ....	225
Figure 5.5	DSC thermogram of coated CAA with SA and G, at heating rate 25°C/min. ....	226
Figure 5.6	<i>In vitro</i> gut release of C from CAA coated with SA and G. ....	228
Figure 5.7	Log-normal particle size distribution of the wax coated CADC granules. ....	230

Figure 5.8 DSC thermogram of wax coated CADC, at heating rate 25°C/min. ....	232
Figure 5.9 <i>In vitro</i> gut release of C from CADC wax coated granules. ....	234
Figure 5.10 Electron microscope images of CADC particles. ....	235
Figure 5.11 Electron microscope images of wax coated CADC particles ....	236
Figure 5.12 <i>In vitro</i> gut release of C from coated CAA mixture with excipients. ....	238
Figure 6.1 DSC thermogram of wax coated CAA in Zinnat <sup>®</sup> compared to that of wax coated CADC, at heating rate 25°C/min. ....	243
Figure 6.2 <i>In vitro</i> gut release of C from Zinnat <sup>®</sup> . ....	244
Figure 6.3 Semilogarithmic plot of plasma C concentrations after a single dose (250mg cefuroxime/5ml). ....	247
Figure 6.4 Linear plot of plasma C concentrations after a single dose (250mg cefuroxime/5ml). ....	247

## TABLE OF TABLES

	Page
Table 2.1 Materials of the <i>in situ</i> perfusion media.....	121
Table 2.2 LLOQ for C analyses using the <i>in vitro</i> gut HPLC method of analyses.....	134
Table 2.3 HPLC Recovery results of C from the <i>in vitro</i> gut TC 199 tissue media.....	134
Table 2.4 Repeatability results of the <i>in vitro</i> gut HPLC method of analyses.....	135
Table 2.5 Precision results of the <i>in vitro</i> gut HPLC method of analyses.....	135
Table 3.1 Amorphous and crystalline CA materials tested.....	143
Table 3.2 Comparative tests for CAA, CAC, CAAC, stored at different conditions.....	144
Table 3.3 Analyses of CAAh and CAAd water content, $T_g$ and $T_m$ .....	157
Table 3.4 Intrinsic dissolution of CA from CAA disks.....	161
Table 3.5 Intrinsic dissolution of CA from CAC disks.....	163
Table 3.6 Dissolution rate of CAAC according to BP 2003 method.....	164
Table 3.7 CA concentration remained in the media after <i>in situ</i> perfusion test.....	166
Table 3.8 <i>In situ</i> perfusion bioavailability results of CA.....	168
Table 3.9 $P_{eff}$ values for CA in the <i>in situ</i> perfusion test.....	169
Table 3.10 <i>In vitro</i> gut percentage C released from CAA to the media.....	170
Table 3.11 Recovery (%) of cefuroxime from the <i>in vitro</i> gut test of the CAA.....	171
Table 3.12 <i>In vitro</i> gut percentage C released from CAC to the media.....	172
Table 3.13 <i>In vitro</i> gut percentage C released from CAAC to the media.....	173
Table 4.1 Materials used in mixtures prepared with CAA and CAC.....	179
Table 4.2 Dissolution %CA release from CAA mixtures with Ac-Di-Sol.....	184
Table 4.3 <i>In vitro</i> gut %C release from CAA mixtures with Ac-Di-Sol.....	185
Table 4.4 Dissolution %CA release from CAA mixtures with Starch 1500...	188
Table 4.5 <i>In vitro</i> gut %C release from CAA mixtures with Starch 1500.....	189
Table 4.6 Dissolution %CA release from CAA mixtures with Aerosil 200.....	191

Table 4.7	<i>In vitro</i> gut C release from CAA mixtures with Aerosil 200.....	192
Table 4.8	Dissolution %CA release from CAA mixtures with SLS.....	195
Table 4.9	<i>In vitro</i> gut % C release from CAA mixtures with SLS.....	196
Table 4.10	<i>In vitro</i> gut release rates (K) of C from all mixtures tested.....	198
Table 4.11	Dissolution %CA release from CADC, CAA and CAC mixtures with the tested excipients.....	203
Table 4.12	<i>In vitro</i> gut release of C from CADC, CAA and CAC mixtures with the tested excipients.....	205
Table 5.1	Waxes studied.....	215
Table 5.2	Melting points of SA and G mixtures at different ratios. ....	216
Table 5.3	Materials studied mixtures with waxes. ....	217
Table 5.4	DSC results of CAA and CADC wax mixtures.....	218
Table 5.5	<i>In vitro</i> gut % C release from coated CAA with SA.....	223
Table 5.6	<i>In vitro</i> gut % C release from CAA coated with SA and G.....	227
Table 5.7	<i>In vitro</i> gut % C release from wax coated CADC.....	233
Table 5.8	<i>In vitro</i> gut % C release from coated CAA mixture with excipients.....	238
Table 6.1	Composition of wax coated CADC dry suspension.....	240
Table 6.2	<i>In vitro</i> gut % C release from wax coated CAA in Zinnat®.....	244
Table 6.3	Mean plasma concentrations of C from Zinnat® and wax coated CADC dry suspension.....	245
Table 6.4	Bioequivalence ratio analyses of data of cefuroxime for $C_{max}$ . ....	246
Table 6.5	Bioequivalence ratio analyses of cefuroxime for $AUC_{0 \rightarrow t}$ .....	246
Table 6.6	Bioequivalence ratio analyses of untransformed data of cefuroxime for $AUC_{0 \rightarrow \infty}$ .....	246

## ABSTRACT

Cefuroxime axetil (CA) is a widely prescribed anti-infectious drug. It exists in an amorphous (CAA) and a number of crystalline (CAC) forms. In this study the physico-chemical properties and dissolution behaviour of the various forms of CA were studied using a combination of analytical techniques and in-vitro dissolution testing.

Thermal analysis indicated that CAA exhibited a glass transition temperature ( $T_g$ ) at  $74^\circ\text{C}$ , while commercially available CAC is processed as two polymorphic forms each with a melting transition at  $130^\circ\text{C}$  and  $180^\circ\text{C}$ , respectively. The amorphous form was found to have higher dissolution and intestinal absorption rates than CAC. The former was also found to have adequate chemical and physical stability upon exposure to high relative humidity conditions. Plasticization effects relating to the uptake of moisture was limited to only small shifts in the  $T_g$  to lower temperatures, with no evidence of a rubbery transition and re-crystallisation. This was shown to be associated with the limited moisture uptake of CAA (maximum 2% at 90%RH,  $25^\circ\text{C}$ ), indicating a distinguished stability of this amorphous form of the drug.

In this study, stability of CAA was also determined under different formulation process conditions, specifically upon compression and coating. It was found that CAA underwent partial crystallisation upon direct compression. This transition was only observed, however, with the DSC technique indicating its potential for detecting the presence of small crystalline content in predominantly amorphous material. The induction of crystallisation by compression was inhibited by introduction of the excipients: Ac-Di-Sol, Starch 1500, and Aerosil 200, either each individually or together.

Such stabilisation is thought to be brought to CAA by the high molecular weight polymers (Ac-Di-Sol and Starch 1500). Thus, the relatively small drug may link its molecular motions to those of the polymers, leading to reduction in its molecular



mobility, and subsequently inhibiting crystallisation. Also, the high T<sub>g</sub> value of Aerosil 200 is also thought to deplasticize CAA upon compression. Thus, the excipients chosen prevented crystallisation of CAA under formulation process conditions.

Wax coating (needed to mask the very bitter taste of CA) was also found to significantly alter the stability of CAA, and led to complete transformation of CAA to CAC.

In vitro gut absorption testing and a pilot bioavailability study conducted on wax coated CAA, in different formulations, indicted a dramatic loss of absorption rate and extent, related to crystallisation of CAA upon coating. Introduction of the studied excipients to the coated granules, maintained 70% of the original absorption rate of CAA.

Thus, stabilisation of CAA under different formulation conditions was possible to achieve by the inclusion of some excipients. This maintained the favourable bioavailability of the amorphous drug.

## CHAPTER 1

### INTRODUCTION

#### 1.1 POLYMORPHISM

Many pharmaceutical solids can exist in a number of different physical forms, which differ in their physicochemical properties. These type of forms include solvates, hydrates, enantiomorphs and pseudopolymorphs of a crystalline material and an amorphous form. Polymorphism is often characterised as the ability of a drug substance to exist in two or more crystalline phases that have different arrangements and/or conformations of the molecules in the crystal lattice (Grant et al, 1999).

Amorphous solids consist of the disordered arrangement of molecules which do not possess a distinguishable crystal lattice. Solvates are crystalline solid adducts containing solvent molecules incorporated within the crystal structure. If the incorporated solvent is water, the solvates are also commonly known as hydrates.

Polymorphism occurs when there exists one or more way to satisfy the energy constraints imposed on molecules as they arrange into a crystalline lattice. The lattice properties of various polymorphs reveal differences in symmetry elements, and intermolecular binding (Elliott et al, 1990). Because intermolecular forces contribute to the properties of a solid, each polymorph is a distinct thermodynamic entity.

Polymorphs exhibit a variety of chemical, physical, mechanical, electrical, and thermodynamic properties. These differences are often observed in their corresponding properties: solubility, melting point, dissolution rate, chemical stability, physical stability, powder flowability, compaction, and particle morphology, (Hancock et al, 1997). These properties can have a direct impact on the processing of the drug substances and the quality/performance of drug products, such as stability, dissolution, and bioavailability.

Conducting early screening studies may eliminate or minimize the effect of discovering an unforeseen polymorph during a later stage of drug development (O'Neil et al, 2003).

### **1.1.1 Screening of polymorphs**

Screening is the first stage in the polymorph life cycle. The goal of polymorph screening is to discover the various polymorphic forms of a molecule. Polymorph screening methods generally rely on dissolving the crystalline phase and permitting the molecules or ions to reassemble under a controlled array of conditions. The rate of nucleation is influenced by the various conditions applied during crystallisation, which can lead to the isolation of the polymorphic forms, (Yu-L et al, 2001).

The solids resulting from each screening experiment are analyzed to determine whether new or different crystalline forms exist. Many analytical tools are required to fully characterise the polymorphic behavior of drug systems. Single crystal X-ray diffraction (XRD) is one of the most routinely used techniques for polymorphic screening (Jenkins et al, 1996).

The most common approach for polymorph screening is based on solvent recrystallisation (Barnett, 2002). However, alternative approaches include recrystallisation from the melt, antisolvent addition, vapour diffusion, solution slurry, and annealing. These approaches are summarised below.

#### **1.1.1.1 Solvent re-crystallisation**

Saturated solutions are prepared by agitating excessive amounts of solids with various solvent systems at a saturation temperature. The mother liquor is separated from the residual solids by filtration and is then heated above the saturation temperature to dissolve any remaining solids. This step is necessary to ensure all solids of the original polymorphic form have been eliminated. The temperature of the solutions is adjusted to the desired growth temperature, and solids are produced by a controlled solvent evaporation and/or by a temperature reduction profile (Mullin et al, 1998).

### **1.1.1.2 Re-crystallisation from the melt**

Re-crystallisation from the melt is often an attractive screening approach because it requires only few milligrams of material and does not require a solvent. The analytical techniques most useful for re-crystallisation from the melt are differential scanning calorimetry (DSC), and hot stage microscopy (HSM). This approach is only applicable to materials that are thermally stable. By manipulating the thermal profile after melting, polymorphic systems can often be frozen in various crystalline forms (Hino et al, 2001).

### **1.1.1.3 Antisolvent addition**

In this approach, saturated (or undersaturated) solutions of a material are prepared in different solvent systems. Rather than using cooling or solvent evaporation to reduce solubility (i.e., generate supersaturation), a set of miscible antisolvents are selected. The direct introduction of a miscible antisolvent to the solutions causes rapid precipitation of the material, due to the large decrease of the solute solubility upon its addition. The possibility exists that the precipitated solid may be in a less stable form than the most stable polymorph as a result of the rapid conversion of the material to solid form. Such crystalline phases are referred to as metastable.

In general, at a given temperature and pressure, the polymorph with the lowest free energy is the most stable form and all other polymorphs are metastable. Metastable polymorphs tend to spontaneously convert into a more stable form (Craig et al, 1999). If the material has sufficiently poor crystallisation kinetics, this approach may even result in an amorphous solid (Blaisdell et al, 2001).

### **1.1.1.4 Vapour diffusion**

Diffusion methods are specialized cases of solvent re-crystallisation. This technique can be useful for materials that exhibit poor crystallisation kinetics and/or are difficult to crystallise. Saturated solutions are exposed to a volatile antisolvent vapour in a closed system, or a second solvent is allowed to slowly diffuse into a saturated solution. As the antisolvent (or second solvent) diffuses into the saturated solution, it reduces the solubility of the drug. Because the system is generally not agitated, the reduction in solubility is slow, causing continually small decreases in the degree of relative supersaturation.

This provides sufficient mobility for the controlled nucleation of single crystals and the growth of existing nuclei and crystals in favour of the formation of nucleation and growth. A relatively small number of significantly sized crystals are typically formed. The slow nature of this approach makes the diffusion method one of the better techniques for isolating single crystals of adequate quality for structure determination using single-crystal XRD, and is the preferred route for high throughput screening techniques in the pharmaceutical industry (Blaisdell et al, 2001).

#### **1.1.1.5 Solution slurry**

Polymorphic forms generally exhibit variations in their solubilities, and the relative solubility of each form (at a given temperature) is dependent on the free energy of the solid and independent of the solvent identity. Slurries are prepared by stirring an excess amount of solid in a variety of solvent systems (Yul et al, 2001). Upon reaching equilibrium, the solution is saturated with respect to the polymorphic form that was dissolved, and supersaturated with respect to any polymorph that is less soluble than the form that was initially dissolved. Under these conditions, a less soluble form can nucleate and precipitate from solution.

#### **1.1.1.6 Annealing**

Polymorphic systems are capable of undergoing direct solid-solid phase transitions. These transitions are often kinetically impaired, making them difficult to detect under the time constraints of screening. One way to overcome this limitation is to first produce the material in the amorphous state. Molecules in the amorphous state have greater mobility than their crystalline counterparts, which results in the amorphous form being less stable than any crystalline forms of the material (Debendetti et al, 1996). Annealing the amorphous form of a drug candidate can result in crystallisation, especially above the glass transition temperature. XRD and DSC are then used to evaluate the resulting crystalline forms.

#### **1.1.2 Characterisation of polymorphism**

The initial step in polymorph characterisation is to confirm that the material generated by the screening experiments is in fact the intended drug candidate and that the screening process itself has not altered the material through decomposition, isomerization, or other inadvertent reaction.

A number of methods have been employed for characterising polymorphs in pharmaceutical solids (Brittain et al, 1999-b). Polarizing optical microscopy and thermomicroscopy have proven to be useful tools. Thermal analysis procedures, such as differential scanning calorimetry (DSC) and thermogravimetric analysis (TGA), can be used to obtain additional information, including phase changes.

These thermal methodologies are employed to distinguish between enantiotropic and monotropic systems. For an enantiotropic system, the relative stability of a pair of solid forms inverts at some transition temperature beneath the melting point while a single form is always more stable beneath the melting point in a monotropic system (Brittain et al, 1999-b).

Each polymorph is generally evaluated by DSC to determine melting point and enthalpy of fusion. This analysis will often indicate other important thermal events such as phase changes or thermal decomposition of the material. If solvents were used in the screening process that generated the polymorphs, thermogravimetric analysis (TGA) of the polymorphs may be used to determine whether the materials are solvated or whether they contain significant residual solvents (Giron et al, 1998).

The utility of solid-state spectroscopy for characterisation of polymorphic systems is becoming exceedingly important. Nuclear magnetic resonance (NMR) (Hogan et al, 2000), infrared absorption and Raman spectroscopy (Sepaniak et al, 2003) are used to study crystal structures. These methods require that either the nuclei of the pair of substances being examined exist in magnetically inequivalent environments or the vibrational modes are sufficiently different between the structural forms to permit differentiation.

The definitive criterion for the existence of polymorphism is via demonstration of a nonequivalent crystal structure, usually by comparison of the x-ray diffraction patterns. Microscopy, thermal analysis methodology and solid state NMR are generally considered as sources of supporting information.

### **1.1.3 Phase transitions**

Most compounds do not exhibit solid-solid phase transitions. For these materials, an accurate determination of the melting enthalpies can be used to determine the stability relationship between the polymorphs.

If phase transitions do occur, they are usually slow in the solid state, but they may be accelerated in the presence of moisture, solvents, or energy input. If the drug candidate exhibits a solid-state phase transition, calorimetry may be used to determine whether the transition is endothermic or exothermic (Burger et al, 1979).

Solubility experiments can also be used to evaluate the energy relationships among polymorphs. For a given solvent, the most stable polymorph has a low solubility at a given temperature. Competitive slurry experiment is another quick method to determine the energy relationship among polymorphs without having to determine their specific solubilities (Mullin et al, 1993). Competitive slurry experiments are performed by placing excess solids of two (or more) forms in contact with a solvent and mixing. Because each form has a different solubility, particles of the form with the low solubility grow at the expense of the more soluble form, which occurs because the more soluble form is slightly undersaturated, and the less soluble form is supersaturated.

Sometimes a competitive slurry experiment results in a polymorphic form that is more stable than either of those initially placed in contact with the slurry solvent. This result can occur when a polymorphic form that has a lower solubility than either of the initial polymorphic forms precipitates from solution. In this case, the two forms initially present are converted into the form that has precipitated (Mullin et al, 1998). Examining thermal data in conjunction with the slurry data can give a general thermodynamic hierarchy for most polymorph systems.

### **1.1.4 Controlling the crystallisation of a polymorphic form**

Developing a robust crystallisation process is the third and final stage in the life cycle for materials that exhibit polymorphism. The final process should be economical, deliver the correct polymorphic form, and provide the desired chemical purity.

Polymorph screening results provide information about the effect of various solvents and crystal growth conditions that lead to the different solid-state forms. These parameters may be used as a starting point to conduct small-scale crystallisation experiments. Crystallisation studies focus on the systematic manipulation of relevant crystal growth parameters (process variables) that are known to influence and control polymorphic forms. Parameters such as temperature, supersaturation, and interfacial tension between the saturated solution and the forming crystallites influence the rates of nucleation of each polymorphic form (Brittain et al, 1999-b).

The process variables that are important in controlling solid-state forms are thermodynamics, hydrodynamics, solvent composition, seeding, impurity profile, time, cooling profile, supersaturation, and reactor geometry (Brittain et al, 1999-b).

To evaluate the scalability of the crystal growth conditions that are established at a small scale, additional large batches are recrystallised at intermediate scales (laboratory to pilot plant) to mimic plant-scale conditions. These experiments provide an insight into the scalability and transferability of the crystallisation process to other facilities. In some cases, crystallisation conditions must be fine-tuned or re-examined if the crystallisation process produces different results when performed at a large scale. Differences can occur as a result of varying impurity profiles of large batches, changes in residual solvent content of reaction mixtures and differences in the reactor heat flow, geometry, and hydrodynamics (Brittain et al, 1999-b).

The ruggedness of a crystallisation process can be evaluated and improved by intentionally altering the crystal growth process variables and determining the amount of variance required to affect the resulting crystalline form. This evaluation can identify the significant process variables that exert a considerable influence on the polymorphic form along with the sensitivity of processing parameters (Wilson et al, 2000).



Thus, during the final stage of developing a synthetic procedure for a new drug entity, a great deal of emphasis is usually placed on obtaining material of high purity and reproducibility in terms of its physical, chemical, and biological properties, and emphasis are placed on what multi polymorphic or solvated crystal forms of the compound can be obtained (Byrn et al, 1982).

### **1.1.5 Amorphous materials**

Most of solid drugs are introduced in pharmaceutical dosage forms in their crystalline form. This is because the physical structures of crystalline materials are generally thermodynamically stable, and are relatively simple to study using techniques such as differential scanning calorimetry and X-ray diffraction (Craig et al, 1999-a).

However in pharmaceuticals, amorphous phases had been intentionally produced to improve the dissolution and bioavailability of poorly soluble compounds (Byrn et al, 1982), to stabilise the tertiary structure of proteins (Carpenter et al, 1994) and to improve the mechanical properties of excipients. The three dimensional long-range order that normally exists in a crystalline material does not exist in the amorphous state, and the position of molecules relative to one another is more random, as in the liquid state. Typically, amorphous solids exhibit short range order over a few molecular dimensions and have physical properties quite different from those of their corresponding crystalline states.

As a result of its higher internal energy e.g.  $\sim 25$  kJ.mol for cephalosporins (Pikal et al, 1978), the amorphous state should have enhanced thermodynamic properties relative to the crystalline state (e.g. solubility, vapour pressure) and greater molecular motion (Zhou et al, 2002). From a pharmaceutical perspective, the high internal energy and specific volume of the amorphous state relative to the crystalline state can lead to enhanced dissolution and bioavailability.

A major phenomenon that a solid amorphous phase exhibits is the glass transition temperature, where there is an abrupt change in its kinetic (molecular mobility) and thermodynamic properties (e.g., heat capacity or thermal expansivity) at the critical temperature.

As pharmaceutical solids rarely exist as 100% crystalline or 100% amorphous phases, it is necessary to consider how partially crystalline or amorphous systems are likely to behave. The coexistence of two thermodynamically different states of a material will probably result in significant and measurable structural heterogeneities and batch to batch variations in physical properties. The presence of one phase in another can act as a focal point for spontaneous phase transitions such as crystallisation (Gerhardt et al, 1994). In addition, as each phase is intimately dispersed in the other, there may not be complete independence in their behavior. For example, the dispersion of crystalline drug in an amorphous carrier has been reported to alter the observed glass transition temperature of the amorphous phase (Broman et al , 2001).

The most common means by which amorphous solids and characteristics are formed are: condensation from the vapour state, super cooling of the melt (quench cooling of a material), mechanical activation of a crystalline mass (e.g. during milling), and rapid precipitation from solution (e.g. during freeze-drying or spray drying) (Hancock et al, 1997).

The general procedure for preparing amorphous solids has been described by (Turnbull et al, 1961, 1986) as a sequence of three steps. First, the material is energized, for example, by melting, grinding, etc. Second, the material is deenergized by means such as quenching. The third step involves kinetically trapping the amorphous form, and is often continuous with the second step. Melt quenching is a technique for preparing an amorphous solid by rapidly cooling the molten form of a material, typically by pouring it into liquid nitrogen. The amorphous form is trapped due to the continuously increasing viscosity (continuous hardening) of the rapidly cooling melt. In contrast, crystallisation of the melt occurs with an abrupt change in viscosity (discontinuous hardening), during which the crystallites grow in the body of the melt. A requisite for glass formation from the melt is that cooling must take place quickly enough to prohibit nucleation and growth of crystals.

Despite the fact that amorphous systems may be desirable, their use is associated with some difficulties. Of these, amorphous materials are thermodynamically unstable and will tend to revert to the crystalline form on storage (devitrification); such behavior had been reported for a number of drugs (Fukuoka et al. 1989; Yoshioka et al. 1994; Hancock et al. 1995). The devitrification process may be so slow so as to be effectively irrelevant within the storage time of a product (Craig et al, 1999-a).

On the other hand, the physical structure of glassy materials is more difficult to characterise and control than that of crystalline systems. The scientific understanding concerning the relationship between  $T_g$  and pharmaceutical product performance has not been fully developed. Furthermore, considerable care must be taken with regards to the use of conventional accelerated stability studies in predicting chemical or physical stability, as the behavior above and below  $T_g$  is not directly comparable (Duddu et al, 1997).

#### **1.1.5.1 Thermal history effects**

Although various techniques can be used to produce an amorphous phase, the increase in free energy of the amorphous phase relative to the crystalline phase of the same compound depends on the technique used.

The dependence of free energy on preparation conditions is referred to as thermal history. The effects of thermal history have been shown to affect relaxation time, stability, and location of the glass transition temperature (Garcia et al, 1997). It has been found that slower cooling rates, when preparing the amorphous material, results in a lower  $T_g$ . The actual value of  $T_g$  may vary by as much as 5%–10% for widely differing cooling rates, although the variation is typically quite small in pharmaceutical systems. Thus, one may not expect glasses of the same material prepared and stored under different conditions to have a single glass transition temperature (Elliott, 1990).

#### **1.1.5.2 Glass transition temperature of the amorphous state**

The nature of the glass transition has been widely described (Elliott, 1990; Angell, 1995; Hancock et al, 1997). Craig et al. (1999-a) illustrated the essential

differences between the formation of amorphous and crystalline systems in terms of their thermodynamic behaviour. These differences are schematically represented in Figure (1.1)

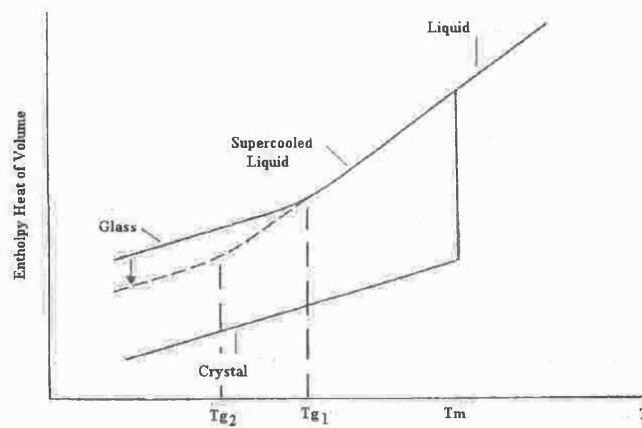


Figure 1.1: Schematic depiction of the variation of enthalpy (or volume) with temperature (Elliott et al. 1983; Zografis et al. 1996; Craig et al. 1999a).

For crystalline systems, when the temperature is reduced from the liquid state to the melting point ( $T_m$ ) a transition to the crystalline form occurs (if no super-cooling is initiated). The crystalline state below  $T_m$  is thermodynamically stable compared to non-crystalline forms. The exothermic crystallisation process leads to a sudden contraction of the system due to a decrease in free volume. Consequently, both the enthalpy ( $H$ ) and specific volume ( $V$ ) decrease at  $T_m$ .

As the temperature is lowered, as a result of heat capacity and thermal contraction effects, a less marked decrease in enthalpy and volume can be observed. For glass-forming materials, the crystallisation process is not favored either due to the molecular size and shape (e.g. proteins) or due to the quench cooling, where the degree of supersaturation is too high for controlled crystallisation to occur. For these materials, no discontinuity in enthalpy or volume is seen on cooling the material below  $T_m$ , and the system forms a super-cooled liquid. Upon further cooling a point is reached ( $T_g$ ) at which the material becomes 'frozen' into a glassy state.

At the  $T_g$ , the bonding between molecules remains essentially the same as that of the liquid but the translational and rotational motions of those molecules are dramatically reduced (Craig et al, 1999-a). The glass transition can then be characterised via a step change in heat capacity  $C_p$  and the transition is dependent on molecular mobility with no associated heat transfer in the process.

At slower cooling rates lower values for  $T_g$  are obtained, as indicated in Figure 1.1. The material is considered to be in the liquid or 'rubbery' above  $T_g$  and in the glassy states below  $T_g$ . Changes in mechanical properties arising as a result of the decrease in molecular motions as the system is cooled through the  $T_g$  will lead to strong or fragile amorphous solids.

To explain the glass transition, it is helpful to consider the entropy of the system (Craig et al, 1999-a), which at equilibrium is related to the heat capacity via  $C_p = T (\Delta S/\Delta T)_p$ . The heat capacities of the glass  $< T_g$ , and crystalline states for a given material are essentially the same. While at temperatures  $> T_g$  the higher values of  $C_p$  observed are caused by the material possessing additional configurational degrees of freedom when in the rubbery state. Consequently, the  $T_g$  may be considered to occur at a given value of excess entropy (Elliott, 1990).

The glass transition may also be explained by the relaxation processes that occur as the liquid is cooled (Craig et al, 1999-a). These relaxation times will be temperature dependent and governed largely by reorganization of hydrogen bonds in the hydrogen bonded fluids. At temperatures above  $T_g$ , the relaxation time of the material ( $t_r$ ) will be short with respect to the time of observation ( $t_0$ ), in this case, the material will appear liquid-like. Consequently, above  $T_g$  the sample is in equilibrium with the cooling program as it will be able to respond to change in temperature with cooling.

Below  $T_g$ , the relaxation process is slow with respect to the timescale of the cooling program, thus  $t_0$  will be  $< t_r$ , and the material will assume solid-like characteristics due of reduced molecular mobility. The glass transition may therefore be considered to occur when  $t_r \sim t_0$ .

Another approach to interpret the glass transition is to consider the free volume of the system. Cohen and Turnbull originally proposed the free volume theory in 1959 (Kasapis et al, 2001 ).

The model was developed for fluids assumed to be composed of thermally oscillating hard spheres. The total volume of the liquid is divided into two parts, the part occupied by the spheres or molecules in the absence of thermal motion, i.e., at 0 K ( $V_{0K}$ ) and the part in which the molecules are free to move, the free volume ( $V_f$ ). The free volume can be further divided into the thermal volume ( $V_{thermal}$ ), which represents the additional volume occupied by a molecule during thermal motion, and the excluded volume ( $V_{excl}$ ), which represents any volume that is never occupied. The model assumes that diffusive motion only occurs when  $V_f$  is above a critical value (Debenedetti et al, 1996).

The free volume can be divided into voids of varying sizes and locations determined by the random motion of the molecules. Redistribution of the free volume occurs without a change in the local free energy. When the liquid is heated,  $V_{thermal}$  increases, corresponding to a decrease in density, while as the liquid is cooled,  $V_{thermal}$  decreases resulting in a liquid with higher density. At temperatures lower than  $T_g$ , the decreased  $V_f$  (higher density) creates an energetic barrier to non-uniform distribution of  $V_f$  (i.e results in a more uniform distribution of  $V_f$ ).

Under these conditions, the thermal expansion coefficient of the glassy phase ( $\alpha_g$ ) is similar to that of the crystalline phase ( $\alpha_c$ ) of the same compound. Below  $T_g$ , a slightly increasing temperature results in increased vibrational molecular motion about effectively fixed positions causing expansion. In this case, the free volume remains uniformly distributed, and the increase in entropy with temperature is small because translational molecular motion does not accompany a change in volume. At  $T > T_g$ , there is enough thermal energy to overcome the energetic barrier, allowing non-uniform distribution of  $V_f$  and translational molecular motion. The thermal expansion coefficient is then liquid-like, and there is a significant increase in entropy with temperature. In this formalism, vitrification occurs when  $V_f$  becomes zero.

Free volume theory is commonly used to describe polymeric systems, where segments of the polymer chain are treated as rigid bodies and  $V_f$  consists of the “holes” present between the segments. At the glass transition temperature, the free volume is insufficient for rearrangement of the polymer backbone to occur. As a result,  $V_f$  is considered a constant at or below  $T_g$  for polymers (Debenedetti et al, 1996).

For a glassy system, the free volume reaches a lower limit at  $T_g$  and is thereafter temperature independent, hence in essence the glass transition occurs when  $V_f$  falls below a critical value (Her et al, 1994).

Ediger et al. (1996) reported that the glass transition can be considered to be a thermodynamic requirement for a super-cooled liquid, since without such a transition the amorphous material would attain a lower enthalpy than the crystalline state at some critical temperature and this critical temperature is known as the Kauzmann temperature  $T_K$ , and is thought to mark the lower limit of the experimental glass transition  $T_g$ , and to be the point at which the configurational entropy of the system reaches zero. The case in which the metastable glass would obtain configurational entropy lower than that of the crystal has been named the Kauzmann paradox (Kauzmann et al, 1948).

Experimental studies of the glass transition are complicated by the existence of many different modes of molecular motion in most systems (e.g. rotational or translational), changes in the scale and type of motions with temperature, and cooperativity or coupling of molecular motions.

At  $T_g$  the mean molecular relaxation time  $t$  associated with the predominant molecular motions is about 100s, and  $T_g$  can be expected to vary with experimental heating and cooling rates. A fast cooling rate produces a higher value for  $T_g$  than does the use of slower rates (Ramos et al, 2004), this can be related to the relaxation behavior of the system. The time scale for the relaxation processes is higher at lower temperatures, i.e. the relaxation will be slower (Moynihan et al, 1996). Consequently, at slower rates the temperature at which the relaxation

process becomes comparable with the time scale of the experiment will be lower, hence the measured  $T_g$  will be lower.

$T_g$  is also affected by the sample molecular mass (Mckenna et al, 1989), sample history, sample geometry, and sample purity (Ford et al, 1999). The experimental glass transition temperature is also influenced by the choice of technique used to measure it because of the varying sensitivities of available techniques to different types and speeds of molecular motions.

Depending upon the magnitude and temperature dependence of the apparent activation energy for molecular motions near and above  $T_g$  in super-cooled liquids, it is possible to classify them as either "strong" or "fragile" amorphous systems (Angell et al, 1988). A strong liquid typically exhibits little changes in its molecular mobility with temperature and a relatively small change in heat capacity at  $T_g$ . Proteins are good examples of strong glass formers, with their changes in heat capacity at  $T_g$  often being so small that they cannot be detected using standard calorimetry techniques (Angell, 1995). A fragile super-cooled liquid has much stronger temperature dependence of molecular mobility near  $T_g$  and a relatively large change in heat capacity at  $T_g$  and will typically consist of nondirectionally, noncovalently bonded molecules (e.g. ethanol).

The behavior of amorphous systems is dependent upon the assumption of constant pressure and composition (Mishima et al, 1991). Pressure effects upon amorphous materials are likely to be significant with effects on molecular packing potentially modifying the glass transition temperature, the thermal expansion behavior, and the strength/fragility of a super-cooled liquid.

Simple mixing rules have been used by many authors to describe the variation of the glass transition temperature with blend composition, however the effects of non-idealities (e.g. immiscibility, molecular size differences, specific interactions, etc) are often significant. The simplest and most reliable approach for use with amorphous pharmaceutical materials appears to be a modified Gordon-Taylor-



equation (Eq.1.1) established by Gordon. M, and Taylor. J in 1952, which is based on free volume theories, for simple two-component mixtures.

$$T_{\text{gmix}} = \frac{(w_1 T_{g1} + Kw_2 T_{g2})}{(w_1 + Kw_2)} \dots\dots\dots \text{Eq.1.1}$$

Where:

$T_g$  : Is the glass transition temperature

$w_1$  and  $w_2$  : Are the weight fractions of components 1 and 2,

$K$  : Can be calculated from the densities  $\rho$  and glass transition temperature  $T_g$  of the components is in Eq.1.2:

$$K = \frac{(T_{g1} \rho_1)}{(T_{g2} \rho_2)} \dots\dots\dots \text{Eq.1.2}$$

Similar equations can be readily derived for mixtures of more than two components. A perfectly miscible system will display a single sharp glass transition event. Immiscibility, incompatibility, or nonideality is often indicated by a poor fit to the theoretical equation and the appearance of more than one  $T_g$  or broadening of the glass transition event.

Simple solution theories also can be used to provide a qualitative understanding of the important factors regulating the glass transition in pharmaceutical systems. This is very important since the presence of very low levels of low molecular weight contaminants or additives (including water vapour) is predicted and observed to have significant plasticizing effects on pharmaceutical glasses. Whereas the addition of low levels of high molecular mass additives often has antiplasticizing effect (Gerhardt et al, 1994).

### **1.1.5.3 Relaxation phenomena**

Relaxation in the glassy state is often referred to as structural relaxation, physical aging, or annealing. The term “structural relaxation” refers to changes in atomic/molecular arrangements that occur during relaxation. The spontaneous conversion from the amorphous to crystalline state is quantified in terms of enthalpy or volume changes with time and temperature. As a glass is aged isothermally below the glass transition temperature, enthalpy, and entropy decrease spontaneously with time towards a temperature-dependent equilibrium value (Super cooled Liquid curve). The process by which the glass contracts toward the lowest free energy state is known as physical aging (McCram et al, 1998). The term was introduced by Struik to distinguish relaxation effects from those produced by chemical reactions, degradation, or changes in crystallinity (Struik et al, 1978). The temperature range in which aging occurs is not restricted to a narrow range just below  $T_g$ . Since the time for molecular relaxation is approximately 100s at  $T_g$ , and of the order of hours to days at temperatures well below  $T_g$  (Hancock et al, 1997) these motions have to be measured using extended experimental techniques, sensitive to motion on the same time-scale.

The Williams-Watts equation has been applied to enthalpy relaxation data to find the temperature where molecular mobility is decreased to a level where it becomes negligible with respect to the expected life time of a drug (William et al, 1970). It has been reported that shelf lives estimated by the Williams-Watts mean molecular relaxation time constant are similar to those determined experimentally (Hancock et al. 1995; Van de Mootor et al. 1999).

### **1.1.5.4 Plasticization of amorphous materials**

A highly important consideration with regard to the glass transition of amorphous materials is the effect of the presence of additional materials, particularly water, on the value of  $T_g$ . The study of mixed systems has been of particular importance in the polymer science field, whereby materials may be multi-component, with the degree of mixing being estimated by observing the glass transitions of the product in relation to those of the individual components. Mixing of amorphous

pharmaceuticals is an approach that may be used to raise the glass transition of a product in order to improve stability (Fukuoka et al, 1989).

Water has a profound effect on the glass transition of amorphous pharmaceuticals, acting as a plasticizer by increasing the free volume of the material, hence leading to a decrease in  $T_g$ . Exactly the same principle applies to the inclusion of plasticizers in polymeric film coats.

In the amorphous state considerably more water may be taken up relative to the crystalline form (Hancock et al, 1997), effectively due to absorption of water into the solid, hence in contrast to crystalline systems the uptake process tends to be dependent on sample mass rather than surface area. As the concentration of water in the solid increases, the  $T_g$  is seen to decrease. Ahlneck et al. (1990) have emphasised that at higher storage temperatures, a lower amount of water is required to lower the  $T_g$  to that particular temperature.

In considering the importance of the amorphous state in determining the solid state properties of pharmaceuticals, four areas are most important: dissolution, crystallisation, chemical degradation, and mechanical responses to stress, (e.g. powder compression in tableting).

#### **1.1.5.5 Amorphous drugs and dissolution**

The solid state characteristics of drugs are known to potentially exert a significant influence on the solubility parameter. Polymorphs of a drug substance can have different apparent aqueous solubilities and dissolution rates. When such differences are sufficiently large, bioavailability is altered and it is often difficult to formulate a bioequivalent drug product using a different polymorph.

Solubility at a defined temperature and pressure is the saturation concentration of the dissolved drug in equilibrium with the solid drug. Aqueous solubility of drugs is traditionally determined using the equilibrium solubility method that involves suspending an excess amount of a solid drug in a selected aqueous medium. The equilibrium solubility method may not be suitable to determine the solubility of a

metastable form, since the metastable form may convert to the stable form during the experiment.

When the solubility of metastable forms of a drug substance can not be determined by the equilibrium method, the intrinsic dissolution method may be useful to deduce the relative solubilities of metastable forms (Amidon et al, 1995). The use of the intrinsic dissolution method assumes that the intrinsic dissolution rate is proportional to the solubility - the proportionality constant being the transport rate constant, which is constant under the same hydrodynamic conditions in a transport-controlled dissolution process.

Polymorphic differences and transformations that result in different apparent solubilities and dissolution rates are generally detected by dissolution testing. This test provides a suitable means to identify and control the quality of a product both from bioavailability and (physical) stability perspectives (Amidon et al, 1995).

It is well recognised that for many drugs, improvement in the dissolution rate may enhance the bioavailability of that drug. One approach for such an improvement is to prepare the drug in an amorphous form. The higher molecular mobility of this form compared to the equivalent crystalline material may lead to enhanced dissolution rate and bioavailability.

A number of examples of enhanced dissolution for amorphous drugs are available in the literature. These include the 9,3''-diacetylmidcamycin (MOM), a 16-membered macrolide antibiotic, was prepared in the crystalline and amorphous forms, and the dissolution behaviour of both at a range of temperatures was compared (Sato et al, 1981). The amorphous form showed higher dissolution rates, although at longer dissolution times the concentration in water decreases due to the formation of crystalline MOM from the supersaturated solution. Similarly, the dissolution rate of amorphous indomethacin has been reported to be greater than for the crystalline material (Fukuoka et al, 1989). Cefuroxime axetil in the amorphous form was found to have a higher dissolution and bioavailability than the crystalline form (Crisp et al, 1985).

Drying or grinding may deliberately or accidentally induce amorphous characteristics. A ground mixture of griseofulvin and microcrystalline cellulose significantly improved both the dissolution rate and bioavailability of the drug compared to a micronised griseofulvin powder preparation (Yamamoto et al, 1974). This was ascribed to an increase in amorphous content of the drug as a result of the grinding process. Grinding of phenytoin with microcrystalline cellulose was also found to enhance drug dissolution rate, this again being attributed to the formation of an amorphous form of the drug (Yamamoto et al, 1976).

Various particle engineering processes such as spray drying may be used to prepare amorphous systems. A review of the physical structure of spray dried products, with special reference to thermal analysis, has been undertaken by Corrigan et al. (2004). The formation of amorphous pharmaceuticals via this process has been demonstrated for a number of drugs such as salbutamol.

#### **1.1.5.6 Crystallisation of an amorphous material**

Since molecules in the amorphous state are thermodynamically metastable relative to the crystalline state, the potential for crystallisation during handling and storage is omni present. Evidence exists to show that such crystallisation can be responsible for phenomena such as postcompression hardening of tablets (Elamin et al, 1994), lyophilized cake collapse and particle aggregation in dry powder inhalers (Ward et al, 1995). It would appear important to be able to anticipate conditions that give rise to such crystallisation and to be able to inhibit it if so desired.

At the point when  $T_g$  drops to the experimental temperature  $T$ , most amorphous (glass) materials have a viscosity of  $10^{12}$  -  $10^{14}$  Pa.S (Levine et al, 1988). In reality, this viscosity is too high to allow crystallisation to occur rapidly. Thus, it is more usual to see crystallisation when  $T_g$  has been significantly reduced below the experimental temperature.

Shalaev described the softening temperature as being the point at which collapse of structures under gravity will occur within a short period of time (Shalaev et al, 1995). Subsequent to the collapse event, the material will crystallise. Again the

rate of onset of crystallisation is dependent upon the extent to which  $T_g$  has been reduced below  $T$ . Crystallisation from the amorphous state is primarily governed by the same factors that determine crystallisation from the melt. For any amorphous system the temperature at which optimal nucleation, and hence crystallisation, should occur will depend primarily on the degree of super-cooling below  $T_m$ , and where the temperature lies relative to  $T_g$ . The closer to  $T_g$  the greater the degree of super-cooling and the lower the molecular mobility.

Gerhardt et al. (1993) showed that the crystallisation temperature for amorphous sugars is reduced by the presence of absorbed water in direct proportion to the plasticizing effects of water on  $T_g$ , and raised by the incorporation of high  $T_g$  additives. This has led to a general conclusion that crystallisation from amorphous state over practical time scale can be prevented by keeping the operating temperature below  $T_g$  (Jolley et al, 1970), by reducing the water content, or by raising the  $T_g$  of the system using additives with high  $T_g$  values (Yoshioka et al, 1995) (e.g. PVP with a  $T_g$  of about 180°C). These strategies have been advocated by many workers, but a clear understanding of the molecular basis for such stabilising effects has not yet been achieved (Yoshioka et al, 1995).

Amorphous systems are expected to exhibit greater chemical reactivity (Pikal et al, 1978), possibly at different rates below and above  $T_g$  (Yoshioka et al, 1994).

In conclusion, amorphous materials are thermodynamically unstable and therefore liable, under certain circumstances such as elevated temperature or relative humidity (RH), to undergo changes in its amorphous structure, or to revert to the stable crystalline form.

#### **1.1.5.7 Characterisation of the amorphous state**

Upon passing into the super-cooled liquid state or through the glass to rubber transition it is possible to observe changes in a multitude of material physical properties including density, viscosity, heat capacity, X-ray diffraction, and diffusion behavior.

Techniques which measure these properties (directly or indirectly) can be used to detect the presence of an amorphous material (glass or rubber), and some of

these methods are sensitive enough to allow quantification of the amount of molecular order or disorder (amorphous content) in a partially crystalline system.

### **Diffraction Techniques**

As there is no long range three dimensional molecular order associated with the amorphous state, the diffraction of electromagnetic radiation (e.g. X-rays) is irregular compared to that in the crystalline state. Diffraction techniques are perhaps the most definitive method of detecting and quantifying molecular order in any system, and conventional, wide angle and small-angle diffraction techniques have all been used to study order in systems of pharmaceutical relevance (Gerhardt et al, 1994).

The specificity and accurate quantitative nature of these nondestructive techniques make them first line choices for studying partially crystalline pharmaceutical materials. Conventional X-ray powder diffraction measurements can be used to quantify non-crystalline material down to levels of about 5% (Gerhardt et al, 1994), and with temperature and environmental control can also be used to follow the kinetics of phase transformations, or to quantify the presence of a crystalline drug in an amorphous excipient matrix (Ward et al, 1995).

Small angle X-ray measurements have been used to study subtle structural (density) changes in polymers in the glassy state upon annealing (Murase et al, 2004), and neutron scattering is gaining wider use in the characterisation of short-range two-dimensional order in amorphous materials.

### **Gas Displacement Technique**

The use of gas displacement pycnometry for quantifying the amorphous content of partially crystalline pharmaceutical systems has been described by (Saleki-Gerhard et al, 1994), and the accuracy achieved was about  $\pm 10\%$ . Liquid displacement pycnometry has also been used to determine the crystallinity of several mannitol samples (Chew et al, 1999). This approach has proved useful for quantifying low levels of disorder in crystalline pharmaceutical samples.

## **Transport Phenomena**

The most characteristic property of the amorphous state is its viscosity (approximately  $< 10^{12}$  Pa.s above  $T_g$  and  $> 10^{12}$  Pa.s below  $T_g$ ). The greater free volume, lower density, and higher molecular disorder of an amorphous material compared to its crystalline counterpart, result in the mechanical properties of amorphous systems, (viscosity, elastic modules) being much more like those of a liquid than those of a solid.

As a consequence of the greater free volume in amorphous materials, diffusive transport processes are usually significantly more rapid than in crystals. Often different diffusion rates are observed above and below  $T_g$ , with significantly faster diffusion occurring above  $T_g$ . This phenomenon can be used to identify the glass transition temperature in some amorphous systems (Duddu et al, 1995). Despite being very difficult to make general predictions about diffusion behavior in amorphous systems because of the large number of system specific variables which can have an effect upon transport properties, it is possible to rank the rates of diffusion in the order liquid  $>$  rubber  $>$  glass  $>$  crystal, assuming all other factors to be approximately equal. Transport properties of amorphous pharmaceutical materials are important because they can be exploited to control drug release in modified release dosage forms (e.g. transdermal patches).

The methods used to study transport phenomena in amorphous pharmaceutical systems include diffusion cells, NMR measurements, and molecular dynamics simulations (Oksanen et al, 1993).

## **Scanning Probe Microscopy**

The development in recent decades of scanning probe microscopy (SPM) techniques such as atomic force microscopy (AFM) has made visualization of surface structures on a nano to micrometer scale feasible (Shakesheff et al. 1996; Craig et al. 2002). In AFM, a tip attached to a cantilever (a spring) is scanned over a surface, while the deflection of the cantilever is monitored by the aid of a laser, as the tip moves over the sample. In this way, the nanoscale topography of the sample can be imaged. Moreover, modern SPM instruments can be run in different



modes to derive indications of surface related properties such as friction and rheology.

AFM has found applications in many areas, such as biology and polymer and materials sciences, and the technique also has considerable potential in the field of pharmaceuticals. It offers a unique means of scanning unprepared samples in different environments, including liquids, and at controlled temperature and relative humidity. A possible application could thus be the examination of solid systems during phase transformation, for example, crystallisation of amorphous materials. AFM can be a valuable tool for monitoring properties of pharmaceutical materials and the measurements can be performed directly, for example on compacts, film coatings, and single particles.

In recent publications, AFM has been used to study different crystal forms of Cimetidine (Danesh et al, 2000), friction, and adhesive forces of lactose (Sindel et al. 2001; Louey et al. 2001) crystallisation of films of amorphous Felodipine, and surface roughness in relation to friction (Berard et al. 2002; Bogdanovic et al. 2002).

A recently developed type of AFM, the microthermal analysis, has also been used to analyze and identify amorphous and crystalline materials (Bond et al. 2002; Royall et al. 2001). However, the AFM technique is restricted to flat sample surfaces, and the height range of the scanner is often limited to approximately 10µm or less. The tip is also sensitive to lateral forces, which can be a problem when scanning rough surfaces. One way to circumvent this problem is to use AC mode, in which the sample is tapped by oscillation of the tip at the sample surface. Information is then extracted from the change in the amplitude of oscillation, rather than from the deflection as in contact mode.

The literature on the use of AFM for the quantification of crystallisation processes is limited. Trojak et al. (2001) reported that the surface roughness increased significantly as a film of amorphous felodipine crystallized. Beekmans et al. (2002) used AFM to study the kinetics of crystal melting of polyethylene oxide.

## **Spectroscopic Techniques**

Spectroscopic techniques are valuable for the characterisation of amorphous systems because of their high structural resolution. Nuclear magnetic resonance (NMR), Raman, infrared (IR) and electron spin resonance (ESR) studies of amorphous pharmaceutical systems have all been described (Taylor et al, 1997).

These methods can be used to determine the glass transition temperature, quantify the presence of amorphous content and determine mean molecular relaxation times as a function of temperature (Taylor et al, 2001).

While there are some advantages in being able to follow the molecular mobility of specific chemical groups within molecule (e.g. resolution of different modes of motion), the conclusions drawn are open question unless supporting evidence can be obtained using complementary techniques (Fevotte et al, 2004). Samples ranging from simple powders or solutions to entire dosage forms can be studied using these nondestructive techniques, and this makes them especially useful for characterising pharmaceutical systems. Dielectric relaxation and dynamic mechanical spectroscopy have also been widely used to study amorphous pharmaceutical materials (Craig et al, 2001). These techniques are especially sensitive to the glass transition event and to secondary thermal transitions which reflect lower order molecular motions. Buckton had shown that it is possible to monitor the crystallisation of amorphous lactose in real time through examination of NIR spectra at certain wavelength (Buckton et al, 1998-a).

Recent studies by Seyer et al. (1997) have indicated that second derivative Near Infra-Red spectroscopy (NIR) spectra are able to quantify small amounts of amorphous materials in crystalline samples, this technique is extremely good at showing the state of water in the sample but not as good as calorimetry methods in quantifying the amorphous content.

Lusting et al. (1997) have shown that solid state NMR has a similar detection limit for amorphous lactose (~0.5%) to that which has been claimed for calorimetric techniques.

## Calorimetric Techniques

### DSC and MTDSC

Thermal calorimetric analytical methods have been widely used to characterise amorphous pharmaceutical systems, and several comprehensive reviews of their use have been published (Giron et al, 1998). These methods can obviously be used to determine fundamental thermodynamic properties (e.g. heat capacity, enthalpy changes) of the amorphous state.

The heat capacity of an amorphous material is always higher than that of its crystalline state, and a change in the rate of heat capacity change with temperature defines its calorimetric glass transition temperature (Weuts et al, 2003). This change in heat capacity at the glass transition temperature  $\Delta C_p$  can be related to the fragility of the amorphous material (Angell et al, 1995).

Glasses are thought to be frozen into an unstable state on normal experimental times scales, but on longer time scales they slowly relax back to the metastable super-cooled liquid state. The enthalpic changes associated with this process was measured using DSC (Hancock et al, 1995). Such relaxation processes were also studied by thermomechanical analysis (TMA) for some sample configurations (Fukuoka et al, 1989). DSC method involves heating or cooling of a sample and reference and the measurement of the differential heat flow (power) between them with respect to temperature.

Hains described two principal approaches of DSC measurements (Hains et al, 1995). Heat flux DSC which involves the measurement of the temperature differential between the sample and reference and the subsequent calculation of the equivalent heat flow according to Eq.1.3:

$$\Delta Q = \frac{(T_s - T_r)}{R_t} \dots\dots\dots \text{Eq. 1.3}$$

where Q is heat,  $R_t$  is the thermal resistance of the cell and  $T_s$  and  $T_r$  are the sample and reference temperatures. Hence at a given scanning rate the heat flow

is displayed against temperature. Power compensation DSC involves the application and measurement of a compensatory power input (P) to one or other pan in order to maintain both at the same program temperature.

Thus, DSC measurements provide qualitative and quantitative information as a function of time and temperature regarding transitions in materials that involve endothermic or exothermic processes, or changes in heat capacity. Some of the advantages contributing to the widespread usage of DSC are the ease of sample preparation, the applicability to both solids and liquids, fast analysis time and wide temperature range.

On the other hand, DSC does have some important limitations. It is often difficult to interpret the heat flow from a DSC experiment if multiple processes are involved over the same temperature range.

In a single component material, different types of transitions can overlap such as, for example, melting and recrystallisation in a semi-crystalline material. In a multicomponent material, transitions of the different compounds can overlap. Moreover it is not always straightforward to identify the nature of a transition, an enthalpic relaxation peak superimposed on the heat capacity variation at the glass transition temperature can be so large that the transition is confused with a melting transition, this renders identification and quantification of  $T_g$  extremely difficult (Verdonck et al, 1999). In addition to the above, there are also a number of practical considerations associated with the measurement of glass transitions using DSC. The baseline shifts may be small, particularly for strong glasses, rendering differentiation from baseline noise a non-trivial problem. However, a true glass transition will be reproducible and should be seen on both heating and cooling. Furthermore, it is essential that adequate baseline calibration is performed to ensure as flat a baseline as possible.

Craig et al. (1999-a) mentioned that the relaxation endotherm arises as a result of one of two processes. Firstly, it may reflect a mismatch in the rate of cooling and subsequent heating of the sample. When cooling is slow the glass that forms has

long relaxation times 'frozen in'. Subsequently, when this material is heated quickly, with a faster rate through the glass transition than was the case on cooling, the relaxation times are slow with reference to the heating rate, thereby producing an overshoot in the enthalpy curve. In other words, the molecules within the glass cannot achieve the motion required for the glass transition within the time scale of the heating rate and the glass briefly superheats (Wunderlich et al, 1990). Once the relaxation times lower to the order of the heating rate the superheated glass reverts quickly towards the liquid line in the enthalpy curve. This overshoot and subsequent recovery in the enthalpy curve produces the characteristic endothermic peak in the  $\Delta C_p$  (or power) curve.

The second reason for the appearance of the endothermic relaxation is that because glasses are not in an equilibrium state. They can relax over time, thereby decreasing the enthalpy and volume of the material and increasing the structural relaxation time. Consequently, such annealing also produces a relaxation endotherm at the glass transition for the same reasons as above, the magnitude of which may be used to calculate relaxation times for the sample (Hancock et al, 1995).

To increase the sensitivity (i.e. signal-to-noise) for the detection of a weak transition, either the sample mass or the scan rate can be increased. For obtaining a better resolution in separating transitions occurring at close temperatures, either smaller samples are used or the scan rate is lowered. Thus, an increased sensitivity is at the expense of the resolution and vice versa.

Besides, the detection of weak transitions is also strongly influenced by the baseline curvature and stability. The determination of a small jump in heat capacity for example, is much more difficult when it is superimposed on a curved baseline than if the baseline is straight. Often the baseline is not straight due to, for example, moisture evaporation from the sample, variations in thermal contact between the sample and the DSC pans during the scan and the overall baseline characteristics of the specific DSC cell.

Some quantities such as the absolute value of a materials heat capacity and its thermal conductivity cannot be determined straightforwardly with DSC and require multiple experiments. Moreover, the heat capacity cannot be determined in an isothermal experiment with DSC.

Modulated Temperature DSC (MTDSC) overcomes these limitations and therefore provides new insight into the materials properties (Royall et al, 1998). A number of instruments are available under the category of MTDSC. The development of MTDSC has removed or reduced some of the difficulties associated with characterising glass transitions (Giron et al. 1998, Craig et al. 1999-c). This technique involves the application of a sinusoidal heating signal superimposed on the linear temperature ramp. Hence, information may be derived from both the sine wave response and the Fourier transformed total heat flow output (equivalent to conventional DSC) (Royall et al, 1988). The advantage of the technique is that changes in heat capacity (i.e. glass transitions) may be seen in isolation from other events, particularly relaxation endotherms, with a considerably enhanced signal-to-noise ratio (Hill et al, 1998).

In the MTDSC sample preparation conditions must be carefully controlled (and stated), particularly in terms of the choice of pans and level of residual moisture or other solvents, as changes to the sample either during or prior to analysis may have a profound influence on the measured  $T_g$ . An investigation by Hill et al. indicated that the measured  $T_g$  of spray dried lactose may vary by  $\sim 35^\circ\text{C}$  depending on pan type (Hill et al, 1998). This is due to the retention of water in hermetically sealed pans, which acts as a plasticizer, thereby reducing  $T_g$  compared to non-hermetically sealed or open pans from which water is lost during the heating run.

Glass transition temperature measurements are ideally performed in cooling rather than heating cycles, as in the former the sample starts from the equilibrium liquid state before entering the nonequilibrium glass, which is a reproducible route compared to starting from the glass in a heating cycle (Wunderlich et al, 1990). However, many pharmaceutical systems such as drugs and freeze dried systems

are heat sensitive and may not withstand cycling. Similarly, other systems are multi-component; hence heating through the  $T_g$  of one component may result in irreversible changes in the structure of the system as a whole. Consequently, most pharmaceutical studies have involved measuring  $T_g$  upon heating.

**Operating principle of MTDSC**

In MTDSC a sinusoidal modulation is overlaid on the linear ramp. As a result of the temperature modulation, the heating rate is no longer constant, but varies in a periodic (modulated) fashion. The average heating rate, corresponding to the rate for a conventional DSC experiment, is called the underlying heating rate. The modulated heating rate varies between a minimum and a maximum value; these are determined by the value of the underlying heating rate, the period (or frequency) and the amplitude of the superimposed temperature wave. Depending on the combination of these three parameters, the minimum modulated heating rate is positive (heat-only), zero (heat-isothermal), or negative (heat-cool).

The resultant heat flow between the sample and reference in a DSC or MTDSC experiment is described by the general Eq.1.4:

$$\frac{dQ}{dt} = C_p b + f(T, t) \dots\dots\dots \text{Eq. 1.4}$$

Where  $dQ/dt$  is the resultant heat flow,  $C_p$  is the heat capacity of the sample,  $b$  is the rate of temperature change ( $dT/dt$ ) and  $f(T,t)$  is heat flow from kinetic processes. For an MTDSC experiment, the resultant heat flow is periodically varying and termed the modulated heat flow.

From the general equation, it follows that the resultant heat flow is composed of two components: one component is a function of the samples heat capacity and rate of temperature change, and the other is a function of absolute temperature and time. In conventional DSC only the sum of the two components is determined and is called the total heat flow. In MTDSC the total heat flow and the two individual components can be distinguished as the heat capacity component ( $C_p b$ )

or reversing heat flow and the kinetic component ( $f(T,t)$ ) or non-reversing heat flow (Cser et al, 1997).

All of these signals are calculated from three measured inputs: time, modulated temperature, and modulated heat flow. The total heat flow in MTDSC is calculated from the average of the modulated heat flow; this average corresponds to the total heat flow in a conventional DSC experiment at the same underlying heating rate. In conventional DSC,  $C_p$  can be calculated from the difference in heat flow between two runs on an identical sample at two different heating rates. In MTDSC,  $C_p$  can be determined in a single experiment because of the periodical variation in heating rate: the heat capacity is calculated from the ratio of the modulated heat flow amplitude and the modulated heating rate amplitude by discrete Fourier transformation. The reversing heat flow is then calculated by multiplication of  $C_p$  with the negative heating rate. The kinetic component or non-reversing heat flow is the arithmetic difference between the total heat flow and the reversing heat flow.

### **Solution calorimetry**

Solution calorimetry has also been used to a small extent to assess powder crystallinity. This approach works on the basis that the heat of solution will be different for the crystalline and the amorphous states of a sample. Previous studies by Ward and Shultz (1995) showed clear differences in the heat of solution of micronised and crystalline salbutamol sulphate samples. These differences were attributed to changes in surface energy.

Thompson et al. (1994) have shown that solution calorimetry can be an effective way of differentiating between drug samples with different degrees of crystallinity. They also showed good agreement between heat of solution and thermal activity measured in an isothermal microcalorimeter over the range 0 – 100% crystallinity. Salvetti et al. (1996) have demonstrated that different physical forms of carbohydrates can be differentiated by measuring heat of solution. Pikal et al. (1978) used heat of solution measurements to correlate the extent of crystallinity to the chemical stability of antibiotics.



### **Microcalorimetry**

Microcalorimetry can be used in a non-isothermal mode to detect glass transition events and secondary transitions in amorphous pharmaceutical solids. It has also been used in several studies to detect physical and chemical instabilities in formulations containing amorphous drugs or excipients (Heidemann et al. 1991; Buckton et al. 1995-c).

A further innovation has been the introduction for microthermal analysis, a technique that combines the principles of atomic force microscopy (AFM) with calorimetry. In essence the tip of the AFM is replaced by a Wollaton wire whereby the platinum sheath is etched away to leave a high resistance tip. On application of a voltage the tip heats in a controlled manner, thereby allowing one to perform thermal analysis on highly specific regions of a sample. For example, one may land the tip on a specific region of a complex material and heat, usually at very rapid rates in the region of 10-20°C/sec. In this manner specific components may be identified and characterised, such as the mixed amorphous and crystalline regions. By landing the tip on these different regions, it becomes possible to identify the material by the temperature at which the material either softens if glassy or melts if crystalline (craig et el, 2002).

Other calorimetric approaches include the gas flow, this approach uses a calorimeter cell in which the powder is housed, which has been constructed to allow a constant flow of humid air. The humidity can be altered in steps or as a ramp. As the powder crystallises, there will be a clear exotherm and also an endotherm associated with the water loss. A number of studies on the use of these gas flow cells in calorimeters have been published, e.g. (Sheridan et al. 1995; Puddipeddi et al. 1996; and Sokoloski et al. 1997).

### **Vapour Sorption Techniques**

Bulk analytical techniques, such as differential scanning calorimetry, powder X-ray diffraction and IR spectra, will measure the properties of the sample as a whole. The detection limits for amorphous content with such techniques can vary, but will generally have a lower cut off of 5–10% (Gerhardt et al, 1994). This detection limit

is related to the fact that these techniques measure the entire sample; thus, the amorphous content becomes a small part of the total signal, and consequently it is difficult to detect with confidence. It may be more appropriate to preferentially investigate the properties of the powder surface only, where amorphous material may predominate.

A powerful way of investigating surface properties is by using the vapour sorption studies, which preferentially probe amorphous (over crystalline) regions due to absorption behavior. As the vapour sorption by amorphous and crystalline pharmaceutical materials is usually quite different, thus it can be used to precisely distinguish between them (Zografi et al, 1994). Typically, crystalline materials adsorb vapours in small quantities at their surfaces in contrast amorphous materials absorb vapours in relatively large amounts. Rubbery amorphous materials usually sorb considerably greater quantities of vapour than their respective glasses, and this phenomenon can be used to identify the state of an amorphous material (Oksanen et al, 1990).

Hancock et al. (1997) described water sorption studies as the preferred means of studying pharmaceutical systems containing low levels of amorphous material. Water sorption has been used in the study of many amorphous and partially amorphous powders. A few examples in the pharmaceutical literature include sucrose by (Gerhardt et al, 1994); Lactose by (Buckton et al, 1996); raffinose by (Gerhardt et al, 1995); and salbutamol sulphate by (Ward et al, 1995).

Another vapour sorption technique is the inverse phase gas chromatography (IGC), in which the powder is packed in a column and known liquid vapours (usually at infinite dilution in a carrier) are passed into probes (Ticehurst et al, 1994). It is possible to assess the surface nature of the material in the column. In keeping with the calorimetric and gravimetric techniques, it is to be expected that this vapour sorption approach will also be able to detect differences in samples due to small amount of amorphous content.

In summary, there are many precise and accurate methods suitable for studying and characterising amorphous pharmaceutical materials in all their configurations, including final dosage forms. As with any scientific method, the use of multiple complimentary techniques which measure the properties most relevant to the problem or material under consideration is preferred. The most notable difference between the techniques described is in their ability to quantify the amount of order or disorder in partially amorphous systems, and in their ability to monitor molecular level processes over a wide range of temperatures (ideally above and below  $T_g$ ), (Buckton et al, 1998-b).

#### **1.1.5.8 Physico-mechanical factors which influence the behaviour of amorphous systems**

In the processing and handling of solid pharmaceuticals there are a number of situations where rheological or mechanical properties are critical for product manufacturability, stability, and performance. Most crystalline materials tend to exhibit high levels of elasticity and brittleness upon exposure to an external stress. In contrast, molecules in the amorphous state tend to exhibit varying degrees of viscoelasticity, depending on their temperature in relation to the  $T_g$ .

Such viscoelastic behavior provides solids with the ability to flow under conditions of mechanical stress and to provide a number of important excipient functionalities. Relief of mechanical stresses through flow would appear to be important in creating tablet bonds after compression of powders (Elamin et al, 1994), and in preventing mechanical failure of polymeric film coats on tablets because of stress relaxation (Sinko et al, 1991).

The use of plasticizers, including water, to lower the  $T_g$  of various cellulose and acrylic polymers utilized in film coating is based on this principle, as is the use of spray dried lactose (about 15% amorphous content), or microcrystalline cellulose (about 30% amorphous content) as direct compression tableting excipients. For example, a critical level of about 4–6% water provides a significant change in the viscoelastic properties of microcrystalline cellulose (Amidon et al, 1995), and is at a level below which direct compaction properties are lost.

### **Chemical reactivity**

Chemical degradation of drugs in the solid state, particularly at elevated temperatures and relative humidities, is a fairly common occurrence with drugs exhibiting susceptibility for degradation when in solution (Byrn et al, 1982). In the amorphous state, the reacting molecules have sufficient free volume and molecular mobility to chemically react. One would expect a comparison of reaction rates of crystalline and amorphous forms of a drug under otherwise identical conditions to reveal greater rates with the amorphous forms than with the crystalline forms, and this has been shown to be the case for a number of systems (Carstensen et al, 1993).

### **Stability and manufactureability**

Polymorphic forms of a pharmaceutical ingredient may have different physical and solid state chemical (reactivity) properties (Byrn et al, 1995). The most stable polymorphic form of a drug substance is often used because it has the lowest potential for conversion from one polymorphic form to another, while the metastable form may be used to enhance bioavailability. Thermodynamic activity and solubility provide a definitive measure of relative polymorphic stability under defined conditions of temperature and pressure.

The relative polymorphic stability may be determined by the examination of the relative apparent solubility of supersaturated solutions of polymorphic pairs. Since the rate of conversion to the more stable form is often rapid when mediated by the solution phase, the less stable polymorph with the greater apparent solubility dissolves, while the more stable polymorph with the lower apparent solubility crystallises out.

Solid-state reactions include solid-state phase transformations, dehydration /desolvation processes and chemical reactions. One polymorph may convert to another during manufacturing and storage, particularly when a metastable form is used.

Since an amorphous form is thermodynamically less stable than any crystalline form, inadvertent crystallisation from an amorphous drug substance may occur. As

a consequence of the higher mobility and the ability to interact with moisture, amorphous drug substances are also more likely to undergo solid-state reactions. In addition, phase conversions of drug substances are possible when exposed to a range of manufacturing processes (Brittain et al, 1999). Milling and micronisation operations may result in polymorphic form conversion of a drug substance (Ward et al, 1995). In the case of wet granulation processes, where the usual solvents are aqueous, one may encounter a variety of transformations between anhydrous and hydrates, or between different hydrates. Spray-drying processes have been shown to produce amorphous drug substances and specially proteins (Pikal et al, 1993).

## **1.2 CEFUROXIME AXETIL**

### **1.2.1 Activity**

Cefuroxime is a second generation cephalosporin antibiotic, which has a broad spectrum of activity against both gram-positive and gram-negative microorganisms. It is generally more active against gram-negative bacteria than first generation cephalosporins, but has a narrower activity in this aspect than the third generation cephalosporins.

Cefuroxime exerts its bactericidal effect by binding to an enzyme or enzymes referred to as penicillin binding proteins (PBPs), involved in bacterial cell wall synthesis. This binding results in inhibition of bacterial cell wall synthesis and subsequent cell death. Specifically, it shows high affinity for PBP3, a primary target for cefuroxime in gram negative organisms such as E.coli., and it has bactericidal activity against a wide range of common pathogens, including many beta-lactamase-producing strains. It is stable to many bacterial beta-lactamases, especially plasmid-mediated enzymes that are commonly found in enterobacteriaceae (De Sommers et al, 1984).

### **1.2.2 Bioavailability**

The compounds use is limited to injectable administration because it is poorly absorbed from the gastro-intestinal tract following oral dosing, where sodium salt of cefuroxime after oral administration is absorbed in less than 1% of applied dose (Ridgway et al, 1991).

Higher bioavailability values are obtained only with cephalosporins that are taken up by carrier systems, or when the polarity of the carboxylic acid group in the 4 position is reduced by esterification (Stoeckel et al, 1995). Therapeutically active drug can, however, be obtained only if the absorbed prodrug ester is readily converted back to the active drug. The success of the prodrug ester approach depends vitally on the solubility and lipophilicity of the prodrug ester as well as its stability to chemical and enzymatic ester cleavage. Crisp et al. (1989) described the synthesis of the 1-acetoxyethyl ester of cefuroxime, now referred to as cefuroxime axetil (CA).

Cefuroxime axetil is a prodrug of cefuroxime which can be orally administered, thereby permitting more convenient and wider therapeutic use of cefuroxime. Esterification of the carboxyl group of cefuroxime renders the molecule more lipophilic and, in contrast to the parent substance, a significant proportion is absorbed after administration.

Chemically, cefuroxime axetil, is (RS)-1-hydroxyethyl (6R, 7R)-7-[2-(2furyl) glyoxylamido]-3-(hydroxymethyl)-8-oxo-5-thia-1-azabicyclo[4.2.0]oct-2-ene-2-carboxylate, 7<sup>2</sup>-(Z)-(O-methyl-oxime), 1-acetate 3-carbamate. Its molecular formula is C<sub>20</sub>H<sub>22</sub>N<sub>4</sub>O<sub>10</sub>S, and it has a molecular weight of 510.48. The structural formula of CA is presented in Figure 1.2.

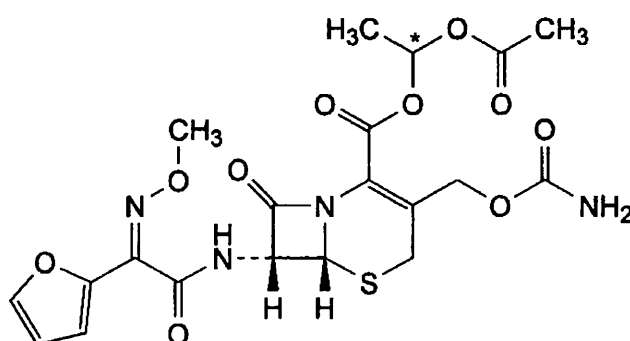


Figure 1.2: Structural formula of cefuroxime axetil

The major structural differences between cefuroxime and other commercially available cephalosporins is that cefuroxime contains a methoxyimino group at

position 7 on the beta – lactam ring and a carbamate group at position 3 on the ring. The methoxyimino group results in stability against hydrolysis by many beta-lactamases and the carbamate group results in metabolite stability.

Cephalosporin prodrug esters exhibit oral bioavailabilities of approximately 50%, after oral administration, CA is absorbed from the gastrointestinal tract and rapidly hydrolyzed by nonspecific esterases in the intestinal mucosa and blood to cefuroxime. Cefuroxime is subsequently distributed throughout the extracellular fluids. The axetil moiety is metabolized to acetaldehyde and acetic acid (Ginsburg et al, 1985).

Cefuroxime axetil suffers from being rapidly hydrolyzed in the intestine, leaving substantial unabsorbable cefuroxime. This premature hydrolysis in the intestine before absorption has been discussed as a possible reason for their incomplete bioavailability (Saab et al, 1988). Hydrolysis can proceed either by enzyme-catalyzed direct hydrolysis to the parent cephalosporin (Mosher et al, 1992), or via a reversible base-catalyzed isomerization yielding the  $\Delta^2$ -cephalosporin ester which is rapidly cleaved to give the biologically inactive  $\Delta^2$ -cephalosporin (Richter et al, 1990). Both pathways will remove some of the cephalosporin available for absorption. The result is incomplete bioavailability of the oral prodrug ester. On the other hand, direct hydrolysis to the non absorbable but biologically active cephalosporin in the gut lumen could affect the gut flora, causing undesirable intestinal side effects (Cullmann et al, 1995). Campbell et al. (1987) reported the isolation and partial characterisation of an esterase enzyme which is said to be responsible for converting CA to cefuroxime in the gut.

The ester portion of CA, namely the 1-acetoxyethyl group, contains an asymmetric carbon atom at the 1-position. Accordingly CA exists in the form of a mixture (mainly 1:1) of two diastereomers designated as *R* (1*R*, 6*R*, 7*R*) and *S* (1*S*, 6*R*, 7*R*). Little is known concerning the relative availability of cefuroxime from each isomeric form. Barrett et al. (1997) used a Caco-2 cell monolayer model to examine the possible stereo selectivity of absorption of CA. This was done by measuring the accumulation and epithelial transport rate in the apical to

basolateral direction of cefuroxime and CA, following application of a mixture or individual diastereomers. Cefuroxime appearance in the basolateral chamber was in the order of mixture > R > S following application of the prodrug. The accumulation of unchanged CA was higher for S than for R, irrespective of the form applied, i.e. individual diastereomer or the mixture. Such stereoselective differences in both absorption and/or hydrolysis may contribute to the observed oral bioavailability (30 – 50 %) of cefuroxime *in vivo* (Barrett et al, 1997).

Mosher et al. (1991) reported that the individual S-isomer of cefuroxime axetil is hydrolyzed in animals much more rapidly than the R-isomer. Accordingly, an R-isomer substantially free of the S-isomer was prepared. The selective administration of the R-isomer was reported by Mosher to cause a surprisingly greater bioavailability of cefuroxime. The latter was said to be readily absorbed in the stomach and intestine well before the esterase enzymes located there are able to hydrolyze the axetil portion of the molecule. Accordingly, oral administration of R-cefuroxime axetil was expected to result in good absorption of antibiotic from the stomach and gut, resulting in drug levels of cefuroxime in the blood sufficient for rapid and effective control and irradiation of the bacterial infection throughout the animal system (Mosher et al, 1991). Just as important, however, is the low incidence of hydrolysis in the intestine, and thus low concentration of cefuroxime as the free acid, which is essentially not absorbed from the gut, and the presence of which results in undesired intestinal irritations.

In concordance to this, Stoeckel et al. (1998) studied the compounds cefetamet pivoxil, cefuroxime axetil, and cefpodoxime proxetil. They found that there occurred a rapid hydrolytic cleavage to the biologically active  $\Delta^3$ -cephalosporin in the intestinal juice, without the concomitant formation of significant amounts of the  $\Delta^2$  isomers. Spontaneous base-catalyzed isomerization to the  $\Delta^2$  ester was significantly slower than hydrolytic cleavage to the  $\Delta^3$  acid. The isomerization process is, therefore, not efficient enough to compete with enzymatic ester cleavage. The incomplete bioavailability of the prodrug esters was related to the efficient enzymatic hydrolysis and not to the  $\Delta^3$  to  $\Delta^2$  isomerization and spontaneous hydrolysis of  $\Delta^2$  esters.



A further relevant observation by Stoeckel et al. is the high stereoselectivity of the enzymatic cleavage reaction. With cefuroxime axetil and cefpodoxime proxetil, both as diastereoisomer mixtures, the S diastereoisomer was hydrolyzed faster than the R, by factors of 2.5 and 5.5, respectively (Stoeckel et al, 1998). Thus, by using the most stable diastereoisomer of the prodrug ester instead of a mixture, higher bioavailabilities can be achieved. Furthermore, elimination of the more rapidly hydrolyzed isomer should reduce the amount of biologically active cephalosporin formed in the gut, leading to improved intestinal tolerability.

Balaguer et al. (1997) studied the intestinal transport of CA in rats. Studies were performed using three CA solutions (11.8, 118 and 200  $\mu\text{M}$ ) in three selected intestinal segments, and one CA solution (118 $\mu\text{M}$ ) in colon of anaesthetized rats. First-order absorption rate pseudo constants,  $k_{ap}$  and effective permeability coefficients,  $P_{eff}$ , were calculated in each set. Absorption of CA was apparently described as a carrier-mediated transport, which obeys Michaelis-Menten and first order kinetics in the proximal segment of the small intestine, and a passive diffusion mechanism in the mean and distal segments. *In situ* intestinal absorption of CA in the proximal segment of the rat, in the presence of variable concentrations of cefadroxil has been also investigated by Balaguer (1997), in order to examine the inhibitory effect of cefadroxil on CA transport. The data suggested that both compounds shared the same intestinal carrier.

As a requirement in the official compendia (USP, BP and JP), CA has been specified as a diastereoisomer of A and B (R and S) of which A should constitute 48 – 55% of the mixture.

### 1.2.3 Physical Forms

It is reported in the literature that CA exists in its amorphous (CAA) and crystalline (CAC) forms. Oszczapowicz et al. (1995) reported that CAC does not exhibit adequate bioavailability upon oral administration. The amorphous form of CA which has higher bioavailability had been prepared by Crisp et al. (1985), as essentially free from the crystalline form. Different processes for preparation of amorphous cefuroxime axetil were reported in the literature, these include spray drying (Crisp et al, 1989) and recovering of CA by drying (Handa et al, 2002).

It was reported by Oszczapowicz et al. (1995) ; Woo et al. ( 2000) ; Guk et al. (2002) that CA shows polymorphism of three forms detected by DSC. Sasinoswka et al. (1995) reported that CA concentration after oral administration to rats depends to a considerable degree on the form as well as on the particle size.

#### **1.2.4 Stability**

Cefuroxime axetil is a relatively stable compound under normal ambient conditions. Fabre et al. (1993) studied the effect of light on CA, where the photoisomerization kinetics of aqueous solutions of CA under irradiation at 254 nm was studied by HPLC. They reported that the overall degradation is the result of a competition between the isomerization of the alkoxyimino group to  $\Delta 2$  isomer and the photolysis of the  $\beta$ -lactam ring. The two diastereomers were found to react at different rates. That was true not only for the photoisomerization step but also for ground-state hydrolysis in alkaline conditions. Photoisomerization of the alkoxyimino group was also observed for the anti isomer of CA and for some of its degradation products. Results of the study indicated that in comparison to the other cephalosporins, bearing the alkoxyimino group, CA was most sensitive under irradiation at 254 nm.

Stoeckel et al. (1996) compared the levels of degradation of cefetamet pivoxil (CT), CA and cefpodoxime proxetil (CD) in 0.6 M phosphate buffer (pH 7.4), and human intestinal juice (pH 7.4) at 37°C over 24 h. Significant differences in the time courses of degradation and in the patterns of degradation products were observed. The relative proportions of the  $\Delta 2$ - and  $\Delta 3$ -cephalosporins were roughly reversed in the two incubation media. In phosphate buffer, the major degradation product was  $\Delta 2$ -cephalosporin while in the intestinal juices it was  $\Delta 3$ -cephalosporin. Generally, the degradation of the prodrug esters progressed faster in intestinal juice than in phosphate buffer. The two diastereoisomers of CA and CD degraded at different rates in intestinal juice.

### **1.2.5 Pharmaceutical Formulations**

Cefuroxime axetil is formulated into tablets and dry suspension dosage forms. Ceftin<sup>®</sup> tablets are administered for the treatment of patients with mild to moderate infections caused by susceptible strains of the designated microorganisms.

Ceftin<sup>®</sup> for oral suspension is administered for the treatment of pediatric patients from 3 months to 12 years of age with mild to moderate infections caused by susceptible strains of the designated microorganisms in the conditions of pharyngitis/tonsillitis, acute bacterial otitis media, and impetigo.

Ceftin<sup>®</sup> for oral suspension was found not to be bioequivalent to Ceftin<sup>®</sup> tablets when tested on healthy adults. Thus, the tablet dosage forms and the powder for oral suspension formulations are not substitutable on a mg/mg basis. The area under the curve for the suspension averaged 91% of that for the tablet, and the peak plasma concentration for the suspension averaged 71% of the peak plasma concentration of the tablets. The safety and effectiveness of both the tablet and oral suspension formulations had to be established therefore in separate clinical trials (Finn et al, 1987).

Absorption of the tablet is greater when taken after food, where the absolute bioavailability increases from 37% to 52% (Finn et al. 1987; Donn et al. 1994). Cefuroxime axetil has an extremely bitter taste which is long lasting and which cannot be adequately masked by the addition of sweeteners and flavors to conventional granules presentations. Tablets are film coated to reduce the bitter taste of the drug.

The tablet core was formulated such that it disintegrates immediately following rupture of the film coat (Deutsch et al, 1990-a). This was achieved by using disintegrants, which provide the desired disintegration properties. The tablet core conveniently contains a disintegrant at high concentrations of 4 to 10% by weight.

Another problem arises from the tendency of CA both in the crystalline and the amorphous form to form a gelatinous mass when in contact with the aqueous media. This gelling effect is temperature dependent, and occurs at temperatures at about 37°C (James et al, 1989). Such gelling would lead to poor dissolution of CA, and hence poor absorption from the gastrointestinal tract, i.e. low bioavailability. In the case of granule formulations, the use of particles of small diameter and high surface area is desirable to avoid gelling (James et al, 1989).

In the formulation of CA powder for dry suspension, it is highly important to avoid the release of the drug into any liquid suspension prior to administration. This has been achieved by formulating CA as lipid coated particles, the coat of which has a limited permeability to water and remains integral (James et al, 1989).

The integral lipid coat has a melting point of 45 – 60°C and is substantially insoluble in water, but readily dispersed or dissolved in gastro-intestinal fluid. The formulated coated particles, while not releasing the bitter CA in the wet environment of the mouth, break down upon contact with gastro-intestinal fluid, thus allowing rapid dispersion and dissolution in the gastro-intestinal tract.

### **1.3 FORMATION OF TASTE MASKED API PARTICLES**

#### **1.3.1 Taste masking approaches**

For ease and safety of administration, most drugs are formulated as tablets or capsules for oral administration. However, children and the elderly often experience difficulty in swallowing solid oral dosage forms. For these patients, drugs are commonly provided in liquid dosage forms such as solutions, emulsions and suspensions. These dosage forms usually permit perceptible exposure of the active drug ingredient to the taste buds, which can be a problem when the drugs have an unpleasant taste or are extremely bitter.

Conventional taste masking techniques such as the use of sweeteners, and flavoring agents are often unsuccessful in masking the taste of highly bitter drugs and other techniques have been and continue to be exploited for the effective taste

masking of such drugs. Extremely bitter drugs, like, quinine, ciprofloxacin, clarithromycin and cefuroxime axetil have been formulated as a fairly acceptable range of products even for pediatric use.

Palatability of oral suspensions is important and may be a substantial factor in determining compliance in young pediatric patients. Dagan et al. (1994) studied acceptance and compliance of such oral antibiotic suspensions. During a 4-month period, lists of children receiving oral antibiotic suspensions were obtained from three major pediatric clinics, and parents were contacted 10 to 14 days after initiation of therapy, at which time information on age, sex, main disease, prescribed drugs and duration of treatment was obtained.

Information regarding acceptance, side effects and compliance were obtained from 11 questions with graded scores. In the study 546 children received one of the following drugs: amoxicillin (n = 222); cefaclor (n = 142); cefuroxime axetil (n = 107); trimethoprim / sulfamethoxazole (n = 75). More than 50% of each group had acute otitis media. The result of the study was that 73% of the cefaclor group reported acceptance of the drug with a pleasurable experience versus 60, 55 and 20% for amoxicillin, trimethoprim / sulfamethoxazole and cefuroxime axetil respectively.

These data demonstrated that marked variations exist in acceptance and compliance of oral antibiotic suspensions with children. The findings influenced the choice of drugs for young pediatric patients with common infections (Dagon et al, 1994).

Taste sensation is presented by taste transduction, which is how the taste cells detect the presence of pleasant-tasting nutrients and bitter-tasting toxins, and store this information in the taste cell. Taste transduction involves the interaction of molecules with taste receptor cells, which reside in specialized structures known as taste buds (Margolskee et al, 1993). Taste buds are located in the papillae of the tongue and are the end organ of taste. The function of taste buds is to relay information to the CNS on the positive (nutrient-rich) and negative (bitter-poison) content of foods. Recent advances in molecular biology and biochemistry of taste

have shown that each taste modality affects receptor cells through a distinct mechanism. The transduction of most bitter and sweet compounds is mediated via G protein coupled receptors (GPCRs), while salty and sour tastes depend on ion channels (McLaughlin et al, 1992).

The G proteins are a class of heterotrimeric proteins that amplify signals generated at the cell surface by ligand-activated receptors. More than 50% of bitter substances activate one or more taste receptors, which catalyze the activation of the taste specific G protein gustducin. Gustducin is homologous to transducin, the G protein of the visual system. Gustducin and transducin have been localized to taste buds and co-localize with taste GPCRs (McLaughlin et al, 1992; 1995).

When gustducin is activated, it dissociates into alpha and beta-gamma subunits. Alpha-gustducin activates intracellular phosphodiesterases leading to decreased cAMP levels (Birnbaumer et al, 1990). Lower cAMP concentrations cause activation of ion channels resulting in a change in the taste cell potential. The beta-gamma subunits are thought to activate phospholipase C, which can generate the second messengers IP3 and DAG. IP3 can then mobilize intracellular stores of calcium modulating the taste cell membrane potential. This complex cascade of biochemical events results in taste cells sending a signal to the brain that is interpreted as bitter and unpleasant.

Most of the non-gustducin mediated bitter substances are thought to traverse the taste cell membrane and directly modulate downstream signal transduction enzymes or ion channels. The bitter taste of caffeine is transduced by inhibition of the taste cell phosphodiesterase (PDE) (Ming et al, 1999).

There is a wealth of information about formulations and processes, including materials and equipment for producing active pharmaceutical ingredient (API) particles designed for taste masking applications. Of these, a review of taste masking in liquid dosage forms was published (Sun et al, 1998), which covered the sensory approaches, chemical approaches, complexation/adsorption approaches and barrier approaches.

Other reviews written by Roy et al. (1994 ; 1997) covered specific formulations and ingredients used for producing taste masked API particles including flavors, sweeteners, amino acids, lipids, lecithin-like substances, surfactants, hydrophilic substances, and polymers/resins (including ion exchange). These studies presented a comprehensive review of the taste masking literature up to the early 1990s.

A review on encapsulation technology focusing on drug delivery applications had been published by Sparks et al. (1999). It comprehensively covered important characteristics of the core particle, selection and formulation of coating materials, equipment and coating procedures, scale up and problems related to microencapsulation.

Gibbs et al. (1999) review on encapsulation in the food industry provided an alternative perspective on materials, processes and equipment used for encapsulation of liquids and solids for purposes of controlled release, stabilisation, physical separation of ingredients and masking of taste and odor.

Tyle et al. (1990) addressed an important issue related to solid oral application of taste masked API through encapsulation. Namely, sensory attributes of particulates including texture and palatability. Although they specifically addressed size, shape and hardness of particles in suspension, the results were said to be applied to solid oral forms as well. The results showed significant differences in sensory perception between different samples based on size, shape and hardness. Aside from particle size, the important discovery from this work is that other particle physical characteristics (shape and hardness) can also affect textural perceptions.

In general, in the pharmaceutical industry, taste-masking science covers physiological and physicochemical approaches to prevent active pharmaceutical ingredient (API) or drugs from interacting with taste buds; thereby eliminating or reducing negative sensory response.

Physiological approaches consist of inhibiting or modifying an API-mediated bitterness response by incorporating agents into a pharmaceutical formulation. Agents like sodium chloride (Breslin et al, 1997), phosphatidic acid, and peppermint flavor (Katsurugi et al, 1997) are known to inhibit bitterness of select API molecules via a mechanism that takes place at the bitterness receptor in the taste buds. Other approaches include the physical approach, presented by encapsulating the API with a coat or barrier material that physically separates the API from the water in saliva, the chemical approach, which is to complex or electrostatically bond the API with another chemical compound.

In the scientific literature, the above approaches were categorized into the following particle configurations: substrate, coated substrate, matrix particulate, drug resinate, microencapsulated API crystal, coated microencapsulated API crystal, and coated matrix particulate.

One challenge is to achieve acceptable human bioavailability while maintaining acceptable sensory attributes. When a barrier approach is used, poor API bioavailability can be averted by judicious selection of a barrier material having suitable properties that allows the API to dissolve in the stomach and intestine.

Another challenge when using a barrier is to prevent or minimize the barrier from becoming physically damaged during the compaction process. Since chewable and orally disintegrating tablets are compacted, the physical barrier material must withstand the stress and strain of the compaction process and chewing without significantly fracturing. Fracturing could be a major cause in API leaking through the barrier prematurely in the mouth, severely reducing the taste masking effectiveness.

Considering the substrate, some can be API crystals alone of which the physical and chemical properties directly relate to its taste masking processing. Ideally, a one step process is required to directly envelop an API crystal with a physical barrier. However, the morphology, crystal size distribution (CSD) and mechanical



strength of most API crystals preclude direct envelopment without an intermediate step to improve these properties.

Significant technological advances are being made to obtain the thermodynamically stable crystal form while simultaneously controlling the API morphology and CSD by employing molecular modeling techniques and novel crystallisation processes (Sridhar et al, 2000).

The shape and size most amenable to the envelopment process is a spheroid with a narrow size distribution. Spherical crystallisation techniques have been reported by Kawashima et al. (1989, 1991 and 1998); Pich et al. (1986); and Espitalier et al. (1997-a, b). These techniques are known as spherical crystal agglomeration (SCA) processing. The unique feature of this technique is that crystal growth and agglomeration occur simultaneously. By manipulation of the process variables, agglomerates are formed with desirable mechanical properties as well as a well-defined CSD and optimal particle morphology. Desirable mechanical properties include high fracture toughness and wearability in withstanding the high-shear forces that occur in typical particle coating processes (e.g. Wurster coating). The ideal CSD was a narrow distribution, with a nominal average particle size equal to 75 to 150 microns.

In the SCA methods, the API is dissolved in a solvent, and the API solution is added to a second anti-solvent which contains a third solvent, called a “bridging” liquid. The API precipitates into fine crystals, which agglomerate through the action of the capillary forces of the bridging liquid and the shear forces/hydrodynamics of the agitation system. Hasan et al. (2001) investigated the effect of bridging liquid composition and concentration on SCA of salicylic acid (SA), and studied the kinetics of SCA of SA through on-line particle size analysis. They concluded that bridging liquid composition and concentration significantly affected the size and shape of agglomerated particles.

The physical properties of the bridging liquid, i.e. solubility, interfacial tension and polarity, correlated with its ability to form SCA particles. Further, based on a shear-

dependent-model, bridging liquids with higher surface tensions produced larger crystal agglomerates, due to formation of stronger liquid bridges during agglomeration (Kawashima et al, 1998). Further, other techniques were developed for controlling and understanding API crystallisation. These included using molecular simulation, solute/solvent control of crystal morphology/crystal size distribution, and spherical crystallisation (Sridhar et al, 2000).

A substrate or core particle may also be a mixture of API with non-taste masking excipients, whose sole purpose is to be subsequently coated. Examples of the substrate particle configuration include: the formulation of spherical particles from theophylline, microcrystalline cellulose, using Glatt GPCG-1 (Pereira et al, 1997). The differences between raw materials in the formulation of the spherical particles and effects of increasing level of drug loading on their quality has also been studied.

For coated substrates the main example, related to this study, is applying a taste-masking layer to the very bitter tasting material ,cefuroxime axetil. James et al. (1989) reported that wax coating of cefuroxime axetil by using suitable lipids . The most common lipids include the high molecular weight ( $C_{10-30}$ ) straight chain saturated or unsaturated aliphatic acid, such as stearic acid or palmitic acid (as in Zinnat<sup>®</sup> commercial preparation). The triglyceride tested was a glyceryl ester of a high molecular weight ( $C_{10-30}$ ) aliphatic acid, such as glyceryl trilaurate or glyceryl trimyristate. The partially hydrogenated vegetable oil tested was cottonseed oil or soyabean oil. While the wax was beeswax or carnauba wax, and the high molecular weight ( $C_{10-30}$ ) straight chain aliphatic alcohol was stearyl alcohol or cetyl alcohol, or a mixture thereof .

Further advancement in the coating process was achieved by improvements in the methodology and apparatus used for coating or microencapsulating solid particles or viscous liquid droplets. This was found applicable to a wide range of particle sizes, and done by using gelatin and glutaraldehyde materials, and by applying microencapsulation process using a heated rotating disc equipment (Spark et al, 1987).

Mauger et al. (1998) used triglycerides in combination with a polymer as a coat for masking the taste of orally administered drugs. The triglyceride tested melt at body temperature, while the polymer was chosen to dissolve at a pH of 5.5. Upon oral administration, the coating remained intact during the brief transit in the mouth but then released the active upon reaching the gastric fluid of the stomach.

Another example of coated substrate particle configuration was undertaken by Holt et al. (2000). They used rapid release spacing layer between core and taste masking layer, which included effervescent agents, EC, poly vinyl pyrrolidone (PVP), and aminoalkyl methacrylate copolymer material. Fluid bed and a wurster were used for such purposes.

The matrix particulate is a mixture of API and taste masking excipients or agents, which may not be subsequently coated. Examples of the matrix particulate configuration include the preparation of clarithromycin with polyvinylacetyl diethyl aminoacetate (AEA) and sodium lauryl sulphate (SLS) (Shimano et al, 1995). The matrix was obtained by dispersion of the drug in AEA solution and spraying it into liquid droplets, followed by subsequent drying into spherical particles.

Another example of matrix particulate particle configuration is via the use of cation exchange resins, which have more effective ion exchange due to the nature of most actives. Ion exchange resin materials have been used with granulation/coating processes using an extruder, fluid bed, spray dryer, and rotary granulation equipments (Hiroshi et al, 1994).

A drug resinate is a drug/resin complex, formed when an ionizable drug reacts with a suitable ion exchange resin for the purpose to taste mask some APIs. Because the drug resinate is insoluble it has virtually no taste, so that even very bitter drugs are masked when converted into a drug resinate (Agarwal et al, 2000). With the correct selection of the ion exchange resin, the drug resinate can be made sufficiently stable such that it does not break down in the mouth, avoiding the unpleasant taste. However, when the drug resinate comes into contact with the gastrointestinal fluids, usually the acid of the stomach, the complex is broken down quickly and completely. The drug is released from the resinate directly into solution

and then absorbed in the usual way. The resin passes through the GI tract without being absorbed. Examples where this technique has been successfully demonstrated include chloroquine phosphate (Agarwal et al, 2000).

Mukherji et al. (2003) prepared a taste masked matrix comprising the process of dissolving the bitter tasting drug, a methacrylic acid copolymer, and a phthalate polymer in a suitable organic solvent, followed by the recovery of the said taste masked matrix from the solution by conventional methods. The optimal taste masking effect was found achieved at total polymer to drug ratio of at least 1:4.

Microencapsulation is the general technology for forming microcapsules, and is divided into two classes known as physical methods and chemical methods (Bakan et al, 1992). The physical methods include spray coating (Fluid bed coating) and wurster coating. These processes rely upon a bottom positioned nozzle spraying the coating material up into a fluidized bed of core particles.

Other physical methods include the annular jet technology, which relies upon two concentric jets (Bakan et al,1992). The innerjet contains the liquid core material, and the outer jet contains the liquid coating material, generally molten, that solidifies upon exiting the jet. This dual fluid stream breaks into droplets much as water does upon exiting the spray nozzle.

Spinning disk is another technique which relies upon a spinning disk and the simultaneous motion of core material and coating material exiting from that disk in droplet form.

In the spray cooling method, a molten matrix material containing minute droplets of the core materials is spray cooled.

Spray chilling process relies on spray-chilling the coat around an atomized core. The resulting capsules move countercurrent to a flow of tempered air and are collected in a large container below the spray nozzle.

The number of methods for chemical encapsulation is actually far less. Two methods are known as water-in-oil and oil-in-water. The oil-in-water process is known as complex coacervation.

A novel process for encapsulating water-insoluble or slightly water-soluble drug was based on to evaporating method in liquid vehicle developed by Morishita et al. (1973). This method provided a process for encapsulating various water-insoluble or slightly water-soluble medicaments, regardless of their physical properties. It is based on dissolving or dispersing a water-insoluble or slightly water-soluble medicament into a solution of a hydrophobic coating material in at least one organic solvent, poorly miscible with water. This was followed by dispersing the resulting solution or dispersion to form fine droplets in a vehicle, and then vapourizing the organic solvent. It was found that when two or more organic solvents are used in the admixture, more fine and excellent encapsulated particles are obtained (Morishita et al, 1973).

Microencapsulation of API crystals has been achieved by the application of a physical barrier directly onto an API crystalline solid to cover the vast majority of solid forms observed in the pharmaceutical industry. Examples of the microencapsulated API crystal particle configuration include microincapsulation of chloroquine diphosphate (CHD), using Eudragit<sup>®</sup> RS100, tetrahydrofuran (THF), cyclohexane, polyisobutylene (PIB) by non-solvent coacervation. Drug crystals were coacervated with Eudragit<sup>®</sup> RS100, using PIB as a well known anti-aggregation agent used during coacervation process (Ndesendo et al, 1996).

Microencapsulated API crystal and coated microencapsulated API crystal particle configurations were applied as taste-masked particles for a variety of dosage forms using EC and MacP, cellulose acetate phthalate (CAP), and hydroxypropylmethyl cellulose phthalate (HPMCP) materials, using phase separation process with fluid bed and microencapsulation tank (Phillip et al, 2001).

Coated substrates, coated matrix particulate and coated microencapsulated API crystal contain an additional coating layer, functioning as a physical barrier. The

coating layer usually consists of polymer, lipid, or carbohydrate chemical classes. An example of coated microencapsulated API crystal is clarithromycin which was first coacervated using gelatin and glutaraldehyde and then subsequently coated by a phase separation technique using methacrylate resins. Friend et al. (1992) concluded that application of the methacrylate resin using a fluid-bed spray process would probably be a better method to use based on the appearance of the coated microencapsulated product.

For simultaneous API crystal growth, agglomeration and encapsulation Cuna et al. (1996 ; 1997-a,b) reported the use of solvent evaporation and solvent extraction to co-crystallise drug and polymer. Mauger et al. (1998) described a pharmaceutical coating for taste masking oral medications which includes a unique combination of triglycerides and a polymer. The triglyceride mixture melts at body temperature and the copolymer causes the coating to dissolve upon reaching the acidic environment of the stomach.

A further flavor masking method for badly tasting pharmaceuticals, which is likewise based on the use of lipids was described as a method for flavor masking based on the embedding of the active ingredient in a mixture of lipids (Paradissis et al, 1988).

### **1.3.2 Evaluation of taste masked API particles**

The ultimate performance tests for taste masking API particles are to conduct human sensory and bioavailability studies. While these tests are pivotal and conclusive, they are costly and time-consuming. Several *in vitro* tests are usually performed prior to the human confirmatory testing (Reo et al, 2001).

Drug release testing can be performed to evaluate the sensory effectiveness and bioperformance. One example of a drug release test for sensory effectiveness has been reported by Shirai et al. (2000). The authors described mixing the processed API in a relatively small volume of water (10 ml) contained in a syringe.

The mixture is gently mixed for 30 seconds, filtered and assayed for API concentration. Bioperformance-indicating drug release tests are usually based on official compendial dissolution testing. Modifications to these tests are frequently implemented to account for drug solubility and particle size of the processed API.

Some common modifications include the chemical composition of the dissolution media and reducing the size of the dissolution basket opening size to prevent particles from escaping. Recently, a novel system has been developed to test *in vitro* taste masking effectiveness. The commercial instrument is called an electronic tongue and consists of several (five to seven) coated potentiometric probes that are immersed into a liquid containing dissolved solids (Reo et al, 2002).

It has been used to assist in optimizing the taste of liquid formulations and may have application to solid dosage forms. Potentiometric response data from all probes for active formulations and placebo formulations are compared using principal component analysis mapping. Formulations having the best taste most closely match the placebo on the map.

Visual assessments of processed API are probably the most common tests performed to determine how the formulation and/or process can be optimized to achieve the desired outcome. Optical microscopy is the oldest test and still prevalently used today. It is quick, easy and can be done during the process. Scanning electron microscopy (SEM) and environmental SEM (ESEM) are commonly used when fine detail of the process API surface is needed.

The most common technique to evaluate the location of the drug in a coated substrate is to combine (ESEM) with energy dispersive X-ray analysis (Gordon et al,1986). This technique can also be a very useful one in evaluation of the efficiency of taste masking of drugs by coating.

Energy dispersive X-ray analysis is limited to elements, if the drug contains an element that is not part of other chemical compounds in the formulation, then it is

highly useful for locating the drug to a resolution region of 3  $\mu\text{m}$  by 3  $\mu\text{m}$  (Gordon et al, 1986). However, when elemental analysis is not appropriate, ESEM can be combined with Time-of-Flight Secondary Ion Mass Spectrometry (TOF-SIMS) for determining drug location, (Patel et al. 2001; Belu et al. 2000).

The TOF-SIMS process involves bombarding a sample surface with a beam of primary ions. When the primary ions collide with atoms and molecules in the surface, they are emitted. Either the positive or negative ions are measured using a mass spectrometer. Some of the key features of TOF-SIMS are sub-micron resolution and parts per million sensitivity. TOF-SIMS can be used to produce a chemical image of a surface by scanning a defined region and recording a spectrum at each pixel within the scan, i.e, a chemical mapping of the surface can be accomplished.

Another imaging technique is Atomic Force Microscopy (AFM). The AFM is a high-resolution surface imaging and surface property mapping technique (Erlandsson et al, 2000). Samples can be studied neat or in a liquid environment. It can be used to detect domains (due to chemical structure) and therefore, location, of one polymer component of a polymer blend when the polymer blend is used as a barrier coating. This type of data could also provide insight to the compatibility of the polymer blend in situ. A related technology of AFM, called Scanning Thermal Microscopy, has enabled polymorphic forms of cimetidine to be identified in ultra small volume on the surface of a sample (Sanders et al, 2000).

## **1.4 ENHANCING DISSOLUTION AND BIOAVAILABILITY OF POORLY SOLUBLE DRUGS**

### **1.4.1 Approaches**

In recent years, an increasing number of active agents which possess low aqueous solubility have come through the discovery laboratories. However, oral delivery of such poorly water-soluble drugs often results in low bioavailability, since the rate-limiting step for absorption from the gastrointestinal tract is the dissolution rate. Several commercial products of these hydrophobic drugs are available, and



different methods had been applied trying to enhance *in vivo* performance. Some of which are described below.

#### **1.4.1.1 Size reduction**

Particle size reduction effectively increases the surface area to volume ratio, thereby increasing the dissolution rate in the GIT and promoting absorption of poorly soluble substances (Kawashima et al, 2001). Various technologies were used for particle size reduction, this include micronisation, nano-ionization and, most recently, supercritical fluid technology (Kerc et al, 1999), which deposits nanometer sized drug particles on a pharmaceutically acceptable support matrix. Particle size reduction must include a method for preventing aggregation, which commonly occurs after milling, and effectively negates any improvement in dissolution gained by particle size reduction.

A common way for reducing the particle size is the disruption of previously formed larger particles by milling techniques, such as jetmilling, milling in a pearl-ball-mill, or high-pressure homogenization (Parrot et al, 1990). However, these methods have several disadvantages resulting from the mechanical disruption process. The micronisation process using mills is inefficient, because of the high-energy input that can alter the surface properties as a thermodynamically activated surface is created. Even a small amount of activated material at the surface can affect the drug substance properties, such as the blending characteristics (Mackin et al, 2002) or flow properties (Feely et al, 1998). Example of this is when the partially amorphous surface recrystallises, leading to changes in the physical properties of the drug (Roberts et al, 1994), where the conversion of crystalline solid surfaces into partially amorphous solid surfaces leads to a dynamic nature of the micronised drug.

Thus, this surface will dominate the size reduced particles and the milled powder is characterised by their surface properties. In the case mentioned above the surface will show poor wetting properties, therefore, because of agglomeration, the increase in the dissolution rate is not as high as calculated from the increase in surface area.

Nanosuspensions are milled by high pressure homogenizers (Jacob et al, 2000). The high pressure used cause changes in the crystal structure, and as a result, the amorphous fraction in the particle increases.

Thus, milling affects several physical properties of the drug, such as powder flow, agglomeration behavior, or electrostatic behavior. Beside these effects, the chemical reactivity or degradation can also be affected (Shalaev et al, 2002). The particle size can also change during storage after micronisation because of stress relaxation processes (Joshi et al, 2002). Beside these problematic properties, a further disadvantage especially of jet-milling processes is a broad size distribution (Muller et al, 1996). On the other hand, because of abrasion, the product can be afflicted with metallic impurities that can affect the chemical stability as a result of catalytic activity.

Due to these disadvantages of milling processes, techniques have been developed that produce the drug directly in the optimal particle size. However, the preparation and stabilisation of small particles is not easy because of their tendency to grow. Because of the high surface that must be created, the established methods need high amounts of stabilising excipients leading to amorphous products.

The most important examples are the so-called hydrosols developed by Gaßmann et al (1994). Hydrosols are colloidal aqueous suspensions containing drug nanoparticles of poorly water soluble drugs for intravenous administration. They are prepared by a precipitation process as the drug solution is mixed with a relatively high volume of water (96-98% water after mixing) in the presence of stabilising agents such as poloxamer and modified gelatins, which act as short term stabilisers (Gaßmann et al, 1994). Hydrosols contain the drug in a particle size of approximately 200 nm and are thus suitable for parenteral application. An example is cyclosporine, which can be formed as a hydrosol in a ratio of drug to gelatin of 1 : 20.

#### **1.4.1.2 Using solid carriers**

Another approach of enhancing solubility was described by Mahesh et al. (2003), with the idea of using solid carriers. This includes a substrate and an encapsulation coat on the substrate. The encapsulation coat can include different combinations of pharmaceutical active ingredients, hydrophilic surfactant, lipophilic surfactants and triglycerides. The composition of the carrier improves the delivery of hydrophilic and hydrophobic drugs and offers potential advantages over micronised drugs, emulsions or solubilized formulations. Solid carriers can easily pass through the stomach, thus making the performance less prone to gastric emptying variability. Further, the problems of leakage and other disadvantages of liquid formulations are not present in solid carrier formulations (Mahesh et al, 2003).

#### **1.4.1.3 Salt formation**

Hanss et al. (2001) reported a method for improving the absorption of ionizable compound through the salt formation. Salts of poorly soluble compounds typically dissolve more quickly in the GIT, thus improving absorption, which is typically limited by the slow dissolution of the parent free acid or base compound. Limitations to this approach involve identifying a counter-ion that will yield a pharmaceutically acceptable salt. Additional salt requirements include the ability to prepare, in sufficient yield, a chemically stable, non or minimally hygroscopic product of sufficiently high melting point to withstand formulation processing.

#### **1.4.1.4 Prodrug formation**

This is a less frequently employed method for improving the solubility and involves attaching a solubilizing moiety to form a prodrug which is cleaved by an endogenous enzyme subsequent to absorption, thereby regenerating the active parent molecule. The added complexity of the prodrug development, which requires additional studies for verifying bioconversion and demonstrating lack of toxicity, has limited the application of this approach (Hanss et al, 2001).

#### **1.4.1.5 Stabilisation of amorphous forms of the drugs**

An infrequently used method for improving the bioavailability of poorly soluble compounds involves stabilising the drug in the amorphous, or high energy solid

state, thereby facilitating its dissolution relative to that of the stable crystalline form (Robinson et al, 1993).

Various stabilising methods have been reported, including the use of polymer excipients having high glass transition temperature ( $T_g$ ). Crystallisation of amorphous sucrose and indomethacin was inhibited by preparing solid dispersion with a small amount of polyvinylpyrrolidone (PVP) (Zografi et al, 1999). Similarly, addition of alginate inhibited the crystallisation of amorphous lactose prepared by spray drying (Takeuchi et al, 2000). The stabilising effect of these excipients was attributed to their antiplasticization effect as well as their ability to interact with sucrose, indomethacin, or lactose. Drug excipient interactions leading to the stabilisation of amorphous drugs have also been reported for the systems of excipients with a pyrrolidone ring (PVP and polyvinylpyrrolidone-co-vinyl acetate) and drugs with hydrogen donor groups (indomethacin, lacidipine, nifedipine, and tolbutamide) (Forster et al. 2001; Aso et al, 1995).

In this same aspect, crystallisation of acetaminophen (ACTA) in solid dispersions with PVP and polyacrylic acid (PAA) has been studied by Miyazaki et al. (2004) to determine the role of drug polymer interaction in the inhibition of crystallisation as well as the effect of moisture on the interaction.

Other examples of stabilising amorphous solids include: the stabilisation of labile biomolecules (e.g. proteins and peptides) through additives. The prevention of the crystallisation is achieved by maintaining the amorphous form within specification on the appropriate storage temperatures to achieve acceptable shelf life, and the prevention of chemical degradation and microbial growth through anti-oxidant, pH buffer, preservatives, etc.

Lyophilisation and spray drying are essential steps in the preparation of protein and peptide formulations (Pikal et al, 1994), and in the preservation of organisms (Crowe et al, 1998). Such treatments can be detrimental to these naturally hydrated species. It has been observed that the proteins, peptides and organisms can be effectively protected against freezing and drying when they are co-

processed with certain excipients, typically carbohydrates and derivatives (sucrose, trehalose, mannitol, sorbitol, etc) (Sun W. et al, 1998). Although the mechanism of stabilisation is not firmly established, it is thought to involve both vitrification and direct interactions.

Vitrification based stabilisation relies on the immobilization and isolation of labile substances in rigid glasses of inert stabiliser molecules. Vitrification is expected to reduce the potential for protein aggregation and diffusion of small molecules required to initiate hydrolysis, oxidation, etc (Lai et al, 1999). The general assessment of the vitrification hypothesis seems to be that vitrification is necessary but insufficient for stabilising labile substances and that direct interactions also are required (Crowe et al, 1998).

In vitrification based stabilisation strategies, the  $T_g$  provides a concrete guide to the selection of stabilisers and storage temperatures. By eliminating plasticizers (e.g. water) and introducing antiplasticizers, one increases  $T_g$  and reduces structural mobility. Shamblin et al. (1998, 2000) showed that antiplasticizers effectively reduce structural mobility in amorphous sucrose. A more sophisticated analysis takes into account of both  $T_g$  and fragility, using the "zero mobility" temperature  $T_0$  as the parameter for ranking the relative stability of potential formulations (Hatley et al, 1999).

Besides vitrification, direct drug excipient interactions are important for stabilisation (Crowe et al, 1998). An example of such interactions is the selective hydrogen bonding between stabilising excipients and the drug molecules. These interactions may resemble the way in which water molecules are integrated into the structures of proteins and peptides (the water replacement hypothesis).

A well developed concept is that conformational change of proteins during freeze-drying is generally detrimental and should be avoided (Carpenter et al, 1994). This is a sound strategy so long as the conformational change is irreversible. In the crystallisation of carbohydrates and other small molecule organics conformational changes upon solidification are common, but often reversible upon dissolution

(Bernstein et al, 1987). In such cases, conformational changes on freezing and drying would not be indicative of structural damage.

It is generally accepted that in order to act as stabilisers, an excipient must mix homogeneously with the drug to be stabilised (Pikal et al, 1994). However, certain excipients (e.g. mannitol) have strong tendency to crystallise, leading to phase separation and loss of stabilising powder. Crystallisation can also lead to the formation of slow dissolving particles, causing slow reconstitution of parenteral products. Despite potential crystallisation problems, excipients with strong tendency to crystallise can sometimes make suitable stabilisers. In the case of mannitol, the crystallisation tendency is compensated by a superior chemical stability against oxidation and hydrolysis in comparison to disaccharides. For example, mannitol is stable at low or high pH where disaccharides undergo hydrolysis. Amorphous sucrose can undergo acid-catalyzed inversion even at very low levels of residual water (Shalaev et al, 2000). In some cases, the “flaw” of mannitol as a poor glass former can be remedied by proteins and peptides themselves, which effectively inhibit crystallisation (Kim et al, 1998).

Molecular mobility that allows physical aging and crystallisation of glasses below  $T_g$  implies that  $T_g$  is unsatisfactory as an indicator for the temperature below which molecular motions cease for practical purposes (Yoshioka et al, 1994). If the parameter  $T_o$  represents the temperature at which the relaxation time goes to infinity (zero mobility), then  $T_o$  rather than  $T_g$  is to be used as a practical guide for selecting storage temperatures. For many fragile glasses,  $T_o$  is approximately 50 K below  $T_g$ . The  $T_g - 50$  K rule is an important reminder of the finite structural mobility below  $T_g$ . For strong materials,  $T_o$  will lie significantly below  $T_g - 50$  K (Hancock et al, 1997).

#### **1.4.1.6 Lipid matrix systems**

Other ways of enhancing dissolution and bioavailability include formulations which solubilize a drug in a lipid or water-miscible co-solvent matrix system. This can provide dramatic improvements in bioavailability by eliminating the need for pre-absorptive dissolution in the GIT (Muller et al, 2001). Due to their immiscibility with water, lipids can maintain a poorly soluble drug in solution, unlike water miscible

co-solvent systems, which often precipitate the drug following dilution in the predominantly aqueous GI fluids. Lipid systems can also be formulated to have self-emulsifying properties, which provides further enhancement to absorption by increasing the surface area of the lipid dispersion presented to the GIT (Muller et al, 2001).

#### **1.4.1.7 Inclusion complex formation**

Cyclodextrins, which are water-soluble molecules containing a hydrophobic pocket, have also been used to form a dissociable inclusion complex with a hydrophobic drug molecule. This resulted in an improvement in the water solubility and bioavailability for poorly water-soluble drugs. The application of this approach is limited by the ability of the cyclodextrin to form the inclusion complex, which is strongly dependent on the molecular characteristics of the drug molecule (Mura et al, 1999).

#### **1.4.1.8 Solid dispersions**

Another common approach to improve the dissolution rate of poorly water-soluble drugs, and, therefore, improved oral bioavailability is by formation of a solid dispersion with a water soluble rate enhancing polymer, such as polyethylene glycol (Chiou et al. 1971; Serajuddin et al. 2004). Typical methods for fabricating solid dispersions include solution methods (Mura et al. 1996 ; Doshi et al. 1997) and melt methods (Mura et al. 1996 ; 1999). These techniques are not readily scalable and have the disadvantages of solvent use and potential drug degradation at elevated temperatures. Broman et al. (2001) described a novel method to fabricate solid dispersions utilizing compression moulding, but this technique also utilized elevated temperature and a thermoplastic polymer.

In another study, cellulose excipients were used to form solid dispersions of enhanced dissolution. Example of this is the use of HPMC (K3L V Premium), by Mitechell et al. (2003), to enhance the rate of dissolution for naproxen, nifedipine and carbamazepine. Three different means of combining HPMC and drug were utilized: dry blending of drug and polymer to produce a simple physical mixture, and compacting the blends by either roller compaction or slugging with subsequent milling. Both the roller compaction and the slugging processes resulted in

enhanced dissolution rate for the poorly water-soluble drugs compared to the drug as received, and the corresponding physical mixture.

The roller compaction and slugging methods produced comparable rate and extent of drug dissolution. Dissolution enhancement by the compaction process was comparable when different types of HPMC, specifically K3LV Premium, E3LV Premium, and E5LV Premium, were used (Mitechell et al, 2003).

The mechanism for how the compaction/milling process yields enhanced dissolution properties was believed to be a microenvironment surfactant effect whereby HPMC dissolution creates a local surfactant concentration in the boundary layer surrounding the drug particles, providing a lower energy pathway for drug dissolution. The compaction processes are believed to be particularly effective at enhancing the rate of drug dissolution because the drug particles are maintained in direct contact with the HPMC particles during drug dissolution. This is in contrast with a physical mixture, where the drug and HPMC particles may quickly disperse and be separated in the dissolution medium.

It was also demonstrated that HPMC presence is critical to the dissolution enhancement mechanism. Samples of the drugs alone subjected to the same slugging and milling procedure did not exhibit faster drug dissolution. Rather, slugged and milled naproxen alone had a dissolution rate that was slower than the drug as received. The compaction and milling procedures did not alter the bulk thermal properties or the X-ray diffractograms of the drugs. Differences were observed between the endotherms for the drug powders compared to the HPMC/drug mixtures. However, in each case the endotherm was unchanged by the compaction and milling processes (Mitechell et al, 2003).

#### **1.4.2 Bioavailability Enhancers**

Bioavailability of drugs is affected by many factors, such factors include the nature of the form of the drug, the physical state, particle size and surface area, presence or absence of adjuvants with the drug, type of dosage form in which the drug is



administered, and pharmaceutical processes used to make the dosage form (Cadwallader et al, 1971).

Manipulations of many of these parameters have been reported in the literature as effective means for increasing drug absorption and bioavailability. As regards to the physical state of the drug, increasing bioavailability of digoxin was achieved by administering the drug in capsule form (Crseswell et al, 1978). Blume et al. (1983) prepared special granular bioavailable formulations of active ingredients, particularly Triamterene and Hydrochlorothiazide. Crisp et al. (1985) reported an amorphous form of cefuroxime axetil with improved bioavailability.

With respect to the use of adjuvants, the use of polyglycerol esters of unsaturated fatty acids enhanced solubility of active drugs (Kaushal et al, 2004). Brickel et al. (1984) reported the use of acid salts of the drug to enhance bioavailability of dipyridamole. Dhanaraj et al. (1998) reported the use of cyclodextrin to enhance the bioavailability of griseofulvin.

Surfactants have also often been used to enhance bioavailability. Examples include the the use of water-soluble polymers and wetting agents to enhance solubility of drugs (Kawata et al, 1983). Tsuji et al. (1974) reported Penicillin prodrugs as having enhanced bioavailability. Ther et al. (1971) discussed the dependence of intestinal drug absorption on blood flow. Cadawallader (1971) suggested that Reserpine and Guanethidine could increase the rate of absorption of orally administered drugs by increasing the blood flow to the GI tract.

Mclean et al. (1978) attempted to explain, via computer modeling, increased bioavailability of drugs such as propranolol or metoprolol after a meal. They predicted that the vasodilator Hydralazine should enhance the bioavailability of Propranolol or similar drugs which require metabolism through the liver to be effective. This prediction was borne out by Schreck et al. (1984), where the authors concluded that the increased bioavailability can be due to hemodynamic effects.

## 1.5 Objectives

It is known in general that the amorphous drugs are metastable and may convert back to its crystalline state (less soluble and absorbable form), during processing and storage. The objective behind this study was to stabilise an amorphous drug, cefuroxime axetil (CAA) upon processing such as compression, crushing and coating, and to protect it from transforming to the crystalline form (CAC).

It is known in the literature that cefuroxime axetil (CA) exists in its amorphous and crystalline states, of which the former is the most soluble and absorbable. The latter was found in this study to be commercialised as a mixture of two polymorphs.

CAA was proved to be sensitive to operation conditions of compression and coating. Compression of the amorphous material led to its partial transformation to the crystalline polymorph of the high melting point, consequently the intestinal absorption rate of the drug was significantly reduced.

On the other hand, wax coating of CA done to mask its very bitter taste in dry suspension formulation, was found to cause complete transformation of CAA to the crystalline polymorphs, thus dramatically reduced its intestinal absorption. This gave bioavailability of CA that is lower than that obtained from the drug in its tablet dosage form.

The concept utilised for stabilising the amorphous CA in this study was based on mixing and processing of CAA with excipients that were expected to deplasticize the amorphous CA, and reduce its molecular mobility, thus inhibiting crystallisation under compression and coating.

Techniques and methods used for testing CAA and its mixtures with excipients were DSC, MTDSC, XRPD, DVS, dissolution *in vitro* gut absorption and bioequivalence. All indicated that the objective of the study was achieved, and that CAA mixed with chosen excipients was protected from crystallisation upon exposure to process conditions.

## **CHAPTER 2**

### **GENERAL MATERIALS AND METHODS**

Different methods had been utilised to characterise and compare physical and chemical properties of different forms and preparations of cefuroxime axetil (CA) used in this study. These methods are described below.

#### **2.1 DIFFERENTIAL SCANNING CALORIMETRY (DSC)**

##### **2.1.1 Introduction**

Thermal analyses is a term used to describe the analytical techniques that measure the physical and chemical properties of a sample as a function of temperature or time (Brown et al, 1998). This physical technique along with complementary analytical structural techniques such as spectroscopy, and, chromatographic methods have become increasingly important in the development of modern day pharmaceuticals. A number of thermo-analytical techniques are currently widely used in the pharmaceutical industry. These include thermogravimetric Analyses (TGA), differential scanning calorimetry (DSC), and thermomechanical Analyses (TMA) (Gallagher et al, 1997). Of these techniques, DSC is the most popular due to its wide applicability, ease of preparation and interpretation (Haines et al, 1995). It provides thermodynamic information that is essential for preformulation studies of pharmaceuticals and the subsequent development of a stable and effective dosage form (Brown et al, 1998). The performance of DSC is dependant on a number of experimental factors. Some of the important factors to be considered are the sample size, the heating rate, the atmosphere, and crucible type (Roy et al, 2003).

This technique is useful to characterise physical properties of raw materials, mixtures of materials or the medical products. A calorimeter measures heat flow into (endothermic) or out of (exothermic) a material as it undergoes a phase change. Examples of thermal transitions measured by DSC are melting, polymorphism, crystallisation, decomposition, out-gassing, glass transition, compatibility, sublimation and thermal stability (Worthington et al, 1999 and Wissing et al, 2000).

It also measures the transition onset and ending temperatures, as well as, the temperature at maximum transition. DSC is useful in monitoring materials to assess their similarities or differences or the effects of additives on the thermal properties of a material. Differential scanning calorimetry is one of the best methods to characterise crystal polymorphism (Haines et al, 1995).

This technique monitors heat effects associated with phase transitions and chemical reactions as a function of temperature. In a DSC the difference in heat flow to the sample and a reference at the same temperature, is recorded as a function of temperature. The reference is an inert material such as alumina, or just an empty aluminum pan. The temperature of both the sample and reference are increased at a constant rate (Brown et al, 1998). A schematic representation of the differential scanning calorimeter is shown in Figure 2.1.

Since the DSC is operated at constant pressure, heat flow is equivalent to enthalpy changes:

$$\left(\frac{dq}{dt}\right)_p = \frac{dH}{dt} \dots\dots\dots \text{Eq. 2.1}$$

The  $dH/dt$  is the heat flow measured in  $\text{mJ sec}^{-1}$ . The heat flow difference between the sample and the reference is:

$$\Delta \frac{dH}{dt} = \left(\frac{dH}{dt}\right)_{\text{sample}} - \left(\frac{dH}{dt}\right)_{\text{reference}} \dots\dots\dots \text{Eq. 2.2}$$

and can be either positive or negative. In an endothermic process, such as most phase transitions, heat is absorbed and, therefore, heat flow to the sample is higher than that to the reference. Hence heat flow ( $\Delta dH/dt$ ) is positive. Endothermic processes which include melting, dehydrations, reduction reactions, and some decomposition reactions. For exothermic process, such as crystallisation, some cross-linking processes, oxidation reactions, and some decomposition reactions, the heat flow ( $\Delta dH/dt$ ) is negative.

The information which is readily obtainable from a DSC curve is the temperature at which a certain process occurs, for example, the melting point. The temperature at which a reaction, such as decomposition, may start is another important parameter. The peak temperature is associated with the temperature at which maximum reaction rate occurs (Mcedo et al, 2001). The enthalpy of a reaction can also be quantified if a known mass of the active is weighed into the pan. Thermodynamic information regarding the process can therefore be determined.

Figure 2.1 shows the differential scanning calorimeter device parts.

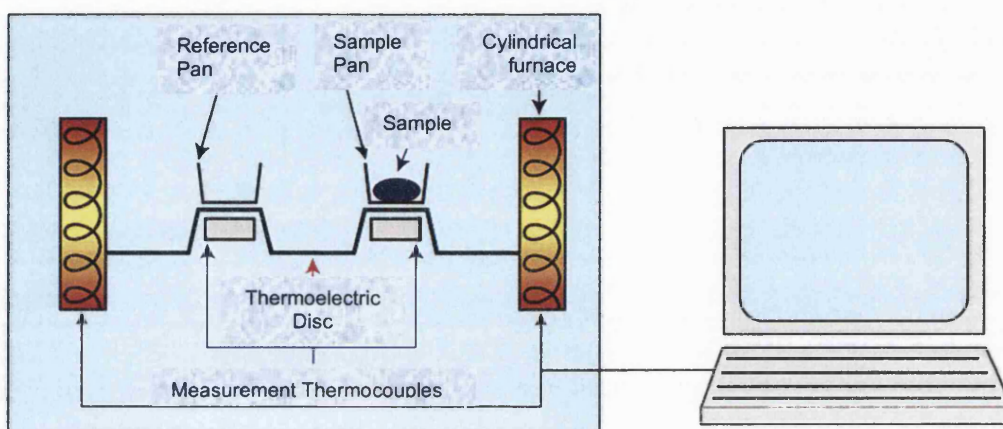


Figure 2.1: Schematic representation of a differential scanning calorimeter (DSC).

### 2.1.1.1 Glass transition temperature ( $T_g$ )

In the case of glass-forming materials, for example, when the cooling process is too rapid for crystallisation, the precipitated material forms a super cooled liquid. Upon further cooling a point is reached at which the material forms a glass, this transition is referred to as the glass transition temperature ( $T_g$ ) (Angell et al, 1995). At this temperature, the bonding between molecules remains the same as in the liquid, but their translational and rotational motions are dramatically reduced. Hence the glass transition is dependent on molecular mobility with no associated heat transfer for the process. It is also rate dependent, with slower cooling rates resulting in lower  $T_g$  values (Craig et al, 1999-a). On the other hand, as a material (e.g. an amorphous polymer) goes from a glassy state to a rubbery state there occurs a change in the heat capacity (Hancock et al, 1997; Angell et al, 1995).

### **2.1.1.2 Crystallisation temperature ( $T_c$ )**

Above the glass transition of an amorphous material, the increase in free volume between molecules will increase the degree of molecular mobility. If there is sufficient mobility and energy to form a critical nucleus, crystallisation will subsequently occur (Royall et al, 2001). As the material undergoes recrystallisation, the excess energy (the enthalpy) gives rise to an exothermic peak in the thermogram.

### **2.1.1.3 Melting temperature ( $T_m$ )**

Heat may allow crystals to form, but upon continued ramping of the temperature, the crystallised material will either undergo melting or decomposition. At the melting temperature the long range order of the crystalline lattice is lost, increasing the degree of molecular freedom. Melting is a first order transition, indicating that at the melting temperature, the temperature of the sample pan will not rise until all the material has undergone the phase transition (Ahlneck et al, 1990). This relates to the need for an increase in the heat flow to the sample pan to melt the crystals and to maintain the temperature rising at the same rate as that of the reference pan. Upon calibration of the system (e.g. with indium) the measured heat flow required during melting provides a quantitative measurement of the thermodynamic process of the melting transition.

A typical DSC thermogram of the thermal transitions of an amorphous substance is shown in Figure 2.2.

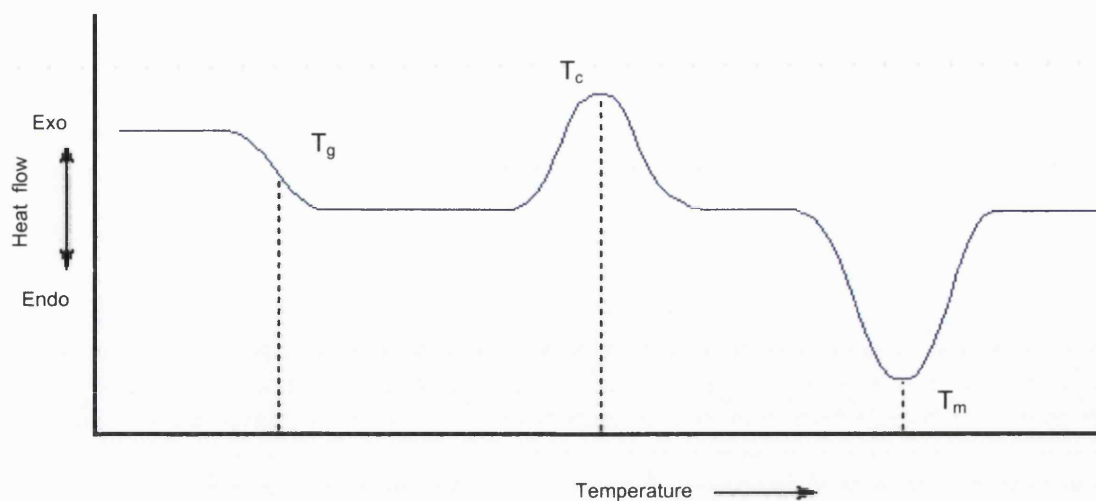


Figure 2.2: A DSC thermogram of an amorphous substance

### 2.1.2 Materials and methods

DSC test procedure:

The sample pan and lid were weighed on the balance and the balance zeroed. After the pan had been put on the movable piece of DSC punch, 10.0 -12.0 mg weight of the material (unless otherwise mentioned) was put in the standard 40 $\mu$ l aluminum crucible with a pinhole in the lid (unless otherwise mentioned) to allow removal of any residual water. The punch was pressed and the closed crucible was weighed again, the weight was recorded.

The instrument (Mettler<sup>®</sup> TA 4000 series) was initially calibrated for temperature and enthalpy values using pure indium. The following parameters were chosen for the ramp: starting temperature 10 $^{\circ}$ C, end temperature 200 $^{\circ}$ C, ramp rate 25 $^{\circ}$ C/min or 10 $^{\circ}$ C/min. Each material was analysed as triplicates.

## 2.2 MODULATED TEMPERATURE DSC (MTDSC)

### 2.2.1 Introduction

#### 2.2.1.1 History

Modulated temperature DSC (MTDSC) is a recently developed extension of standard DSC. It was first presented by Reading et al. at the 1992 NATAS conference (Sauerbrunn et al, 1992; Reading et al, 1993-a, 1993-b). The technique has subsequently been extensively studied (Gill et al, 1993; Boller et al, 1994; Reading et al, 1994; Schawe, 1995-a, 1995-b, 1996-a; Varma-Nair, 1996) and applied to the characterisation of materials such as inorganic glasses (Schawe, 1996-b; Tomasi et al, 1996), polymers (Reading et al, 1994; Boller et al, 1995; Hourston et al, 1995; Sauerbrunn et al, 1995; Boller et al, 1996) and more recently to pharmaceutical and food systems (Barnes et al, 1993; Alden et al, 1995; Coleman et al, 1996; Izzard et al, 1996; Craig et al, 1998; Hill et al, 1998; Bustin et al, 1999).

In an MTDSC operation, a modulated sinusoidal wave is superimposed over the conventional linear (or isothermal) heating or cooling temperature program. MTDSC confers to the same theory as standard DSC in which the heat flow signal is a combination of the specimen heat capacity (heat rate dependent component) and of any temperature dependent, often irreversible, 'kinetic' component. The resultant heat flow can be represented by (Saklatvala et al, 1999):

$$\frac{dQ}{dt} = C_{p,t} \frac{dT}{dt} + f(t,T) \dots\dots\dots \text{Eq. 2.3}$$

where Q is the heat flow absorbed by the specimen,  $C_{p,t}$  the specimen heat capacity, T the absolute temperature, t the time and f (t,T) the kinetically-limited heat flow rate (i.e. it represents the contribution to the total heat flow rate given by the reversible events taking place with a kinetics that is slow when compared to the experimental time-scale). In MTDSC, the applied temperature program can be expressed as:

$$T(t) = T_0 + bt + B\sin(\omega t) \dots\dots\dots \text{Eq. 2.4}$$



where  $T_0$  is the starting temperature,  $b$  the underlying or average heating rate,  $B$  the amplitude of the oscillation and  $\omega$  the frequency of the oscillation. Assuming that for a small temperature modulation the response of the rate of the kinetic process to temperature is linear over a modulation interval, the heat flow can be written as (Craig et al, 1999-b):

$$\frac{dQ}{dt} = C_{p,t}(b + B\omega \cos(\omega t)) + f'(t, T) + C \sin(\omega t) \dots \dots \dots \text{Eq. 2.5}$$

where  $f'(t, T)$  represents the contribution to the total heat flow rate given by true irreversible events;  $C$  is the amplitude of the kinetic response to sine wave modulation and the term  $(b + B\omega \cos(\omega t))$  is the derivative modulated temperature.

The cyclic component of the heat flow signal depends on the value of  $b$ ,  $\omega$  and  $C$ . In most kinetically-controlled processes,  $C$  may be approximated to zero such that the response to the cyclic perturbation originates from the thermodynamic heat capacity contribution only, resulting in:

$$\frac{dQ}{dt} = C_{p,t}(b + B\omega \cos(\omega t)) + f'(t, T) \dots \dots \dots \text{Eq. 2.6}$$

A discrete fourier transform (DFT) algorithm is then used to separate this cyclic response of the specimen from its response to the underlying heating rate and to quantify these two signals separately.

The heat capacity  $C_{p,t}$  may be determined from the measurement of  $b$ ,  $\omega$  and  $B$ . The product of  $C_{p,t}$  and the underlying heating rate may then be calculated to yield the cyclic heat flow component, also called the reversing heat flow. The non-reversing heat flow is obtained by simply subtracting the reversing heat flow component from the calculated total heat flow.

It is worthy to note that, by applying this procedure, all short-term noise is removed from the deconvoluted signals and the heat capacity, which is calculated using modulation amplitudes, is not affected by instrumental baseline curvature. Thus, thermal events such as glass transition and some melting events will be distributed in the reversing heat flow whereas the non-reversing heat flow will refer to

enthalpic relaxation, evaporation, crystallisation, thermal decomposition, cure and some melting events.

MTDSC is nowadays a widely recognised technique yielding particular advantages over conventional DSC. One of the major advantages of MTDSC is that the technique allows direct measurement of the glass transition in the first heating scan when an associated enthalpic relaxation is also present (Craig et al, 1999-b). The enthalpic relaxation may arise over the glass transition region either due to a difference in the cooling and heating rates used in the preparation and characterisation of an amorphous material, or by stress relaxation on storage (Moynihan et al, 1996). The presence of this thermal feature is frequently problematic as it occurs over the same temperature range as the glass transition, thereby rendering visualization of the latter difficult. Furthermore, the similarity in appearance between the relaxation endotherm and a melting response may result in confusion with regard to whether a melting or glass transitional event is taking place.

On the other hand, the presence of water, which lowers the  $T_g$  of amorphous systems, has concomitant implications for product stability. The relationship between water content and  $T_g$  has been explored in a number of publications in the pharmaceutical literature (e.g. Hancock et al, 1994). However, if one is attempting to quantitatively model the relationship between  $T_g$  and water content, the errors in  $T_g$  measurement arising due to the presence of the relaxation endotherm may be considerable. It is possible to temperature cycle the sample in order to minimize the relaxation endotherm, although this may alter the sample in relation to the original system under study either due to changes in water distribution or to non-reversible alterations in structure such as collapse of freeze dried products.

There are, therefore, significant advantages in measuring the  $T_g$  during the first temperature cycle, in isolation from the relaxation endotherm. All the benefits listed make MTDSC a powerful technique provided that the choice of the experimental parameters as well as the  $C_p$  calibration of the calorimeter are carried out properly.

### **2.2.1.2 Choice of MTDSC parameters**

The general precautions that are necessary to ensure reliable and accurate results include careful specimen preparation, appropriate specimen size, use of adequate pans and purge gas, selection of appropriate purge gas flow, and calibrations carried out under conditions identical to those used for specimen measurement (Craig et al, 1999-a).

Other general recommendations which apply for all types of thermal events is to select an optimized set of MTDSC parameters. This includes the underlying linear heating rate ( $R$ ), which should be 1–5°C/min; a value of 5°C/min should not be exceeded to allow for the specimen to follow the modulation; values below 1°C/min should be preferred whenever possible to ensure enough oscillations (at least 5–6 cycles) across the thermal event studied. The modulation period ( $P$ ) should be 40–100s, a value of 60s is generally recommended when using standard aluminium crimped pans and nitrogen purge gas. The temperature modulation amplitude ( $A$ ) is better to be  $\pm 0.1 - \pm 3^\circ\text{C}$  for a given linear heating rate. Larger period values enhance sensitivity, while smaller values enhance resolution. In the specific case of the glass transition which involves  $C_p$  measurement, the following additional recommendations also apply, the use of large modulation period values (80–100 s), which allows for a maximum time for heat transfer across the specimen and is necessary to yield precise heat capacity values. For weak glass transition signals, a larger value of the amplitude should be preferred, typically around 1.5–2°C (working in ‘heat-and-cool’ instead of in ‘heat only’ mode is not a problem when dealing with reversible events such as a glass transition). However, this value should not be too large to prevent the modulation from over-spanning the transition width.

A general approach for selecting appropriate experimental parameters would be to first run the specimen in standard mode to evaluate the possible need for MTDSC, then choose the temperature modulation period and the underlying linear heating rate and finally select the temperature modulation amplitude.

### 2.2.1.3 Heat capacity ( $C_p$ ) calibration and measurement

The heat capacity is obtained by continuously dividing the amplitude of the heat flow by the amplitude of the modulated heating rate, as expressed in the following equation (Craig et al, 1999-b):

$$C_p = K_{(Cp)} \frac{Amp_{MHF}}{Amp_{MHR}} \dots\dots\dots \text{Eq.2.7}$$

where  $K_{(Cp)}$  is the heat capacity constant,  $Amp_{MHF}$  the amplitude of the modulated heat flow and  $Amp_{MHR}$  the amplitude of the modulated heating rate. Once the appropriate set of MTDSC parameters has been chosen, the calorimeter must be calibrated by both performing a  $C_p$  baseline run and determining the heat capacity constant,  $K_{(Cp)}$ , a multiplying factor which allows for the quantitative measurement of the heat capacity. These calibrations must be carried out under the same experimental conditions as those chosen for specimen analyses using closely mass matched DSC pans, (Varma-Nair et al, 1996).

The heat capacity constant,  $K_{(Cp)}$ , is given by the ratio of the theoretical heat capacity of a reference material to the measured heat capacity of the material studied ,as expressed in Eq. 2.8:

$$K_{(Cp)} = \frac{C_{p, \text{theoretical}}}{C_{p, \text{measured}}} \dots\dots\dots \text{Eq. 2.8}$$

As the MTDSC parameters can significantly affect the  $K_{(Cp)}$  value, it is compulsory to be in the so-called plateau zone of the three-dimensional ( $K_{(Cp)}$ , period, amplitude) graph. A safe-operating zone that ensures reliable determination of the heat capacity constant. This zone corresponds typically to period values comprised of between 60 and 100s (a value of 100s should be preferred for best accuracy) and amplitude values ranging from 90.1 to 92s. By doing so, acceptable values of  $K_{(Cp)}$  can be obtained, typically less than 1.1, by using either helium or nitrogen purge gas.

Several approaches can be applied for heat capacity measurements. These include isothermal (Jin et al, 1993; Boller et al, 1994) and non isothermal methods

(Varma-Nair et al, 1996), with the choice being dependant upon the degree of accuracy required and the time which can be devoted to the measurements. The quasi-isothermal MTDSC method (Boller et al, 1994) is a unique way of performing  $C_p$  measurements with an average heating rate value of zero, thus keeping the specimen continuously close to equilibrium. It involves measuring the specimen heat capacity at a given temperature for 20–30 min while applying a fixed modulation period and temperature amplitude.

This procedure is repeated for several temperatures within the studied temperature range. The quasi-isothermal MTDSC method allows for obtaining highly precise  $C_p$  values and is advantageous when dealing with specimens that are sensitive to fast temperature changes. This method, however, is time consuming.

The MTDSC dynamic method is fast and easy. Over the temperature range of interest, there should only be, however, a small variation in  $K(C_p)$  values, on the order of less than 93% of the average value (within the experimental precision limits of the technique).

### **2.2.2 Materials and methods**

MTDSC analyses were undertaken with Mettler® DSC 822 Module, equipped with a refrigerated cooling accessory. The DSC was calibrated for baseline using empty pans of matched masses, and for temperature and enthalpy using indium standards. For purging of the samples nitrogen gas was used, and measurements were made using pairs of samples and standard aluminum pans.

Analyses was performed using lids with 50 $\mu$ m pinhole in order to work under self generated atmosphere. Accurate samples weights of 3.0 - 5.0 mg were taken, and measurements were done at heating rate of 1°C/min, amplitude of 0.5°C, at period of 48 seconds for the range of 30°C - 100°C. These conditions were chosen to obtain 5 – 6 cycles across the thermal event studied.

## **2.3 LASER PARTICLE SIZE ANALYSES**

### **2.3.1 Introduction**

Particle sizing is an important aspect of pharmaceutical development and validation processes, particularly as the particle size of active ingredients strongly affects their solubility and, thus, bio-availability. There are many methods available for particle size and distribution determination. In general, these techniques can be divided into three basic categories: ensemble methods, counting methods, and separation methods (Syvitsia et al, 1991).

An ensemble method takes a snap shot of a sample and then elucidates the distribution of particles sizes based on the physical properties revealed by the measurement. A counting method characterises the sample one particle at a time in a more direct manor. The accumulative account of the particle provides the size distribution. A separation method, on the other hand, first physically separates the sample according to their particle size, then various techniques are applied to determine the relative amount of each fraction. The advantages and disadvantages of each technique are presented below.

#### **2.3.1.1 Ensemble techniques**

Common ensemble techniques include Low Angle Laser Light Scattering (LALLS), Photon Correlation Spectroscopy (PCS), and Back-Scattering Spectroscopy, (Jillaven-Katesa et al, 2002).

#### **Laser Diffraction**

This is more correctly called Low Angle Laser Light Scattering (LALLS). This method has become the preferred standard in many industries for characterisation and quality control. The applicable range according to ISO13320 is 0.1- 3000 $\mu\text{m}$ .

Instrumentation has been developed in this field over the last twenty years or so, the method relies on the fact that diffraction angle is inversely proportional to particle size. The laser particle size analyser instruments consist of a laser as a source of coherent intense light of fixed wavelength. He-Ne gas lasers ( $\lambda=0.63 \mu\text{m}$ ) are the most common as they offer the best stability (especially with respect to temperature) and better signal to noise than the higher wavelength laser diodes.

The instrument also includes some means of passing the sample through the laser beam. In practice it is possible to measure aerosol sprays directly by spraying them through the beam. Particles in suspension can be measured by recirculating the sample in front of the laser beam.

The latest instruments use the Mie theory which solves the equations for interaction of light with matter. This allows accurate results over a large size range typically (0.02 -2000 $\mu\text{m}$ ) (Cooper et al, 1998; Rame et al, 2002). Refractive indices of the material and medium need to be known and the absorption part of the refractive index known or approximated. These values are either generally known or can be measured.

Laser diffraction has the following advantages over other methods. It is an absolute one set in fundamental scientific principles, hence there is no need to calibrate an instrument against a standard. Equipment can be validated, to confirm that it is performing to certain traceable standards. It works in a wide dynamic range, the best laser diffraction equipment allows the user to measure in the range from 0.1 to 2000 microns. Smaller samples 1nm – 1 $\mu\text{m}$  can be measured with the photon correlation spectroscopy technique as long as the material is in suspension and does not sediment.

An important feature of the instrument is its flexibility. It has extensive application in pharmaceutical and agricultural industries. Dry powders can be measured directly, although this may result in poorer dispersion than using a liquid dispersing medium. However, in conjunction with a suspension analyses it can be valuable in assessing the amount of agglomerated material in the dry state.

Particle properties in liquid suspensions and emulsions can be measured via a recirculating cell, which gives high reproducibility and allows dispersing agents (e.g. 0.1% Calgon, sodium hexametaphosphate solution for  $\text{TiO}_2$ ) and surfactants to be employed to ascertain the primary particle size. The preferred method would be to measure in liquid suspension (aqueous or organic). Another important feature is that the entire sample is measured, thus all the sample passes through the laser beam and diffraction is obtained from all the particles.

### **Photon Correlation Spectroscopy (PCS)**

For smaller particles, a dynamic light scattering system is preferred. A PCS method uses laser light with well defined properties, (wavelength, polarisation, etc) (Brown et al, 1993), to determine the velocity distribution of particles by measuring dynamic fluctuations of scattered light intensity. The typical scattering angle is 90 degrees. To avoid multiple scattering, high dilution is required. The main disadvantage is that small particles can get lost in the crowd of larger particles.

### **Back Scattering Spectroscopy**

To overcome the difficulties encountered in conventional dynamic light scattering system, back scattering spectroscopy has been developed to utilise the information at high scattering angle (Brokovec et al, 2000). One such system involves the use of a single fiber optics that provides both the probing and scattering beam. The most important advantage of this technique is the ability to measure particle size and distribution for concentrated samples without dilution (Allegra et al, 1972).

#### **2.3.1.2 Counting Techniques**

In a counting technique, each particle is identified and counted at a time. Among the popular counting methods are electrozone counter, optical counter, time of flight, and microscope.

### **Electrozone Measurement (Coulter Counter)**

This technique was developed in the mid 1950's for sizing blood cells. The principle of operation is that a glass vessel has a hole or orifice in it, and a dilute suspension is made to flow through this orifice with a voltage applied across it. As particles flow through the orifice the capacitance alters and this is indicated by a voltage pulse or spike (Allen et al, 1992).

The method is not an absolute one but is more of a comparative nature. For real industrial materials, there are a number of fundamental drawbacks in this technique. It is, for example, difficult to measure emulsions, sprays and dry powders which need to be suspended in a medium and cannot be measured directly. Using this technique one must measure in an electrolyte; for organic based materials this is difficult. On the other hand this method requires calibration



standards which are expensive and change their size in distilled water and electrolyte (Allen et al, 1992).

### **Optical Counter**

In this technique particles are forced through a counting chamber (Gouesbet et al, 1988), where a focused laser beam is partially blocked as the particle passes. The light counter has resolution and accuracy comparable to electrozone and LALLS methods.

### **Time of Flight (TOF) Counter**

In a time of flight counter a very dilute particulate suspensions in water is first "nebulized". After the evaporation of water, particles are carried by airflow through two adjacent detectors. The advantages of this technique include high resolution and reasonable dynamic range. The disadvantage is that particle may aggregate during the evaporation of solvent.

### **Microscopy**

Using this, relatively cheap, technique the shape of the particles can be seen. it is not ,however, suitable as a quality or production control technique as only few particles are examined, and there is the real danger of unrepresentative sampling.

### **2.3.1.3 Separation Techniques**

A separation method exerts an external force to a sample and physically groups the particles according to size. Once the particles are separated, the characterisation of individual groups of particles can be conducted using either a counting method or an ensemble method. Common separation techniques include sieves, gravitational sedimentation, disc centrifuge, capillary hydrodynamic fractionation, packed column chromatography, and sedimentation field flow fractionation.

### **Disc Centrifuge Methods**

A disc centrifuge method uses a rotating optically clear disc that is filled with slurry to be analysed (Fitz-patrick et al, 1995). The particles suspended in the liquid move at rates that depend on particle size, large particles move much faster than

small ones. A light beam detector is used to monitor the amount and the size of particles that pass through the edge of the disc.

### **Capillary Dynamic Fractionation**

In capillary hydrodynamic fractionation (CHDF) system, a very dilute suspension of particles flows through a very thin capillary. A parabolic velocity profile is developed for each particle size group (Barth et al, 1984). The method is capable of measuring particles in the range of 0.01-2 microns, and the resolution is usually poor.

### **Gravitational Sedimentation**

The applicable range for this method is 2-50 microns (Allen et al, 1992). The principle of measurement is based on the Stokes' Law. The viscosity factor indicates that it is needed to control temperatures very accurately (Beckers et al, 1989). On the other hand, measurements with this technique tends to be extremely slow and repeat measurements are tedious.

### **Sedimentation Field Flow Fractionation**

In this instrument a rotating disc provides a flow chamber for the particle suspension to be analysed (Schimpf et al, 2000). The method can provide extremely good resolving power for particles that are less than 3-5 microns, but is based on the highly convoluted separation mechanisms, thus, the run time is typically long (1 hour or more).

### **Packed Column Chromatography**

In this technique, the capillary is packed with chromatographic materials that create many tiny channels for the suspended particles to flow through. An advantage of the technique is the increased resolution for particles with small size difference.

### **Sieving**

Is an old technique but has the advantage that it is cheap and is readily usable for large particles. Allen et al. (1992) discussed the difficulties of reproducible sieving, but the main disadvantages are that by sieving it is difficult to measure sprays, emulsions, and dry powders under 400# (38 $\mu$ ).

In this study; Laser particle size analyses was the method of choice for samples testing.

### **2.3.2 Materials and methods**

Particle size analyses was performed using Analysette<sup>®</sup>22 (Fritsch, Germany) Laser particle sizer, together with a liquid dispersing unit for small quantities of suspended material. The instrument was tested using the “Fritsch” starch standard, before being used for samples testing.

The liquid dispersing unit was filled with small quantities of Benzene (it has been found the most suitable dispersing liquid for the material to be tested, as water and other organic solvents dissolved it).

A background measurement was performed before starting analyses. The sample was gradually added until the absorption was between 7% and 15%. The measurement was started automatically as the specified value was reached. When the measurement was finished, the raw data were stored and the particle size distribution was calculated from these data.

## **2.4 X-RAY POWDER DIFFRACTION**

### **2.4.1 Introduction**

X-ray powder diffraction (XRD) has been used extensively in pharmaceutical industry for a number of years. Historically, diffraction started with the development of film methods, where the intensity of the diffracted beams was measured by the blackening on a photographic film (Kenkins et al, 1996). The 1940s saw the advent of the powder diffractometer which contained a detector designed to scan across the area previously occupied by the film (Klug et al, 1974). Until recently, instrument development has focused mainly on detector technology and sample environment.

In recent years, however, the introduction of sources that can focus an x-ray beam into a small area and two dimensional detectors for rapid data collection have opened new horizons for x-ray powder diffraction.

The XRPD technique takes a sample of the material and places a powdered sample in a holder, then the sample is illuminated with x-ray of a fixed wave-length and the intensity of the reflected radiation is recorded using a goniometer (Erko et al ,1996). This data is then analysed for the reflection angle to calculate the inter-atomic spacing (D value in Angstrom units- $10^{-8}$  cm). The intensity (I) is measured to discriminate (using I ratios) the various D spacings and the results are compared to identify possible matches (Nielsen et al, 2001).

#### **2.4.1.1 X-Ray generation and properties**

X-rays are electromagnetic radiation with typical photon energies in the range of 100 eV – 100 keV. For diffraction applications, only short wavelength x-rays (hard x-rays) in the range of a few angstroms to 0.1 angstrom (1 keV – 120 keV) are used. Because the wavelength of x-rays is comparable to the size of atoms, they are ideally suited for probing the structural arrangement of atoms and molecules in a wide range of materials. The energetic x-rays can penetrate deep into the materials and provide information about the bulk structure (Warren et al, 1990).

X-rays are produced generally by either x-ray tubes or synchrotron radiation. In an x-ray tube, which is the primary x-ray source, x-rays are generated when a focused electron beam accelerated across a high voltage field bombards a stationary or rotating solid target. As electrons collide with atoms in the target and slow down, a continuous spectrum of x-rays are emitted, which are termed Bremsstrahlung radiation (James et al, 1982). The high energy electrons also eject inner shell electrons in atoms through the ionization process.

When a free electron fills the shell, an x-ray photon with energy characteristic of the target material is emitted. Common targets used in x-ray tubes include Cu and Mo, which emit 8 keV and 14 keV x-rays with corresponding wavelengths of 1.54 Å and 0.8 Å, respectively (Christopher et al, 1997). The energy E of an x-ray photon and it's wavelength is related by the equation  $E = hc/\lambda$ , where h is Planck's constant and c the speed of light.

In recent years synchrotron facilities have become widely used as preferred sources for x-ray diffraction measurements. Synchrotron radiation is emitted by electrons or positrons travelling at near light speed in a circular storage ring (Authier et al, 2001). These powerful sources, which are orders of magnitudes are more intense than laboratory x-ray tubes, have become indispensable tools for a wide range of structural investigations and brought advances in numerous fields of science and technology.

The diffracted beam may be detected by using a moveable detector such as a Geiger counter, which is connected to a chart recorder. In normal use, the counter is set to scan over a range of  $2\theta$  values at a constant angular velocity.

Routinely, a  $2\theta$  range of 5 to 70 degrees is sufficient to cover the most useful part of the powder pattern. The scanning speed of the counter is usually  $2\theta$  of 2 degrees  $\text{min}^{-1}$  and therefore, about 30 minutes are needed to obtain a trace.

Figure 2.3 represents a schematic of the principle mode of operation of an X-ray diffractometer.

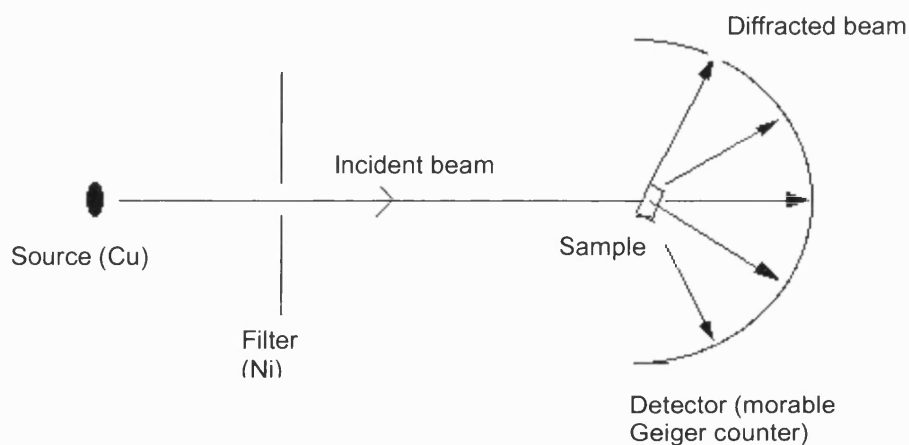


Figure 2.3: Scheme of an X-ray powder diffractometer

#### 2.4.1.2 Lattice Planes and Bragg's Law

X-rays primarily interact with electrons in atoms. When x-ray photons collide with electrons, some photons from the incident beam will be deflected away from the

direction in which they were originally travelling. If the wavelength of these scattered x-rays did not change (meaning that x-ray photons did not lose any energy), the process is called elastic scattering (Thompson Scattering) in that only momentum has been transferred in the scattering process (Guinier et al, 1994). These are the x-rays that are measured in diffraction experiments, as the scattered x-rays carry information about the electron distribution in materials.

In an inelastic scattering process (Compton Scattering), x-rays transfer some of their energy to the electrons and the scattered x-rays will have different wavelength than the incident x-rays (Guinier et al, 1994).

Diffracted waves from different atoms can interfere with each other and the resultant intensity distribution is strongly modulated by this interaction. If the atoms are arranged in a periodic fashion, as in crystals, the diffracted waves will consist of sharp interference maxima (peaks) with the same symmetry as in the distribution of atoms. Measuring the diffraction pattern therefore allows us to deduce the distribution of atoms in a material.

The peaks in an x-ray diffraction pattern are directly related to the atomic distances. For a given set of lattice plane with an inter-plane distance of  $d$ , the condition for a diffraction (peak) to occur can be simply written as  $2d\sin\theta = n\lambda$ . It is presented in Figure 2.4, and is known as the Bragg's law, after W.L. Bragg.

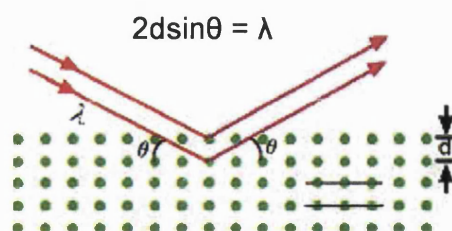


Figure 2.4: Bragg's Law

Where  $\lambda$  is the wavelength of the x-ray,  $\theta$  the scattering angle, and  $n$  an integer representing the order of the diffraction peak. Bragg's law is one of most important laws used for interpreting x-ray diffraction data (Zachariasen et al, 1997).

## **2.4.2 Materials and methods**

X-ray powder diffraction (XRPD) patterns were obtained with a Phillips analytical X-ray powder diffractometer (Bath, UK) utilizing a  $\text{CuK}_\alpha$  source at 1.5418 Å. Each sample of approximate weight of 1gm was analysed by a single  $2\theta$  sweep, with a step size of  $0.02^\circ$ / step and step time of 13 s.

## **2.5 DYNAMIC VAPOUR SORPTION**

### **2.5.1 Introduction**

Many amorphous materials are able to crystallise by the process of water absorption, which lowers the  $T_g$  and gives sufficient molecular mobility to allow crystallisation to proceed rapidly. The availability of microbalance assemblies with good temperature and humidity control (as in the dynamic vapour sorption apparatus) makes it rather simple to detect changes in crystallinity gravimetrically (Buckton et al, 1999).

Water sorption has been used in the study of many amorphous and partially amorphous powders. A few examples in the pharmaceutical literature include sucrose (Gerhardt et al, 1994), lactose (Buckton et al, 1995-b), raffinose (Gerhardt et al, 1995) and salbutamol sulphate (Ward et al, 1995).

Vapour sorption by amorphous and crystalline pharmaceutical materials is usually quite different and can be used to precisely distinguish between them (Buckton et al, 1995-b). Typically, crystalline materials adsorb vapors in small quantities at their surfaces. In contrast, amorphous materials absorb and adsorb vapors in relatively large amounts. Vapor sorption in glassy and rubbery amorphous systems have been widely studied experimentally and modeled extensively, particularly with polymers (Vrentas et al, 1993). The models most applicable to pharmaceutical materials are based on solution theories and assume no specific interactions between sorbent and sorbate.

Rubbery amorphous materials usually sorb a considerably greater quantity of vapour than their respective glasses, and this phenomenon can be used to identify the state of an amorphous material (Oksanen et al, 1990). Many sorbent vapours plasticize the amorphous material into which they absorb, and thus at a critical

partial vapor pressure the glass to rubber transition can be induced at a constant temperature. Temperature effects on vapour sorption tend to be small, usually with an increased level of sorption with decreasing temperature .

Water vapor sorption has been most widely used in the study of amorphous drugs and excipients, and the predominant techniques are the vacuum microbalance and desiccator-saturated salt solution gravimetric methods. Other Volumetric and potentiometric methods have also been used (Kontny et al, 1985).

The sensitivity of water vapor sorption techniques to amorphous material is of the order of a few weight percent, and thus these techniques are the preferred means of studying pharmaceutical systems containing low levels (<10%) of amorphous material. The plasticizing effects of water vapor on amorphous pharmaceutical materials have been described in some details (Oksanen et al, 1990), and can potentially induce unwanted effects such as spontaneous phase transitions and lyophile collapse. Isothermal microcalorimetric techniques can be used in conjunction with water vapor sorption methods to study such phase transitions from the amorphous state (Angberg et al, 1988). The influence of additives on the kinetics of amorphous to crystalline phase transition in lactose has been widely investigated (Buckton et al, 1998-b), as has the physical stability of amorphous drugs.

### **2.5.2 Materials and methods**

The moisture sorption profile was determined by dynamic vapor sorption (DVS; DVS-1 from Surface Measurement Systems Ltd., Bath, UK). Approximately 10 mg of sample was weighed into the DVS sample cell and subjected to a sorption-desorption cycle using 10% RH increments between 0 and 90% RH. Equilibrium mass, at each RH, was determined with a  $dm/dt$  of  $0.0005\% \text{ min}^{-1}$ .

## **2.6 SCANNING ELECTRON MICROSCOPY**

### **2.6.1 Introduction**

Electron microscopes use a beam of highly energetic electrons to examine objects on a very fine scale. This examination can yield information on topography (surface features), and crystallography (how the atoms are arranged in the object) (Mohanty



et al, 1982). Electron microscopes were developed due to the limitations of light microscopes (Watt et al, 1997), which are limited by the physics of light to 500x or 1000x magnification and a resolution of 0.2  $\mu\text{m}$ .

The transmission electron microscope (TEM) was the first type of electron microscopes to be developed and is patterned exactly on the light transmission microscope except that a focused beam of electrons is used instead of light. It was developed by Max Knoll and Ernst Ruska in Germany in 1931.

The scanning electron microscope generates a beam of electrons in a vacuum. That beam is collimated by electromagnetic condenser lenses, focused by an objective lens, and scanned across the surface of the sample by electromagnetic deflection coils. The primary imaging method is by collecting secondary electrons that are released by the sample (Chapman et al, 1986). The secondary electrons are detected by a scintillation material that produces flashes of light from the electrons. The light flashes are then detected and amplified by a photomultiplier tube (Chapman et al, 1986). The intensity of the electrical current induced in the specimen by the illuminating electron beam is used to produce an image (Lyman et al, 1990).

Scanning electron microscopes are often coupled with x-ray analysers. The energetic electron beam-sample interactions generate x-rays that are characteristic of the elements present in the sample (Reimer et al, 1985).

The instrumentation of an electron microscope, and X-ray ejected from electron beam hitting the samples are presented in Figure 2.5.

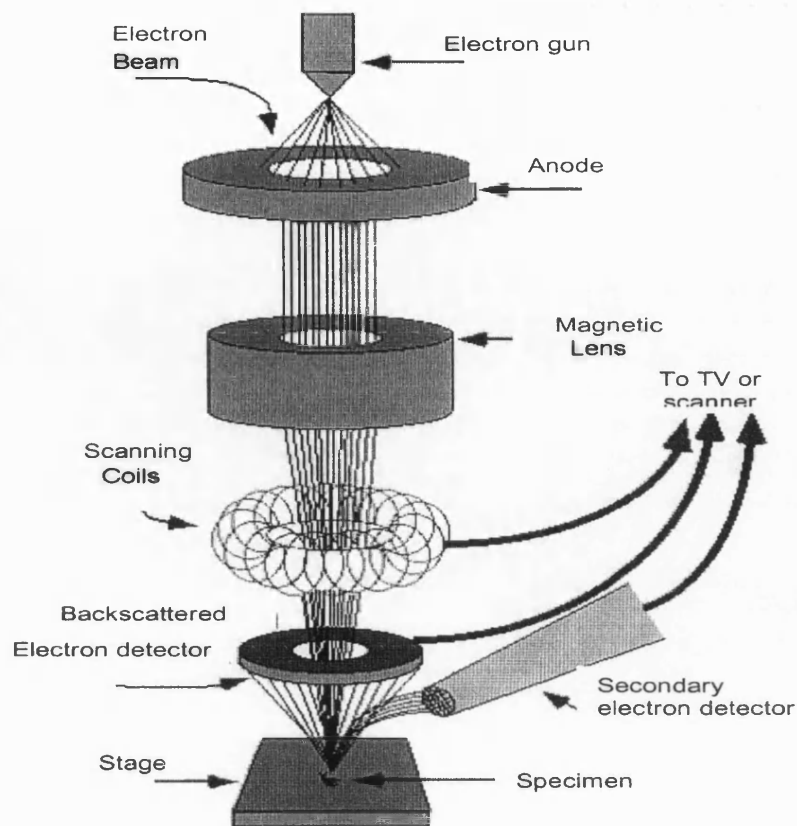


Figure 2.5: Electron microscopy instrumentation

### 2.6.1.1 Scanning process

In a typical SEM configuration, electrons are thermo-ionically emitted from a tungsten or  $\text{LaB}_6$  cathode filament towards an anode (Chesco et al, 1990). The beam then passes through the objective lens, where pairs of scanning coils deflect the beam over a rectangular area of the sample surface. As the primary electrons strike the surface they are inelastically scattered by atoms in the sample (Reimer et al, 1985).

Interactions with the surface lead to the subsequent emission of electrons and x-rays, which are then detected to produce an image as shown in Figure 2.6.

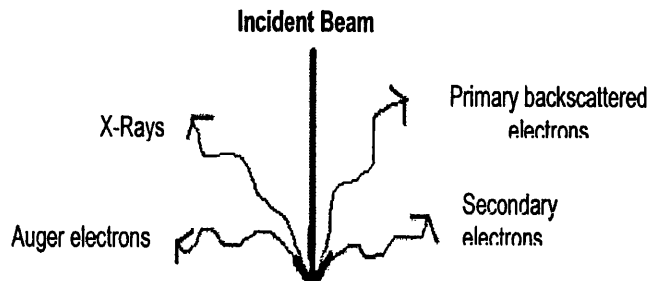


Figure 2.6 Electrons and X-rays ejected from electron beam hitting the samples

### 2.6.1.2 Detection of secondary electrons

The most common imaging mode monitors low energy (<50 eV) secondary electrons (Heywood et al, 1971). Due to their low energy, these electrons must originate within a few tenths of a nanometer from the surface. The electrons are detected by a scintillator-photomultiplier device and the resulting signal used to modulate the intensity of a cathod ray tube that is rastered in conjunction with the raster-scanned primary beam. Because the secondary electrons come from the near surface region, the brightness of the signal depends on the surface area that is exposed to the primary beam (Crang et al, 1988).

Because the SEM utilises vacuum conditions and uses electrons to form an image (Chapman et al, 1986), special preparations must be done to the sample. All water must be removed from the samples because the water would vaporize in the vacuum. All non-metals need to be made conductive by covering the sample with a thin layer of conductive material (e.g. gold). This is done by using a device called a sputter coater.

### 2.6.2 Materials and methods

Instrument used was 6310 Cryo System, and samples were coated with gold for measurement. For the cooling system with liquid nitrogen, SEM cold stage and anticontaminator were purged with nitrogen gas at a pressure of 0.5kg/cm<sup>2</sup> (7psi) for 1-2 minutes. Particles examined under electron microscope were initially passed through the sieve 0.2mm.

## **2.7 DISSOLUTION**

### **2.7.1 Introduction**

The measurement of dissolution rate is utilised for the functionality and characterisation of bulk drug substances and products. The dissolution rate and bioavailability of a drug substance is influenced by its solid state properties, i.e. crystallinity, polymorphism, hydration, solvation, particle size, and particle surface area (Banakar et al, 1992). It is also influenced by extrinsic factors, such as hydrodynamics (e.g. test apparatus, shaft rotation speed) and test conditions (e.g. temperature, fluid volume and viscosity, pH, and buffer strength in the case of ionizable compounds) (Byrn et al, 1995). The official approved dissolution apparatus for testing dissolution include, apparatus I (Basket), apparatus II (Paddle), apparatus III (reciprocating cylinder), and apparatus IV (flow through the cell).

In these, testing of pharmaceutical dosage forms typically calls for using a buffer solution or a hydrochloric acid (HCl) solution as the dissolution medium. Usually basket speed is 100 rpm, while the paddle speed is 50 rpm. Both tests require sampling of the solution after specific intervals, called time points. These are usually 15, 30, 45, and 60 minutes when testing immediate-release products. The compendial time points are usually a single point of either 30 or 45 minutes.

A discriminating dissolution procedure yields data that distinguishes important differences in composition and/or method of manufacture between dosage forms (Junginger et al, 2003). The discriminatory power of the dissolution method depends on the method's ability to detect changes in the drug product (Banakar et al, 1992). Of these, manufacturing variables which can come from many sources, e.g. the drug substance (different particle sizes, crystal habits, solvation, surface areas, or synthetic pathways) (Mauger et al, 1996), the drug product's formulation, and/or the drug product's process of manufacturing.

The method sensitivity to drug product formulation changes can be challenged by testing products with different amounts of excipients or by testing formulation changes (Rohrs et al, 2001). If the data show a measurable difference for the key

variables, then the method may be considered as a discriminating test for critical manufacturing variables.

With regard to stability, the dissolution test should appropriately reflect relevant changes in the biopharmaceutical performance caused by temperature, aging, humidity, and photosensitivity.

On the other hand, the implementation of similarity analyses is becoming important for demonstrating formulation equivalencies among semi-solids, immediate release and extended release oral solid dosage forms. Test methods for these analyses involve the use of the USP apparatus I and II (Fares et al, 1995). For active pharmaceutical ingredients (API) “sameness” analyses became possible by the development of the intrinsic dissolution test (Viegas et al, 2001). The evaluation of the intrinsic dissolution of an API is a way to demonstrate chemical purity and equivalency, after changing the synthesis final crystallisation steps, the particle size and the surface area. Polymorphism and scale up issues regarding batch size and manufacturing site can also be assessed by intrinsic dissolution (Viegas et al, 2001).

The intrinsic dissolution rate is defined as the rate of dissolution of a pure pharmaceutical active when conditions such as surface area, temperature, agitation-stirring speed, pH and ionic strength of the dissolution medium are kept constant, (Mauger et al, 2003). The intrinsic dissolution apparatus is shown in Figure 2.7. The assembly is immersed, pellets side up, into the bottom of a flat-bottom dissolution vessel containing 900 ml dissolution medium at 37°C. The apparatus II paddle is positioned 1 inch above the die and rotated at 50 rpm.

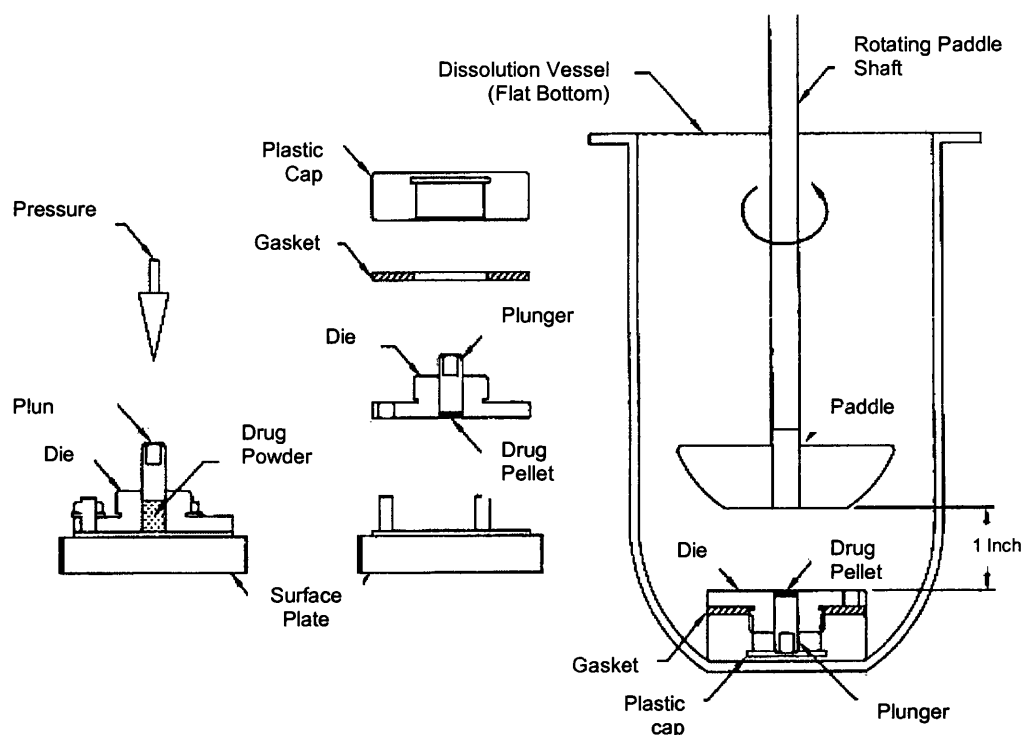


Figure 2.7: The apparatus for intrinsic dissolution test (Vigas et al, 2001).

## 2.7.2 Materials and methods

### 2.7.2.1 Intrinsic dissolution

Disc preparation: 6 Discs were prepared from each material, compressed at pressure of 2000 – 3000 psi for 2 minutes and 30 seconds at weighs of around 0.125 gm.

Standard preparation: 35.0 mg of cefuroxime axetil reference standard (CARS) was transferred to 100 ml volumetric flask containing 10 ml methanol. The solution was sonicated for 10 minutes and then completed to volume with the dissolution media. 4 ml of the solution was transferred to 100 ml volumetric flask and diluted to volume with the same media.

Sample preparation: Each disk was placed in a dissolution vessel, as shown in figure 2.7, and the dissolution test was started as the conditions mentioned below. At the specified time intervals (5,10, 20, 30 & 45 min), 20 ml samples were withdrawn from the dissolution vessels, filtered using 0.45 $\mu$ m filter previously saturated with 10 ml of the dissolution media, and then analysed.

Dissolution conditions: Dissolution conditions mentioned under CA tablets in BP 2000 were applied. These are, dissolution apparatus II used together with the intrinsic dissolution disks (Erweka DT 60), 900ml 0.1N HCl medium maintained at  $37^{\circ}\text{C}\pm 1^{\circ}\text{C}$ . The speed of the paddle was set at 50 rpm.

Measurements: the absorbances of the standard preparation and the samples taken were measured at 278 nm using "Varian Cary I" UV spectrophotometer. The dissolution media was used as a blank.

#### **2.7.2.2 Dissolution using apparatus II**

Dissolution conditions adopted were those mentioned in BP 2000 monograph for CA tablets. These include the use of apparatus II (Erweka DT 60), set at 50 rpm speed, and 900ml 0.1N HCl, maintained at  $37^{\circ}\text{C} \pm 1^{\circ}\text{C}$ .

Standard preparation: 34.0 mg CARS was transferred to a 100 ml volumetric flask, 10 ml methanol was added and sonicated for 10 minutes, then volume was completed with the dissolution media. 4ml of the solution was transferred to 100 ml volumetric flask, then volume was made up with the same media.

Sample testing: a weight from the sample preparation equivalent to 125mg cefuroxime was transferred to each of the 6 dissolution vessels at the beginning of the test. At the time intervals of 5, 10, 15, 20 & 30 minutes samples (10 ml each) were withdrawn. Substitution with 10ml media was done gently and directly, samples were then filtered through 0.45microns filter, diluted with the same dissolution media (if necessary), and analysed for the amount of dissolved CA.

Measurements: the absorbances of the standard preparation and the samples tested were measured at 278 nm using "Varian Cary I" UV spectrophotometer. The dissolution media was used as a blank.

The % release of CA was calculated at each time interval using the following equations:

$$\frac{\text{Abs of sample}}{\text{Abs of standard}} \times \text{Conc. of CARS} = \text{Conc. of CA in the sample} \dots\dots\dots \text{Eq. 2.9}$$

$$\text{Conc. Of CA mg/ml} \times 900\text{ml} = \text{amount of CA released to the media} \dots\dots\dots \text{Eq. 2.10}$$

$$\frac{\text{Amount of CA released}}{125/0.8} \times 100\% = \% \text{ Release of CA to the media} \dots\dots\dots \text{Eq. 2.11}$$

## **2.8 RAT INTESTINAL ABSORPTION MEASUREMENTS**

### **2.8.1 Introduction**

The intestinal epithelium is a gatekeeper, i.e. it controls the entry of nutrients and active pharmaceutical ingredients. Knowledge of the absorption and metabolism of these substances at the intestinal mucosal level is, thus, of great importance. Drug absorption is considered to be a complex transfer process across the intestinal lining, which includes passive diffusion through the paracellular space and/or membranes of absorptive cells, vesicular uptake (endocytosis / pinocytosis), and release at the basolateral space, transcytosis (Lennerans, 1998). This transport may or may not be receptor-mediated, entailing uptake across the apical domain with subsequent passive diffusion into the basolateral space.

Each transport mechanism depends on the physico-chemical properties of the absorbed compound, such as its stereochemistry, partition into membranes, molecular weight and/or size, molecular volume, pKa, solubility, chemical stability and charge distribution. Physiological factors such as gastric emptying, gastrointestinal motility, intestinal pH, blood flow, lymph flow, pathological state, drug interactions, nutrition, and mucus dissolution, also need to be considered when evaluating absorption (Pade et al, 1998; Wikman et al, 1993).

Possible routes and mechanisms of transport of molecules across the intestinal epithelium are illustrated in Figure 2.8.



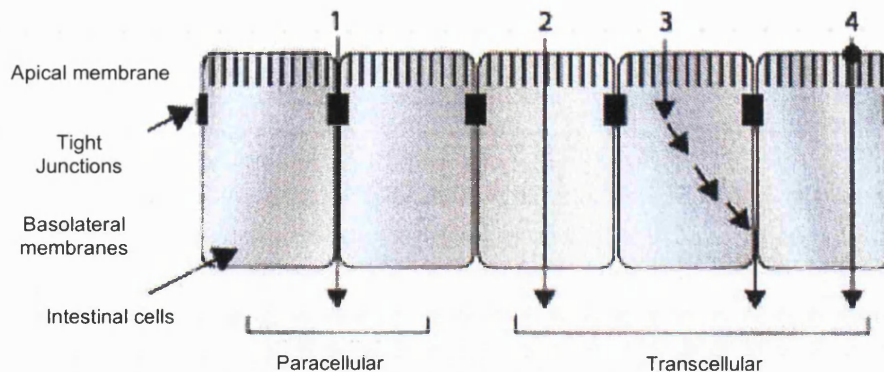


Figure 2.8: Routes and mechanisms of transport of molecules across the intestinal epithelium 1) Paracellular; 2) transcellular passive diffusion; 3) transcytosis; 4) carrier-mediated uptake at the apical domain followed by passive diffusion across the basolateral membrane.

Upon ingestion, compounds have to be liberated from their dosage form, which includes dissolution into a complex medium containing numerous compounds (bile salts, ions, lipids, cholesterol and enzymes) (Welling et al, 1984). This medium can vary considerably, depending on the individual, the intestinal segment, the diet, etc.

Measurements of absolute solubility and dissolution are performed routinely during drug development, however, knowledge of intestinal drug dissolution is limited, due to the non-physiological aspects of *in vitro* systems. For example, instead of using intestinal fluid, buffer systems are commonly employed, which may result in an overestimation or underestimation of the actual events *in vivo* (Galia et al, 1998; Dressman et al, 1998). Since the intestinal fluid is rich in enzymes derived from dying enterocytes and/or the intestinal flora, gastrointestinal stability includes both physico-chemical and enzymatic stability.

The intestinal cell lining is covered with a viscous and elastic gel produced by the goblet cells of the villous epithelium. The physico-chemical properties of this gel can influence the rate of diffusion from the bulk to the site of absorption. Furthermore, metabolic enzymes could be associated with the mucus layer.

Thus, the gel is considered to be the first in a series of absorptive barriers (Winne et al, 1979). The enzymatic barrier to oral absorption could consist of several layers, depending on the physico-chemical properties of the active compound.

As well as the enzymes within the intestinal lumen, there are additional enzymes located in the absorptive cells themselves, such as several cytochrome P450 (CYP) isoforms. In combination with P-glycoprotein (P-gp), these enzymes are responsible for the intestinal first-pass effect.

The intestinal mucosa is characterised by the presence of villi that constitute the anatomical and functional unit for nutrient and drug absorption (Pacha et al, 2000). The presence of villi and microvilli provides enormous surface area for absorption (approximately 250m<sup>2</sup> in a human). The mucosa consists of the epithelial layer, the lamina propria (collagen matrix containing blood and lymphatic vessels) and the muscularis mucosa. Therefore, any drug entering the bloodstream has to pass through the epithelial layer, part of the lamina propria, and the wall of the respective vessel.

A series of methods have emerged for investigating the principal mechanisms of absorption in animals, namely, *in vivo*, *in situ* and *in vitro* methods. The choice of model depends totally on the questions to be answered with respect to the test compound being studied.

#### **2.8.1.1 *In vivo* models**

The main advantage of *in vivo* models is the integration of the dynamic components of the mesenteric blood circulation, the mucous layer and all the other factors that can influence drug dissolution (Amidon et al, 1988).

The most frequently used animal model is the rat, since it better reflects the human situation with respect to paracellular space and metabolism than the dog, which is significantly different to the human, particularly in relation to metabolism, and overestimation of the absorption of paracellularly restricted compounds (Kararli et al, 1995). However, oral studies in rats also have limitations, and tend to provide

false-positive results. It has therefore been stated that “the only real model for man is man” (Wilding et al, 2000).

The disadvantage of *in vivo* models is that it is impossible to separate the variables involved in the process of absorption, i.e. it is not possible to identify individual rate-limiting factors.

### **2.8.1.2 *In situ* models**

The development of stable, vascularly perfused preparations of the small intestine has provided a powerful research tool for the investigation of intestinal transport and metabolism. In this approach, the abdominal cavity of an anaesthetised animal is exposed by laparotomy. The intestinal segment into which the drug solution is introduced can be either a closed loop or an open loop.

*In situ* methods have significant advantages over *in vivo* models. This includes bypassing the stomach, which means that acidic compounds are not likely to precipitate, so dissolution rates do not confuse intestinal drug concentrations and therefore plasma levels. Furthermore, *in situ* tests allow the experimentalist to assess formulation-independent breakdown in the stomach under acidic conditions. Although the animal has been anaesthetised and surgically manipulated, mesenteric blood flow remains intact.

Rat single-pass intestinal perfusion is an *in situ* technique wherein the blood supply, innervation and clearance capabilities of the animal remain intact. Input of drug can be closely controlled in terms of concentration, pH, osmolality, composition, intestinal region and flow rate (Thomas et al, 1992). The drug is measured in buffer or perfusate, thus facilitating assay of drug by specific chromatographic means. This technique has been used extensively in establishing a database for permeabilities with correlation to human absorption data, as well as to elucidate absorption mechanism (Amidon et al, 1988). The basic principle of perfusion experiments is that the absorption is calculated from the disappearance rate of the drug from the perfused segment.

The value of effective permeability ( $P_{\text{eff}}$ ) provides the best description of the transport process across the intestinal barrier (Lennerans et al, 1992, 1995-a and

1995-b). Calculation of  $P_{\text{eff}}$  is dependent on the hydrodynamics within the segment, which in turn is determined by the perfusion technique, its rate, and the degree of intestinal motility.

The intestinal  $P_{\text{eff}}$  represents a direct measurement of the local absorption rate in man and reflects the transport velocity across the epithelial barrier. Intestinal perfusion models, which measure the clearance disappearance of the drug from the perfusion solution, directly describe uptake into the epithelial cell.

Intracellular metabolism in the enterocyte, for instance CYP 3A4, does not occur in the vicinity of the outer leaflet and is therefore considered less likely to influence the disappearance rate ( $P_{\text{eff}}$ ) (Lande et al, 1994; 1995). Intracellular metabolism is, however, a part of the first-pass effect and can therefore be a further limitation to the bioavailability of the drug. In contrast to intracellular metabolism, metabolism in the lumen and/or at the brush-border will interfere directly with the determination of the  $P_{\text{eff}}$  (Langguth et al, 1994; Krondahl et al, 1997).

*In vivo* studies permit the determination of absolute or relative bioavailability, but are also more complex in terms of plasma assay development and assessing where rate limiting processes occur. *In vitro* or *in situ* models are of particular utility if they project when absorption is rate limiting to systemic availability and permeability is rate limiting to absorption.

There are few publications (Artursson et al, 1991; Conradi et al, 1993; Kim et al, 1993) that compare the three widely used intestinal absorption models, possessing individual strengths and weaknesses. They show that each absorption model rely on a different mean of determining membrane transport. The rat *in situ* single-pass intestinal perfusion system base permeability calculations on steady state disappearance of the compound from the intestinal lumen (Conradie et al, 1993).

The rat everted intestinal ring method use the tissue accumulation of compound *in vitro* to determine drug uptake rate (Kim et al, 1993). The human colon adenocarcinoma cell line (Caco<sub>2</sub>) is grown on membrane filters mounted in

diffusion chambers, the rate of compound appearing in the receiver compartment is the basis of the permeability measurement (Artursson et al, 1991).

There are factors that add weight in selecting the appropriate *in vitro* or *in situ* methods for evaluating drug absorption. These factors include the ease and cost of preparation, maintenance, control of experimental conditions, reproducibility and ease of drug analyses.

### **2.8.1.3 *In vitro* models**

#### **Organotypic models**

All intestinal cell types (for example, enterocytes, caliciform cells and lymphocytes) are present in organotypic models, which are used to study formulation effects, intestinal metabolism/stability, and regional differences in permeability. Some studies have shown that permeability to various marker molecules varies along the intestinal canal. In general, permeability decreases in the order jejunum > ileum > colon (Davis et al, 1982). The half-lives of these models are short (1-3 hours).

#### **Everted gut sacs**

The everted gut sac of the rat small intestine can be used to determine kinetic parameters with high reliability and reproducibility (Barthe et al, 1999). Oxygenated tissue culture media and specific preparation techniques ensure tissue viability for up to 2 hours. The technique can be used to study drug transport across the intestine and into the epithelial cells, provided that sensitive detection methods are employed.

This technique has been previously used to study the transport of macromolecules and liposomes. More recently, it has mainly been used to quantify the paracellular transport of hydrophilic molecules and to estimate the effects of potent enhancers on their absorption (Ceppert et al, 1994). Molecules that cross the epithelial barrier by transcellular route have a much higher permeability, which can also be accurately quantified by using the everted sac system.

This kind of model (everted or not) is suitable for measuring absorption at different sites in the small intestine (Chowhan et al, 1977), and for performing preliminary

experiments on the colon (Bratthe et al, 1999).

It is also useful for estimating the first-pass metabolism of drugs in intestinal epithelial cells. A potential disadvantage of this approach is the presence of the muscularis mucosa, which is not usually removed from everted sac preparations. This model, therefore, does not reflect the actual intestinal barrier, because compounds under investigation pass from the lumen into the lamina propria (where blood and lymph vessels are found) and across the muscularis mucosa. Thus, the transport of compounds with a propensity to bind to muscle cells might be underestimated.

The rat everted gut sac system was first reported for the study of the transport of glucose and amino acids (Wilson et al, 1954). In the original method, and all subsequent reports of the use of the method, sacs were incubated in simple salts-containing media/buffers, sometimes with the addition of glucose. Viability of the intestinal tissue was doubtful under such conditions. In histological studies Levine et al. (1970) showed that after 30 min incubation in a salt-buffered medium, 50-75% of the normal epithelium had disappeared, and at 1 h there was total disruption of the epithelial border.

In a histological study of various gut preparations Plumb et al. (1987) observed that when everted gut sacs were incubated for 20 min in simple media, there was severe interstitial oedema and disruption of the villus epithelium. Similar observations were made by Bridges (1980). As a result, the basic method was modified to an organ culture system by using tissue culture medium (TC 199), in place of simple salt buffers. The use of tissue culture medium greatly enhances the viability of the tissue and the system was successfully used to quantify *in vitro* the intestinal uptake of macromolecules (Rowland et al, 1981). This modified method has been used in uptake studies of liposomes, synthetic polymers (Blundell et al, 1993), and to precisely quantify the paracellular transport across the rat intestine.

Stewart et al. (1994) showed the histology at the electron microscope level, of everted sacs incubated for 1h in TC 199. It was shown that the general cell structure and tissue morphology were well preserved. A simple biochemical test of sac integrity was in the ability of the tissue from the duodenum and proximal

jejunum to transport glucose via active transport and to maintain a glucose concentration gradient inside the sacs (serosal side) up to 3.7 times higher than the outside (mucosal) concentration.

The active transport of glucose requires metabolic energy and so clearly if the sacs were not biochemically active, or if they were not physically intact, such a concentration gradient would not be maintained.

From the recovery of total glucose in the system, it was clear that the cells were metabolically active, with approximately 20% - 30% of the total glucose in the system being utilised by the sacs during 60 min of incubation. During these studies it was also observed that the sacs actively transported H<sup>+</sup> ions (Stewart et al, 1994).

The *in vitro* gut experiments tissue culture medium contained a colored indicator that facilitated a visual estimation of the pH of the medium. Careful and gentle handling of the tissue during preparation was found to be very important. The intestine needs to be removed as quickly as possible from the animal and the sacs prepared with the entire intestine are bathed in warmed TC 199 medium with constant oxygenation.

*In vitro* gut intestinal absorption offers a relatively quick and inexpensive technique for measuring uptake of drug into tissue. These considerations are important in comparing the methods, as the everted ring technique does not entail the considerable time and expense of start-up and maintenance of the Caco<sub>2</sub> cells, nor does it require the greater number of animals, with associated husbandry costs needed for statistical power with the perfusion method. Rings can be prepared from virtually any segment of intestine, permitting study of axial differences in uptake.

### **Techniques used in the study**

In this study two techniques were used to test absorption of CAA, the intestinal *in situ* perfusion and the *in vitro* gut sac absorption.

*In situ* perfusion was conducted to determine the  $K_{abs}$  (absorption rate constant) and  $t_{0.5}$  of absorption of CA across the rat intestinal membrane. Calculation was then done to determine the rate of absorption in the human intestine.

Only one concentration was tested, because the mechanism of CA absorption is well known and reported as via an active transport mechanism (Balaguer et al, 1997). Further, absorption in only one region of the intestine was studied (jejunum, first 15 cm), as the proximal part of the intestine was determined as the major site of absorption (Balaguer et al, 2002).

In this study cefuroxime axetil drug was tested for *in situ* and *in vitro* absorption. It is known that the parent drug (cefuroxime) is not absorbed, whereas the prodrug CA showed absolute bioavailabilities in human of 36% and 52% in the fasted and fed states respectively (Carretro et al, 2000). It had also been shown that during absorption from the GIT, CA was rapidly hydrolyzed by non-specific mucosal esterases to cefuroxime (C) and acetaldehyde (Balaguer et al, 1997).

As mentioned above, the mechanism of CA absorption is via a carrier mediated transport, which obeys Michaelis-Menten and first order kinetics in the proximal segment of the small intestine, and a passive diffusion mechanism in the mean and distal segments of the intestine. In another study, using Caco<sub>2</sub> cells, it was reported that CA enters the Caco<sub>2</sub> cells by simple diffusion (Dantzig et al, 1999).

In the *in vitro* gut tests, the gut sacs were not everted and were taken as sacs of 50 cm long from proximal and mean parts of the small intestine, they were filled with the drug dispersed in 0.01N HCl, and then isolated at both sides. Each sac was soaked in 50 ml TC 199 media in a flask at 37°C with oxygen aeration. A 0.01N HCl solution was chosen in accordance with the published literature which states that CA undergoes gelling in water (Deutsch et al, 1990-b and James et al, 1989). No evidence of gelling occurred in 0.01 N HCl (pH < 4). Also CA was stable in the solution for more than 3 hours as the stability of CA in this media revealed. The drug which was transported from inside the intestine to outside was withdrawn from the media at constant time intervals (every 15 min for 120 min), and analysed for the concentration of transported C.



The efficiency of the transport system was controlled by monitoring the followings:

1. Changes in the pH of the TC 199 media in the flask. This could be immediately noticed by changes in the color of the media if any leakage of 0.01N HCl from inside intestine to outside occurred, as the media is pink and it changes to yellow under acidic conditions.
2. CA analyses in the media, as if any destruction or leakage from the intestinal membrane occurred, CA would be found in the withdrawn samples from the media. For this purpose stability of CA in the TC199 media at 37°C was studied for 2 hrs, and it was found that > 85% of CA was recovered. Thus CA could be detected in the release media, if presented.
3. The viability of the membrane ,this was assured by the linear transport of the drug to the release media with respect to time.

Each *in vitro* gut absorption test (in this study) was conducted in triplicates.

## **2.8.2 Materials and methods**

### **2.8.2.1 *In situ* perfusion**

The *in situ* perfusion test was conducted according to methods previously published by Fagerholm et al. (1996).

The materials shown in Table 2.1 were used for the preparation of the perfusion media.

No.	Materials	Quantity
1.	NaCl Batch No.: 3264613358 Exp. Date: 11/03 Source: Scharlau	5.616 gm
2.	KCl Batch No.: 46891 Exp. Date: 05/06 Source: Scharlau	0.804 gm
3.	Mannitol Batch No.: E6LCI Source: Roguette	12.74 gm
4.	Glucose Batch No.: K19714474 Source: Merck	3.6 gm
5.	Na <sub>2</sub> HPO <sub>4</sub> Batch No.: 44474 Exp. Date: 01/06 Source: Sharlau	7.96 gm
6.	NaH <sub>2</sub> PO <sub>4</sub> Batch No.: K91116195907 Exp. Date: 10/03 Source: Sharlau	10.32 gm

Table 2.1: Materials used for the *in situ* perfusion media

### Media preparation method

The materials mentioned in Table 2.1 were transferred to a 2L volumetric flask and the volume was made up with Milli-Q water to 1500 ml volume with stirring. The pH was adjusted to 6.5 using NaOH or H<sub>3</sub>PO<sub>4</sub> solutions. Volume was adjusted with Milli-Q water to 2L.

### Solution preparation

A solution of CA in the perfusion media was prepared at a concentration of 0.1 mg/ml C. The drug was solubilised with the aid of sonication for 10 min upon cooling. CA was analysed initially using the HPLC method mentioned under section 2.9.2.2, and the results were recorded as the initial assay. The concentration in the perfusion study was chosen as (0.1 mg/ml), based on the fact that the dose of the drug given to the rat should be equivalent to the dose given to human. The equivalent dose was determined using the following equation.

$$\text{Dose (RAT)} = \frac{\text{wt of rat}}{\text{wt of human}} \times \text{Dose of human at a specified weight} \dots\dots\dots \text{Eq. 2.12}$$

$$\text{Dose (RAT)} = \frac{300 \text{ gm}}{15000} \times 125 = 2.5 \text{ mg Cefuroxime}$$

The volume of the in situ perfusion solution was 24 ml. This relates to the media flow rate previously reported of 0.2 ml/min for 2 hrs (120 min) (Fagerholm et al, 1996). Thus, a 0.1 mg/ml drug (C) concentration was needed for the in situ perfusion experiments.

***In situ* perfusion procedure**

A rat of weight 250g – 350g, fasted for 24 hr, was anaesthetised using ether compartment, followed by administration of 1M Ketamine (1ml). Labotomy was done starting from the large intestine and upwards. The intestine was traced to take the first segment from the jujenum(15 cm).

A partial cut was done away from the mysentry to allow the tip of infusion tube (1) to be entered, and the same was done at the end of the segment to put another infusion tube tip (2). Both were tied tightly to the intestine.

A 50 ml syringe filled with saline was flushed through the sealed intestine at a rate of 1 ml/min. The intestine was subsequently purged with air to remove any saline residue. A wet gauze was fitted on the exposed part of the stomach trying, as much as possible, to retain intestine parts inside.

Another syringe filled with filtered drug solution (using a saturated 0.45µm filter), was connected to the syringe pump at a rate of 0.22 ml/min. A long tube was used to heat the solution via a water bath, to 37°C, before entering to the intestine. The timer was started from the moment the drug solution entered the intestine. Meanwhile an ice bag was placed above the syringe to minimize CA hydrolysis, while a second tube and a clean graduated cylinder 10 ml were fitted to other end of the intestine.

Samples were collected every 10 min, for 100 min. The collected samples were immediately filtered using 0.45µm nylon filter, and stored in eppendorfs at -20°C. Samples were subsequently withdrawn and analysed using the method described under section 2.9.2.2.

### **2.8.2.2 *In vitro* gut absorption**

Preparation of the test media:

The content of TC 199 bottle (10g) was placed in a 1L volumetric flask, 0.35g NaHCO<sub>3</sub> were added, and volume was completed with purified water. The media was kept cool.

Rat Preparation:

Rats of weight around 0.3 kg were fasted for 24 hr, then anaesthetized by ether until death. The abdomen was incised, the intestine was traced from the beginning of the large intestine upward, and with avoiding the 15 cm of the ileum it was cut. About 50 cm from the small intestine was taken (length was measured accurately). The intestine was washed with 20 ml of saline water and squeezed gently to empty.

The intestine was assured to be viable by keeping it all time in the media and not allowed to dry. This was done either by putting the intestine on a spread media over a tray or in a beaker filled with the media.

After washing, the empty intestine was weighed and then one end of the intestine was tied up using a medical thread. Using a syringe, the drug suspension was loaded slowly, while avoiding any spillage. The second end of the intestine was then tied up and weighed upon loading. The drug remaining in the syringe and the volumetric flask were analysed for CA content.

A volume of 50 ml of TC 199 media was placed in a conical flask, which was pre-heated to 37°C and aerated with Carbogen gas (95% O<sub>2</sub>, 5% CO<sub>2</sub>). The intestine was then soaked in the media and timing of the measurements started. Measurements were undertaken after the initial immersion and then every 15 min for 120 min. Total of 2ml volume was withdrawn from each measurement and

substituted immediately with another fresh 2 ml media. Aeration of the conical flask was undertaken after each sampling, flasks were stoppered, and the samples taken were filtered and stored at -20°C for post analyses using the HPLC method described under section 2.9.2.3.

After 120 min, the intestine was removed from the flask, weighed after drying its surface with a guaze, and emptied in a test tube with squeezing. Washing of the inner surface of the intestine was done with 10 ml of saline water (Wash Sample), and the intestine gently squeezed. The samples were stored at -20°C for analyses using the HPLC method described under section 2.9.2.3.

To digest the intestine (for the purpose to obtain the residual cefuroxime) it was soaked in 2.5N NaOH for 2 hrs at 37°C in a water bath. This, however, led to complete destruction of the cefuroxime structure as confirmed by analyses of CA upon exposure to the same conditions.

#### **Drug suspension preparation**

A quantity of CA, equivalent to 25 mg cefuroxime, was transferred to a 10 ml volumetric flask. Prior to each experiment, the volume was made up with 0.01N HCl, with shaking to ensure complete wetting.

Cefuroxime dose was based on a 10X dose of the drug, which was chosen for easy quantitation of the material during analyses. The dose for the study was calculated as follows:

30 kg child → the dose is 250 mg cefuroxime.

0.3 kg rat → the dose is 2.5 mg cefuroxime.

10 X = 25 mg cefuroxime dose given to the rat.

## 2.9 HPLC ASSAY METHODS

### 2.9.1 Introduction

The USP, British and European pharmacopeia current editions issued monographs for testing of CA raw material . All HPLC assay methods mentioned in there included the same method conditions, parameters, instrumentation and materials. This indicated a reliable and valid method for analyses of CA. Because of this, it has been adopted in this study for the analyses of CA and C, and was tested for its suitability for detection and quantitation of C in the samples of the *in situ* perfusion and *in vitro* gut tests.

Changes in the method were needed to eliminate the interference of the tissue culture media (TC 99) with CA and C analyses, such changes were accompanied with validation to ensure the method suitability and validity.

A few non-pharmacopeial HPLC methods had been developed and published for analyses of CA. Of these, a simple reversed phase HPLC method for detection of C in the serum has been developed by Koot et al (1992). This method was based on cleaning up the serum with 93.3% solution of perchloric acid in water, and analyses using cefuroxime as an internal standard. Detection was made using a UV detector, at a wavelength of 275 nm.

Holt et al. (1990) reported a simultaneous assay method for some additional antibiotics found in combination in clinical samples. No interference was detected between these in urine, serum or cerebrospinal fluids. In another published method, an HPLC method for analyses of CA was described for the study of comparative pharmacokinetics of 2 brands of CA following a single intramuscular injection. The detection was based on UV method at 280 nm (Irshiad et al, 1995).

Rossel et al (1997) established a sensitive and selective method for determination of C in bronchoalveolar lavage fluid. The HPLC method included a UV detection at 280nm, a C18 column and a mobile phase of acetonitril 0.05M and ammonium phosphate buffer pH 3.2 (15 : 85) v/v. The method was found to be sensitive, selective and linear.

Another method reported by Klaus et al. (1998) was used for detecting the stability of CA in human intestinal fluid. The method utilised a C18 column maintained at room temperature, mobile phase I (0.002M Perchloric acid), mobile phase II (Acetonitril), a flow rate of 1 ml/min and a detector at wavelength of 265 nm. The separation eluent consisted of 84.0% mobile phase I for the first 6.5 min, and then it was changed to 62.0% for the 28.5 min, followed by washing with 84.0% mobile phase I for the 40 min.

Another assay method published by Sasinowska et al. (1995) described the use of the HPLC chromatography for the permeability determination of CA across the biological membrane, which included monitoring the absorbance at 280 nm.

## **2.9.2 Materials and methods**

### **2.9.2.1 HPLC assay method for testing CA content and homogeneity in mixtures**

For the analyses of the homogeneity of distribution and the content of CA in the mixtures prepared, the following assay of CA according to BP 2000 was applied .

Reference solutions:

Reference solution (a): 1 ml of the test solution was diluted to 100.0 ml with the mobile phase.

Reference solution (b): 5 ml of the test solution was heated at 60°C for 1hr to generate the  $\Delta^3$ -isomers.

Reference solution (c): 5 ml of the test solution was exposed to ultraviolet light at 254 nm for 24 hr to generate E isomers.

Standard solution: The solution was prepared immediately before use. 40.0 mg of cefuroxime axetil reference standard (CARS ) (BP, batch no. 2024) was dissolved in 20 ml of the mobile phase and then diluted to 200.0 ml with the same solvent.

Sample preparation (test solution): the solution was prepared immediately before use. A known mass of the material, equivalent to 40 mg cefuroxime, was transferred to a 200 ml volumetric flask containing 10 ml of methanol. The solution was cooled and sonicated for 10 minutes. The volumetric was subsequently filled

with the mobile phase, and upon complete dissolution of the drug, the solution was filtered using a 0.45µm filter that had been previously saturated with 20 ml standard solution. It was then stored at 2°C – 8°C.

The chromatography was carried out using the HPLC system (Waters 2690 Separations Module “Alliance”), column 0.25m long and 4.6 mm internal diameter, packed with trimethylsilyl silica gel for chromatography (L13) (5 µm), and the mobile phase was a mixture of 36% v/v of methanol R and 64% v/v of a 23 g/L solution of ammonium dihydrogen phosphate R. The flow rate was at 1.0 ml/min. The photodiode array detector was set at a wavelength of 278 nm. 20µl of each of reference solutions a, b, c and the standard solution were injected.

When the chromatograms were recorded in the prescribed conditions, the retention times relative to CA diastereoisomer A (second peak) were approximately 0.9 for CA diastereoisomer B, 1.2 for the CA  $\Delta^3$  – isomers, and 1.7 and 2.1 for the E isomers. The test was not considered valid unless in the chromatogram obtained with the standard solution, the resolution between the peaks corresponding to CA diastereoisomers A and B was at least 1.5. In the chromatogram obtained with reference solution b, the resolution between the peaks corresponding to CA diastereoisomers A and CA  $\Delta^3$  – isomer was at least 1.5.

The standard solution was injected six times. The assay was not considered valid unless the relative standard deviation of the sum of the peaks corresponding to CA diastereoisomers A and B was at most 2.0%.

The percentage content of  $C_{20}H_{22}N_4O_{10}S$  was calculated from the sum of areas of the two diastereoisomer peaks and the declared content of  $C_{20}H_{22}N_4O_{10}S$  in CARS.

#### **2.9.2.2 HPLC assay method for testing CA and C content in the *in situ* perfusion test**

Since CA undergoes hydrolysis in the intestinal conditions and is converted to cefuroxime sodium (C), both compounds CA and C were analysed. The method used was based on the BP 2000 monograph for analyses of CA, and its suitability



for analyses of both CA and C was confirmed by its validation for C analyses, as mentioned under 2.9.3.

Standard preparation – about 40 mg weights of cefuroxime, as cefuroxime axetil reference standard (CARS, batch no. 2024, BP) and cefuroxime working standard (CWS, batch no. CUC 05512, Orchid), were transferred to a 200 ml volumetric flask. 20 ml methanol was added, sonicated with cooling, and the volume was then completed with the mobile phase. The standard preparation was diluted with mobile phase to obtain standards with concentrations of 0.02, 0.005 and 0.002 mg/ml.

Sample preparation: each sample of the in situ perfusion test was taken from the freezer 30min before analyses, and sonicated for 7 minutes with cooling. The solution was then filtered using 0.45 $\mu$ m nylon filter that had been previously saturated with 30 ml standard preparation.

Reference solutions:

Reference solution (a). 1.0 ml of the standard preparation was diluted to 100.0 ml with the mobile phase.

Reference solution (b). 5 ml of the standard preparation were heated at 60°C for 1h to generate the  $\Delta^3$ -isomers.

Reference solution (c). 5 ml of the standard preparation were exposed to ultraviolet light at 254 nm for 24 hr to generate E isomers.

The chromatographic test was carried out using the HPLC system (Waters 2690 Separations Module “Alliance”). A 0.25m column with a 4.6 mm internal diameter packed with trimethylsilyl silica gel for chromatography (5  $\mu$ m) was used. The mobile phase – at a flow rate of 1.0 ml/min – was prepared as a mixture of 36% v/v of methanol R and 64% v/v volumes of a 23 g/L solution of ammonium dihydrogen phosphate R. The photodiode array detector was set at a wavelength of 278 nm.

20µl of each of reference solutions (a), (b), (c) and the standard solution were injected. When the chromatograms were recorded in the prescribed conditions the retention times relative to CA diastereoisomer A (second peak) were approximately 0.9 for CA diastereoisomer B, 1.2 for the CA Δ<sup>3</sup> – isomers, 0.35 for C and 1.7 and 2.1 for the E isomers.

The test was not considered valid unless in the chromatogram obtained with the standard solution, the resolution between the peaks corresponding to CA diastereoisomers A and B was at least 1.5. In the chromatogram obtained with reference solution (b), the resolution between the peaks corresponding to CA diastereoisomer A and CA Δ<sup>3</sup> – Isomer was at least 1.5.

The standard solution was injected six times. The assay was not considered valid unless the relative standard deviation of the sum of the peaks corresponding to CA diastereoisomers A and B is at most 2.0%, and the relative standard deviation of the peaks corresponding to C is at most 5% for the 0.005 mg/ml standard solution.

Volumes of 20µl sample preparation were injected into the chromatograph, the chromatograms were recorded, and the responses for the major peaks were recorded. The concentration of cefuroxime (mg/ml) present in each sample was calculated in the form of CA , and C as shown in equations 2.13 and 2.14 respectively:

$$\frac{\text{Sum peak area of diastereoisomers A + B in the sample}}{\text{Sum peak area of diastereoisomers A + B in the CARS}} \times \text{Conc. of CA RS} \quad \text{Eq.2.13}$$

$$\frac{\text{Peak area of C in the sample}}{\text{Peak area of the C in the WS}} \times \text{Conc. of C WS} \quad \dots\dots\dots \text{Eq. 2.14}$$

### **2.9.2.3 HPLC assay method for testing CA and C content in the *in vitro* gut absorption tests**

Since CA undergoes hydrolysis in the intestine and is converted to C, both compounds CA and C were analysed using the same HPLC method. Method used for *in situ* perfusion samples analyses mentioned under section 2.9.2.2, was tested for suitability for the analyses of *in vitro* gut sac samples, but was found to be not suitable, due to the interference of the test medium having TC 199 with the C peak. Thus, the method was altered as described below, and was validated to confirm its suitability and validity for *in vitro* gut samples analyses (as shown under section 2.9.3).

The mobile phase contained a filtered and degassed mixture of 0.2M monobasic ammonium phosphate and methanol (64 : 36). The 0.2M Monobasic ammonium phosphate was prepared by dissolving 23.0 g of monobasic ammonium phosphate in 1000 ml water.

Standard solutions were prepared by adding 40mg weights of cefuroxime, as CARS and as CWS in a 200 ml volumetric flask. 20 ml methanol was added, sonication with cooling was done and volume was completed with mobile phase. Standard preparation was diluted with the mobile phase to obtain standards of 0.02, 0.005 and 0.002 mg/ml concentrations with the mobile phase. CARS and CWS standards used for *in vitro* gut analyses were the same as those mentioned under section 2.9.2.2.

The liquid chromatography (Waters 2690 Separations Module "Alliance") HPLC system was equipped with a 320 nm (Waters 996 Photodiode Array) detector and a 4.6 mm × 25 cm column containing 5 µm packing L13. The flow rate was about 1.0 ml per minute. The resolution (R) between the CA diastereoisomer A and B peaks was not less than 1.5, the column efficiency was not less than 3000 theoretical plates when measured using the CA diastereoisomer A peak. The relative standard deviation for replicate injections was not more than 2.0%, and the relative standard deviation of the peaks corresponding to C was at most 5% for 0.005 mg/ml standard solution.

All frozen samples were taken from the freezer and kept at room temperature for 30 min before analysis, it was then sonicated with cooling and shaking for 5 min and immediately analysed after filtration using a 0.45 µm nylon filter saturated with 30 ml of standard preparation.

These samples include the followings:

Media samples: Those withdrawn (2ml) samples from the TC 199 medium surrounding the intestinal sac.

Intestinal (Wash & inside samples): Those taken from inside the intestine and its wash after the test. Samples were centrifuged before freezing for 10 min at 4,000 rpm in a cooled centrifuge.

Syringe wash samples: for the undissolved CA remaining in the syringe, the syringe was loaded with 3.5 ml methanol, shaken well after closing its end, to completely dissolve CA. The syringe content was then transferred to a 10 ml volumetric flask, swirled, sonicated for 10 min with cooling and shaking. Volume was completed to 10 ml with ammonium dihydrogen phosphate (23 g/L), followed by sonication with cooling for about 5 min.

Equal volumes (20µl) of the standard preparation and each sample preparation were separately injected into the chromatograph, the chromatograms were recorded and the responses for the major peaks were measured. The concentration of cefuroxime (mg/ml) present in each sample was calculated in the form of CA and C as mentioned under section 2.9.2.2, equations 2.13 and 2.14, respectively.

### **2.9.3 Validation of the HPLC methods**

#### **2.9.3.1 Validation of the HPLC method used for the *in situ* perfusion**

To ensure that the HPLC method mentioned in BP 2000 for CA analyses is also suitable and valid for analyses of C, the validation was done from different aspects, these included linearity, selectivity and stability.

#### **Linearity**

The linearity of the HPLC method was tested on 10 points calibration curve in the range of 0.99 to 79.20 µg cefuroxime/ml. Two solutions of each single

concentration were prepared and injected three times. Figure 2.9 shows the linearity results of this method.

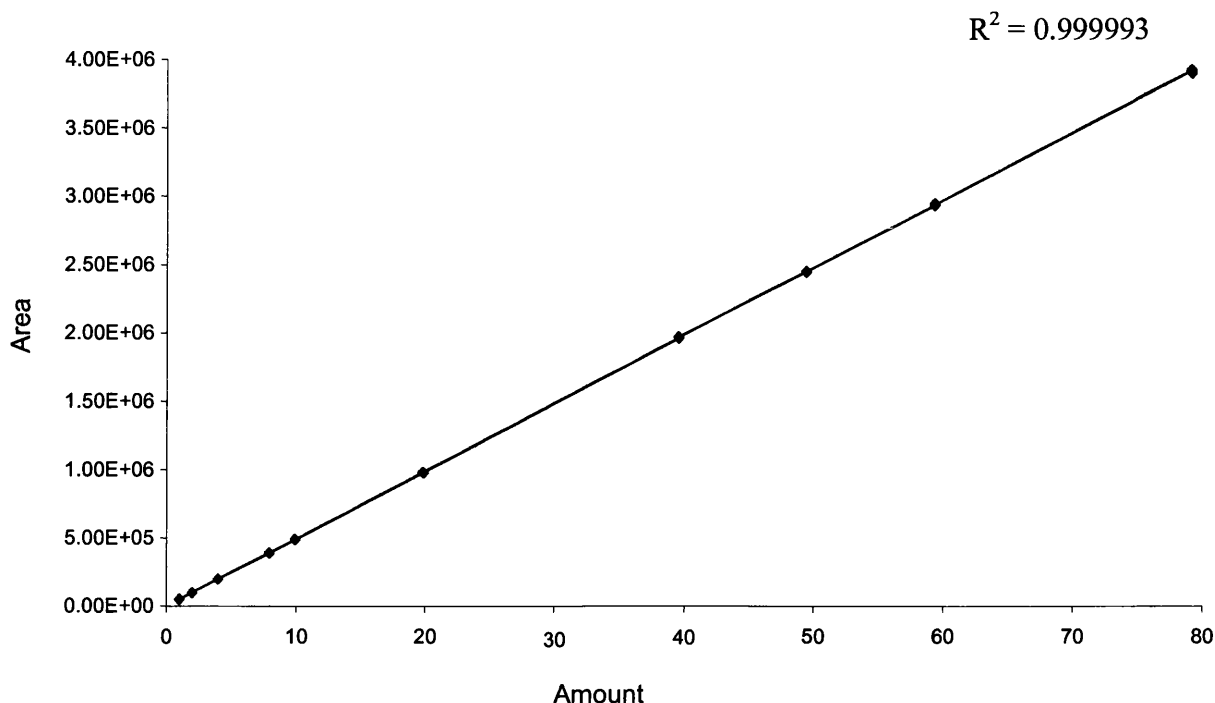


Figure 2.9: Linearity of C using the BP 2000 HPLC method of CA analyses

The linear regression coefficient of  $R^2 = 0.999993$ , indicated that the analytical method was quantitative.

#### ***In situ* perfusion media interference with the HPLC analyses of CA and C**

The standard solution was prepared as described in the method. A further sample was prepared exactly in accordance with the standard preparation, however with the exception to the dilution using solution 1 and solution 2 mentioned below.

Solution 1: obtained by passing 200 ml of the perfusion solution in the rat intestine.

Solution 2: the perfusion media itself, without passing through the intestine.

After the analyses, the chromatograms revealed that there was no interference of any of the solutions 1 and 2 with CA or C analyses.

### **Stability of CA in the perfusion media**

This test was done to study the effect of the perfusion media on the hydrolysis of CA, and to see the effect of the test conditions e.g. heat on the degradation of CA to  $\Delta^3$ -Isomer.

A weight of CAA, equivalent to 20 mg cefuroxime, was taken and transferred to a 200 ml volumetric flask containing 100ml perfusion media. The solution was sonicated for 15 min with cooling to avoid degradation and the volume was then made up to 200 ml with the same media. The solution was then filtered through 0.45 $\mu$ m nylon filter and analysed. The remainder of the solution was kept in a water bath adjusted at 37°C. Samples were analysed, at 0 and 2 hrs.

Results of this test indicated that CA degradation occurred with time in the perfusion media at 37°C. After 2 hrs, there was a loss of assay at 10% – 15% level, related to degradation of CA to C and to  $\Delta^3$ -Isomer. Thus cooling of the solution was necessary during *in situ* perfusion studies.

### **Adsorption of CA to the walls of syringes and tubes used for the *in situ* perfusion test**

A weight of CA equivalent to 50 mg cefuroxime was taken and transferred to 500 ml volumetric flask containing 100ml perfusion media. The solution was sonicated for 15 min, and the volume was made up with the same media. The solution was then filtered using 0.45 $\mu$ m filter and tested for the initial assay. A portion of the solution was stored at 2°C – 8°C, and considered as a reference solution.

A volume of the solution (60 ml) was transferred to a syringe, left for 2 hrs soaked in ice, and then analysed. Also 6 ml of the solution were passed into a tube (Enteplin, disposable infusion set), which was then closed from both sides and immersed in ice. Initial and two hours samples were taken and analysed for C and CA content.

Another simulation test was conducted where the parameters used for *in situ* perfusion were applied. The only exception was that the intestine was not

connected to the tubes during this study. Samples were collected through out the 100 min, and analyses was done for initial and every 30 min samples.

Results of these tests indicated that there was no adsorption of CA to the walls of the syringe or the tubes used for the in situ perfusion experiments, but there was a loss of CA assay related to its hydrolysis and degradation to C and  $\Delta^3$  isomer in the perfusion media under the conditions of the test.

### 2.9.3.2 Validation of the *In vitro* gut HPLC method

#### Lower limit of quantitation

2 $\mu$ g of cefuroxime/ml was taken as the LLOQ for this method. Table 2.2 shows LLOQ for C analyses.

Acceptance Criteria	Result
The analyte response at the LLOQ > 5 times the response of blank	5
RSD of analyte peak $\leq$ 20%	5.2%

Table 2.2: LLOQ for C analyses using the *in vitro* gut HPLC method of analyses

#### Recovery from tissue media

Recovery of cefuroxime from tissue media was tested in triplicate, by applying the method to samples of tissue media having amounts of C working standard added at a concentration range of 1 to 80 $\mu$ g/ml. Results were as presented in Table 2.3.

Acceptance Criteria	Result
% Recovery from LLOQ = 100 $\pm$ 20%	111.1
% Recovery from other preparations = 100 $\pm$ 15%	102.95

Table 2.3: HPLC Recovery results of C from the *in vitro* gut TC 199 tissue media.

According to the obtained results, it was concluded that this analytical method was accurate.

## Precision

Repeatability results for 6 injections are shown in Table 2.4.

C ( 4.983 $\mu\text{g}$ cefuroxime / ml)							%RSD
Injection #	1	2	3	4	5	6	
Peak area	10193	10545	10197	10541	9993	10228	2.12
R.T (min)	4.142	4.141	4.143	4.141	4.136	4.147	0.09

Table 2.4: Repeatability results of the *in vitro* gut HPLC method of analyses

## Intermediate precision:

Intermediate precision results of the HPLC method at the same concentration tested for precision, from analyst to analyst, and from day to day are as shown in Table 2.5.

Acceptance Criteria	Result
Repeatability of injection %RSD < 5	2.12%
Intermediate precision %RSD < 10%	From analyst to analyst = 0.40% From day to day = 0.40%

Table 2.5: Precision results of the *in vitro* gut HPLC method of analyses

According to the obtained results, it was concluded that this analytical method was precise.

## Linearity

The linearity of the HPLC method was tested on 10 points calibration curve in the range 0.99 to 79.20  $\mu\text{g}$  cefuroxime/ml. Two solutions of each single concentration were prepared and injected three times. Results shown in Figure 2.10 were obtained.



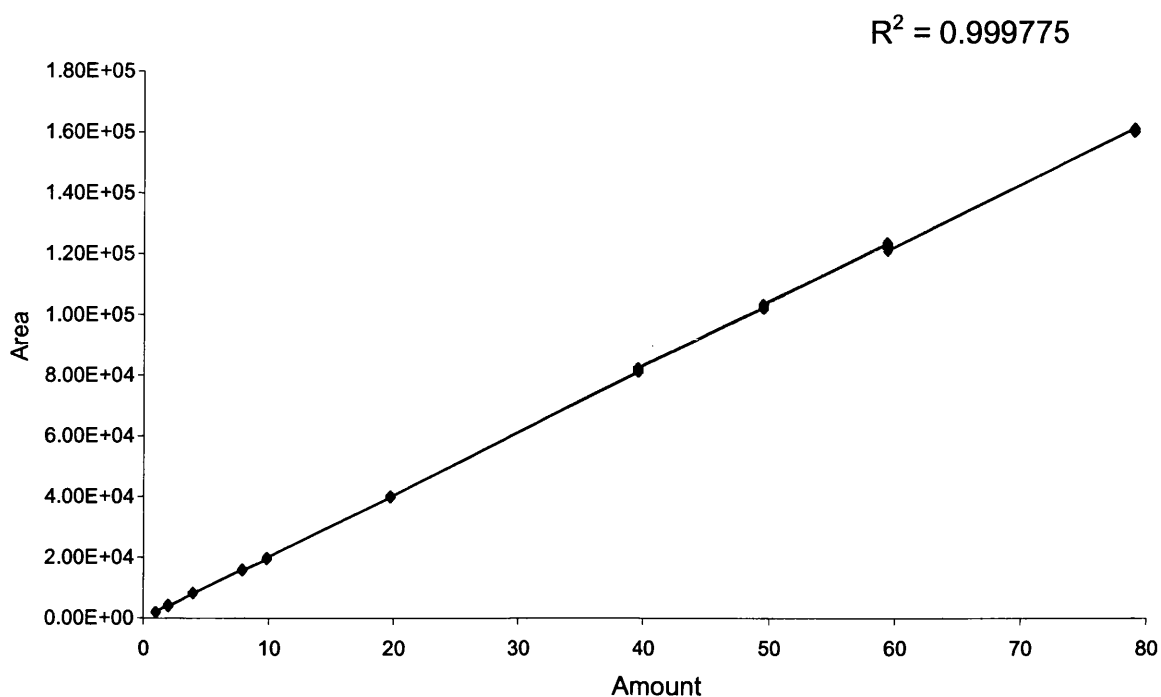


Figure 2.10: Linearity of C in the *in vitro* gut HPLC method of analyses

According to the obtained results, it was concluded that the analytical method is linear.

### Selectivity

The results of HPLC method selectivity for C and CA from tissue media indicated that the tissue media does not interfere with C or CA analyses.

### Stability

To determine the stability of C during analyses of *in vitro* gut samples, a solution of C in tissue media (4.983  $\mu\text{g}$  of cefuroxime/ml) was stored for 17 hrs at ambient temperature, and for 4 hrs at  $37^\circ\text{C} \pm 1$ , and then analysed. The test revealed that C concentration decreased by 6.0% and 10% when stored dissolved in tissue media at ambient temperature for 17 hrs, and at  $37^\circ\text{C} \pm 1$  for 4 hrs respectively.

A typical chromatogram of a standard solution of the *in vitro* gut HPLC method is shown in Figure 2.11.

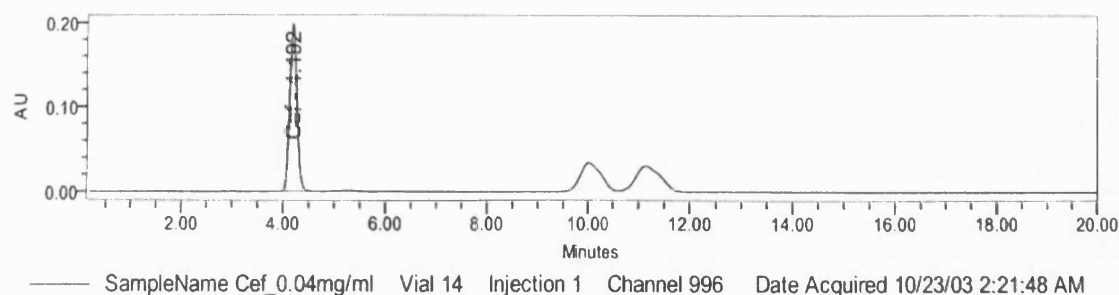


Figure 2.11: Typical chromatogram for a standard solution of the *in vitro* gut HPLC method of analyses.

## 2.10 KARL FISHER (WATER CONTENT) DETERMINATION

### 2.10.1 Introduction

The Karl Fischer titration is a moisture determination method specific for water and is suitable for samples with high moisture content (titrimetry) and also for those with water contents in the ppm range (coulometry). It was originally developed for non aqueous liquids (Harris et al, 1995), but is also suitable for solids if these are soluble or if the water they contain can be removed by heating in a stream of gas or by extraction.

The Karl Fischer method is used for many substances as a reference method. It is a chemical analyses procedure which is based on the oxidation of sulfur dioxide by iodine in a methanolic hydroxide solution. In principle, the following chemical reaction takes place (Skoog et al 1994):



The titration can be performed volumetrically or coulometrically. In the volumetric method a Karl Fischer solution containing iodine is added until the first trace of excess iodine is present. The amount of iodine converted is determined from the burette volume of the iodine-containing Karl Fischer solution. In the coulometric

procedure, the iodine participating in the reaction is generated directly in the titration cell by electrochemical oxidation of iodide until again a trace of unreacted iodine is detected.

### **2.10.2 Materials and methods**

A volume of 35-40ml methanol were transferred to the titration vessel. Titration with the Karl Fischer reagent to the electrometric endpoint was done to consume any present moisture in the sample.

An accurately weighed quantity of 100 mg sample to be tested was mixed and titrated with Karl Fischer reagent to the electrometric endpoint. Water content of the specimen was calculated in mg, as shown in equation 2.15:

$$\text{Water content} = S \times F \dots\dots\dots \text{Eq 2.15}$$

Where S is the volume in ml of Karl Fischer reagent consumed in the titration. F is the water equivalence factor of the Karl Fischer reagent.

## CHAPTER 3

### PHYSICAL PROPERTIES OF CEFUROXIME AXETIL AMORPHOUS POWDER (CAA) AND COMPRESSED (CAA<sub>c</sub>) AND CEFUROXIME AXETIL CRYSTALLINE (CAC)

#### 3.1 INTRODUCTION

It has been reported that cefuroxime axetil (CA) exists in an amorphous (CAA) and a series of crystalline forms (CAC) (Oszczapowicz et al, 1995; Sansinowska et al, 1995; Crisp et al, 1985). Sasinowska et al. have reported that CA serum concentration after oral administration in rats was dependant on the form as well as the particle size of the drug (Sasinowska et al, 1995).

The levels of cefuroxime in the serum 15 min after oral administration of CAA with a median particle size of 0.09 mm were found to be significantly greater ( $\geq 63\%$ ) than administration of particles with a median particle size of 0.4 mm. In addition, for the same particle size distribution, cefuroxime serum levels 15 min after administration of the amorphous CA were 120% greater than the crystalline form.

Oszczapowicz observed three forms of cefuroxime axetil, named A<sup>I</sup>, A<sup>II</sup> and K, all of which were found to be significantly different (Oszczapowicz et al, 1995). Form A<sup>I</sup> was found to possess the highest solubility values in different media, while form A<sup>II</sup> showed a slightly lower solubility in chloroform, methylene chloride, and N,N-dimethyl acetamide. The absolute bioavailability values were  $25.85\% \pm 1.53\%$  and  $23.95\% \pm 0.62\%$  for forms A<sup>I</sup> and A<sup>II</sup> respectively. When thermal DSC analyses was done, it showed an endothermic peak for form A<sup>I</sup> between 84°C – 86°C and for A<sup>II</sup> between 135°C-138°C. The form A<sup>I</sup> showed a higher solubility and a better bioavailability than form A<sup>II</sup>, indicating a higher molecular packing in the latter, thus a reduced dissolution rate.

Form K showed a melting peak between 179°C-181°C. This form was found to have the lowest solubility and absolute bioavailability ( $19.68\% \pm 0.37\%$ ) of all. This was related to being the crystalline form of the drug which has the lowest solubility and bioavailability.

The *in vitro* dissolution behaviour of these forms was also compared in the study. Forms A' and A'' were readily suspended in the total volume of gastric fluid and, subsequently, dissolved rapidly. The dissolution of form A' was found to be slightly greater. In the case of the crystalline form K, both suspension formation and dissolution were comparatively slow (Oszczapowicz et al, 1995). However data from this thesis show different interpretation of results of analysis for the different forms of cefuroxime axetil (CA).

Crisp et al. (1985) had first prepared CA in the substantially pure amorphous form. It was found that despite the well known tendency of amorphous materials to have inferior chemical stability to the crystalline form, and the known tendency for highly pure amorphous material to crystallise, this was not the case with amorphous CA. The crystalline form was surprisingly not found to have the best balance of properties for commercial use, and contrary to previous experience in the cephalosporin field, CA was advantageously used in a highly pure substantially amorphous form. Crisp et al. also determined that CA in its pure amorphous form had higher bioavailability upon oral administration with respect to the crystalline form. Moreover, the amorphous form of CA had adequate chemical stability upon storage (Crisp et al, 1985).

Amorphous preparation of CA by Crisp et al. contained less than 5% w/w of impurities. Any residual solvent was in concentration of less than 2% w/w. Typical impurities which were found to be present were the  $\Delta^3$ -isomers of CA and its corresponding E-isomers. The prepared CA ester was essentially free from the crystalline form, i.e. it contained < 5% CAC, and it was in the form of a (1:1) mixture of its R and S isomers. Such a mixture was found to have a substantially improved solubility as compared with amorphous R isomer or amorphous S isomer alone. It was prepared by recovery of CA from a solution under conditions whereby the highly pure substantially amorphous form of the product was obtained. Techniques that were employed included the rapid removal of solvent Lacquer to precipitate the drug. Other satisfactory methods included spray drying, roller drying, solvent precipitation and freeze drying (Crisp et al, 1985).

Following intensive work on the preparation of substantially pure amorphous form of CA, Crisp et al. confirmed that spray drying technique was the best method for obtaining the pure amorphous form of the drug (Crisp et al, 1989). In this technique a suitable organic solvent for dissolving CAC was used (e.g. ketones, alcohols, acetonitrile, tetrahydrofuran, esters, chlorinated solvents), or mixtures with other solvents (e.g. water) (Crisp et al, 1991). The drying gases tested were inert gases such as nitrogen, argon, and carbon dioxide. The gas inlet temperature to the spray dryer was chosen according to the solvent used, and was in the temperature range of 50°C-140°C. The gas outlet temperature was similarly dependent on the solvent and was in the range 45°C-100°C.

The spray dried product had a consistent range of particle sizes, and it had the form of hollow microspheres which could conveniently be used for pharmaceutical compositions.

It was subsequently reported that the prior art processes for the preparation of amorphous form of CA suffered several disadvantages, and were not suitable for operation at a large scale (Handa et al, 2002). These disadvantages included the requirement of large volumes of solvents for dissolving CA, because of its poor solubility in the solvents utilised. This was considered uneconomical on a commercial scale because large size reactors were necessary. Furthermore, because of the poor solubility of CA, higher temperatures were required. These disadvantages made the process operationally tedious and inefficient.

Handa et al. (2002) analysed a method for preparing CAA, which comprised dissolving CAC in a solvent such as formic acid, present in an amount just sufficient to dissolve the CAC. The resulting CA solution was added to water all at once, leading to rapid precipitation (dumping) due to the anti-solvent effect of water on CA. The crystallinity of the resulting product was greatly reduced via dumping, i.e., the product was highly amorphous by use of the rapid precipitation method. Additionally, it had been determined that in order to precipitate an amorphous product that contained minimal amount of crystalline material, a specific volume of water is required in relationship to the weight of the starting material (CAC).

Handa et al. (2002) applied the same process for the preparation of the pure CAA by dissolving CAC in acetic acid instead of formic acid, including at least 5% v/v water. Thus these new methods opened the door for highly efficient methods to obtain CAA.

Since CAC was not found to possess the necessary bioavailability characteristics, the amorphous CA was registered throughout the world. This remained until Zenoni et al. prepared a comparable bioavailable form of CAC. This was achieved by treating the crystalline and the amorphous forms with a mixture of water or water miscible organic solvent at a temperature between 20°C – 60°C, followed by cooling (Zenoni et al, 1997).

More recently, Woo et al. (2000) confirmed what Oszczapowicz et al. published in 1995, of that CA exists as a crystalline form having a melting point of about 180°C, and two other forms of endothermic peaks at about 70°C and 135°C. The same was also reported by Guk et al. (2002) who stated that CA can be found as a crystalline form which has a melting point at 175°C, and as other two forms having endothermic peaks at 80.25°C and 137.7°C, respectively. These different forms were obtained due to different preparation parameters and conditions, such as cooling rate during crystallisation.

It was noticeable, however, from the published data that the onset temperatures of the endothermic peak for amorphous CA are different. Such differences were also found in this study, and can be related to dynamic shifts in the  $T_g$  temperature at different water content levels in the material.

This shifted  $T_g$  of CAA has been shown in this study to revert back to its original temperature under vacuum drying. This has not been the case with the other known amorphous pharmaceutical systems, e.g. Lactose (Mahlin et al, 2003; Buckton et al, 1996) which upon exposure to elevated conditions of temperature and/or relative humidity undergoes irreversible changes in its physical properties (crystallisation). This indicates a superior stability of CA amorphous system, which enables it to maintain the state of desirable physical properties even upon fluctuation in the storage conditions.

Woo et al. (2002) previously reported that the water absorbed in CA is judged to be bound water which causes physico-chemical changes in the drug, leading to shifting in its endothermic peak onset.

The current commercially available CA formulations, Ceftin<sup>®</sup>, are prepared from the highly pure amorphous CA produced by the spray drying method under careful processing to avoid the possible conversion to the crystalline form upon storage (Somani et al, 2003).

Current BP, USP and Eur. Ph monographs for CA do not specify a requirement for the form of the drug. That is, it may be in either amorphous or crystalline forms, but both forms should meet the criteria for dissolution when in its tablets form (>60% after 15 min and >75% after 45 min).

In this study, both CAA and CAC forms were investigated in order to further understand their physical properties. The effect of some processes on these forms was also studied, e.g. the effect of compression on CAA. The compressed form of CAA was defined as CAAc.

### 3.2 MATERIALS AND METHODS

Table 3.1 defines the tested amorphous and crystalline preparations of CA .

Material Parameter	CAA	CAC
Batch No.	CAFAA/003/00	CRCB030005
Assay	81.8% (as cefuroxime)	83.4 (as cefuroxime)
Water Content	0.99%	0.16%
Retesting Date	12/2003	02/2006
Source	Orchid	Orchid

Table 3.1: Amorphous and crystalline CA materials tested.



The compressed cefuroxime axetil amorphous (CAAc) was prepared by compacting CAA powder into 10 mm biplanar tablets with a hardness range between 70–90 N, using a single punch compression machine (Erweka EKO).

Tablets were then crushed through 0.2mm screen. The crushed powder was subsequently passed through a set of sieves, and particles passed through the 63µm sieve were collected. This final step was done to obtain a similar particle size distribution for CAAc to CAA and CAC materials used in the study.

Conditioned forms of the amorphous and crystalline materials were prepared upon exposure to elevated relative humidity. The particles were exposed to a saturated solution of di-sodium hydrogen phosphate dodeca hydrate ( $\text{Na}_2\text{HPO}_4 \cdot 12\text{H}_2\text{O}$ ) in a sealed vessel. The saturated atmosphere had a relative humidity (RH) of 95%, at 25°C. CAA and CAC were placed in the sealed vessel for 10 days, samples were called CAAh and CACH, respectively.

DSC testing and water content analyses of the stored samples were done prior and at different time intervals (3 days, 1 week and 10 days) upon exposure to 95%RH at 25°C. Further, a one week sample of the CAAh powder was taken, dried in a vacuum oven for 10 hours, and subsequently analysed. This sample was labelled CAAd.

### 3.2.1 Methods of testing CAA, CAC and CAAc

All materials were compared by the testing methods summarised in Table 3.2.

Material	DSC chapter 2 section 2.1.2	MTDSC chapter 2 section 2.2.2	Particle size distribution chapter 2 section 2.3.2	XRPD chapter 2 section 2.4.2	DVS chapter 2 section 2.5.2	Intrinsic dissolution chapter 2 section 2.7.2.1	Dissolution using App II chapter 2 section 2.7.2.2	<i>In situ</i> perfusion Chapter 2 section 2.8.2.1	<i>In vitro</i> gut test chapter 2 section 2.8.2.2	<i>Karl Fisher</i> chapter 2 section 2.10.2
CAA	✓	✓	✓	✓	✓	✓	x	✓	✓	✓
CAAh	✓	x	x	x	x	x	x	x	x	✓
CAAd	✓	x	x	x	x	x	x	x	x	✓
CAAc	✓	✓	✓	✓	✓	x	✓	x	✓	x
CAC	✓	✓	✓	✓	✓	✓	x	x	✓	✓
CACH	✓	x	x	x	x	x	x	x	x	✓

Table 3.2: Comparative tests for CAA, CAC, CAAc, stored at different conditions.

✓ : Tests performed    x : Tests not performed

### 3.3 RESULTS AND DISCUSSIONS

#### 3.3.1 Particle size distribution

##### 3.3.1.1 Particle size distribution of cefuroxime axetil amorphous (CAA)

The particle size distribution of CAA in the Log-normal form is presented in Figure 3.1.

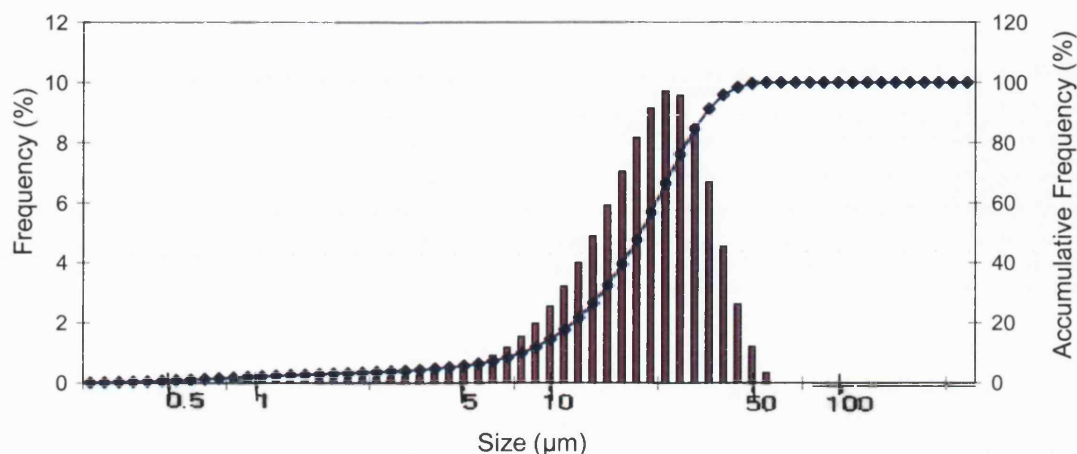


Figure 3.1: Log-normal particle size distribution of CAA

The geometric mean diameter (median diameter) for CAA tested was 19.5 µm.

The geometric standard deviation ( $\sigma$ ) of the particle size distribution was calculated as shown in equations 3.1 and 3.2 below.

$$\begin{aligned} \sigma &= \frac{d_{50}}{d_{15.78}} \dots\dots\dots \text{Eq. 3.1} \\ &= \frac{19.5 \mu\text{m}}{12.0 \mu\text{m}} = 1.63 \end{aligned}$$

and

$$\begin{aligned} \sigma &= \frac{d_{84.13}}{d_{50}} \dots\dots\dots \text{Eq. 3.2} \\ &= \frac{34.5 \mu\text{m}}{19.5 \mu\text{m}} = 1.75 \end{aligned}$$

The results above indicated that fine particles of CAA material were used in the study. The standard deviation ( $\delta$ ) of the CAA particle size distribution indicated a log-normal distribution.

### 3.3.1.2 Particle size distribution of cefuroxime axetil crystalline (CAC)

The Log-normal CAC particle size distribution is shown in Figure 3.2.

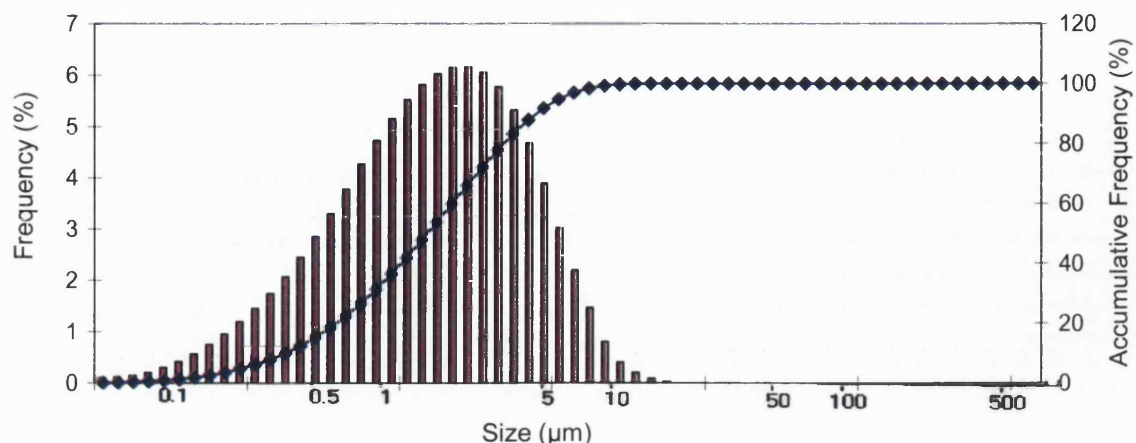


Figure 3.2: Log-normal particle size distribution of CAC

The geometric mean diameter (median diameter) of tested CAC was determined to be 3.3 µm. The geometric standard deviation of the particle size distribution was calculated according to equations 3.1 and 3.2.

$$\sigma_g = \frac{d_{50}}{d_{15.78}} = \frac{3.3 \mu\text{m}}{1.59 \mu\text{m}} = 2.0$$

and

$$\sigma_g = \frac{d_{84.13}}{d_{50}} = \frac{6.72 \mu\text{m}}{3.3 \mu\text{m}} = 2.0$$

Results indicated that the particle size of the CAC material used in the study was less than 5µm. This can be related to the fact that manufactures of CAC tend to micronize the material, aiming to increase the surface area, thus enhancing the dissolution and bioavailability of this form of the drug. The standard deviation ( $\delta$ ) of the CAC particle size distribution indicated a log-normal distribution.

### 3.3.1.3 Particle size distribution of compressed cefuroxime axetil amorphous (CAAc)

Figure 3.3 represents the log-normal particle size distribution of CAAc.

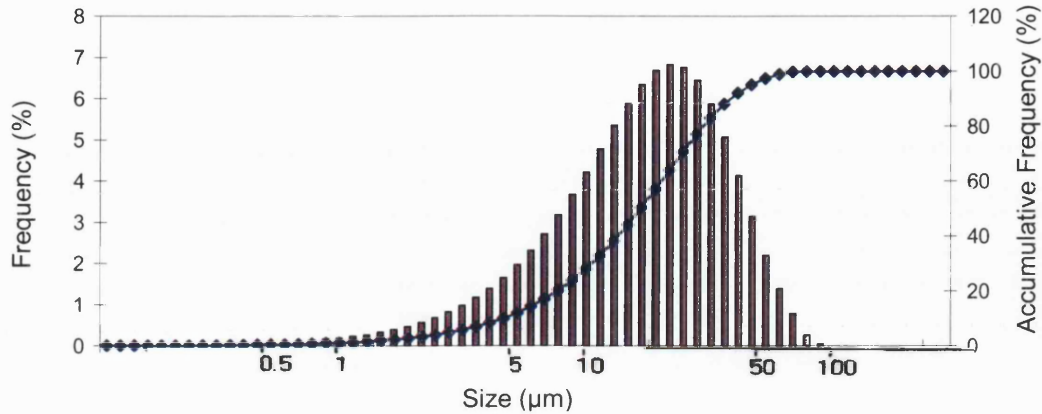


Figure 3.3: Log-normal particle size distribution of CAAc

The geometric mean diameter (median diameter) of tested CAAc was determined to be 21.9µm. The geometric standard deviation of the particle size distribution was calculated according to equations 3.1 and 3.2.

$$\sigma_g = \frac{d_{50}}{d_{15.78}} = \frac{21.9 \mu\text{m}}{10.9 \mu\text{m}} = 2.0$$

and

$$\sigma_g = \frac{d_{84.13}}{d_{50}} = \frac{44.4 \mu\text{m}}{21.9 \mu\text{m}} = 2.0$$

The particle size distributions of CAA, CAC and CAAc revealed that CAA and CAAc particles tested had similar d50 values, (around 20µm), while the CAC had the finest particles (d50 = 3µm). The standard deviation ( $\delta$ ) of the CAAc particle size distribution indicated a log-normal distribution.

### 3.3.2 DSC and MTDSC testing

DSC thermograms for CAA, CAAc and CAC are shown in Figures 3.4-a, b, and c, respectively.

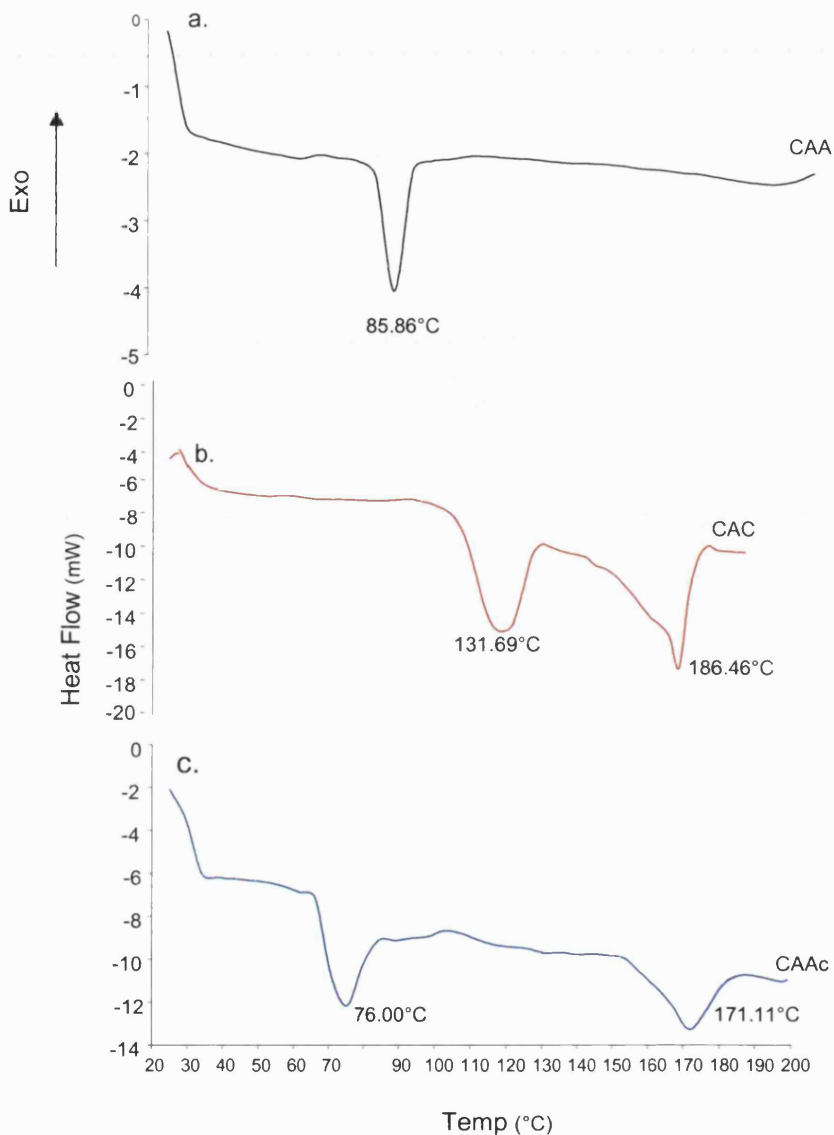


Figure 3.4: DSC thermograms of CAA(a), CAC(b) and CAAC(c), at the heating rate 25°C/min.

The DSC thermogram of CAA material showed an endothermic peak at 85.9°C. The CAAC thermogram showed two endothermic peaks, one at 76.0°C and the other at 171.1°C. For CAC, two endothermic peaks were also detected at 131.7°C and at 186.5°C.

To further elucidate the endothermic peaks in the DSC tested samples, MTDSC analyses was also undertaken. The heat flow and the heat capacity ( $C_p$ ) thermograms of CAA are shown in Figures 3.5 and 3.6 respectively.

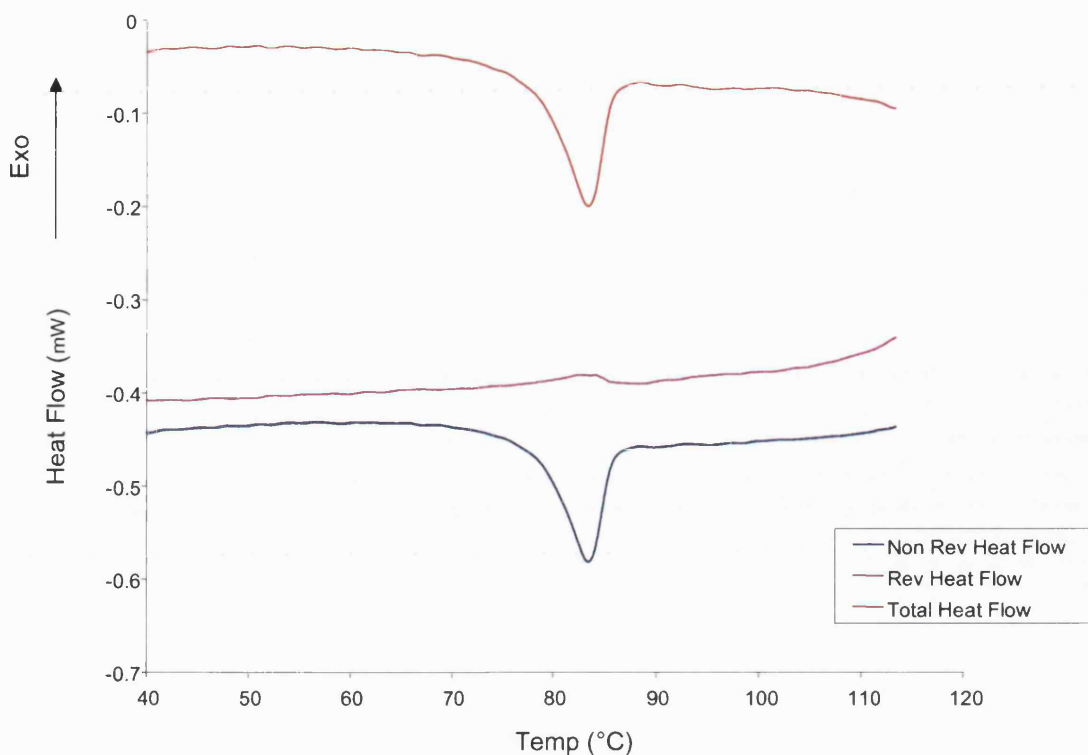


Figure 3.5: MTDSC heat flow thermograms of CAA, at heating rate 1°C/min, amplitude 0.5°C/48 seconds.

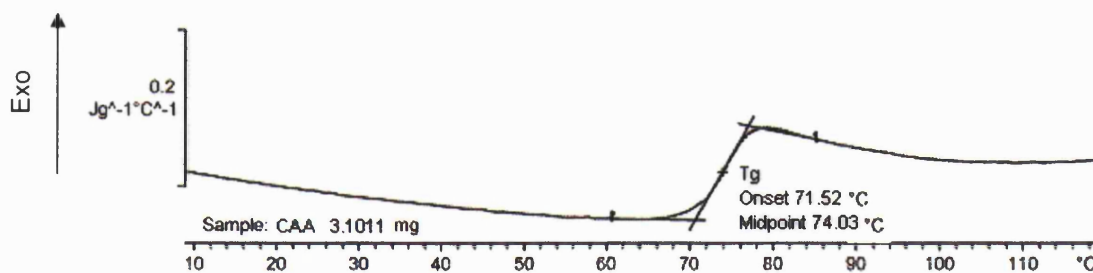


Figure 3.6: Heat capacity curve (C<sub>p</sub> complex) of CAA, at heating rate 1°C/min, amplitude 0.5°C/48 seconds

The MTDSC heat flow thermograms of CAC are presented in Figure 3.7. Figures 3.8 and 3.9, respectively, show the heat flow and C<sub>p</sub> thermograms of CAAC.

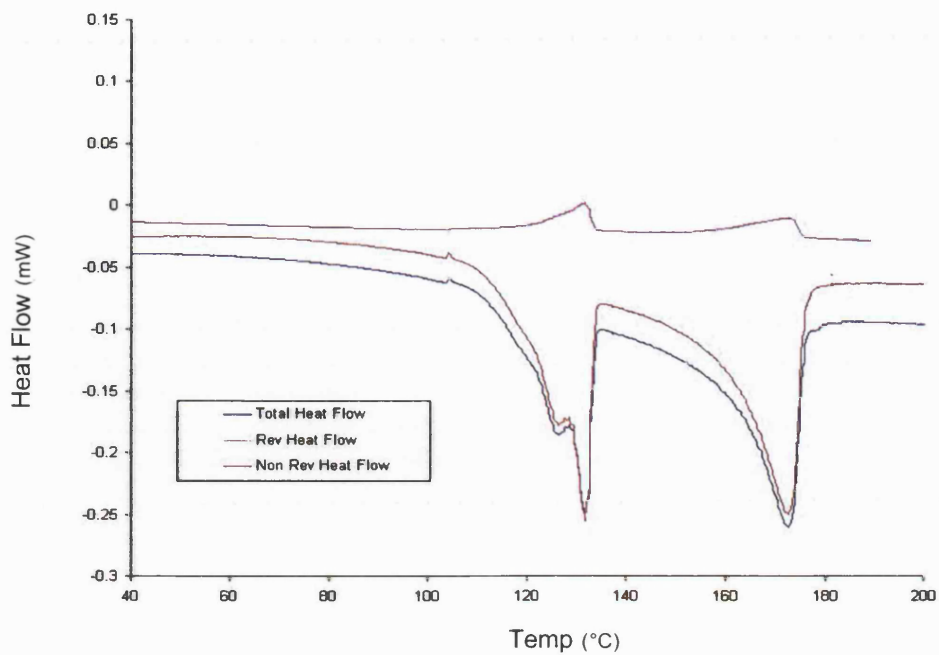


Figure 3.7: MTDSC heat flow thermograms of CAC, at heating rate 1°C/min, amplitude 0.5°C / 48 seconds.

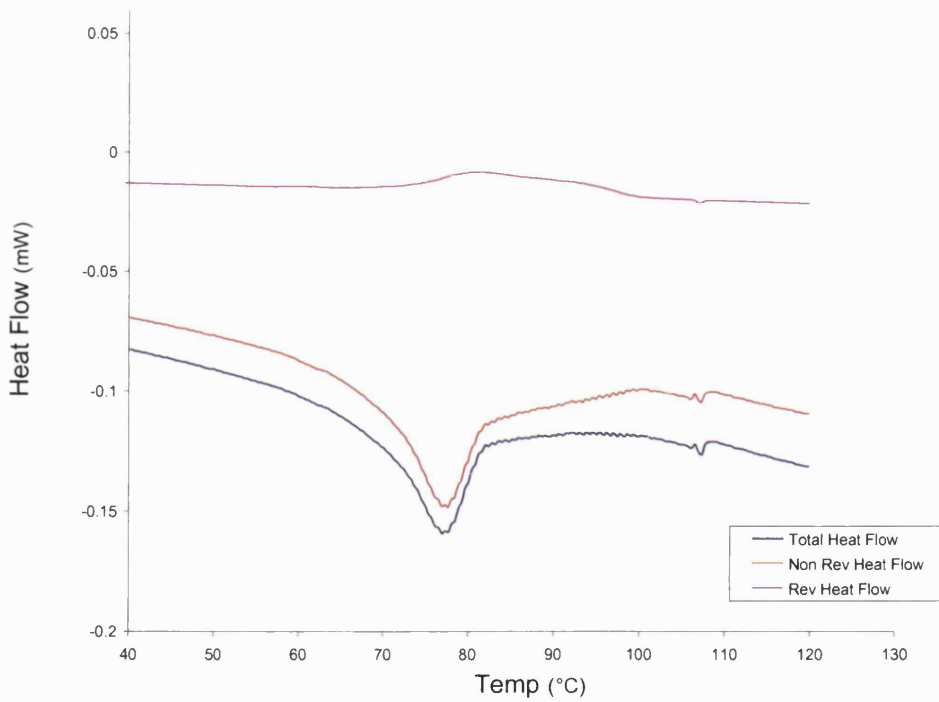


Figure 3.8: MTDSC heat flow thermograms of CAAC, at heating rate 1°C/min, amplitude 0.5°C / 48 seconds.

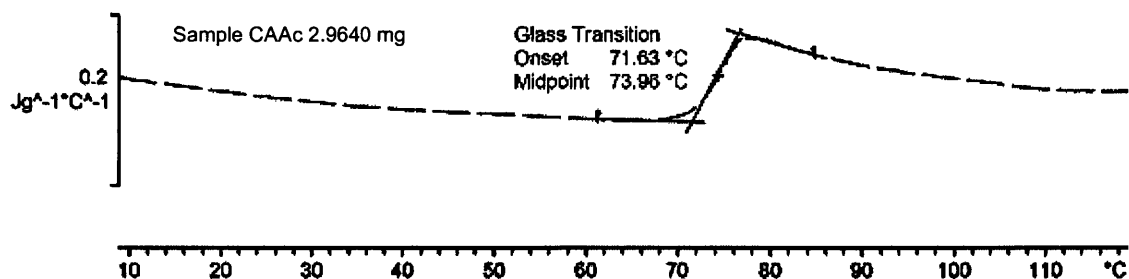


Figure 3.9: Heat capacity curve ( $C_p$  complex) of CAAC, at heating rate  $1^\circ\text{C}/\text{min}$ , amplitude  $0.5^\circ\text{C}/48$  seconds.

From the MTDSC results shown above, the endothermic peaks of CAA and CAAC at around  $80^\circ\text{C}$  were interpreted as the glass transition temperature of the amorphous material with a mid point of  $74^\circ\text{C}$ , overlapping the relaxation peak. For CAA and CAAC, the non-reversing heat flow curves show a relaxation peak which was separated from the glass transition temperature using the MTDSC. While for CAC, the reversing heat flow curve did not reveal glass transition at any temperature. It might indicate, however, a second polymorph of the crystalline form of the drug.

When CAC samples from different raw material sources were tested, similar results were obtained. This may indicate that manufacturers of the crystalline material prepare the CAC as a mixture of two polymorphs, one of which has a lower melting temperature at  $135^\circ\text{C}$ . This can either be related to the manufacturing or crystallisation procedures, or to aimed selection, to possibly enhance dissolution and bioavailability.

After compression, the DSC thermogram of CAAC gave rise to a new melting peak characteristic of the crystalline form of the drug at  $171^\circ\text{C}$ . When the melting enthalpy ( $9.3\text{J}/\text{g}$ ) of the generated CAC peak was fitted to CAC enthalpy/concentration curve (Figure 3.10), it revealed an approximate content of 15% crystalline material in the sample. This suggested that compression may result in partial transformation of the pure amorphous CA to the crystalline form. This may be related to the heat and pressure generated during compression and crushing of CAA. These may have significant plasticization effect on the material, and can



lower the  $T_g$  below the experimental temperature under compression or slugging. Thus increasing the entropy of the molecules and enhancing crystallisation. The amount of crystallised material would be dependant on how much heat and pressure are generated, and on how the drug was distributed in the slugged matrix.

This may also be related to the fact that pressure effects on CAA may be significant enough to affect its molecular packing, potentially reducing the volume and enthalpy, leading to crystallisation in some parts of the slugs where the compressive load is at maximum.

An enthalpy/concentration calibration curve was established (using DSC analyses) for the determination of crystalline content in CAA material. The calibration curve was established for 5mg mixtures containing different concentrations of CAC (1%, 2%, 4%, 5%, 25%, 50%, 75% and 100%) with CAA material. Melting enthalpy values of the crystalline peak were obtained at the different concentrations of CAC. Results were as shown in Figure 3.10. Also a calibration curve based on relaxation enthalpy values of the different concentrations of CAA in the same mixtures was plotted and results were compared to those of the CAC calibration curves. It was unexpectedly found that data from both curves were comparable.

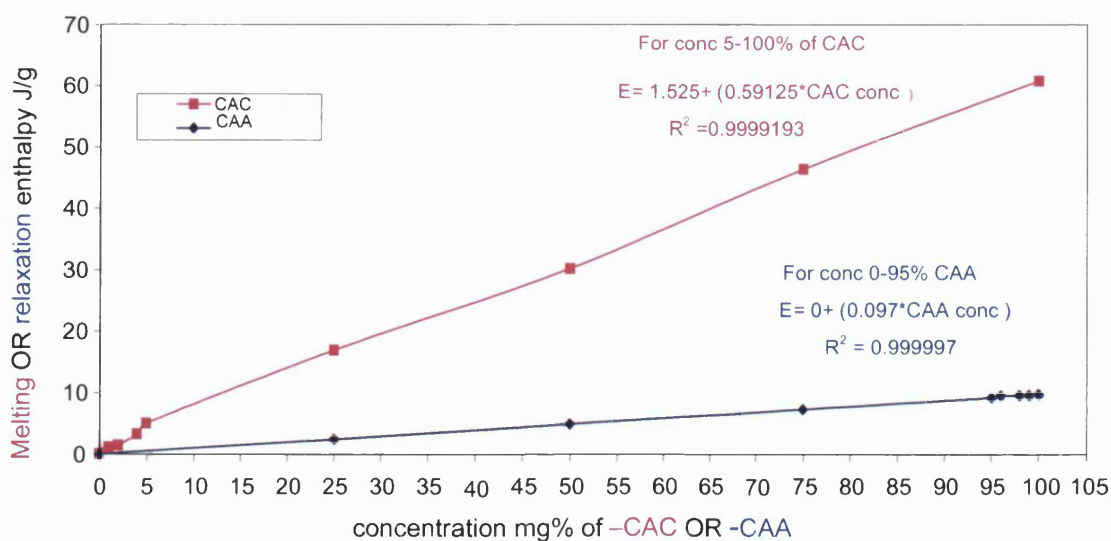


Figure 3.10: Enthalpy/concentration calibration curve of CAA mixtures with CAC

Results above indicated that the DSC is a good technique for the detection of down to 1% w/w CAC in a mixture with CAA, although not quantitative for concentrations below 5% w/w (as the both curves showed loss of linearity below this concentration).

It was noticed that the DSC thermograms of different CAA samples show different onset values for  $T_g$ . This was further studied and found to be related to plasticization effect of water on samples having different water content levels.

Figure 3.11 shows the plasticization effect of water on the  $T_g$  of CAA. The thermograms of CAAh demonstrated that there is a shift in the  $T_g$  towards lower temperatures upon exposure to humid conditions. This may be related to the increasing water content in the amorphous material. The plasticization effect of the sorbed water can be summarised by increasing the free volume, reducing the viscosity of CAA and increasing its molecular motion. Thus reducing the  $T_g$  of the amorphous material (Royall et al. 1999; Zografis et al. 1990). The thermogram of CAA<sub>d</sub> indicated that upon vacuum drying the conditioned material loses its water, and its  $T_g$  reverts back to its original temperature.

These data demonstrated an unusual stability of the amorphous form of CA compared to other pharmaceutical amorphous systems, which may undergo crystallisation upon short term exposure to humid conditions. Of these, amorphous sucrose which crystallises at conditions above 21% relative humidity at 30°C (Oksanen et al, 1999). Spray dried amorphous lactose has also been reported to recrystallise after 11 hrs of storage at 53% RH at 25°C (Mahlin et al, 2003; Buckton et al, 1996). Price et al (2003) also studied the recrystallisation transformation of amorphous lactose during moisture uptake at 58%RH and 75%RH. They suggested that a secondary nucleation and growth process occurs at these humid conditions, and that primary nucleation requires an elevated relative humidity (94%RH). Other reported examples of unstable amorphous systems include the crystallisation of amorphous indomethacin and phenobarbital at temperatures below their glass transition temperatures (Yoshioka et al, 1994; Fukuoka, 1989).

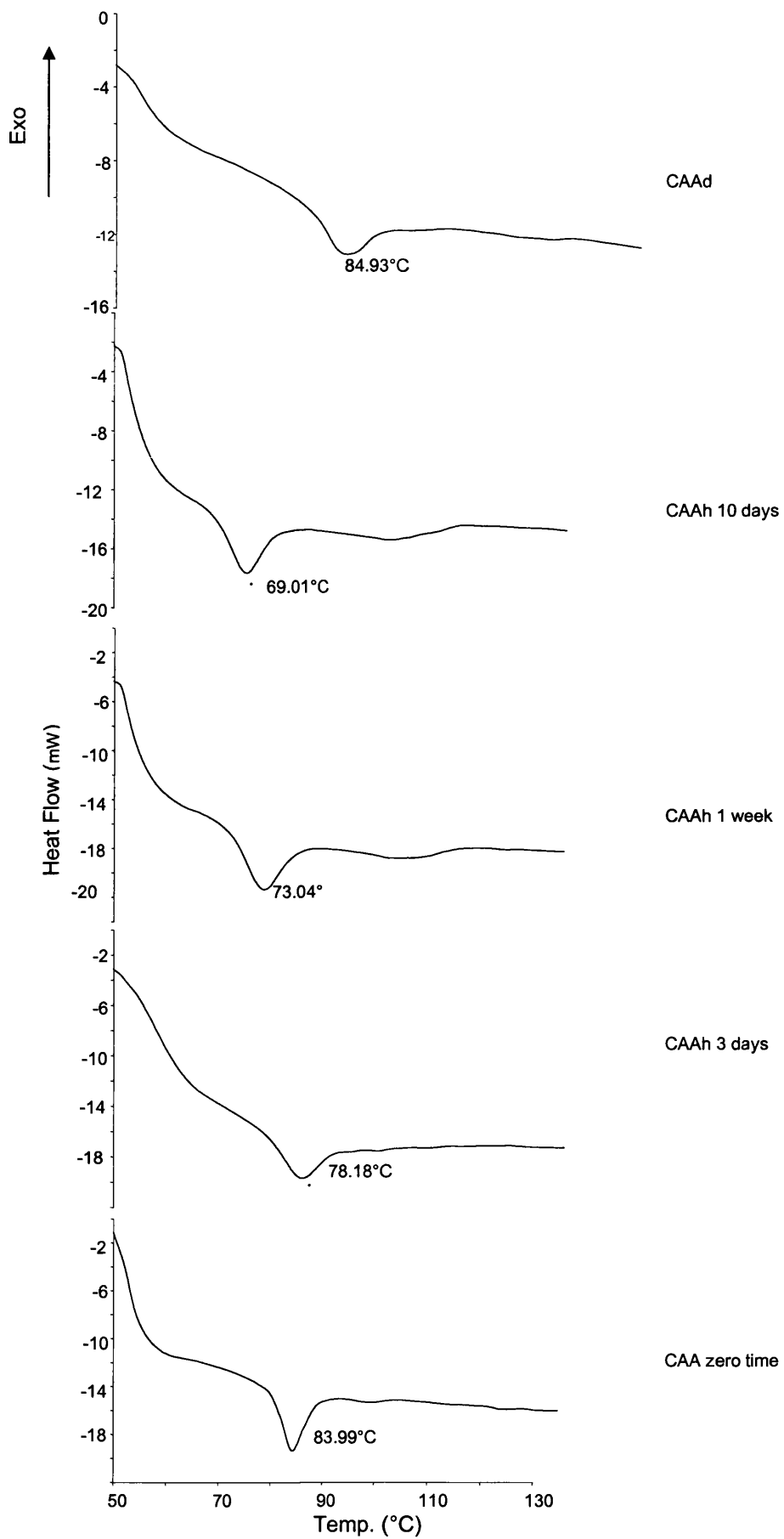


Figure 3.11: DSC thermograms of CAAd and CAAh after storage under 95%RH humidity for different time intervals, at the heating flow 25°C/min.

The stability of CAA is presented by maintaining the  $T_g$  value of the material well above that of the experimental conditions, even after extended exposure (10 days) to elevated relative humidity conditions (95%RH, 25°C). Under these conditions, the maximum water uptake by the material was 1.3%, associated with a 15°C reduction in  $T_g$  value.

Thus, the potential crystallisation of CAA would be difficult to induce upon exposure to humidity under the normal experimental and storage conditions (15°C-30°C). This is most probably related to the low water affinity of CAA material which is non-hygroscopic. Absorbed water can not, therefore, form a saturated solution at CAA surface, consequently the plasticization effect of water on it will be very limited.

When water was withdrawn from CAA, its  $T_g$  value increased again to its original value. This, further, supports the physico-chemical stability of the material under fluctuations in storage conditions.

In conclusion, exposure of CAA to conditions of elevated relative humidity were not significant to induce its crystallisation. A case which is rare to find with other amorphous materials that crystallise under lower humidity conditions than the 95%RH. The latter severely limited the use of amorphous pharmaceutical dosage forms in the pharmaceutical industry.

Thermograms of crystalline CA upon exposure to elevated relative humidity showed no shift in the melting peaks as demonstrated in Figure 3.12. This highlighted the insignificant plasticization effect of water on crystalline materials, associated with its low moisture uptake (Columbano et al. 2002; Ahlneck et al. 1990).

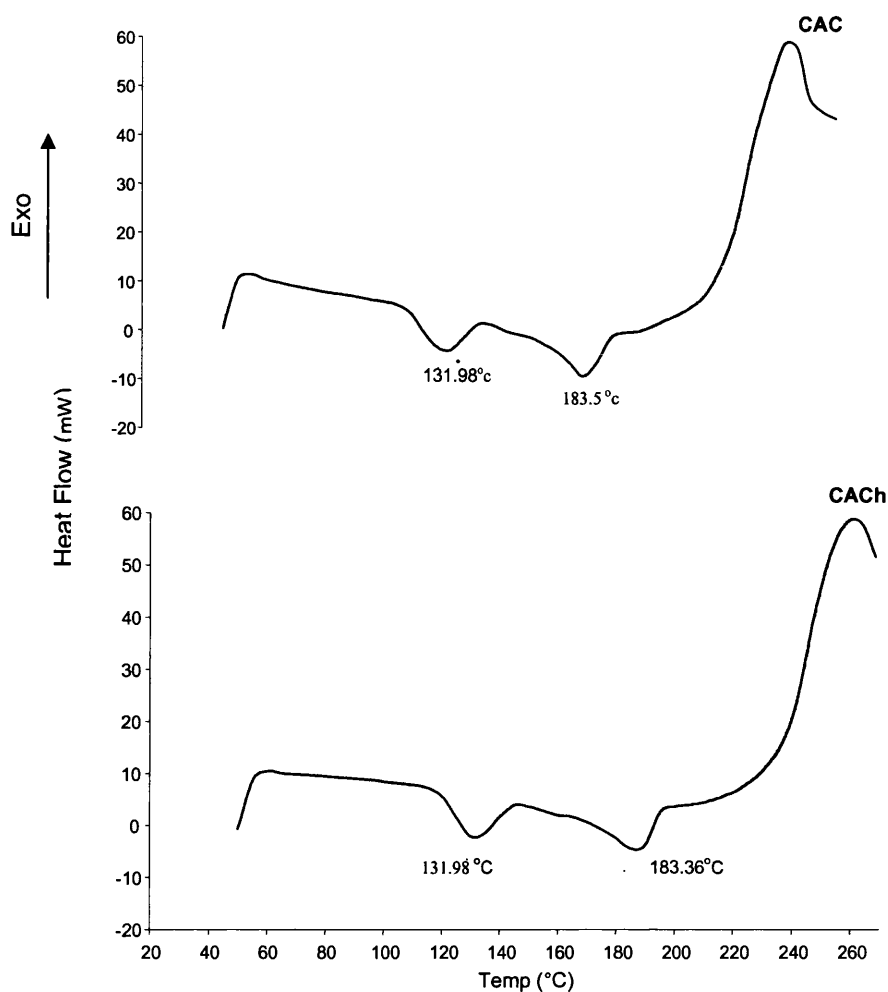


Figure 3.12: DSC thermogram of CACH after storage for one week at 95%RH humidity, at the heating rate 25°C/min.

### 3.3.3 Water content determination (Karl Fisher)

Table 3.3 shows the water content,  $T_g$ , and melting temperatures ( $T_m$ ) of CAAh and CACH after different storage times under 95%RH. It also shows the results for the dried CAAd sample.

No.	Storage Period	Storage Condition	T <sub>g</sub> or T <sub>m</sub>	Water Content
1.	CAA zero time	Ambient	83.99°C (T <sub>g</sub> )	0.99%
2.	CAAh 3 days	95%RH,25°C	78.18°C (T <sub>g</sub> )	1.80%
3.	CAAh 1 week	95%RH,25°C	73.04°C (T <sub>g</sub> )	2.10%
4.	CAAh 10 days	95%RH,25°C	69.01°C (T <sub>g</sub> )	2.30%
5.	CAAd	Dried under vacuum	84.93°C (T <sub>g</sub> )	0.70%
6.	CAC zero time	Ambient	131.98°C (T <sub>m</sub> ) 183.50°C (T <sub>m</sub> )	0.16%
7.	CACh 1 week	95%RH,25°C	131.98°C (T <sub>m</sub> ) 183.36°C (T <sub>m</sub> )	0.24%

Table 3.3: Results of analyses of CAAh and CAAd at different storage conditions

Results above indicated that the water content increased in CAA upon storage for 10 days at humid conditions (95%RH), until it reached a maximum at 2.3% (from 0.9%). Results also indicated that higher water content led to a shift in the T<sub>g</sub> towards lower temperatures. The highest shift observed in the T<sub>g</sub> was 15°C.

For CAC, the water content started initially low (0.16%). After one week of storage at the humid conditions, water content increased only to 0.24%.

Upon vacuum drying of CAA exposed to humidity (CAAh, one week sample), the loss in water was associated with a shift in the T<sub>g</sub> to 84°C.

### 3.3.4 X-Ray powder diffraction (X-RPD)

Figures 3.13a, b and c, show the XRPD diffractograms of CAA, CAC, and CAAc, respectively. The broad diffuse peaks in Figure 3.13a clearly indicated the lack of resolved reflections, and the absence of any significant crystalline long-range order in CAA. In contrast, the XRPD of CAC in Figure 3.13b shows characteristic sharp diffraction peaks associated with a highly crystalline material.

The diffractogram of CAAc (the partially crystalline material) showed an apparent absence in crystallinity within the material, as demonstrated by the presence of a broad halo which lacked the resolved reflections associated with the long-range order.

This suggested that the XRPD technique was not sensitive enough for the detection of crystalline material in a nominally amorphous drug at 15% concentration. While XRPD technique was previously reported to be a sensitive technique for the detection of amorphous material in a crystalline drug at a lower concentration of 5%–10% (Gerhardt et al, 1994), the converse was not observable.

On the contrary, the DSC technique utilised for testing the samples as mentioned under section 3.3.2 was capable of detecting 1% of the crystalline material within the amorphous CA.

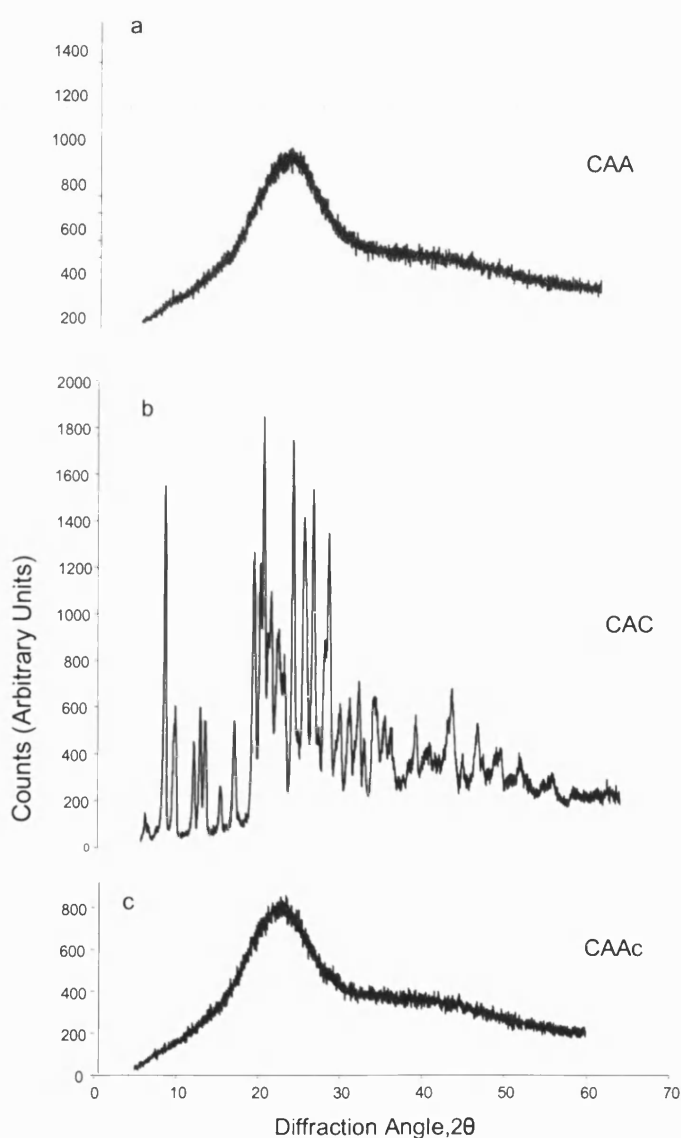


Figure 3.13: X-Ray powder diffraction for CAA(a), CAC(b), CAAC(c).

### 3.3.5 Dynamic vapour sorption (DVS)

The moisture sorption and desorption isotherms of CAA, CAC, and CAAC at  $25 \pm 0.5^\circ\text{C}$  are shown in Figures 3.14, 3.15, and 3.16, respectively. Figure 3.14 indicated that CAA adsorbed water slowly up to 2.0 – 2.5 %w/w at 90%RH. This indicated a limited water affinity of CAA, related to its low hygroscopicity. Thus, it would be difficult to plasticize CAA under the applied humid conditions, and it showed resistance to crystallisation even after exposure to high relative humidity conditions.

This behaviour is significantly different from other pharmaceutical amorphous materials. Spray dried Lactose which was found to increase its moisture uptake by 11% w/w at 50%RH,  $25^\circ\text{C}$  (Price et al, 2004). Increasing the partial water vapor pressure to > 50%RH led to a dramatic weight loss, associated with the expulsion of water during the recrystallisation process. This behaviour was not observed for CAA at  $25^\circ\text{C}$  even at 90%RH, indicating a distinguished stability of the amorphous CA compared to conventional pharmaceutical ingredients.

The desorption isotherm indicated that CAA can readily displace the adsorbed moisture, as indicated with the minimal hysteresis in the sorption/desorption curves.

The sorption isotherm of CAC at  $25^\circ\text{C}$  is shown in Figure 3.15. The water uptake is considered negligible as humidity increases to 50%RH. A slight water uptake of about 0.2% occurs at 60%RH, followed by a further 1.5% increase in water content between 70 – 90 %RH. The maximum water uptake achieved was 2.0%, a similar value to that obtained with the CAA material, indicating a limited affinity of both CAA and CAC forms to water uptake. The absorbed water was easily expelled in the desorption isotherm of CAC.

Figure 3.16 showed a similar sorption and desorption isotherms of CAAC to CAA, suggesting that this technique, which is sensitive to the presence of amorphous material, is not sensitive in detecting small quantities of crystalline content in a predominantly amorphous system. It was previously reported that DVS technique can detect down to 0.5% w/w amorphous content in a crystalline material (Buckton et al, 1995-b).



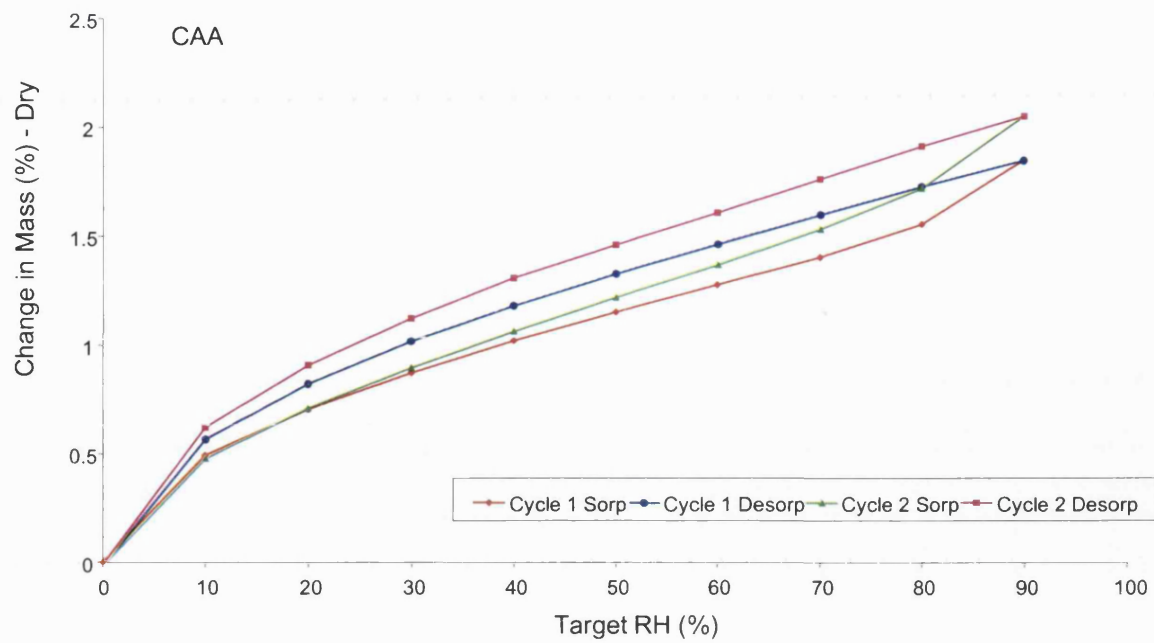


Figure 3.14: Dynamic vapour sorption/desorption isotherms of CAA

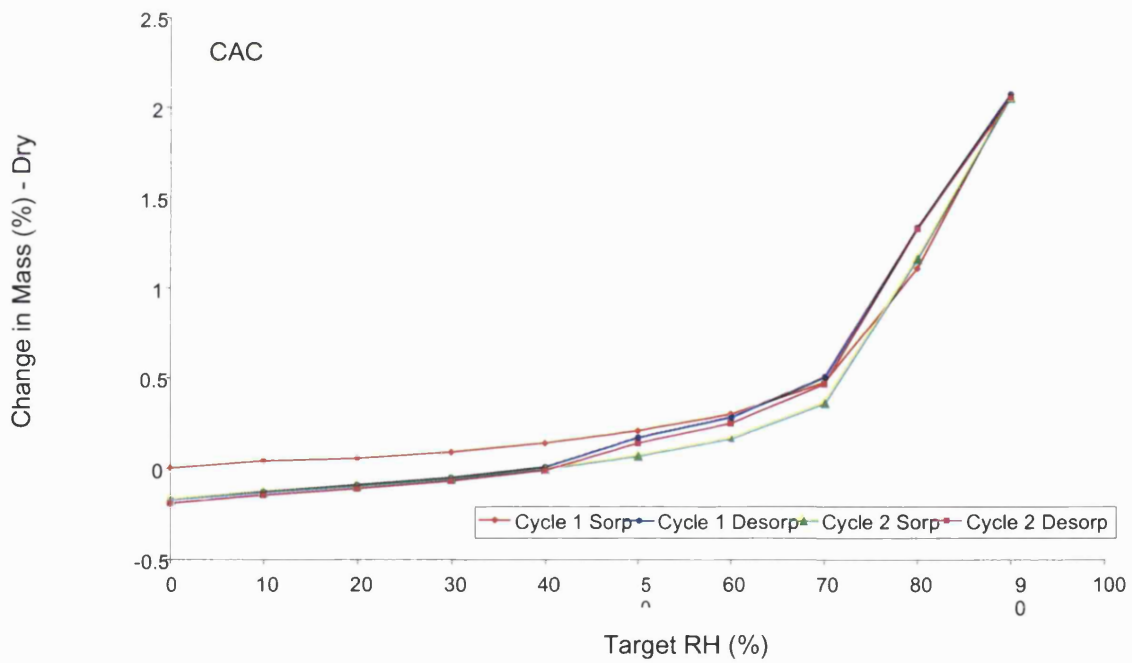


Figure 3.15: Dynamic vapour sorption/desorption isotherms of CAC

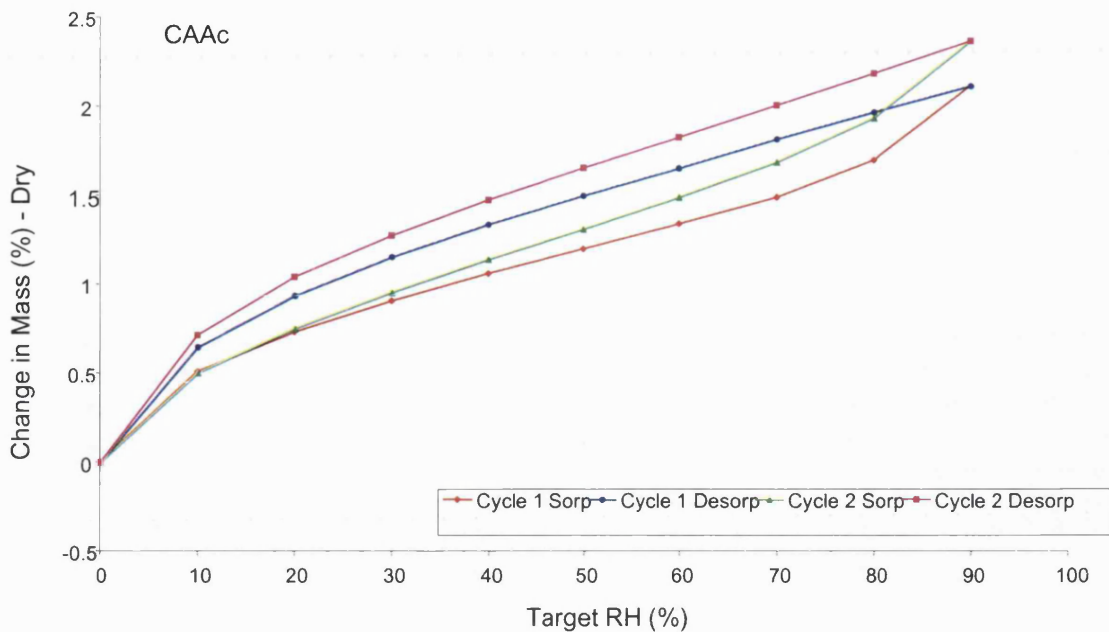


Figure 3.16: Dynamic vapour sorption/desorption isotherms of CAAC

### 3.3.6 Intrinsic dissolution

#### 3.3.6.1 Intrinsic dissolution of CAA

The CA cumulative amount released from CAA disks at different time intervals are shown in Table 3.4 and Figure 3.17. The area of exposure of the disk to dissolution media, and the intrinsic dissolution rate of CAA were calculated using equations 3.3 and 3.4 respectively.

$$\begin{aligned} \text{Area of exposure of CAA disks} &= (r^2) \pi \dots\dots\dots \text{Eq. 3.3} \\ &= (0.4)^2 \pi = 0.5027 \text{ cm}^2 \end{aligned}$$

Time (min)	Cumulative amount release of CA in (mg/cm <sup>2</sup> )	
	Average	± SD
5	1.00	0.34
10	3.16	0.82
15	5.77	1.53
20	8.58	2.24
30	12.14	2.52
45	16.98	3.07

Table 3.4: Intrinsic dissolution of CA from CAA disks, n=6.

$$\text{Intrinsic dissolution rate of CAA} = \frac{\text{Cumulative amount released (mg/min)}}{\text{Area of exposure of disks (cm}^2\text{)}} \dots \text{Eq. 3.4}$$

$$= 0.4 \text{ mg/min/cm}^2$$

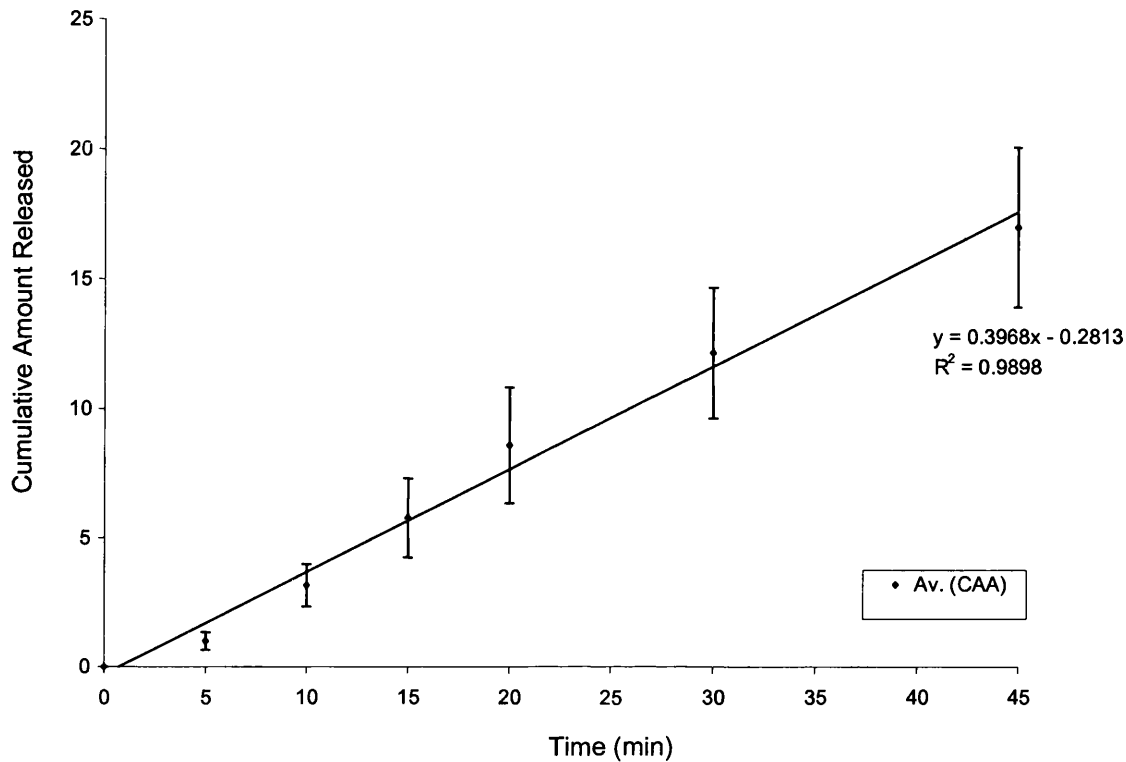


Figure 3.17: Intrinsic dissolution profile of CA from CAA, n=6.

The above release profile of CAA indicates a linear zero order release pattern. The lag time (1 min) is related to the compression of the material into a disc, leading to delay in the release onset.

### 3.3.6.2 Intrinsic dissolution of CAC

Table 3.5 and Figure 3.18 show the cumulative amount release of CA from CAC at various time intervals. The area of exposure of CAC disks was calculated as:

$$(r^2) \pi = (0.4)^2 \pi = 0.5027 \text{ cm}^2$$

Time (min)	Cumulative amount release in (mg/cm <sup>2</sup> )	
	Average	± SD
5	4.43	0.83
10	6.15	0.42
15	6.26	0.92
20	4.41	0.72
30	3.89	0.29
45	5.11	1.60

Table 3.5: Intrinsic dissolution of CA from CAC disks, n=6.

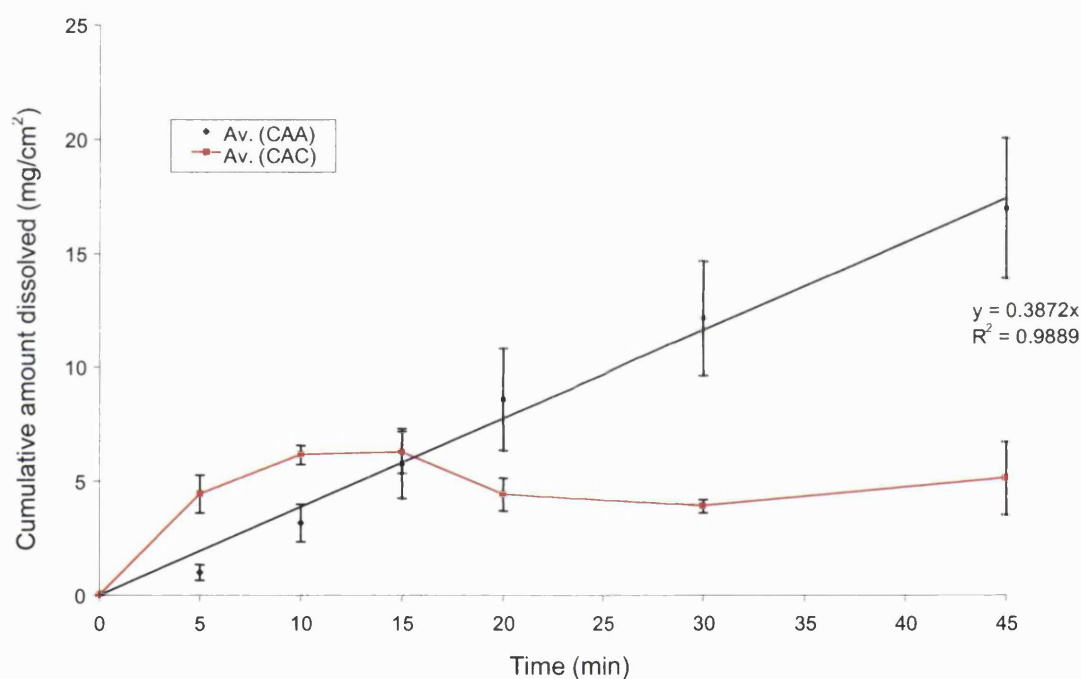


Figure 3.18: Intrinsic dissolution profiles of CAA and CAC disks, n=6.

Figure 3.18 shows the comparative intrinsic dissolution profiles for CAA and CAC. It demonstrated that during the first 15 minutes CAC showed a higher amount released than the CAA, for an equivalent area of exposure. This may be related to smaller particle size of CAC ( $d_{50}=3.3\mu\text{m}$ ), compared to CAA ( $d_{50}=20\mu\text{m}$ ), leading to faster and higher initial dissolution results. This may also be due to the fact that compressibility of the amorphous materials is higher than that of the crystalline (Berggren et al, 2004), leading to a higher CAA disk hardness, thus lower initial

dissolution results. This remains the case until the solubility of CAC reaches a plateau (solubility limit), after which saturation occurred and CAC crystallized out in the media leading to the slight noticed decrease in the dissolution results .

After the first 20 minutes, the amount dissolved from CAA became significantly higher with time compared to that from CAC. After 45 minutes, the cumulative amount dissolved from CAA was around 3 times higher than that from CAC.

### 3.3.7 Dissolution using apparatus II

Intrinsic dissolution was considered not suitable for testing CAAC, as the material was compressed, and crushed, i.e. it underwent processing. Dissolution using the BP 2003 method was seen the most appropriate to measure the dissolution rate of CAAC. Results were compared to the official compendial (BP & USP) specified limits for release of CA from tablets.

Table 3.6 and Figure 3.19 show the results of dissolution of CAAC granules tested according to BP 2003.

Time (min)	% Release of CA	
	Average	± SD
5	35.89	1.99
10	48.72	2.94
15	54.82	2.01
20	59.50	2.64
30	65.32	3.29
45	70.29	2.86

Table 3.6: Dissolution rate of CAAC according to BP 2003 method, n=6.

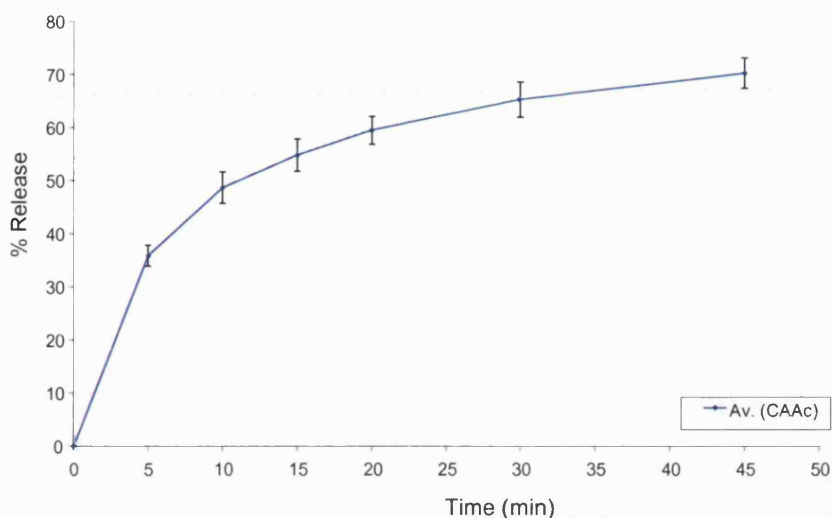


Figure 3.19: Dissolution profile of CAAC using BP 2003 method, n=6.

It can be shown from the above profile that the dissolution results of CAAC (55% after 15 min) is lower than that requested by the official compendia (> 60%).

### 3.3.8 *In situ* perfusion of CAA

Only CAA was tested for *in situ* perfusion as the material needed to be solubilised in the *in situ* perfusion medium before being loaded in the intestine. In this case, the issue of concern is the CA absorption rate across the rat intestinal membrane after being dissolved, and not the rate of dissolution and absorption of its different forms.

The concentration of cefuroxime remaining in the *in situ* perfusion media was corrected to volume for each time point, and presented in Table 3.7 and Figure 3.20.

Concentration of CA (mg/ml)					
Time (min)	Rat 1	Rat 2	Rat 3	Av.	SD
0	0.084	0.094	0.084		
10	0.072147465	0.07316129	0.056709677	0.0673395	0.00922
20	0.061640553	0.081774194	0.077640553	0.0736851	0.010634
30	0.086588645	0.112626728	0.076313364	0.0918402	0.018719
40	0.074661751	0.066176115	0.067261106	0.076106	0.009508
50	0.080875576	0.080552995	0.070967742	0.0774654	0.005629
60	0.084193548	0.096239631	0.064700461	0.0817112	0.015915
70	0.073824885	0.081290323	0.069262673	0.0747926	0.006072
80	0.041474654	0.081387097	0.061124424	0.0613287	0.019957
90	0.041474654	0.067741935	0.076497696	0.0619048	0.018227
100		0.069308756	0.068018433	0.0686836	0.000812

Table 3.7: CA concentration (mg/ml), remained in the media after *in situ* perfusion test.

The concentration values in the table above includes the concentration of CA remaining in the media, plus the concentration of C resulted from the hydrolysis of CA by the intestinal enzymes, and the concentration of  $\Delta^3$ - Isomers generated from the degradation. Both were converted by calculation to CA, and the sum concentration had been corrected according to the volume collected at each time point. The HPLC chromatograms for CA *in situ* perfusion at zero time and after 70 minutes are presented in Figure 3.21.

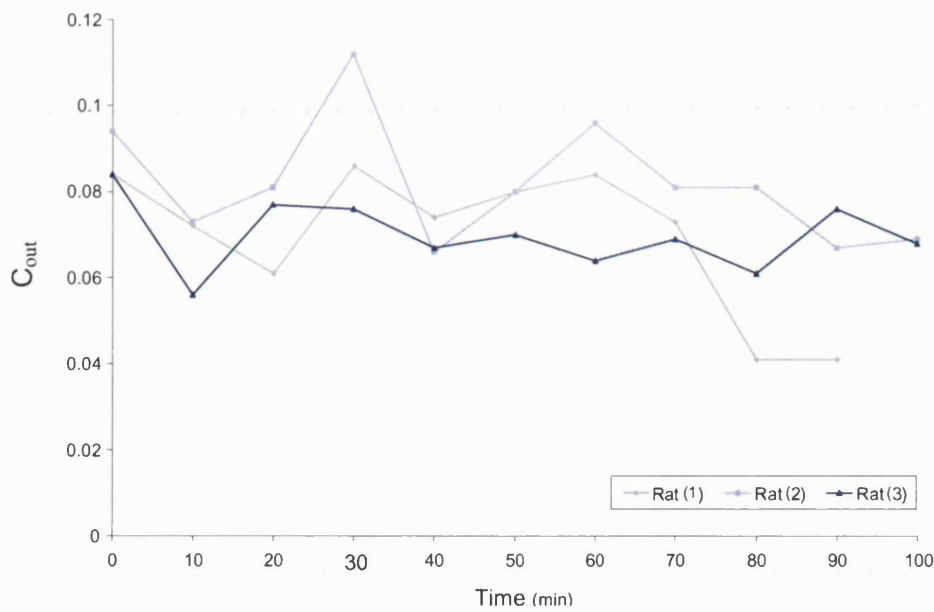


Figure 3.20: CA concentration (mg/ml), remained in the media (taken out) after *in situ* perfusion test.

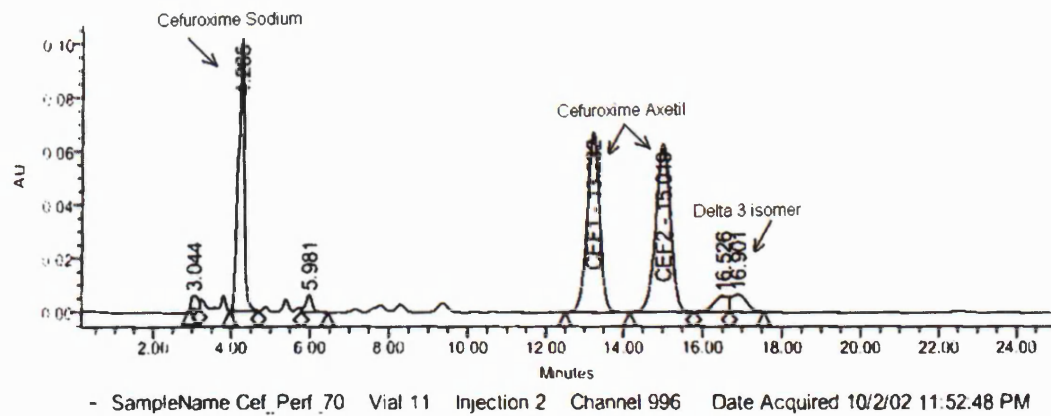
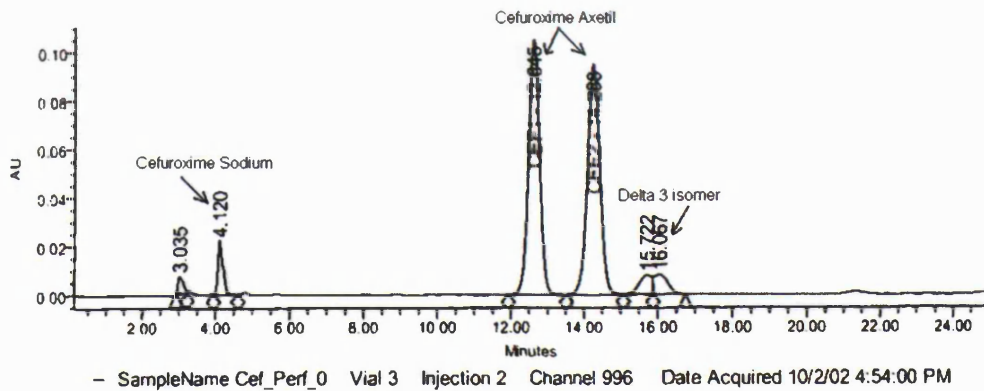


Figure 3.21: *In situ* perfusion HPLC chromatograms of CAA at zero and 70 minutes.



The bioavailability F was then determined as  $(1 - C_{out}/C_{in})$  versus time. This is shown in Table 3.8.

F value of CA					
Time (min)	Rat 1	Rat 2	Rat 3	Av.	SD
0	0	0	0	0	0
10	0.198361495	0.238696251	0.340585146	0.2592143	0.073298
20	0.315104967	0.149071867	0.097202872	0.1871266	0.113826
30	0.837992832	-0.17197428	0.112635302	-0.0071154	0.147569
40	0.168202765	0.103276637	0.217661558	0.163047	0.057366
50	0.101382488	0.161779444	0.174793698	0.1459852	0.039171
60	0.064516129	-0.00145298	0.24766906	0.1035774	0.129073
70	0.179723502	0.154106945	0.194620084	0.1761502	0.020492
80	0.539170507	0.15309993	0.289250884	0.3271738	0.195809
90	0.539170507	0.295089121	0.110491909	0.3149172	0.215026
100		0.27878506	0.209087986	0.2439365	0.049283

Table 3.8: *In situ* perfusion bioavailability results of CA.

$P_{eff}$  values for CA were calculated at each time point according to equation 3.5, Fagerholm, (1996).

$$P_{eff} = \frac{-Q \ln \frac{C_{out}}{C_{in}}}{2\pi r l} \dots\dots\dots \text{Eq. 3.5}$$

Q = Flow Rate, 0.22 ml/min = 0.00362 ml/sec

r = 0.19 cm

l = 13.5 cm for Rat 1 & 15 cm for Rat 2 and Rat 3

Average of the three readings at each point was taken. The results obtained are tabulated in Table 3.9.

Time (min)	P <sub>eff</sub> (cm/sec)			P <sub>eff</sub> (Av.)
	Rat 1	Rat 2	Rat 3	
0				
10	4.9642E-05	5.51099E-05	8.41436E-05	6.297E-05
20	8.498E-05	3.26201E-05	2.08834E-05	4.609E-05
30	8.69663E-06	-3.2067E-05	2.41475E-05	2.591E-07
40	4.13501E-05	2.20275E-05	4.96024E-05	3.766E-05
50	2.40013E-05	3.56606E-05	3.88226E-05	3.283E-05
60	1.49739E-05	-2.9339E-07	5.75057E-05	2.406E-05
70	4.44816E-05	3.38194E-05	4.37369E-06	4.068E-05
80	0.000173946	3.3579E-05	6.89949E-05	9.217E-05
90	0.000173946	7.06616E-06	2.366E-05	8.942E-05
100		6.60411E-05	4.73999E-05	5.672E-05

Table 3.9: P<sub>eff</sub> values for CA in the *in situ* perfusion test

The results of P<sub>eff</sub> show steady state constant values between 40–70 minutes, thus only average of these values were taken. The values for 10 and 30 minutes were excluded due to erratic absorption noticed at the beginning. The end values from 80-100 minutes were also excluded due to water absorption from the small intestine leading to differences in drug concentration.

The average of P<sub>eff</sub> ± SD was calculated to be (3.381E-5 ± 7.257E-6 cm/sec).

The first order absorption rate constant (K<sub>abs</sub>) and the half life (t<sub>1/2</sub>) were then calculated according to equations 3.6 and 3.7, respectively (Fagerholm, 1996).

$$K_{abs} = \frac{2P_{eff}}{r} \dots\dots\dots \text{Eq. 3.6}$$

$$T_{0.5} = \frac{\text{Ln}2}{K_{abs}} \dots\dots\dots \text{Eq. 3.7}$$

The  $K_{abs}$  value obtained was  $1.281\text{hr}^{-1}$ , with a half life of 32.46 min in rats. The  $P_{eff.rat}$  of CA was correlated to its human effective permeability ( $P_{eff.man}$ ) according to equation 3.8 (Lennerans, 1998).

$$P_{eff.man} = 3.6X P_{eff} + 0.03 X 10^{-4} \dots\dots\dots \text{Eq. 3.8}$$

The effective permeability in man was determined to be  $12.17\text{E-}5$  cm/sec. The first order absorption rate constant ( $K_{abs}$ ) was then calculated to be  $4.612\text{hr}^{-1}$ , with a half life of 83.035 min in human.

It was determined that the  $t_{0.5}$  absorption of CA in the jejunal membrane of the rat is around 32.5 minute, while in human (by correlation) it could be approximated to 83.0 min. This can be considered an adequate absorption rate for an antibiotic drug. A recent finding by Sanjuan et al (2000), indicated a similar  $P_{eff}$  value for CA in rat intestine, with a value of  $3.1\text{E-}5$  cm/sec.

### 3.3.9 *In vitro* gut absorption

#### 3.3.9.1 *In vitro* gut absorption of CAA

Results of *in vitro* gut percentage release of C from CAA to media are shown in Table 3.10 and Figure 3.22.

Trial \ Time (min)	15	30	45	60	75	90	105	120
Average (%)	4.22	7.97	12.76	17.37	21.48	25.37	30.07	34.54
SD	2.41	3.54	4.88	5.14	6.09	6.88	5.81	6.02

Table 3.10: *In vitro* gut percentage C released from CAA to the media, n=3.

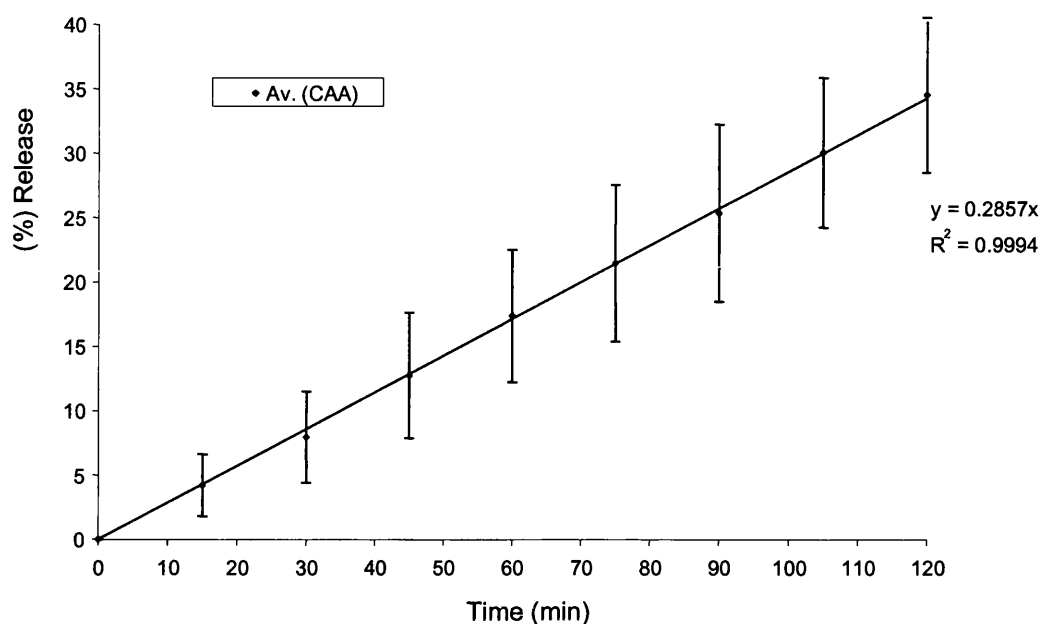


Figure 3.22: *In vitro* gut release of C from CAA to the media, n=3.

The above data shows a linear zero order release kinetics of C from CAA, with a 34% (i.e. 9 mg) transported across the rat intestine after 120 min. This indicated that around 4 times the dose needed for rat was absorbed. Thus the bioavailability of the amorphous form of CA was adequate.

The percentage recovery was also calculated by determining the amount of cefuroxime (as C and CA) released to the media at the end of the test, remained inside the intestine, and found in the wash. Results are presented in Table 3.11.

Trial	Cefuroxime release to the media (mg), as		Cefuroxime remained inside the intestine (mg), as			Cefuroxime found in the wash (mg), as	Cefuroxime amount (mg)		% Recovery
	C	CA	C	Degraded $\Delta^3$	CA	C	Total	Initial	
1	10.00	0.00	3.10	0.00	0.00	0.04	13.10	16.8	78.0
2	8.50	0.00	5.10	0.00	0.00	0.07	13.60	16.8	81.0
3	7.30	0.00	6.10	0.00	0.00	0.06	13.40	20.5	65.4

Table 3.11: Recovery (%) of cefuroxime from the *in vitro* gut test of CAA

From the above, it was shown that the recovery of C after testing was in the range of 65% - 81%, which indicated that some amounts of the drug remained on the membrane brush after the experiment, which could not be recovered.

It was also shown that 40% of CA was hydrolysed to C in the intestine, a matter which reduced the percentage drug absorbed. This was in agreement with previously published work by Mosher et al. (1991) that the intestinal hydrolysis of CA to C lead to an incomplete and erratic absorption of the drug, resulting in the wide absorption variations that may occur.

### 3.3.9.2 *In vitro* gut absorption of CAC

Table 3.12 and Figure 3.23, show the results of the *in vitro* gut release of C from CAC to the media. The release rate of C from CAA is also shown for comparison.

Time (min)	15	30	45	60	75	90	105	120
Average (%)	0.60	1.69	3.34	5.53	7.90	10.18	12.56	15.10
SD	0.20	0.12	0.15	0.47	0.89	1.06	1.75	1.39

Table 3.12: *In vitro* gut percentage C released from CAC to the media, n = 3.

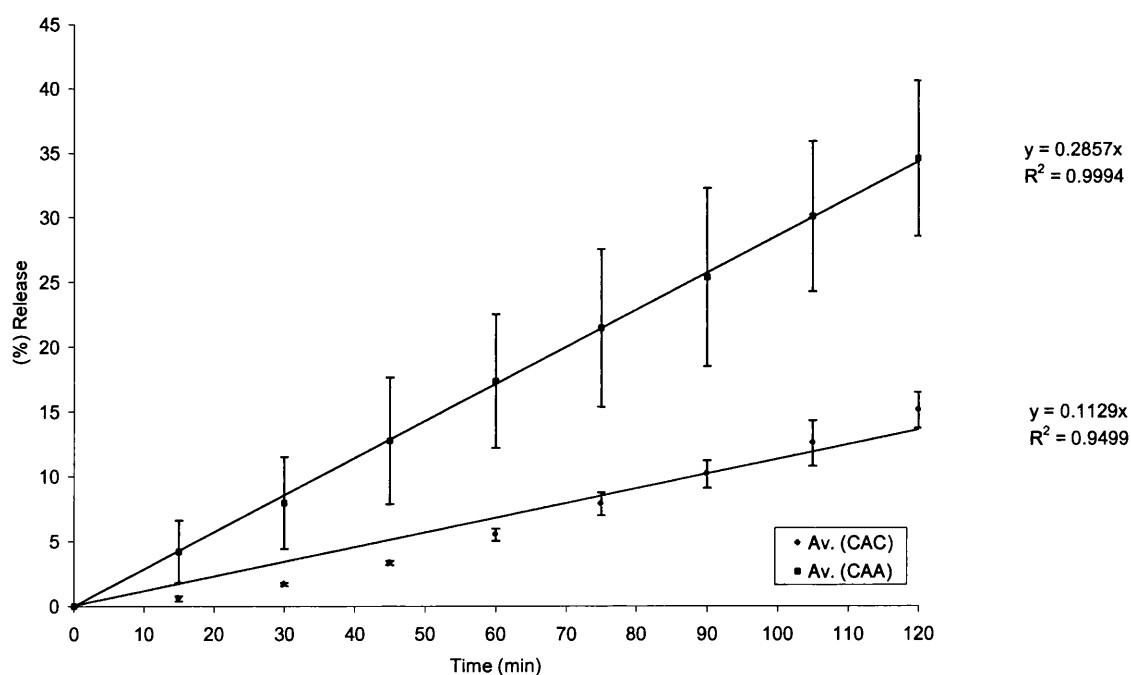


Figure 3.23: *In vitro* gut release of C from CAC to the media, n=3.

The results above indicated that CAC has a linear zero order release kinetics. The rate of C release (K) from CAA, however, was found to be over two folds higher than that from CAC (K= 0.286 and 0.113, respectively). This confirmed the significantly higher absorption rate of CAA than CAC, as reported in previous related studies (Somani et al, 2001, 2003; Guk et al, 2002; Crisp et al, 1991; Zenoni et al, 1997; James et al, 1989).

### 3.3.9.3 *In vitro* gut absorption of CAAC

Results of *in vitro* gut percentage release of C from CAAC to the media are shown in Table 3.13 and Figure 3.24. The release rate of CAA is also shown for comparison.

Trial \ Time (min)	15	30	45	60	75	90	105	120
Average (%)	0.94	3.17	5.93	9.50	13.11	16.01	19.71	22.49
SD	3.16	2.14	3.60	4.23	5.25	4.87	2.57	3.33

Table 3.13: *In vitro* gut percentage C released from CAAC to the media, n = 3.

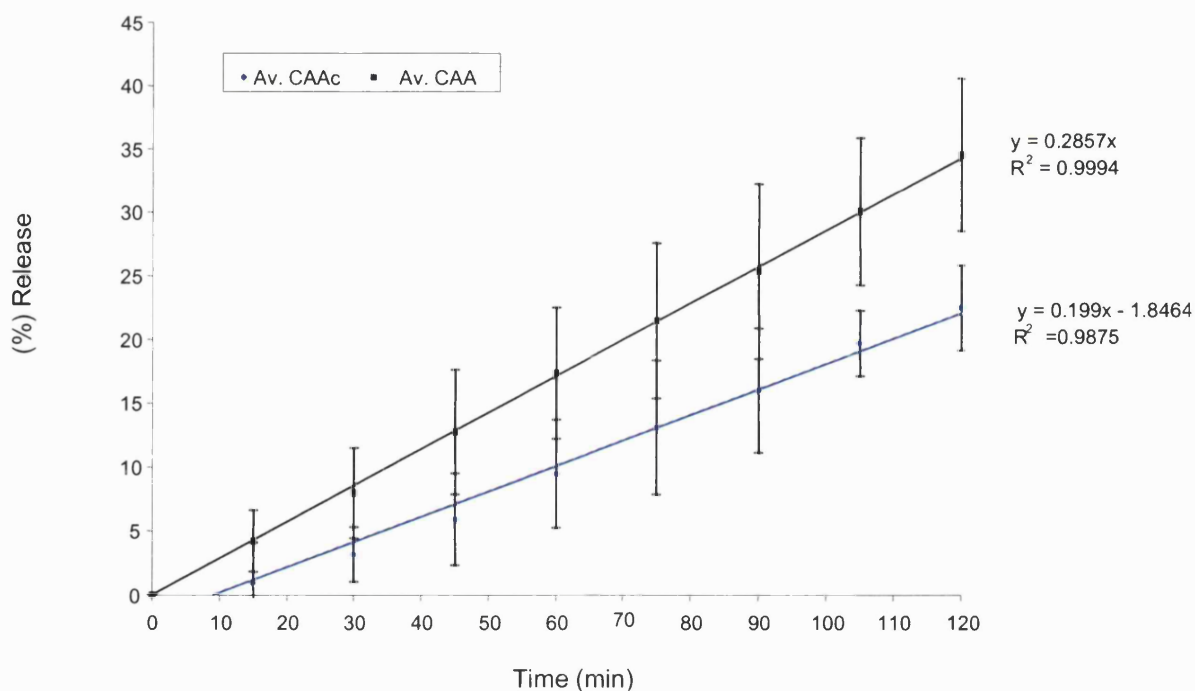


Figure 3.24: *In vitro* gut release of C from CAAC to the media, n=3.

The above results indicated a zero order release for C from CAAC, with a lag time for the first minutes, related to the time needed for granules to disintegrate before dissolution. There was a noticeable decline in the absorption rate of C from CAAC compared to that from CAA related to partial transformation of CAA to CAC upon compression, as the DSC thermograms revealed (section 3.3.2). Thus, compression resulted in a decrease in the release rate (K) of CAA across the rat intestines by 30% from (0.288 to 0.199).

Statistical two-way ANOVA of the two materials CAA and CAC showed that they were significantly different ( $P < 0.05$ ). The same statistical evaluation was applied to determine if CAA is different from CAAC, and the two release rates were found also significantly different ( $P < 0.05$ ).

### 3.4 CONCLUSIONS

Results of tests conducted on CAA and CAC indicated differences in their physical properties. The amorphous form, which has a  $T_g$  at a mid point temperature of 74°C showed a significantly higher dissolution rate and bioavailability than CAC. The latter showed two distinct DSC melting peaks at about 135°C and 180°C, representing two polymorphs of the crystalline drug. This indicated that the commercial form of CAC is a mixture of two polymorphs.

Upon compression, CAA showed a degree of instability presented by a partial transformation of the pure CAA to CAC (at 15% w/w). Thus, DSC testing of CAAC showed a melting peak at around 180°C characteristic of the crystalline form. The formation of the crystalline material may be a function of the heat and pressure generating during compression.

X-ray powder diffraction testing of both the pure and the partially crystallised CAA showed no evidence of crystallinity, indicating that this technique is not adequate in detecting relatively low percentages of crystalline content of CAC (up to 15% w/w) upon compression of the amorphous (CAAC) material.

The vapor sorption isotherms of CAA showed a limited (2%) water uptake at high relative humidity (90%) at 25°C, with no evidence of crystallisation, indicating a very stable amorphous drug. Furthermore, the water uptake of CAA at 90%RH was close to that of CAC. The desorption isotherms of both forms indicated that the sorption and desorption of condensed water was reversible.

The similar sorption isotherms of CAAC to CAA indicated that the DVS technique was not sensitive in detecting small levels of crystalline content in the amorphous drug.

The only technique which was highly efficient in detecting small levels of crystalline CAC material in the CAAC sample was the DSC. Furthermore, the enthalpy/concentration calibration curves indicated the possibility of detecting as low as 1% w/w CAC in the amorphous material.



The intestinal absorption studies indicated that the absorption rate of the crystalline (CAC) drug was the lowest, despite being introduced in the study as the finest particles ( $d_{50} = 3\mu\text{m}$ ). This suggested that the form of the drug (i.e. crystalline or amorphous) was more determinant to the rate of CA absorption than its particle size. The compression effect on CAA was demonstrated by lower *in vitro* gut absorption rate of CAAC (by 30%) compared to that of CAA.

The experimentally determined  $P_{\text{eff}}$  value of CA indicated sufficient bioavailability of the drug, regardless of the rapid and extensive hydrolysis of CA in the rat intestine and under the test conditions.

The  $T_g$  onset of CAA material was found to be affected by the presence of water, which has a plasticization effect on the material. This was indicated by the reduction in the  $T_g$  value of CAA to an extent related to water uptake upon exposure to high humidity condition. However, the limited uptake of moisture (1.3%) upon exposure to 95%RH, remained insufficient to induce crystallisation within the amorphous drug. Furthermore, the  $T_g$  value of CAA reverted back to its original value upon vacuum drying, indicating that CAA material can withstand fluctuations in storage conditions. This demonstrated a stable amorphous drug, a case which has rarely been seen in other amorphous pharmaceutical systems.

## CHAPTER 4

# EFFECT OF SOME EXCIPIENTS ON THE PHYSICAL PROPERTIES OF CEFUROXIME AXETIL CRYSTALLINE (CAC) AND CEFUROXIME AXETIL AMORPHOUS (CAA) AS POWDER BLENDS AND COMPRESSED MIXTURES

### 4.1 INTRODUCTION

Only limited studies had been undertaken on mixing, formulation properties and the possibility of enhancing stability, solubility, and bioavailability of CA with the introduction of excipients. Of these, the use of citric acid sodium salt in a tablet formulation containing CA, microcrystalline cellulose, SLS, croscarmellose sodium and calcium carbonate (Somani et al, 2001). The addition of sodium salt of citric acid was undertaken to inhibit the tendency of CAA to form a gel that prolonged the disintegration time and retards the dissolution of the tablet formulation. The dissolution behaviour of the formulated tablets was satisfactory (77% after 45 min), and the product was bioequivalent to the commercial Ceftin<sup>®</sup> preparation, containing pure CAA.

Crisp et al. (1991) described compositions for oral administration whereby enhanced absorption of CA via the GIT was achieved. These pharmaceutical compositions took the form of tablets or capsules prepared by conventional processes with pharmaceutically acceptable excipients such as binding agents (e.g. PVP, or HPMC), fillers (e.g. starch, lactose, microcrystalline cellulose or calcium phosphates), disintegrants (e.g. potato starch, or sodium starch glycolate), wetting agents (e.g. SLS), and lubricants (e.g. Mg-stearate, hydrogenated vegetable oils, talc, silica or PEG).

In another study, a solid dispersion of CA was prepared by dissolving CA and a surfactant (e.g. Tween<sup>®</sup>, Cremophor<sup>®</sup>, Myrj<sup>®</sup>, Poloxamer<sup>®</sup>, Migloyol<sup>®</sup>, Labrafil<sup>®</sup>, Imvitor<sup>®</sup>, and Span<sup>®</sup>) in an organic solvent (e.g. alcohol, acetonitril, THF, dichloromethane, and chloroform), followed by suspending a water insoluble inorganic carrier (e.g. silicon dioxide, hydrotalcite, aluminum magnesium silicate,

aluminium hydroxide, titanium dioxide and talc) in the resulting solution and drying the resulting suspension to remove the organic solvents (Woo et al, 2000).

The solid dispersant showed an improved bioavailability and increased the stability of CA. The dispersant was used for the preparation of tablets containing microcrystalline cellulose, cross-linked povidone and Mg-stearate, tablets were further coated with a regular film coat. The dissolution of these tablets was comparable to those of the control drug (Zinnat<sup>®</sup> tablets)(> 90% after 45 minutes). This high dissolution rate of these tablets can be related to the rapid rupturing of the film coating in the GIT fluids, after which the core disintegrates quickly and CAA becomes rapidly exposed to the absorption media (Deutsch et al, 1990-a,b). The coat composition was made up to HPMC 5 or 6, propylene glycol, methyl hydroxy benzoate and propyl hydroxy benzoate.

Somani et al. (2003) developed a method for preparing CAA from an admixture of CAC with one or more pharmaceutically accepted excipients (e.g. NaCl, CaCO<sub>3</sub>, Lactose, Starch, Microcrystalline cellulose, Colloidal Silica, Talc, and SLS). The mixture was then subjected to a milling action. Upon milling pure CAA was obtained, which contained less than 5% CAC.

In another study, a solid dispersion technique was used to obtain and stabilise the amorphous form of the drug (Guk et al, 2002). Upon dissolving CAC in a mixture of acetone, methanol and methylene chloride at ambient temperature, PVP K-30, HPMC and PEG were added each individually to the solution while stirring. The solution was sprayed into a vessel with supercritical CO<sub>2</sub> (100 bar, 45°C) which acted as anti solvent. The solid dispersion containing CAA showed similar solubility to that of CAA in the reference product Zinnat<sup>®</sup> tablets.

Sherman et al. (2000) published a method for stabilisation of CA by forming an admixture of CA with zinc chloride in a 0.1 – 4% concentration. The zinc salt was added to CAA co-precipitate with a water soluble diluent (e.g. sorbitol). Accelerated stability testing on the prepared tablets from the admixture (60°C for 7 days) revealed a low increase in impurities, indicating good stability.

As discussed in chapter 3, compression of CAA resulted in reduction in its dissolution and intestinal absorption rates, due to its partial crystallisation.

In this chapter, mixtures of CAA were prepared with some excipients with and without compression, for the objective of characterising their effect on enhancing the dissolution and bioavailability of CA.

A powder blend and a compressed mixture of CAA with all excipients was also prepared to determine their possible synergistic effect. The same study was repeated with CAC to determine whether these excipients have any significant effect on the solubility and intestinal permeability of the crystalline form of the drug.

## 4.2 MATERIALS AND METHODS

Table 4.1 summarises materials used in this study.

No.	Material	Batch No.	Assay	Water Content	Source	Retesting Date
1.	Cefuroxime axetil amorphous (CAA)	CAFAA/003/00	81.8%	0.99%	Orchid	12/2003
2.	Cefuroxime axetil crystalline (CAC)	CRCB030005	83.4%	0.16%	Orchid	02/2006
3.	Crosscarmellose sodium (Ac-Di-Sol)	T506C	--	2.2%	FMC	02/2000
4.	Pregelatinized starch	IN 502729	--	8.6%	Colorcon	03/2003
5.	Colloidal silicon dioxide (Aerosil 200)	C2711011	--	0.1%	Degussa	01/2003
6.	Sodium lauryl sulphate (SLS)	00015026	--	0.87%	Hankel	02/2002

Table 4.1 Materials used in the mixtures prepared with CAA and CAC.

### 4.2.1 Preparation of Mixtures

#### 4.2.1.1 Powder blends preparation

Mixtures of 20 gm weight were prepared for each of the following excipients with CAA at the following concentrations: Ac-Di-Sol at 15% and 50%, starch 1500 at 30% and 50%, SLS at 15% and 50%, and Aerosil 200 at 3% and 50%.

The mixtures were prepared by accurately weighing each material at the quantities needed using a calibrated Mettler balance. Materials for each mixture were then transferred to a beaker of a suitable size and mixed using a spatula for 5 minutes.

#### **4.2.1.2 Compressed mixtures preparation**

From each of the prepared powder blends mentioned under section 4.2.1.1, 10 gm were taken and compressed into tablets with a hardness of 70–90N using an “Erweka EKO” single punch machine. Tablets were crushed into granules using an “Erweka” crusher, and then passed through a 0.2 mm sieve.

In order to exclude differences in particle size distribution, compressed granules of each mixture were sieved through a set of sieves ranging 50-200 $\mu$ m. Only granules at the size range of 90–100 $\mu$ m were collected, analysed for homogeneity, and tested as described under section 4.2.3 below.

#### **4.2.2 Powder blends and compressed mixtures prepared**

##### **4.2.2.1 Mixtures of CAA with Ac-Di-Sol**

Croscarmellose sodium (Ac-Di-Sol), a cross linked polymer of carboxymethyl-cellulose sodium, is a non crystalline fibrous material of high molecular weight of 90 K -700 K. It is most commonly used in oral pharmaceutical formulations as a disintegrant for capsules, tablets and granules (Botzolakis, 1988; Gorman et al. 1982). It is generally regarded as an essentially nontoxic and nonirritant material.

In tablet formulations, croscarmellose sodium may be used in both direct compression and wet granulation processes. When used in wet granulation the croscarmellose sodium is best added both intra and extra-granular, so that the swelling ability of the disintegrant is best utilised (Khattab et al, 1993).

Two ratios of CAA powder mixtures with Ac-Di-Sol were prepared, the 50:50 (Mixture 1), and the 85:15 (Mixture 2). The compressed granules were only prepared from mixture 2.

##### **4.2.2.2 Mixtures of CAA with pregelatinized starch 1500**

Pregelatinized Starch 1500 performs key functions in direct compression formulations as a binder, disintegrant and a self-lubricant (Shangraw et al, 1981). It also promotes formulation flexibility by complementing and enhancing other excipients. Starch is a semi crystalline material, it loses its crystalline properties when pregelatinized.

Powder mixtures of CAA with pregelatinized starch 1500 were prepared in 50:50 ratio (Mixture 3), and 70:30 ratio (Mixture 4). The compressed granules were only prepared from mixture 4.

#### **4.2.2.3 Mixtures of CAA with Aerosil 200**

Colloidal silicon dioxide is an amorphous material with a large specific surface area. It is widely used in pharmaceuticals, cosmetics and food products to give it the desirable flow characteristics which are exploited to improve the flow properties of dry powders in a number of processes (Lerk, 1977).

Colloidal silicon dioxide is also used to stabilise emulsions and as a thixotropic, thickening, and suspending agent in gels and semisolid preparations.

Powder mixtures of CAA with Aerosil 200 were prepared in 50 : 50 ratio (mixture 5), and 97 : 3 ratio (mixture 6). The compressed granules were prepared from mixture 6 only.

#### **4.2.2.4 Mixtures of CAA with SLS**

Sodium lauryl sulfate is an anionic surfactant. It is a crystalline material having a molecular weight at 288.38. It is employed in a wide range of non parenteral pharmaceutical formulations and cosmetics as a detergent and wetting agent which is effective in both alkaline and acidic conditions (Wang et al, 1990).

Powder mixtures of CAA with SLS were prepared in 50 : 50 ratio (Mixture 7), and 85 : 15 ratio (Mixture 8). The compressed granules were prepared from mixture 8 only.

#### **4.2.2.5 Blends of CAA and CAC with Ac-Di-Sol, Starch 1500 and Aerosil 200**

A powder blend composed of the followings was prepared with 600 gm of each of CAA and CAC:

Ac-Di-Sol	: 100.0 gm
Starch 1500	: 180.0 gm
Aerosil 200	: 20.0 gm

CAA or CAC, Starch 1500 and Aerosil 200 were mixed using the “Niro PMA” high sheer mixer of a 10L container for 2 minutes. Ac-Di-Sol was then added and mixed with the rest of the blend at low speed for 1 minute.

The compressed mixture was prepared from the CAA mixture with excipients. The obtained granules were called cefuroxime axetil direct compression granules (CADC). A compressed mixture of CAC with excipients was not prepared, as the dissolution results of its powder blend indicated insignificant role of the excipients on this form of the drug.

### **4.2.3 Mixtures testing**

#### **4.2.3.1 HPLC method for mixtures analyses**

Mixtures were tested for homogeneity of CA distribution by analyses of 5 different samples from each. The test was undertaken on powder quantities equivalent to the weight needed for sample preparation according to the HPLC method mentioned in chapter 2, section 2.9.2.1.

#### **4.2.3.2 DSC testing of the mixtures**

To study the physical and chemical compatibility of CA with each of the tested excipients, DSC testing on 1 : 1 CAA mixtures with excipients was performed according to the method described in chapter 2, section 2.1.2. Each excipient was also tested alone and results were compared with those of related mixtures.

#### **4.2.3.3 MTDSC testing of the mixtures**

MTDSC testing using the method described in chapter 2, section 2.2.2, was applied for CAA and CAC mixtures with all excipients chosen. This included the compressed mixture (CADC).

#### **4.2.3.4 Dissolution testing of the mixtures**

Dissolution rate of CA from each mixture was tested using BP 2003 method described in chapter 2, section 2.7.2.2.

#### **4.2.3.5 *In vitro* gut absorption testing of the mixtures**

*In vitro* gut absorption of CA from each mixture was tested as described in chapter 2, section 2.8.2.2.

### **4.3 RESULTS AND DISCUSSIONS**

#### **4.3.1 Mixtures of CAA with Ac-Di-Sol**

##### **4.3.1.1 Homogeneity measurements**

The homogeneity results of CA in mixture 1 (50:50, CAA : Ac-Di-Sol), and mixture 2 (85:15, CAA : Ac-Di-Sol) were 47.0 – 54.0 mg% and 80.0 – 89.0 mg% CA, respectively. Results of compressed mixture 2 were 78.0 – 92.0 mg% CA. The obtained results indicated good blend homogeneity ( $\pm 10\%$ ).

##### **4.3.1.2 DSC measurements**

The DSC thermogram of mixture 1 showed two endothermic peaks, one at 84.3°C representing the  $T_g$  of CAA overlapping the relaxation peak, and another wide peak for Ac-Di-Sol at 131.8°C. DSC thermogram of Ac-Di-Sol alone showed one wide endothermic peak at 130.3°C.

These measurements indicated that Ac-Di-Sol is physically and chemically compatible with CA upon mixing, and that there is no apparent effect of Ac-Di-Sol on the  $T_g$  value of CAA upon mixing.

##### **4.3.1.3 Dissolution testing**

The results of CA release from mixtures of CAA with Ac-Di-Sol are shown in Table 4.2 and Figure 4.1.



Time	Average %C release ( $\pm$ SD)		
	Powder blends		Compressed
	Mixture 1	Mixture 2	Mixture 2
5	67.2 $\pm$ 3.0	83.5 $\pm$ 1.3	93.1 $\pm$ 6.0
10	78.5 $\pm$ 5.9	99.8 $\pm$ 0.8	107.2 $\pm$ 0.3
15	81.0 $\pm$ 7.2	98.8 $\pm$ 2.0	103.3 $\pm$ 0.4
20	85.9 $\pm$ 2.5	100.6 $\pm$ 1.6	103.0 $\pm$ 0.6
30	88.0 $\pm$ 2.0	100.9 $\pm$ 1.6	103.6 $\pm$ 0.6

Table 4.2: Dissolution CA% release from CAA mixtures with Ac-Di-Sol, n=6.

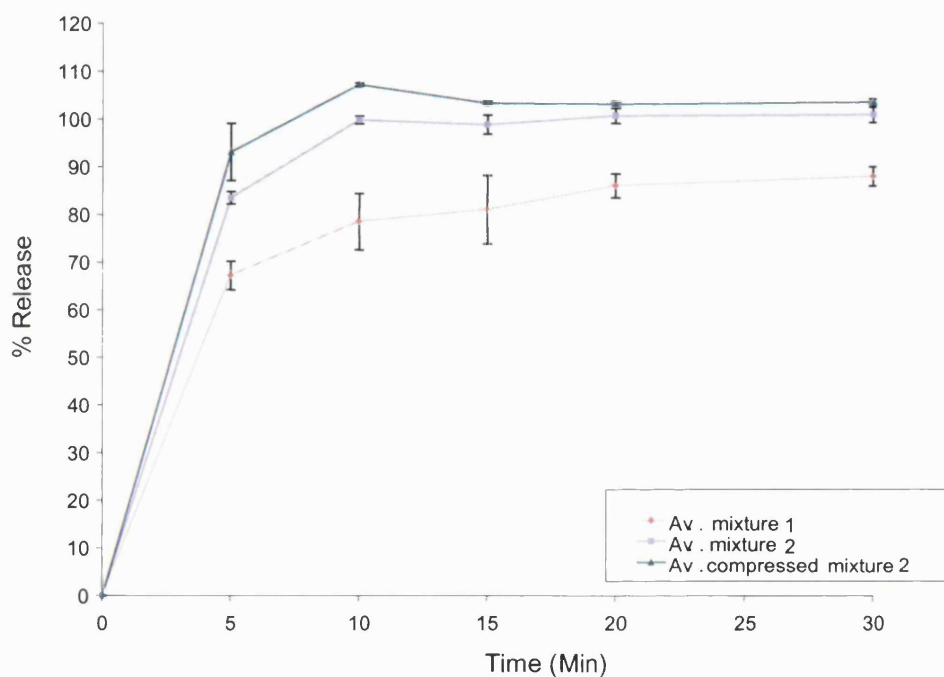


Figure 4.1: Dissolution CA% release from CAA mixtures with Ac-Di-Sol, n=6.

As shown above, the dissolution results of CA from all mixtures with Ac-Di-Sol were compliant with BP and USP current specifications for the dissolution of CA tablets (> 60% after 15 min and > 75% after 45 min).

The dissolution rate of CA was higher from mixture 2 than that from mixture 1. This is related to the fact that mixture 1 contained 50% (by weight) insoluble Ac-Di-Sol material, which settled at the bottom of the dissolution vessel, thus, trapping and retarding the complete release of CA. This was not observed with mixture 2 which

contained 15% Ac-Di-Sol only. This last concentration led to a fast and efficient dispersion and dissolution of CAA particles in the dissolution media.

Results also indicated that the rate of dissolution of CA from compressed mixture 2 was significantly higher than that from CAAC, as shown in chapter 3, section 3.3.7. This indicated that compression had no detrimental effect on the release of CAA when in the form of a mixture with Ac-Di-Sol.

Also, the release rates of CAA from mixture 2 and compressed mixture 2 were both high, with a slight increase observed with the latter. This may be related to the micro-environment that Ac-Di-Sol could provide to CAA material upon compression, which led to a better enhancement in CAA dissolution rate compared to being in the form of a blend that is immediately dispersed when loaded into the media.

#### 4.3.1.4 *In vitro* gut absorption test

The *in vitro* gut results of C release from compressed and uncompressed mixture 2 are presented in Table 4.3 and Figure 4.2.

Time (min)	Average %C release ( $\pm$ SD)	
	Mixture 2	Compressed mixture 2
15	2.02 $\pm$ 2.50	5.45 $\pm$ 1.30
30	5.32 $\pm$ 5.10	7.31 $\pm$ 3.33
45	9.92 $\pm$ 4.30	12.65 $\pm$ 2.87
60	15.77 $\pm$ 2.75	19.47 $\pm$ 3.66
75	21.74 $\pm$ 3.37	24.78 $\pm$ 5.80
90	26.75 $\pm$ 4.82	30.47 $\pm$ 6.20
105	33.36 $\pm$ 5.00	34.33 $\pm$ 7.50
120	38.04 $\pm$ 3.00	41.08 $\pm$ 7.20

Table 4.3: *In vitro* gut C% release from CAA mixtures with Ac-Di-Sol, n=3.

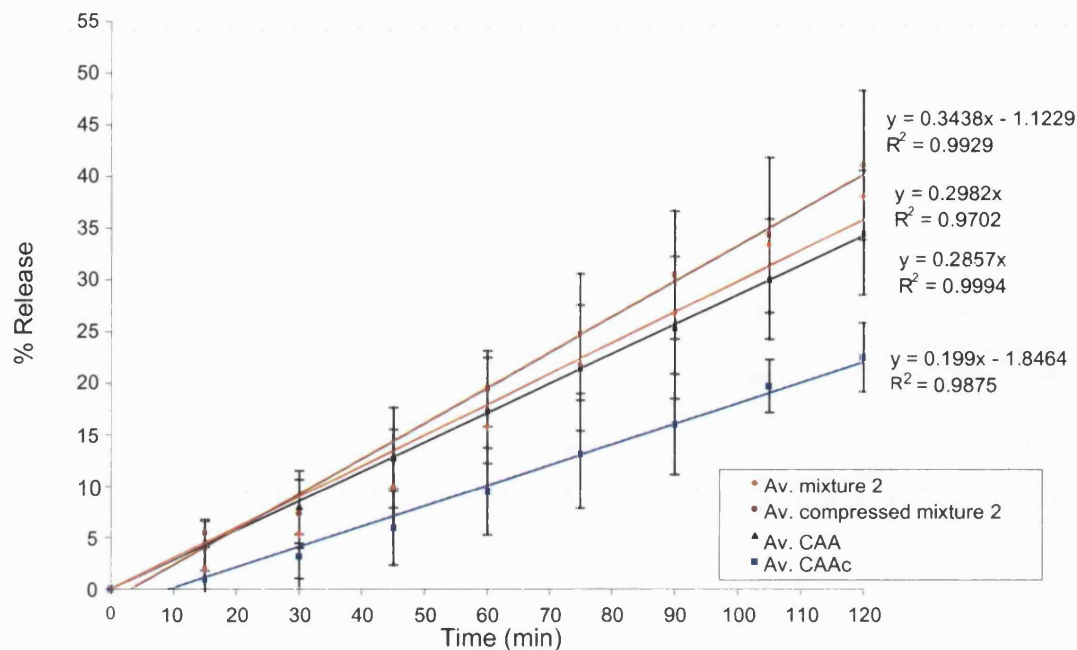


Figure 4.2: *In vitro* gut release of C from compressed and uncompressed CAA mixtures with Ac-Di-Sol, n=3.

The above figure shows a linear zero order *in vitro* gut release of C from mixture 2, the rate of which was found similar to that from CAA alone. This indicated that Ac-Di-Sol in the ratio used in mixture 2 retained the intestinal absorption rate of CAA. A linear zero order release rate of C was also observed for the compressed mixture 2, which was close to that of the uncompressed mixture.

The reduction in intestinal absorption rate of CAA upon compression, related to partial crystallisation of CAA (chapter 3), was not noticed with the compressed mixture 2. This may be related to the inhibition of crystallisation by the introduction of Ac-Di-Sol within the compressed CAA granules. Thus, compression of CAA in the presence of AC-Di-Sol maintained its original absorption rate, unlike compression of CAA alone, which significantly reduced its rate of absorption.

The above may be related to mixing of CAA with the highly fibrous non crystalline material (Ac-Di-Sol), which might have diluted the effect of heat and pressure generation upon compression. This was aided by the fact that Ac-Di-Sol is a relatively poorly compressible material compared to other polymers such as PVP,

(Gissinger, 1980). It may also be considered the hydrogen bonding between CA and Ac-Di-Sol polymer, which might have reduced the molecular mobility of CAA in the mixture, thus linking its local motions to that of the polymer and preventing crystallisation. Thus Ac-Di-Sol stabilised the amorphous form of the drug and inhibited its crystallisation during compression.

The lag time noticed in Figure 4.2 for compressed mixture 2 release curve is related to time needed for the compressed granules to disintegrate, and the powder to be dispersed in the media before absorption started.

Statistical analyses (two way Anova) was applied to determine similarity of the *in vitro* gut release rates of C from mixture 2 and from CAA. Data obtained indicated that these two were not significantly different ( $P>0.05$ ), but both were significantly different from that of the compressed CAA alone (CAAc), ( $p<0.05$ ).

#### **4.3.2 Mixtures of CAA with pregelatinized starch 1500**

##### **4.3.2.1 Homogeneity measurements**

Homogeneity results of CA in mixture 3 (50:50, CAA : Starch1500) were 45.0mg – 51.0mg% CA, for mixture 4 (70:30, CAA : Starch1500) and compressed mixture 4 results were 67.3mg – 72.5mg%, and 63.5mg – 71.5mg % CA, respectively. This indicated good blend homogeneity ( $\pm 10\%$ ).

##### **4.3.2.2 DSC measurements**

The DSC thermogram of mixture 3 had an endothermic peak at 83.0°C representing the  $T_g$  of CAA overlapping the relaxation peak, and a wide endothermic peak for Starch 1500 centred at 141.1°C. Testing of Starch 1500 alone showed one wide endothermic peak at 142.7°C. Thus, the DSC results indicated that starch 1500 was chemically and physically compatible with CA, and that there was no effect of Starch 1500 on the  $T_g$  value of CAA.

##### **4.3.2.3 Dissolution testing**

The results of CA release from its mixtures with starch 1500 are shown in Table 4.4 and Figure 4.3.

Time	Average %CA release ( $\pm$ SD)		
	Powder blends		Compressed
	Mixture 3	Mixture 4	Mixture 4
5	57.70 $\pm$ 14.76	68.0 $\pm$ 3.1	86.39 $\pm$ 9.17
10	69.26 $\pm$ 15.39	79.7 $\pm$ 2.9	105.58 $\pm$ 0.96
15	70.00 $\pm$ 10.16	85.0 $\pm$ 2.0	102.26 $\pm$ 1.22
20	68.93 $\pm$ 8.69	85.2 $\pm$ 2.2	99.29 $\pm$ 2.69
30	68.91 $\pm$ 10.14	83.7 $\pm$ 1.1	100.72 $\pm$ 0.89

Table 4.4: Dissolution CA% release from CAA mixtures with Starch 1500, n=6.

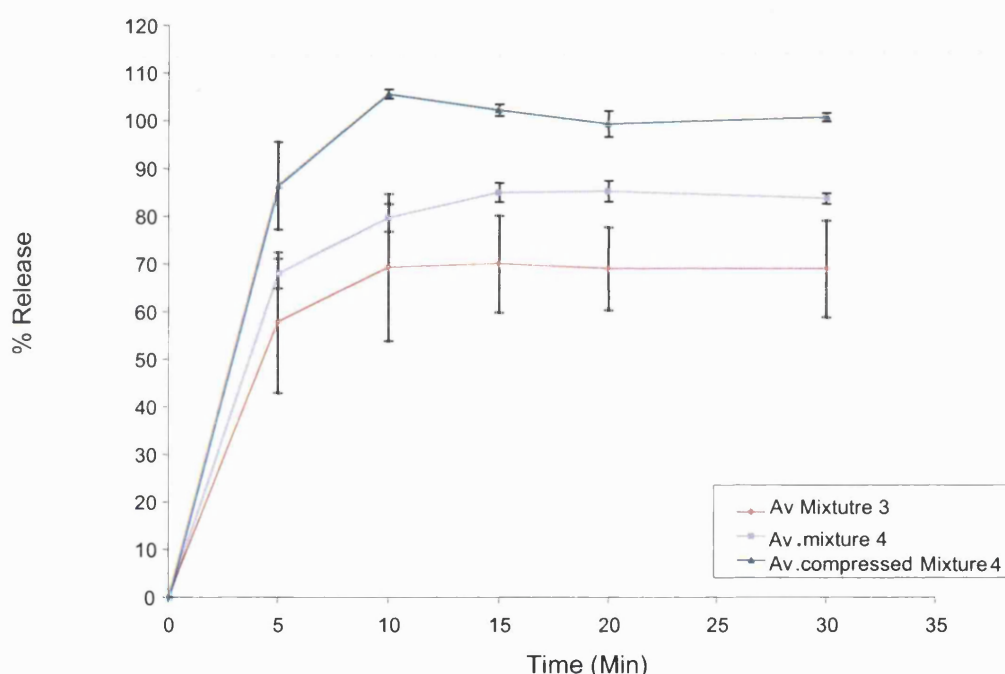


Figure 4.3: Dissolution CA% release from CAA mixtures with Starch 1500, n=6.

The above data show that the dissolution rate of CA from mixture 4 was in compliance with BP and USP current specifications for dissolution of tablets, ( $\geq 60\%$  after 15 minutes). It was also shown that the dissolution rate of CA in mixture 4 was higher than that in mixture 3. This can be related to the fact that mixture 3 contained 50% (by weight) insoluble material (Starch 1500) which settled at the bottom of the dissolution vessel, trapping and retarding the complete release of CAA. This case was not found with the 30% Starch 1500 content in mixture 4.

It was also evident that in compressed mixture 4 the rate of dissolution of CA was

higher than that from the uncompressed mixture. This may be related to the compaction of the mixture which brought the disintegrant (Starch 1500) particles in close proximity to the CAA particles, thus potentially providing it a faster dispersion and a higher surface area of exposure in the dissolution media.

#### 4.3.2.4 *In vitro* gut absorption

The *in vitro* gut results of C release from compressed and uncompressed mixture 4 are presented in Table 4.5 and Figure 4.4.

Time (min)	Average %CA release ( $\pm$ SD)	
	Mixture 4	Compressed Mixture 4
15	5.34 $\pm$ 1.58	2.52 $\pm$ 0.50
30	8.98 $\pm$ 2.74	4.03 $\pm$ 1.47
45	14.40 $\pm$ 3.78	8.78 $\pm$ 2.00
60	20.61 $\pm$ 5.60	13.97 $\pm$ 3.35
75	27.10 $\pm$ 2.93	20.15 $\pm$ 4.20
90	31.08 $\pm$ 4.72	26.03 $\pm$ 5.67
105	34.73 $\pm$ 5.08	31.49 $\pm$ 6.33
120	37.34 $\pm$ 2.30	37.25 $\pm$ 5.27

Table 4.5: *In vitro* gut C% release from CAA mixtures with Starch 1500, n=3.

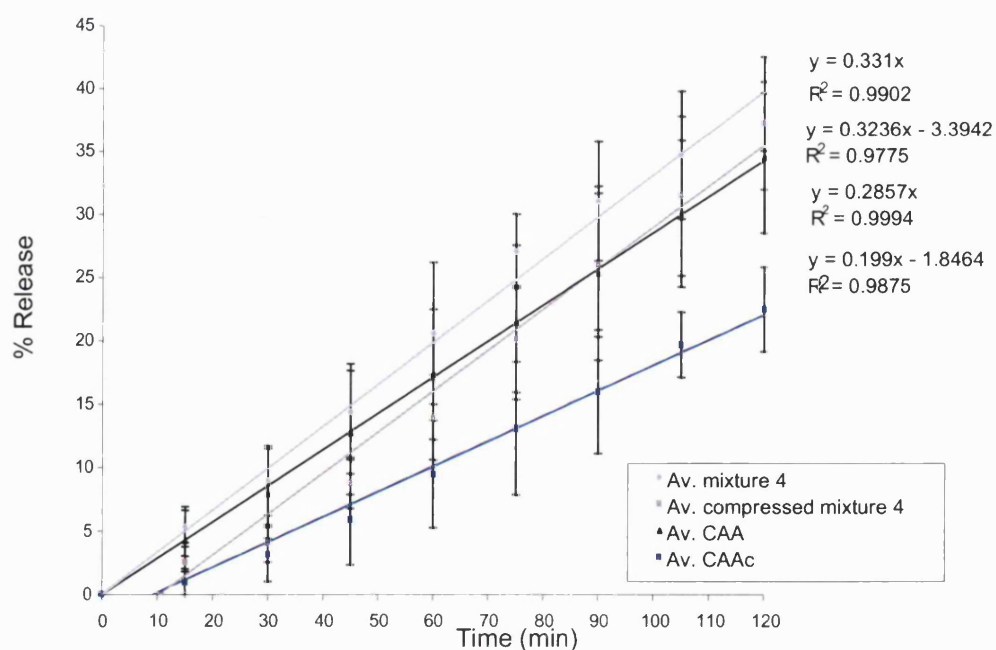


Figure 4.4: *In vitro* gut release of C from compressed and uncompressed CAA mixtures with Starch 1500, n=3.

The figure above shows a linear zero order *in vitro* gut release rate of C from mixture 4, which was found close to that from CAA alone. Thus, the introduction of starch 1500 in mixture 4, at the 30% ratio, retained the intestinal absorption rate of CAA. The few minutes lag time seen in Figure 4.4 for compressed mixture 4 is related to time needed for the compressed granules to disintegrate and disperse in the media before absorption started.

It was also clear that the absorption rate of CA from compressed mixture 4 was similar to that uncompressed. This indicated that compression of CAA in the presence of starch 1500 maintained its original absorption rate, which was different from what was noticed with compression of CAA alone, where absorption rate was reduced significantly. The reduction in dissolution rate of CAA after compression was referred to partial transformation of CAA to the crystalline form. Starch 1500 was found to minimize such an effect, thus it stabilised CAA and inhibited its crystallisation upon compression.

On the other hand, the possible hydrogen bonding formation between CAA and this polymer might have hindered its molecular mobility, and prevented crystallisation. It was also reported that the compressibility of Starch 1500 was less than that in other polymers (as PVP) (Gissinger, 1980). Thus, less pressure and heat would be generated in the slugs, hence reducing the plasticization and possible crystallisation of the amorphous drug.

Statistical analyses (two way Anova) was applied to determine similarity of the *in vitro* gut release rates of C from mixture 4 and from CAA. Data obtained indicated that these two were not significantly different ( $P > 0.05$ ), but both were significantly different from that of the compressed CAA alone (CAAc), ( $p < 0.05$ ).

### **4.3.3 Mixture of CAA with Aerosil 200**

#### **4.3.3.1 Homogeneity results**

The homogeneity results of CA in mixture 5 (50:50, CAA : Aerosil 200) and mixture 6 (97:3, CAA : Aerosil200) were 46.0mg – 53.0mg%, and 92.0mg – 99.0mg%CA, respectively. For compressed mixture 6, results were 93.0mg – 103.0mg% CA. This indicated good distribution of CA in all mixtures tested ( $\pm 10\%$ ).

#### 4.3.3.2 DSC measurements

The DSC thermogram of mixture 5 indicated physical and chemical compatibility of Aerosil 200 with CA. The endothermic peak characteristic of CAA  $T_g$  overlapping a relaxation peak at 82.8°C was detected, together with a  $T_g$  for Aerosil at 302.0°C. Testing Aerosil 200 alone indicated a  $T_g$  at 303.3°C.

#### 4.3.3.3 Dissolution testing

The results of CA release from its mixtures with Aerosil 200 are shown in Table 4.6 and Figure 4.5.

Time	Average %CA release ( $\pm$ SD)		
	Powder blends		Compressed
	Mixture 5	Mixture 6	Mixture 6
5	31.8 $\pm$ 6.5	70.1 $\pm$ 0.3	75.98 $\pm$ 11.88
10	49.3 $\pm$ 9.4	91.0 $\pm$ 3.4	99.30 $\pm$ 2.13
15	69.3 $\pm$ 8.4	91.5 $\pm$ 3.9	98.43 $\pm$ 4.05
20	78.3 $\pm$ 2.8	91.2 $\pm$ 0.9	99.49 $\pm$ 1.61
30	88.8 $\pm$ 2.0	91.0 $\pm$ 2.5	99.59 $\pm$ 0.76

Table 4.6: Dissolution CA% release from CAA mixtures with Aerosil 200, n=6.

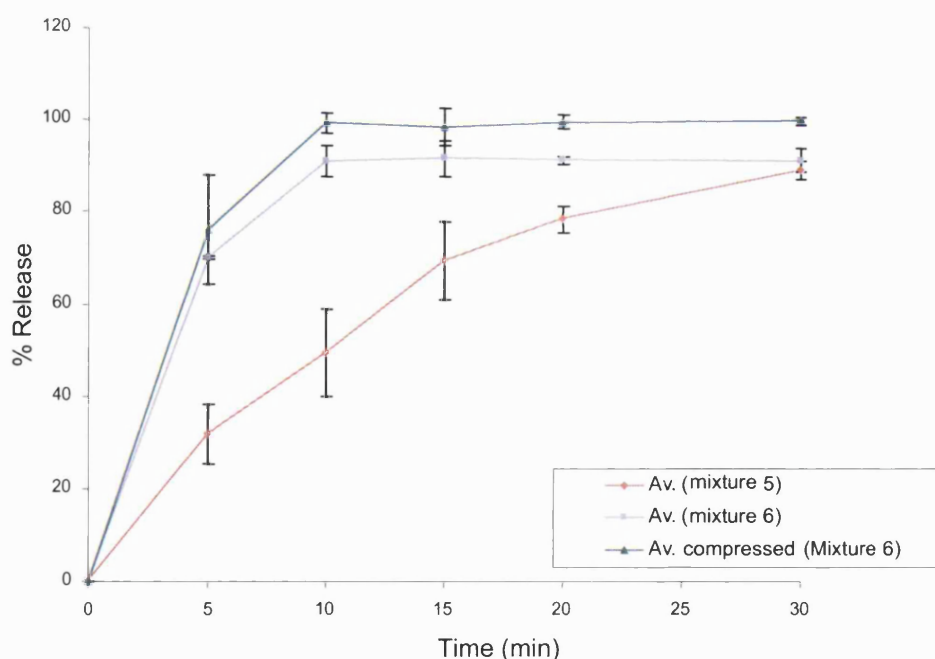


Figure 4.5: Dissolution CA% release from CAA mixtures with Aerosil 200, n=6.



The results above show that the dissolution rate of CA in mixture 6 was slightly enhanced with regards to mixture 5. This may be related to the high surface area of the water insoluble mesh formed by Aerosil around CAA particles at the 50:50 ratio in mixtures, which minimized CA contact with the dissolution media. A 3% concentration of Aerosil 200 in mixture 6 did not, however, show such an effect.

The slight decrease in CA% dissolved from uncompressed mixture 6 compared to the compressed at different time points can be possibly related to the observed creaming of CAA particles on the surface of the dissolution media. This may be due to the fluffy and light particles of Aerosil 200, which creamed some of the smaller CAA particles to the surface of the media during testing. A case that was not noticed upon compression of the mixture.

#### 4.3.3.4 *In vitro* gut absorption

The results of *in vitro* gut C release from compressed and uncompressed mixture 6 are presented in Table 4.7 and Figure 4.6.

Time (min)	Average %C Release $\pm$ SD	
	Mixture 6	Compressed Mixture 6
15	2.66 $\pm$ 0.22	3.82 $\pm$ 0.80
30	7.50 $\pm$ 1.87	5.58 $\pm$ 1.53
45	13.01 $\pm$ 3.59	10.14 $\pm$ 2.76
60	18.83 $\pm$ 5.87	15.21 $\pm$ 3.31
75	23.46 $\pm$ 4.44	19.96 $\pm$ 4.85
90	28.75 $\pm$ 5.55	24.42 $\pm$ 5.66
105	33.25 $\pm$ 3.73	29.39 $\pm$ 6.30
120	37.04 $\pm$ 4.93	33.74 $\pm$ 6.10

Table 4.7: *In vitro* gut C release from CAA mixtures with Aerosil 200, n=3.

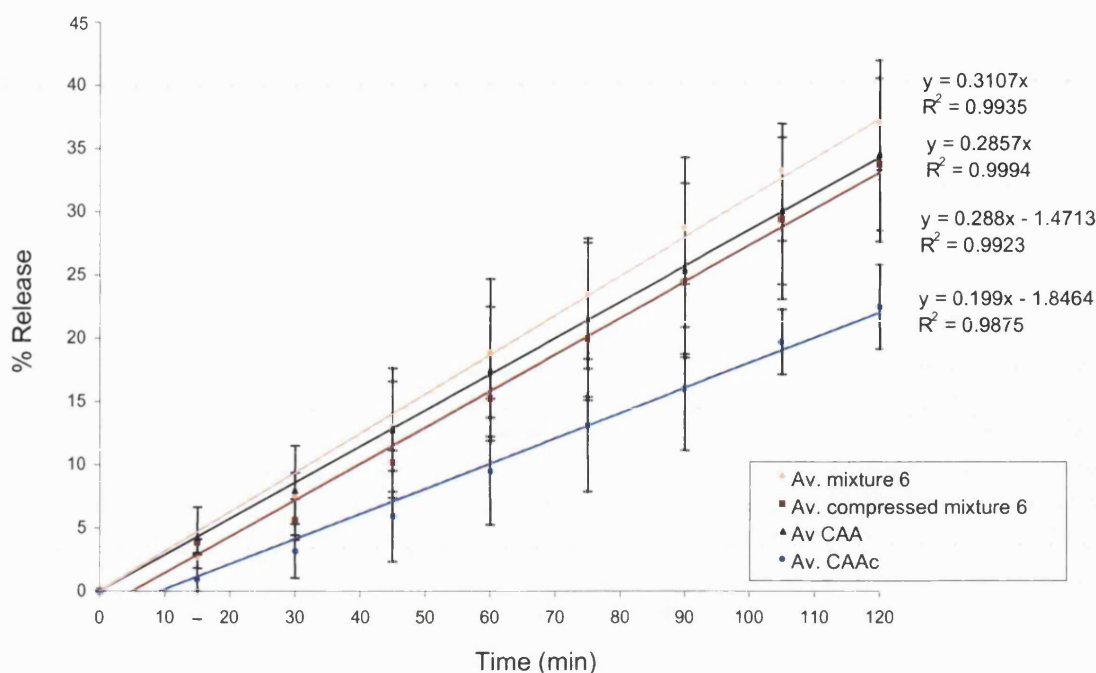


Figure 4.6: *In vitro* gut release of C from compressed and uncompressed CAA mixtures with Aerosil 200, n=3.

The C release profiles from CAA mixtures with Aerosil, shown in Figure 4.6, reflected linear zero order release rates. The few minutes lag time noticed with compressed mixture 6 may be related to time needed for the granules to disintegrate and disperse in the media before absorption started.

The *in vitro* results indicated that Aerosil 200 in the ratio applied in mixture 6 maintained the intestinal absorption rate of CA from CAA. It was also noticed that compression didn't reduce the absorption rate of CA from compressed mixture 6, as it did with CAA alone. This, once again, indicated that Aerosil 200 prevented the transformation of CAA to CAC. Thus, although it did not form an ideal mixture with CAA as each material retained its  $T_g$  value upon mixing, Aerosil 200, by having a higher  $T_g$  value (300°C), tended to stabilise CAA and to prevent its crystallisation, thus it maintained its original absorption rate.

Such stabilisation mechanism of small amorphous drugs by materials having higher  $T_g$  values was previously reported by Craig et al.(1999-a).

On the other hand, because of the high surface area of Aerosil 200, it efficiently covered CAA particles in the mix, this might have an aid in relieving the effect of compression on the amorphous drug.

Another reason for Aerosil being enhancing the dissolution and maintaining the absorption rate of CAA may be related to the fact that silicon dioxide can act as a micro-environmental pH adjustor around CA, and as an anti-gelling agent for the drug (James et al, 1989). It was confirmed in the lab that at pH > 5.5 decomposition rate of CA increased. When CA was mixed with silicon dioxide to prepare solid formulation for oral administration, the micro-environment around CA was maintained with an acidic state between 3.5 and 5.5, which increased its stability.

Thus, despite the relatively small amount of Aerosil 200 mixed with CAA, it had evenly distributed between the particles due to its large surface area. Thereby the attractive forces between CAA particles was reduced, and its gelation was subsequently prevented. Consequently good dissolution and absorption rates of the drug were maintained.

Statistical analyses (two way Anova) was applied to determine similarity of the *in vitro* gut release rates of C from mixture 6 and from CAA. Data obtained indicated that these two were not significantly different ( $P>0.05$ ), but both were significantly different from that of the compressed CAA alone (CAAc), ( $p<0.05$ ).

#### **4.3.4 Mixtures of CAA with SLS**

##### **4.3.4.1 Homogeneity measurements**

The homogeneity results of CA in mixtures 7 (50:50, CAA : SLS) and 8 (85:15, CAA : SLS) were 48.0mg – 55.0mg% and 79.5mg – 91.0mg% CA, respectively. The compressed mixture 8 results were 81.0mg – 92.0mg% CA. This indicated good distribution of CA in all mixtures tested ( $\pm 10\%$ ).

##### **4.3.4.2 DSC measurements**

The DSC thermogram of mixture 7 revealed 3 endothermic peaks, one for the  $T_g$  of CAA overlapping a relaxation peak at 82.0°C, and the others for SLS at 113.5°C

and 195.3°C. The DSC thermogram of SLS alone showed its characteristic two endothermic peaks at 115.1°C and 196.2°C.

#### 4.3.4.3 Dissolution testing

The results of CA release from its mixtures with SLS are shown in Table 4.7 and Figure 4.7.

Time	Average %CA release ( $\pm$ SD)		
	Powder blends		Compressed
	Mixture 7	Mixture 8	Mixture 8
5	10.0 $\pm$ 7.0	16.5 $\pm$ 9.3	27.17 $\pm$ 10.53
10	18.0 $\pm$ 5.0	24.1 $\pm$ 8.6	34.66 $\pm$ 8.86
15	23.0 $\pm$ 4.0	28.6 $\pm$ 7.1	38.80 $\pm$ 7.18
20	28.0 $\pm$ 3.0	32.1 $\pm$ 5.6	41.54 $\pm$ 7.85
30	30.0 $\pm$ 6.0	36.6 $\pm$ 4.5	46.58 $\pm$ 7.76

Table 4.8: Dissolution CA% release from CAA mixtures with SLS, n=6.

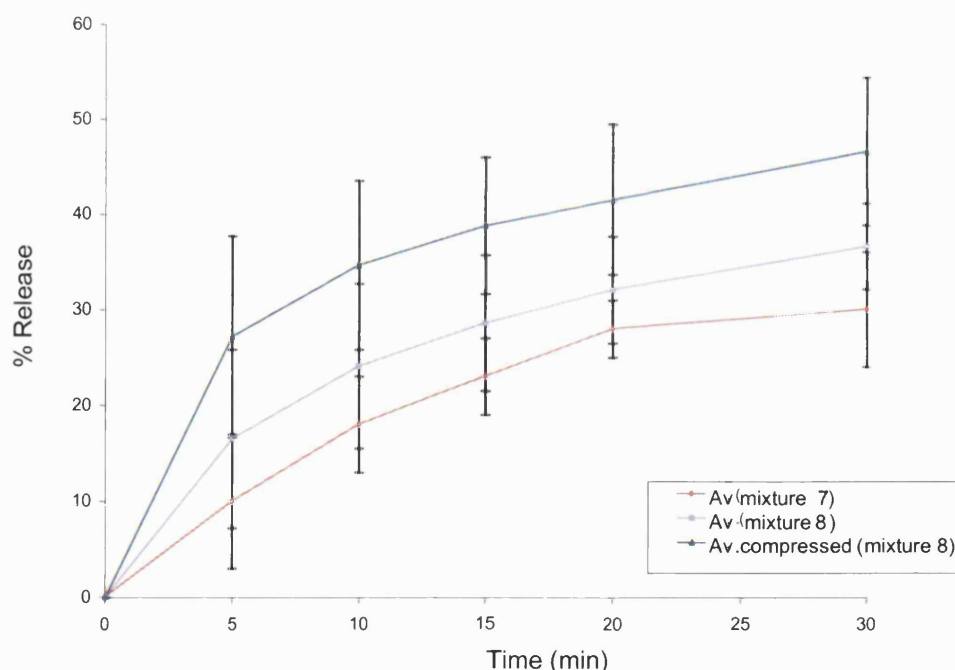


Figure 4.7: Dissolution CA% release from CAA mixtures with SLS, n=6.

The results above indicated that SLS did not significantly enhance the dissolution rate of CAA when compared to other excipients. The % release of CA from both mixtures 7 and 8 were similar, with a slight increase noticed with compressed

mixture 8 at each time point. The reason for having such low dissolution results, despite of SLS being a wetting agent, may be related to the basicity of SLS compared to other tested excipients. The increased pH of the solution (by SLS) around CAA to 6.3 caused its gelation and limited its dissolution enhancement. Hence, dissolution results of CAA as a mixture with SLS were all below the stated pharmacopeial limits (> 60% after 15 minutes), and much lower than what was obtained from mixtures with other tested excipients.

#### 4.3.4.4 *In vitro* gut release testing

The results of the *in vitro* gut C release from compressed and uncompressed mixture 8 are presented in Table 4.9 and Figure 4.8.

Time (min)	Average % C release ( $\pm$ SD)	
	Mixture 8	Compressed Mixture 8
15	1.10 $\pm$ 0.25	1.49 $\pm$ 0.23
30	3.03 $\pm$ 1.30	1.68 $\pm$ 0.56
45	6.10 $\pm$ 2.65	3.39 $\pm$ 1.00
60	10.48 $\pm$ 4.57	5.67 $\pm$ 0.90
75	14.12 $\pm$ 4.53	7.89 $\pm$ 2.10
90	17.73 $\pm$ 5.77	10.48 $\pm$ 3.03
105	21.49 $\pm$ 6.85	13.41 $\pm$ 3.00
120	25.21 $\pm$ 7.00	15.84 $\pm$ 2.87

Table 4.9: *In vitro* gut C% release from CAA mixtures with SLS, n=3.

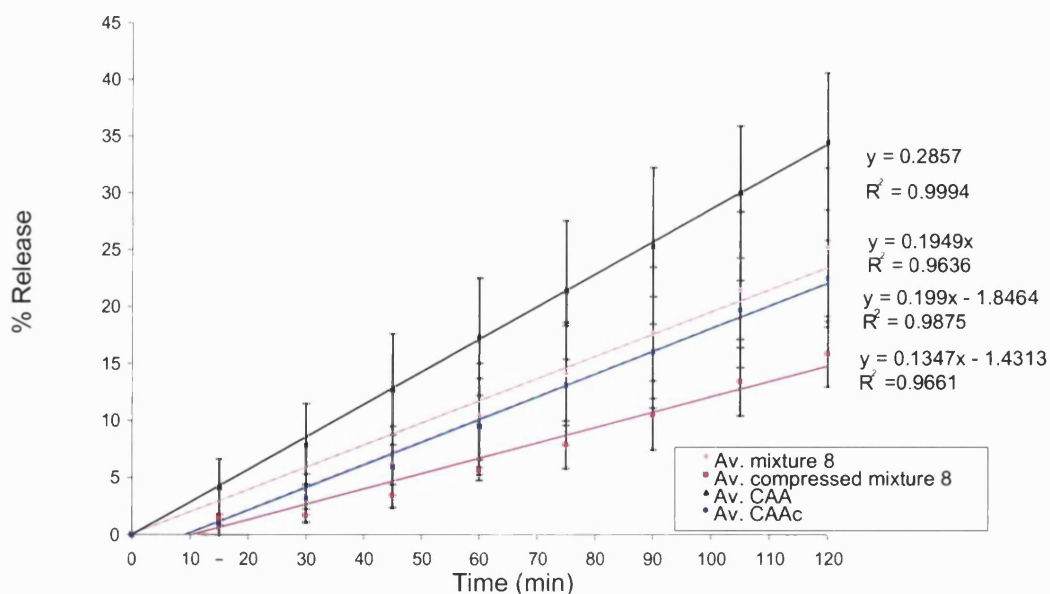


Figure 4.8: *In vitro* gut release of C from CAA mixtures with SLS, n=3.

Figure 4.8 shows the zero order linear release rate of C from CAA mixtures with SLS. The few minutes lag time for the compressed mixture can be related to time needed for granules to completely disintegrate and disperse in the media before absorption started.

The results above showed that despite of SLS being a wetting agent, it led to a significant reduction in the absorption rate of CAA (by 35%). The CA absorption rate from SLS mixtures was found to be significantly lower than those previously obtained with other mixtures (namely mixtures 2, 4 and 6). This may be due to the fact that SLS is a basic material which induced gelation of CAA, thus reduced CAA absorption rate significantly.

Statistical analyses (two way Anova) was applied to determine similarity of the *in vitro* gut release rates of C from mixture 8 and from CAA. Data obtained indicated that these two were significantly different ( $P < 0.05$ ).

#### **4.3.5 *In vitro* absorption results summary Table**

Table 4.10 summarises the C release rates (K) from all mixtures studied. It shows that the release rate of CAA was maintained when mixed at the chosen ratios with Ac-Di-Sol, Starch 1500, and Aerosil 200.

Compressed mixtures also showed similar release rates to that of CAA, with no significant difference ( $P > 0.05$ ). This indicated that the effect of compression on CAA was limited when mixed with any of these excipients. Thus, they minimized the effect of pressure and heat generated during compression, potentially preventing the partial crystallisation of CAA upon compression.

SLS showed the lowest K value because of its basic properties that increased the environmental pH around CAA, and led to gelation of the material in the media, thus, significantly reduced the absorption rate.

Material	% CAA Content	C Release rate (K value)	
		Compressed	Uncompressed
CAA	100%	0.20	0.29
CAA + Ac-Di-Sol (Mixture 2)	85%	0.34	0.30
CAA + Starch 1500 (Mixture 4)	70%	0.32	0.33
CAA + Aerosil 200 (Mixture 6)	97%	0.29	0.31
CAA + SLS (Mixture 8)	85%	0.13	0.19

Table 4.10: *In vitro* gut release rates (K) of C from all mixtures tested

#### 4.3.6 Mixtures of CAA, CAC with all tested excipients

It was shown above, the enhancement effect of Ac-Di-Sol, Aerosil 200 and Starch 1500 on the dissolution rate of CAA upon compression. The additive enhancement effect of these excipients (together) on dissolution and bioavailability of CA from both CAC as a powder blend, and CAA as a powder blend and compressed mixture (CADC) was studied as described below.

##### 4.3.6.1 Homogeneity measurements

The homogeneity results of CA content in the powder blends of all the above mentioned excipients, with CAC were 61.5 – 67.0 mg %CA, with CAA were 62.0mg – 68.5mg%, and in CADC 67.8mg – 72.5mg %CA, respectively. This indicated good homogeneity ( $\pm 10\%$ ).

##### 4.3.6.2 DSC measurements

The DSC thermograms of CAA and CAC powder blends showed no significant change compared to those obtained with each form tested alone (as shown in chapter 3, section 3.3.2).

DSC and MTDSC thermograms of CADC shown in Figures 4.9, 4.10 and 4.11 below revealed a  $T_g$  for CAA at about 74°C overlapping a relaxation peak. No melting peak for CAC was detected, as was obtained with the compressed CA (CAAc).

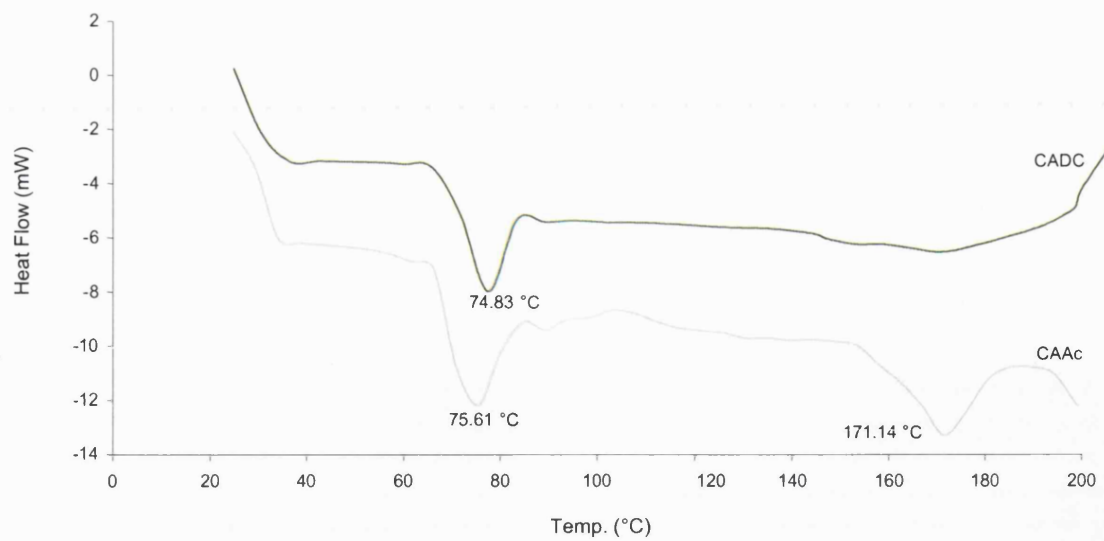


Figure 4.9: DSC thermograms of CADC compared to CAAC, at heating rate 25°C/min.

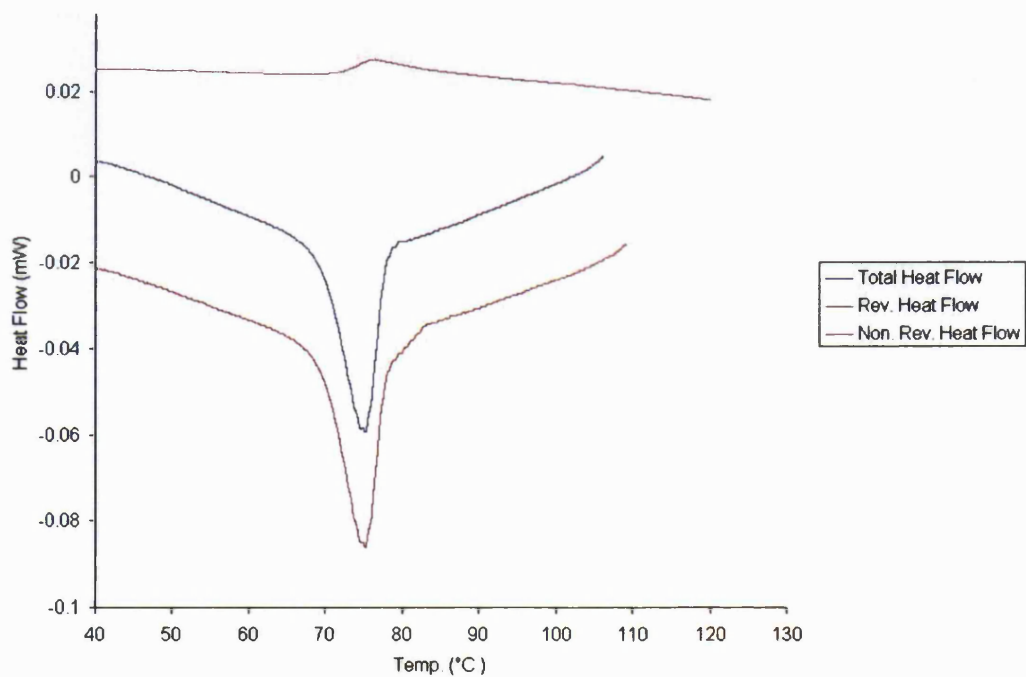


Figure 4.10: MTDSC heat flow thermograms of CADC, at heating rate 1°C/min, amplitude 0.5°C / 48 second



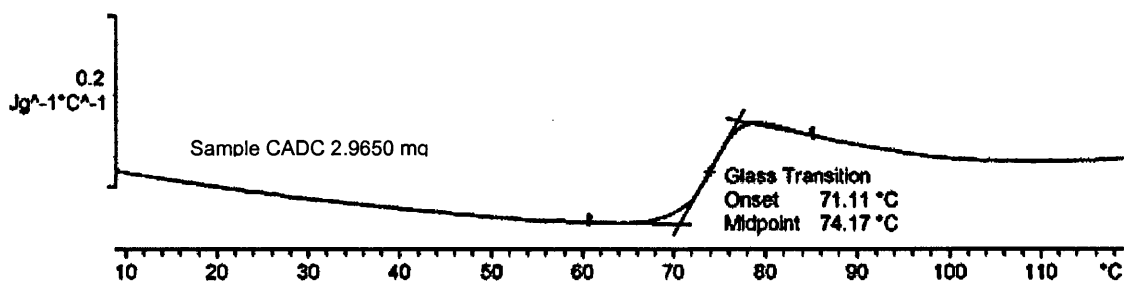


Figure 4.11: Cp complex of CADC, at heating rate 1°C/min, amplitude 0.5°C/48 seconds.

The above DSC thermograms indicated that the crystalline form of CA was not generated upon compression of CAA in a mixture with the excipients (Ac-Di-Sol, Starch 1500, Aerosil 200).

This stabilisation may be related to the fact that the relatively small drug molecule of CAA dispersed in the polymers (Ac-Di-Sol and Starch 1500) physically interacted by hydrogen bonding, thus had its molecular motions coupled with those of the polymers, leading to prevention of crystallisation. Also, Aerosil 200 was found to stabilise CAA due to its high Tg value.

To better understand the effect of the chosen excipients on stabilisation of CAA, a DSC test was done for each of the CAA, compressed CAA (CAAc) and compressed mixture of CAA with the chosen excipients (CADC). A heating - cooling - heating cycle was applied for each form at 10°C/min rate, for the range 30°C - 100°C. In this case hermetically sealed lids were used to keep water inside, and to get a better estimation of the stability of the material as is. Relaxation curves were obtained from the difference between the first and second heating curves of each run. Results obtained for CAA, CAAc and CADC are as shown in the below 4.12, 4.13 and 4.14 Figures, respectively.

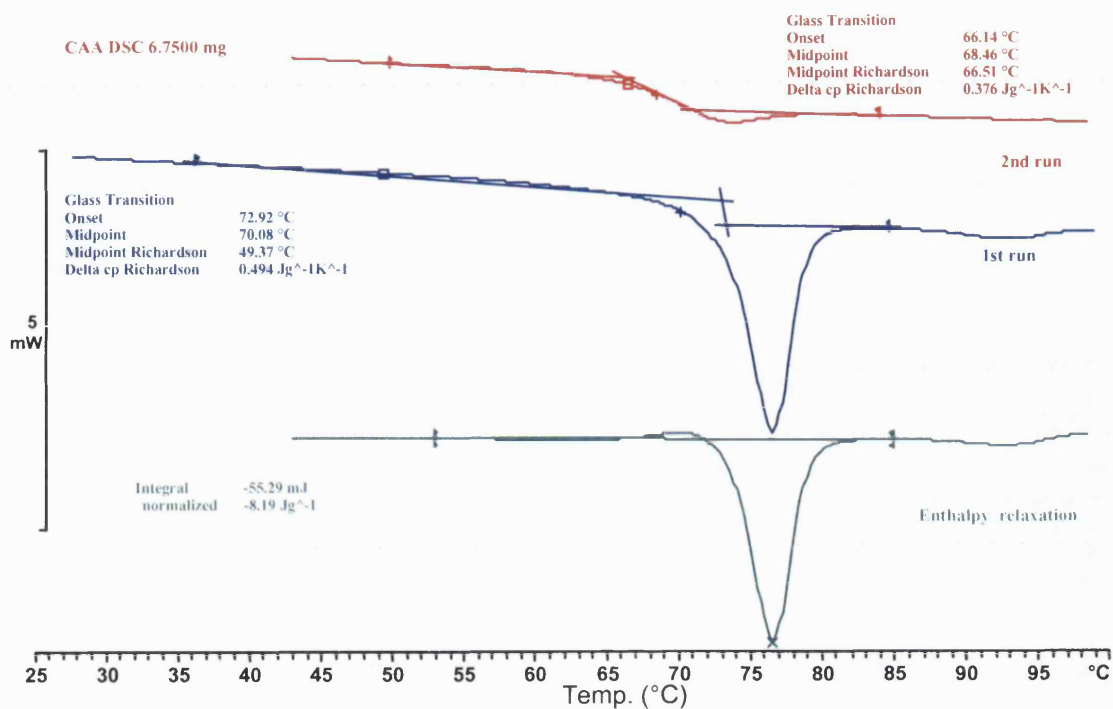


Figure 4.12: DSC thermograms of CAA, heating – cooling – heating cycle, at rate of 10°C/min.

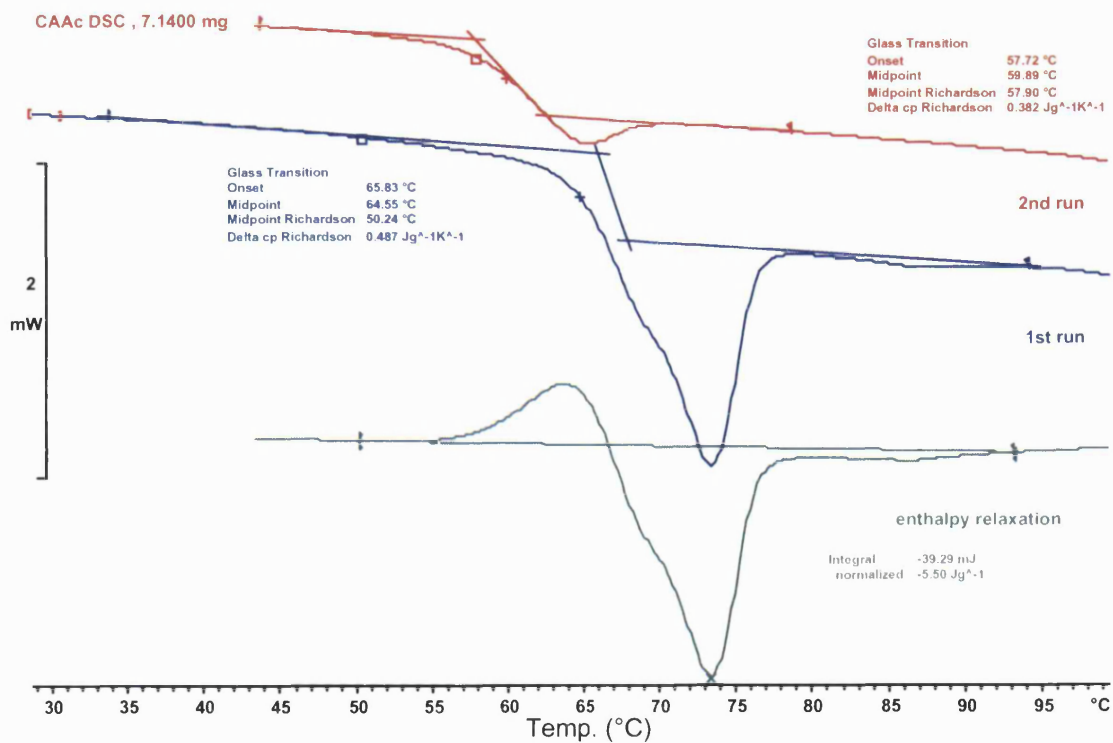


Figure 4.13: DSC thermograms of CAAC, heating – cooling – heating cycle, at rate of 10°C/min.

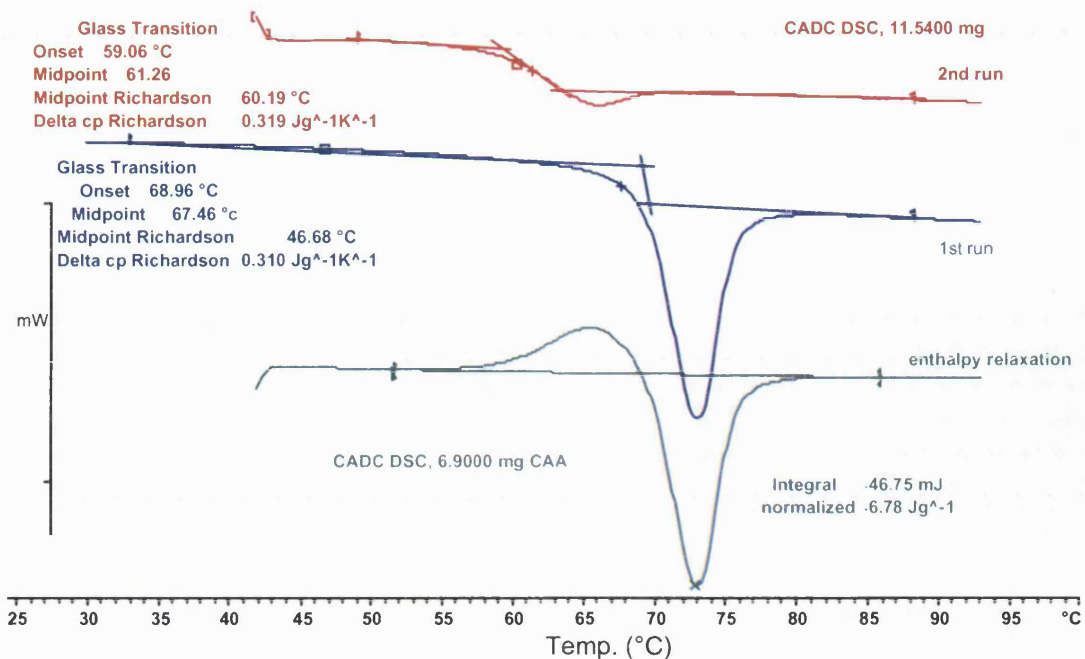


Figure 4.14: DSC thermograms of CADC, heating – cooling – heating cycle, at rate of 10°C/min.

The results above showed the thermal history effect (Relaxation), presented in the first heating run in all tested samples. This effect was not seen in the second heating run as relaxation did not occur in the samples upon ramping up to 100°C. The thermograms also indicated that the  $T_g$  value for CADC is lower than that for CAA (by 6°C). This may be related to the effect of higher water content in the former (2.5%) compared to that of the latter (0.9%). The higher water content in CADC caused plasticization and reduction of  $T_g$  of the amorphous material to 60°C.

On the other hand, the  $T_g$  of CADC in the second heating run was higher by 2°C than that of CAAC. This is despite of CADC having a higher water content than that in CAAC by 1.5%. The  $T_g$  of CAAC was also found to be lower by 8°C than that of the pure amorphous, which indicated that the compressed material (CAAC) was less stable than the pure CAA and also was less stable than CADC.

This, while compression would lower the stability of CAA (reduces its  $T_g$ ), the presence of the formulation excipients limited such an effect and provided stabilisation for CAA against compression generated heat and pressure.

Similar suggested stabilisation effect of some polymers on amorphous drugs were found in the literature. Examples include, stabilisation of amorphous sucrose (Zografi et al. 1999; Shamblin et al. 1996, 1998) and amorphous indomethacin with polyvinylpyrrolidone PVP (Yoshioka et al. 1994, 1995; Zografi et al. 1999), and stabilisation of amorphous acetaminophen using PVP, and polyacrylic acid (Miyazaki et al, 2004). These were in the form of solid dispersions and not as physical mixtures.

The difference observed in this study was that stabilisation of CAA under process conditions was achieved by only physical mixing (i.e. solid dispersion was not needed) with the chosen excipients. This may be related to the fact that CAA is a highly stable amorphous material.

#### 4.3.6.3 Dissolution testing

The percentage release of CA from the compressed CAA mixture with excipients (CADC) and from CAA, CAC blends with the excipients are presented in Table 4.11 and Figure 4.15.

Time	Average %CA release ( $\pm$ SD)		
	Blended mixtures		Compressed mixture
	CAA	CAC	CADC
5	72.0 $\pm$ 5.0	9.72 $\pm$ 1.31	78.0 $\pm$ 8.00
10	81.0 $\pm$ 4.0	18.51 $\pm$ 3.20	92.0 $\pm$ 4.00
15	89.0 $\pm$ 5.0	25.27 $\pm$ 2.93	98.0 $\pm$ 4.00
20	98.0 $\pm$ 2.0	30.35 $\pm$ 2.18	101.0 $\pm$ 1.50
30	101.0 $\pm$ 3.0	33.12 $\pm$ 0.98	100.0 $\pm$ 2.30

Table 4.11: Dissolution CA% release from CADC, CAA and CAC mixtures with the three excipients, n=6.

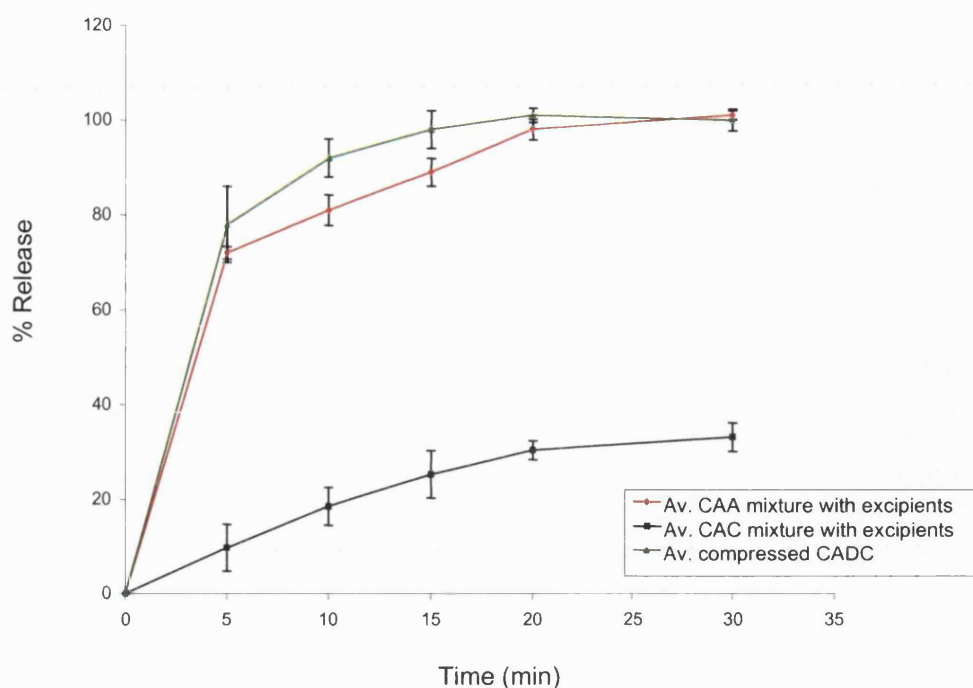


Figure 4.15: Dissolution %CA release from CADC, CAA and CAC mixtures with the three excipients, n=6.

The dissolution profile of CAA with the addition of the excipients together (Ac-Di-Sol, starch 1500 and Aerosil 200) was similar to those obtained from mixtures of CAA with each excipient individually (as shown in sections 4.3.1.3, 4.3.2.3 and 4.3.3.3). Thus, the excipients either added singular or together enhanced the dissolution rate of CAA to the same degree.

Upon compression, CADC granules showed similar dissolution profile to that of CAA powder blend with the excipients, with a slight higher rate for the former. This may be due to the micro-environment these excipients provided to CAA when in its close proximity, thus, providing better enhancement of dissolution than if being purely mixed.

It was also observed that the dissolution results of CA from CAC mixture with excipients were lower than that from the CAAs'. Indicating that the studied excipients did not have the same dissolution enhancement effect as is the case with CAA.

Thus, these excipients could stabilise the amorphous CA and maintained its physical properties, but couldnot enhance the solubility of the crystalline form.

#### 4.3.6.4 *In vitro* gut absorption

The *in vitro* gut absorption results of CADC and CAA, CAC mixtures with excipients are shown in Table 4.12 and Figure 4.16.

Time (min)	Average % release of C $\pm$ SD		
	Mixtures of all excipients with		CADC
	CAA	CAC	
15	1.97 $\pm$ 1.22	2.29 $\pm$ 0.30	3.06 $\pm$ 1.41
30	4.98 $\pm$ 2.97	1.87 $\pm$ 0.25	6.30 $\pm$ 2.45
45	9.06 $\pm$ 3.45	3.41 $\pm$ 0.75	10.64 $\pm$ 2.41
60	14.95 $\pm$ 3.13	5.60 $\pm$ 1.30	15.78 $\pm$ 3.15
75	20.76 $\pm$ 4.25	8.01 $\pm$ 2.50	19.82 $\pm$ 3.73
90	26.48 $\pm$ 5.25	10.60 $\pm$ 3.40	25.38 $\pm$ 5.35
105	31.52 $\pm$ 6.78	13.08 $\pm$ 1.73	30.89 $\pm$ 7.50
120	35.47 $\pm$ 3.52	16.36 $\pm$ 2.42	34.63 $\pm$ 8.45

Table 4.12: *In vitro* gut release of C from CADC, CAA and CAC mixtures with the three excipients, n=3.

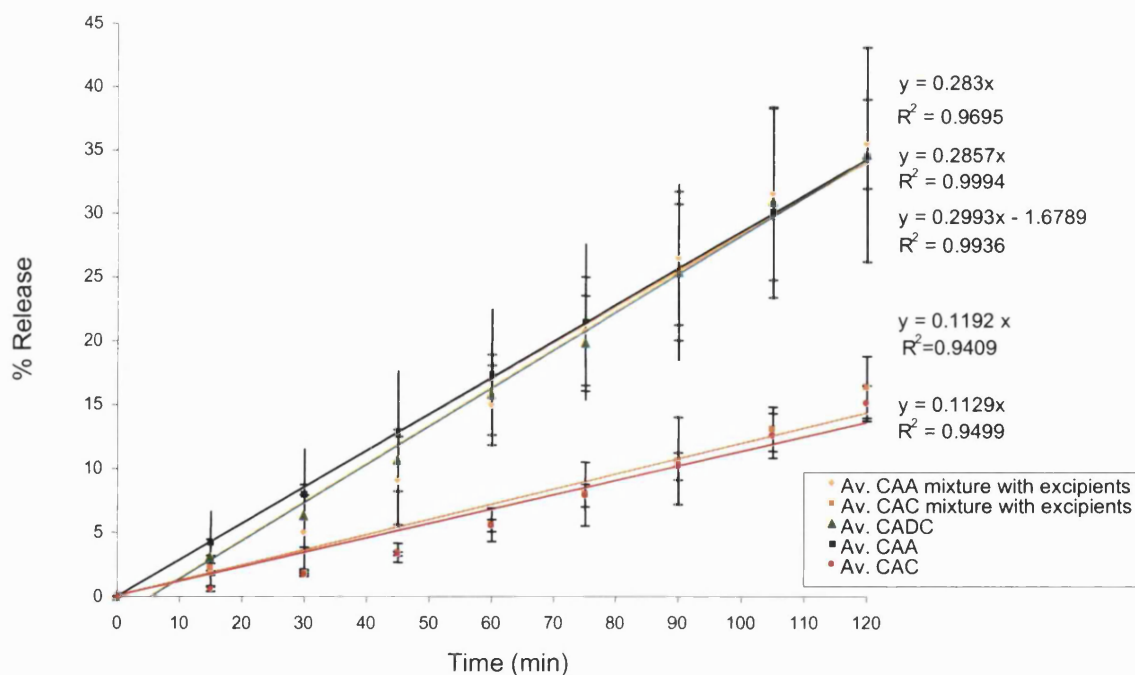


Figure 4.16: *In vitro* gut release of C from CADC, CAA and CAC mixtures with the three excipients, n=3.

It is shown in Figure 4.16 that the studied excipients maintained similar absorption rate to that of CAA, but they had no enhancement effect on CAC.

It was also observed that CADC showed similar absorption rate to that of CAA, which confirmed that the excipients restored the original absorption rate of CAA upon compression.

The absorption rate of C from CAC mixture with excipients was significantly lower (by 60%) than that from the CAAs', but similar to that from CAC alone. This indicated that these excipients were not able to enhance the solubility or bioavailability of the crystalline form of the drug.

Statistical analyses (two way Anova) was applied to determine similarity of the *in vitro* gut release rates of C from the compressed CAA mixture with excipients (CADC) and from CAA. Data obtained indicated that these two were not significantly different ( $P>0.05$ ), but both were significantly different from that of the compressed CAA (CAAc), ( $p<0.05$ ).

#### **4.4 CONCLUSIONS:**

From the DSC studies, it was clear that the thermal behavior of CAA was not affected by the presence of any of the studied excipients, indicating their physical and chemical compatibility with it. From the dissolution studies, it was shown that the optimum ratios for the studied mixtures with CAA were 15%w/w Ac-Di-Sol, 30%w/w Starch 1500, and 3%w/w Aerosil 200.

Compared to dissolution results of CAA alone, CAA mixed with the excipients either singular or together indicated good dissolution profiles ( $> \pm 90\%$  after 45 minutes). This indicated that the introduction of the excipients enhanced the dissolution rate of CAA by providing it a higher contact surface area with the dissolution media. When these mixtures were compressed, slightly higher dissolution results were obtained.

The prepared CAC mixture with the same excipients showed low dissolution rate, characteristic of the low solubility of the crystalline form of the drug. Thus,

dissolution of CAC could not be enhanced by the presence of the formulation excipients.

*In vitro* gut studies showed similar intestinal absorption profiles for CAA and CAA mixtures with excipients, which indicated that they maintained its absorption rate. Upon compression, CAA was shown to undergo partial transformation to CAC (Chapter 3). This may be related to compression generated heat and pressure which caused plasticization and partial crystallisation of CAA. However, mixing of CAA with a variety of formulation excipients (e.g. Ac-Di-Sol, Starch 1500, and Aerosil 200) prevented crystallisation and, further, stabilised the amorphous form the drug.

Stabilisation achieved by these excipients may be related to hydrogen bonding with CAA which reduced its molecular mobility. It may also be related to the high molecular weight of the polymers, and the high  $T_g$  (300°C) of Aerosil 200, both factors reduced the effect of temperature and pressure on the compressed material, thus inhibited CAA crystallisation potential.

The introduction of the wetting agent SLS with CAA did not, however, enhance the dissolution rate to the same extent as obtained with other excipients. Similarly the *in vitro* gut absorption results showed that the absorption rate of CAA was reduced when mixed and/or compressed with SLS. This may be related to the fact of SLS being a basic material, thus, its dispersion with CAA gave rise to an increase in the pH to 6.3. This induced the gelation of CAA, and reduced the extent of the material availability at the absorption site.

The *in vitro* gut absorption results of CAC mixed with the same excipients were confirmatory to the dissolution results, and showed a similar profile to that of CAC alone. This indicated that the selected excipients could only stabilise the amorphous form of CA, but did not enhance the permeability and absorption rate of the crystalline form.



## CHAPTER 5

### EFFECT OF WAX COATING ON CEFUROXIME AXETIL AMORPHOUS (CAA) AND CEFUROXIME AXETIL COMPRESSED MIXTURE WITH EXCIPIENTS (CADC)

#### 5.1 INTRODUCTION

In previous chapters, it was shown the effect of compression on the release and intestinal permeability of CAA, both in the absence and the presence of excipients.

In this chapter, the effect of another important process factor is described, which is the wax coating of CA. It is considered an important factor because in the marketed oral suspension, CA particles are processed with integral lipid coatings in the form of granules to mask the very bitter taste of CA (James et al, 1989). The aim of the lipid coating is to avoid release of the drug into the liquid suspension or in the mouth. The coat which has a limited permeability to water is readily dispersed or dissolved in the gastro-intestinal fluid.

The melting point of the lipid used is sufficiently high to prevent melting of the coated particles in the mouth and release of the bitter tasting active ingredient. In order to prevent melting of the active ingredient and/or its chemical degradation during the coating process, the lipid or mixture of lipids used have a melting point between 40°C and 70°C.

James et al. (1989) reported that wax coating of CAA can be achieved by using suitable lipids (e.g fatty acids , monohydric alcohols, fixed oils, fats, waxes, sterols, phospholipids and glycolipids). The most common lipids include the high molecular weight (C<sub>10-30</sub>) straight chain saturated or unsaturated aliphatic acid, such as stearic acid or palmitic acid (as in Zinnat<sup>®</sup> commercial preparation). The triglyceride tested was a glyceryl ester of a high molecular weight (C<sub>10-30</sub>) aliphatic acid, such as glyceryl trilaurate or glyceryl trimyristate. The partially hydrogenated vegetable oil tested was cottonseed oil or soyabean oil. While the wax was beeswax or carnauba wax, and the high molecular weight (C<sub>10-30</sub>) straight chain aliphatic alcohol was stearyl alcohol or cetyl alcohol, or a mixture thereof .

Of the above, the lipid of choice in providing the best bioavailability and physical properties, and which was particularly compatible with CA was stearic acid in an admixture with palmitic acid in a 1:1 ratio by weight (James et al, 1989).

James et al. described that CA can be first under-coated with a substance of good coating properties. This undercoating serves to protect CA from chemical interactions with the lipid coat. The undercoat is preferably a water soluble and a film forming agent that can be applied from aqueous or non-aqueous systems (e.g polysaccharides such as maltodextrin, alkylcellulose such as methyl or ethyl cellulose, hydroxyalkylcellulose, polyvinylpyrrolidone and polymers based on methacrylic acid).

Wax coated CA particles with an undercoat contained from 5 to 15% by weight of CA. If no undercoating was employed the lipid coated particles contained approximately 10 to 30% by weight of CA. Particles provided with an integral lipid coating to mask the bitter taste of the CA had a diameter of less than 250µm.

The size of the coated particles was found to be an important factor with respect to the bioavailability of CA and the acceptability of its products for oral administration. Particle sizes in excess of 250µm mean diameter by volume gave an undesirable gritty taste, so the mean diameter by volume was maintained below 100µm. The coated particles were prepared by atomizing a dispersion of particulate CA in a molten lipid and cooling the coated particles thereby. For Zinnat<sup>®</sup> wax coated particles, the dispersion is prepared by adding CAA powder to the molten lipid of stearic acid and palmitic acid in the ratio of about 1:1 w/w. The molten dispersion is then atomized to give particles of lipid coated CA upon cooling.

Techniques used to coat CA particles have included the use of conventional atomizers such as rotary atomizers, pressure nozzles, pneumatic nozzles and sonic nozzles. The atomizing gas supplied to the nozzle was air or an inert gas such as dry nitrogen. During the coating process, the temperature at which the molten dispersion was maintained was in the range of 10° to 20°C above the melting point of the lipid or mixture of lipids used. This is in order to provide a dispersion having the desired viscosity for atomization. The atomizing pressure was controlled in order to produce coated particles of the preferred size. The

coated particles were solidified and collected by applying a stream of cool air or dry nitrogen to the spray chamber, at a temperature of 5°C-20°C, until cooling and solidification of the particles were completed. The undercoat was applied to CA using conventional coating techniques, e.g. spray coating using a coater or a spray drier, or coating with a rotary granulator (James et al, 1989).

It has been reported that even after wax coating, CA continues to have bitter taste which is long lasting and cannot be adequately masked by the addition of sweeteners and flavors to the granules (Kremminger, 2003).

It has also been reported (Physicain Disk Reference 2000) that oral suspension of CA is not bioequivalent to CA tablets when tested on healthy adults. The tablets and powder for oral suspension formulation cannot be substituted on a milligram per milligram basis. The area under the curve for the suspension averaged 91% of that for the tablets. Therefore, the safety and effectiveness of both tablets and oral suspension formulations have to be established in separate clinical trials.

Reo et al. (1999) reported another method of masking the taste of the drug in particulate form, which was based on mixing CA with a lipid at a temperature below that where significant drug degradation occurs. This was done by addition of an emulsifier having a hydrophilic-lipophilic balance value (HLB) of 10 – 18, in the presence of 5–25% by weight of the wax/emulsifier coating. Emulsifiers tested included polyglycerol esters, polysorbates, mono and diglycerides of fatty acids, propylene glycol esters, sucrose fatty acids esters, propylene glycol esters, and polyoxethylene derivatives of sorbitan fatty acids esters. The waxes tested were carnauba wax, beeswax, lanolin, bay berry, sugar cane, candelilla wax, microcrystalline waxes, petrolatum wax, carbowax, rice bran wax, paraffin wax and mixtures thereof. The wax was presented in an amount of 80 – 90 % of the coating. The coating provided rapid dissolution and enhanced long term stability of CA.

Sanz et al. (2003) provided a composition comprising CA in particulate form with integral coatings of lipid or mixture of lipids, similar to what James et al. (1989) proposed. He applied a sweetener system (e.g. Saccharin, sodium saccharin,

sodium cyclamate, acesulfame potassium, thaimatin, neohesperidin dihydrochalcone, ammonium glycyrrhizinate and aspartame) at a concentration of 0.3–5% by weight. It further contained a texture modifier, and any thickener or binding agent which may optionally form a part of the composition.

The introduction of the texture modifier was to improve the mouth feel reducing the gritty texture and to enhance easy swallowing. These modifiers included povidone K30, sodium carboxy methyl cellulose, hydroxyethyl cellulose, hydroxypropyl cellulose, guar gum, or xanthan gum.

Mukherji et al. (2003), masked the very bitter taste of CA by coating the active particles in two enteric coating polymers, comprising a methacrylic acid copolymer, and a phthalate polymer added into the matrix to enhance the release of the drug from the methacrylic acid coat. A 1:1 ratio of methacrylic acid copolymer to phthalate polymer was optimal for the taste masking effect. The total polymer to drug ratio was at least 1:4. It was shown that the obtained coat composition effectively masked the taste of the drug without compromising the dissolution rate.

The CA methacrylic acid copolymer and the phthalate polymer were dissolved in a suitable organic solvent. This was followed by the recovery of the matrix from the solution obtained by conventional methods, which included vacuum evaporation, tray drying, spray drying, and drum or belt film drying. Spray drying was the preferred method for solvent removal, because it kept the drug in a finely dispersed state within the polymers, preventing the exposure of the bitter tasting drug to the taste buds.

The methacrylic acid copolymers used included methylmethacrylic ester copolymers, such as Eudragit S and Eudragit L and copolymers of ethyl acrylate and methacrylic acid as Eudragit L-100-55. The phthalate polymers included cellulose acetate phthalate, ethyl vinyl phthalate, polyvinyl acetate phthalate and hydroxyl alkyl cellulose phthalates. The solvent system chosen was one in which both the active ingredient and the polymers are either soluble or swellable. Preferred solvents included water, ketones, alcohols, esters and their mixtures.

The process of spray drying provided highly porous material thereby requiring a secondary granulation to improve the taste masking.

Channeling agents were used to further tailor the drug release from the granules. Channeling agents helped in opening up the granules within a specific media. These included disintegrants (e.g. croscarmellose sodium, crospovidone and sodium starch glycolate), diluents (e.g. lactose, mannitol, sodium chloride, talc, polyvinyl pyrrolidone) and gelling agents (e.g. carbopol, and xanthan gum). The CA acrylate / phthalate taste masked granules were mixed with flavoring agents such as natural or artificial flavors, citric and tartaric acids, sweeteners such as saccharin and aspartame, and with other pharmaceutically acceptable excipients. They were then formulated as conventional chewable or dispersible tablets, dry syrups, suspensions, sachets or any other suitable oral dosage forms.

In another study, Cuna et al. (1997-a, b) developed a microencapsulated form of CA using pH-sensitive acrylic polymers. CA was encapsulated in pH-sensitive acrylic microspheres in order to be used in the suspension dosage form. Using this microencapsulated form it was expected to prevent leaching of the drug from the microspheres into the suspension medium and to ensure the release of the drug in the first part of the intestine, thus avoiding changes to its bioavailability. For this purpose, CA was microencapsulated within several types of acrylic polymers by the solvent evaporation and the solvent extraction techniques.

The acrylic polymers selected were Eudragit E (positively charged and soluble at pH 5), Eudragit L-55 (negatively charged and soluble at pH > 5.5) and Eudragit RL (neutral, insoluble, but readily permeable). The influence of the polymer electrical charge on the stability and *in vitro* release of CA was investigated. Though Eudragit E microspheres presented good morphological characteristics and dissolution behaviour, the analyses of the stability of CA in the presence of Eudragit E by HPLC indicated a negative interaction between both compounds. However, formulations made of Eudragit L-55 and RL in the ratios tested (100:0) and (90:10) were adequate in terms of the stability of the encapsulated CA.

The dissolution studies showed a critical pH between 5.2 and 6.0, which allowed the complete release of CA in a short period. Furthermore, these polymer microspheres were shown to be efficient in masking the taste of CA.

Cefuroxime axetil (CA) was also microencapsulated within various cellulosic polymers having a pH-dependent solubility (Cuna et al, 1996). Cellulose acetate trimellitate (CAT), Hydroxypropylmethyl cellulose (HPMC) P-5 and P-50 were used, with the aim to mask CA taste while assuring its release in the intestinal cavity. The drug release studies and the stability assay of the encapsulated molecule showed that the HPMCP-55 microspheres represented an useful approach in achieving the specific objective.

The dissolution properties of coated CA with stearic acid (SACA) systems with a view to investigating the effects of the dissolution medium on both the release rate and the physical integrity of the microspheres, were studied by Robson et al (1999, 2000-a). The release from the spheres was found to be highly dependent on the media used. Systems in distilled water (pH 6.8) and pH 5.9 Sorensens modified buffer showed a relatively slow release which exhibited linearity with the square root of time, implying a diffusion process. The rate of release from systems in pH 7.0 and 8.0 buffer was considerably faster and did not follow simple diffusion kinetics. Examination of the microspheres after immersion in various media indicated a change in the integrity of the spheres in those media which showed the most rapid release.

This was particularly marked when the systems were dried in the buffer, with disintegration observed in the higher pH systems. It was suggested that the release of the drug is dependent both on diffusion through the intact microspheres and changes in the physical integrity of the spheres as a result of a reaction with the surrounding medium (Robson et al, 1999).

In another study, Robson et al. (2000-b) tested the influence of buffer composition on the release of CA from the stearic acid microspheres, with particular emphasis on establishing the relationship between buffer composition and release at a single pH value. Studies of drug dissolution and release from spheres in pH 7.0 citrate phosphate buffer (CPB), boric acid buffer (BAB), phosphate buffer mixed (PBM),

and Sorensens modified phosphate buffer (SMPB) indicated marked differences in release profiles from the spheres, with an approximate rank order of SMPB > CPB ~ BAB > PBM. The role of added sodium was then investigated by examining the release profiles in SMPB and PBM to which sodium ions had been added. Increases in the sodium content from 0.11 to 0.2 M were found to decrease the release rate from the SMPB, while an increase from 0.007 to 1.0 M sodium in PBM resulted in a maximum release being seen for the systems containing 0.05 M sodium. Studies on surface disintegration, using scanning electron microscopy (SEM) and sodium uptake using flame emission spectroscopy, indicated an interrelationship between medium composition, disintegration and release.

Microspheres (SACA) were studied using DSC to examine the interaction between the spheres and a range of buffer systems, with a view to further enhance the understanding of the mechanism of drug release from wax coated particles (Robson et al, 2000-c).

DSC studies indicated that upon immersion in SMPB pH 5.9, followed by washing and drying, no change in the thermal properties of the spheres was detected up to 60 min of immersion. A single endotherm was noted at 56°C, which corresponded to the melting of stearic acid used in this study, similar results were obtained for systems immersed in distilled water (Robson et al, 2000-c).

After immersion in SMPB pH 7.0 and 8.0, however, a second peak was noted at approximately 67°C, which increased in magnitude, relative to the lower temperature endotherm, with increasing exposure time to the medium. Spheres that had not been previously washed prior to drying showed complete conversion to the higher temperature endotherm for those two buffers. Systems which had been exposed to a range of pH 7.0 buffers CPB, PBM, BAB were then examined. Only the CPB systems showed evidence conversion to the higher melting form. PBM systems to which further sodium had been added were then examined. A maximum conversion was found at 0.05 M sodium (Robson et al, 1999, 2000-b).

In this chapter the effect of wax coating on CAA physical properties was investigated. The wax coat chosen was a mixture of stearic acid and a hemisynthetic glyceride, and was used at around 40% w/w. Both thermal behavior and *in vitro* release of wax coated CAA and CADC were tested and compared to those of uncoated particles.

## 5.2 WAX MIXTURES PREPARED

### 5.2.1 Materials and methods

Table 5.1 summarises wax materials studied in this chapter.

<b>Materials</b>	Stearic Acid	Gelucire 39/01
<b>Batch No.</b>	605021900	OE2504-2
<b>Retesting Date</b>	04/2002	06/2003
<b>Source</b>	Croda	Gattefosse

Table 5.1: Waxes studied for coating

The BP and the USP describe SA as a mixture of stearic acid (SA) ( $C_{18}H_{36}O_2$ ) and palmitic acid ( $C_{16}H_{32}O_2$ ). The content of SA is not less than 40.0% and the sum of the two acids is not less than 90.0%. The USP also contains a monograph for purified SA.

SA is widely used in oral and topical pharmaceutical formulations. It is mainly used in oral formulations as a tablet and capsule lubricant (Mitrevej et al, 1982). It may also be used as a binder, or in combination with shellac as a tablet coating. SA is also used in cosmetics and food products. It is generally regarded as a nontoxic and nonirritant material, with a melting point of 57°C-60°C (Kibbe et al, 2000).

Gelucire 39/01 (G), a Hemi-synthetic glyceride (glycerol ester of  $C_{12}$ - $C_{18}$  saturated fatty acid esters) is an excipient used for hard gelatin capsules. It is also used as a bioavailability regulator for sustained release formulation to protect it against oxidation and hydrolysis and in formulation of low density products or toxic or low dose active drugs. It has a hydrophilic-lipophilic balance of 1 and a melting point of 37.5°C-41.5°C (Kibbe et al, 2000). SA was used in this study either purely or as a mixture with G, added to lower the high melting point of SA.



### 5.2.1.1 Wax mixtures preparation

Mixtures were prepared by weighing the waxes in quantities equivalent to the percentage specified for each mixture in Table 5.2. Each mixture was prepared as 2 gm batches. Materials were transferred to beakers immersed in a water bath containing hot water at 60°C.

Mixing was undertaken until waxes were completely melted. Finally, flasks were cooled at room temperature with continuous mixing until solidification occurred.

### 5.2.1.2 Melting point testing:

The melting point of each mixture was tested using a capillary tube filled to 4mm with the sample. The parameters of the instrument were set as initial temperature of 30°C, heating rate of 2°C/min, and a final temperature of 60°C. When the furnace was heated up to the starting temperature, the sample tube was inserted in the sample holder.

When the start temperature increased, the furnace temperature also increased at the selected heating rate until the sample melted, the melting point was then recorded on a digital display. Testing for each sample was repeated three times.

## 5.2.2 Results and discussions

Table 5.2 shows the results of melting point depression of SA when mixed with G in different ratios.

Gleucire 39/01	Stearic acid	Melting Point
100%	-	37.0°C – 37.8°C
90%	10%	36.3°C – 36.5°C
80%	20%	43.3°C – 42.3°C
70%	30%	46.9°C – 47.1°C
60%	40%	49.6°C – 48.4°C
50%	50%	51.4°C – 51.2°C
40%	60%	52.3°C – 52.7°C
30%	70%	53.9°C – 53.7°C
20%	80%	54.6°C – 54.6°C
10%	90%	55.2°C – 55.3°C
-	100%	56.7°C – 56.7°C

Table 5.2: Melting points of SA and G mixtures at different ratios, n=3.

The results in Table 5.2 indicated that the melting point of SA was lowered when mixed with varying amounts of G.

Increasing G content to more than 40% caused softening of the wax mixture. Thus 60:40 ratio was found to be optimum for achieving the melting point depression , while retaining wax solid properties.

### 5.3 MIXTURES OF CAA AND CADC WITH WAXES

Mixtures of CAA and CADC were prepared with SA and G individually and together to study their effect on the physical and chemical properties of CA. These mixtures were tested as described below.

#### 5.3.1 Materials and methods:

Table 5.3 summarises materials studied as wax mixtures.

Materials	CAA	SA	G	CADC
Batch No.	CAFAA/003/00	605021900	OE2504-2	Granules prepared as in chapter 4, section 4.2.2.5
Assay	81.8%	04/2002	06/2003	
Water content	0.99%	--	--	
Exp. Date	12/2003	--	--	
Source	Orchid	Croda	Gattefosse	

Table 5.3: Materials studied as wax mixtures

#### 5.3.1.1 Wax mixtures prepared

The following mixtures were prepared (3 gm of each mixture):

1 : 1 SA with CAA, and, SA with CADC

1 : 1 G with CAA, and, G with CADC

1 : 1 : 1 SA with G with CAA, and, SA with G with CADC

#### 5.3.1.2 Method of preparation

For each mixture, the materials were accurately weighed, and the wax was transferred to a glass beaker and melted at (60°C–70°C). The CAA or CADC was added in the specified ratio with continuous stirring until a homogenous dispersion was obtained. Mixing was continued with cooling until the whole mixture solidified.

### 5.3.1.3 Testing of mixtures

Compatibility of CA with each wax mixture was tested using the HPLC and DSC methods mentioned under chapter 2, sections 2.9.2.1 and 2.1.2, respectively.

### 5.3.2 Results and discussions

#### 5.3.2.1 HPLC analyses

All HPLC analyses results of CA in the wax mixtures were 97.0-101.0 mg% CA. This indicated good homogeneity ( $\pm 10\%$ ). Chromatographic purity revealed pure peaks with no degradation products, indicating that CA was chemically stable in the wax mixtures tested.

#### 5.3.2.2 DSC Measurements

DSC testing results of CAA and CADC wax mixtures are presented in Table 5.4.

Material	Endothermic peaks	Material	Endothermic peaks
CAA	84.0°C – 85.0°C	CADC	79.8°C – 81.9°C
SA	56.0°C – 58.0°C	CADC with SA	80.5°C – 80.7°C 57.4°C – 57.8°C
G	37.0°C – 39.0°C	CADC with G	80.6°C – 82.3°C 36.8°C – 37.9°C
CAA with SA	83.3°C – 83.7°C 57.4°C – 58.6°C	CADC with SA and G	80.6°C – 82.2°C 52.9°C – 53.4°C 36.3°C – 36.7°C
CAA with G	84.1°C – 84.4°C 38.6°C – 39.5°C		
CAA with SA and G	83.0°C – 84.0°C 52.2°C – 53.5°C 37.1°C – 37.2°C		

Table 5.4: DSC results of CAA and CADC wax mixtures.

From the DSC results in Table 5.4 it was observed that the melting point of SA was depressed when mixed with G, confirming the results obtained from the melting point testing of the mixtures, presented under section 5.2.2.

Furthermore, the endothermic peak in each of CAA and CADC thermograms, relating to the  $T_g$  of CAA overlapping a relaxation peak, was not affected by the waxes. Thus, waxes tested were physically and chemically compatible with CA.

## **5.4 COATING OF CAA WITH SA**

In this section, effect of SA wax coating on the properties and release of C from CAA coated particles was studied.

### **5.4.1 Materials and methods**

The following materials (mentioned in Table 5.3) were used to prepare the wax coated CAA with SA:

Cefuroxime axetil amorphous (CAA)	: 500
Stearic acid (SA)	: 400
Isopropyl alcohol (IPA)	: 2900 ml extra pure

The solvent IPA was chosen because it dissolves SA, and is considered less hazardous to the environment than other halogenated hydrocarbons used usually for organic coatings.

#### **5.4.1.1 Method of coating**

The coating solution was prepared by dissolving SA in IPA with the aid of gentle heating. CAA was then coated with the coating solution prepared, using the Niro Aeromatic Multi Processor (MP1) at exhaust air temperature of 14°C–18°C.

Coating was continued with frequent sampling to test the bitter taste masking achieved as a function of time during coating. Approximately all the coating solution was consumed to achieve masking of the bitter taste. The coated particles were subsequently passed through a 0.20 mm sieve.

#### **5.4.1.2 HPLC assay testing of coated particles**

HPLC method mentioned in chapter 2, section 2.9.2.1, was applied to determine the content and homogeneity of CA in 5 samples of CAA coated particles with SA. The powder was taken in quantities equivalent to the weight needed for sample preparation in the HPLC method.

#### **5.4.1.3 Particle size distribution of coated particles**

Wax coated CAA particles with SA were tested for particle size distribution using the laser particle size analyses method mentioned under chapter 2, section 2.3.2.

#### 5.4.1.4 DSC of coated particles

Wax coated CAA particles with SA were analysed by DSC, using the method described under chapter 2, section 2.1.2, after being gently crushed using a mortar and a pestle.

#### 5.4.1.5 *In vitro* gut absorption testing of coated particles

Wax coated CAA particles with SA were tested for intestinal absorption as described under chapter 2, section 2.8.2.2, and samples were analysed as described in section 2.9.2.3.

### 5.4.2 Results and discussions

#### 5.4.2.1 HPLC analyses

The homogeneity results of CA in the SA coated CAA powder were 50.0 – 60.0 mg% CA. This indicated good homogeneity ( $\pm 10\%$ ). Around 45% wax coating was needed to achieve the desirable bitter taste-masking of CAA.

#### 5.4.2.2 Particle size analyses

Figure 5.1 shows the particle size distribution results of coated CAA with SA.

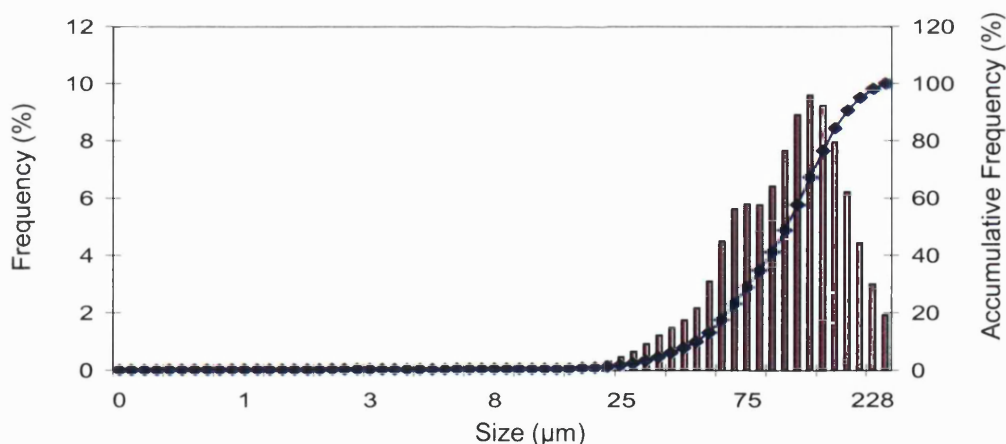


Figure 5.1: Log-normal particle size distribution of CAA coated with SA

The geometric mean diameter (median diameter) of the SA coated CAA was 107.0µm.

The geometric standard deviation of the particle size distribution was calculated as was mentioned in chapter 3, equations 3.1 and 3.2. Results were as follows:

$$\sigma_g = \frac{d_{50}}{d_{15.78}} = \frac{107.0 \mu\text{m}}{64.8 \mu\text{m}} = 1.7$$

and

$$\sigma_g = \frac{d_{84.13}}{d_{50}} = \frac{182.2 \mu\text{m}}{107.0 \mu\text{m}} = 1.7$$

The particle size of the SA-coated CAA powder was approximately 5 times higher than that before coating ( $d_{50} = 20\mu\text{m}$ ). This can be related to the agglomeration of CAA powder during wax coating. The standard deviation ( $\delta$ ) of particle size distribution indicated a log-normal distribution.

#### **5.4.2.3 Dissolution testing**

As wax coated CAA particles have very low solubility in 0.01N HCl (media of dissolution test in BP 2000), this test was not conducted on wax coated particles. Instead all comparisons were based on *in vitro* gut intestinal absorption results.

#### **5.4.2.4 DSC measurements**

Figure 5.2 shows the DSC thermogram of CA particles coated with SA. The thermogram revealed three endothermic peaks, one for melting of SA at 57.0°C, the second is characteristic of CAC at 178.0°C, and the third found at 153.3°C, which is representative of a secondary polymorphic form of CAC.

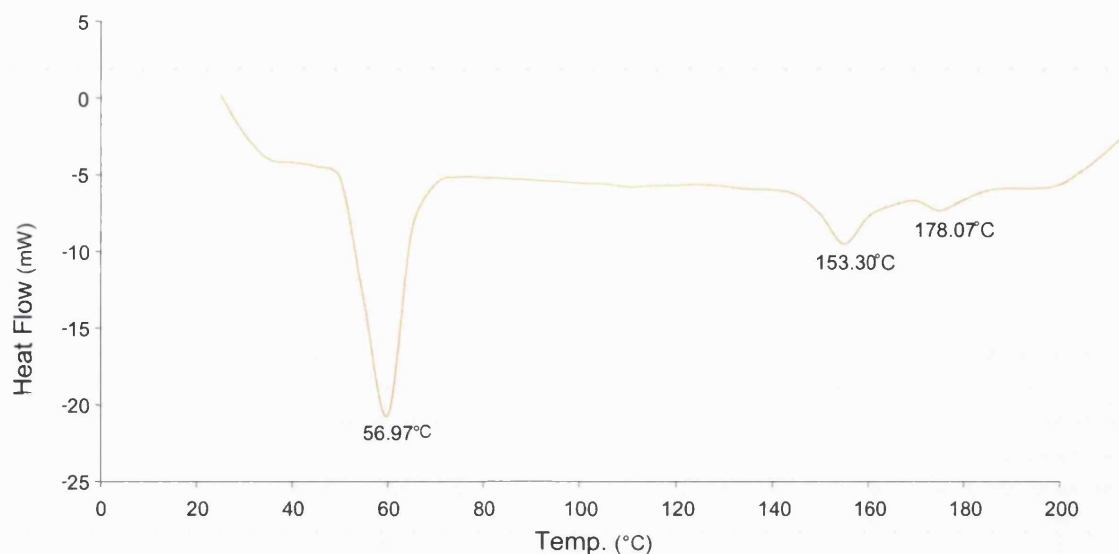


Figure 5.2: DSC thermogram of CAA coated with SA, at heating rate 25°C/min

The DSC thermogram indicated that the wax coating process may have converted the pure CAA to CAC polymorph of the melting peak at 178°C, plus another form of a lower temperature endothermic peak (153.3°C), which is expected to be another polymorph for CAC. This may be attributed to the heat generated from the friction of the fluidized particles during coating process which would plasticize CAA and enhance crystallisation. It may also be related to the possible dissolution of CAA in IPA and subsequent recrystallisation on the particles surface exposed to coating solution.

#### 5.4.2.5 *In vitro* gut absorption testing

Table 5.5 and Figure 5.3 show the results of *in vitro* gut % C released from SA-coated CAA.

Time (min)	Average % C release ( $\pm$ SD)
15	0.75 $\pm$ 0.20
30	0.88 $\pm$ 0.18
45	1.24 $\pm$ 0.22
60	1.47 $\pm$ 0.42
75	2.17 $\pm$ 0.56
90	2.86 $\pm$ 0.37
105	3.06 $\pm$ 0.83
120	3.61 $\pm$ 1.05

Table 5.5: *In vitro* gut C% release from coated CAA with SA, n=3.

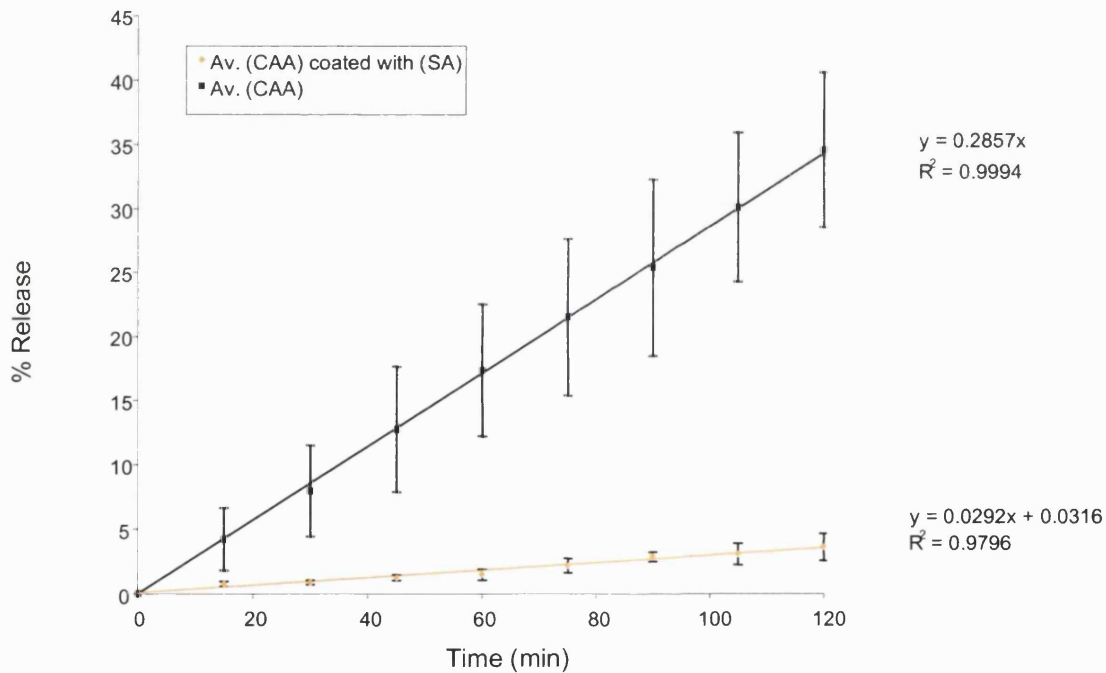


Figure 5.3: *In vitro* gut release of C from CAA coated with SA, n=3.

The above *in vitro* gut results indicate a linear zero order release rate of C from CAA coated with SA. The lag time noticed for wax coated CAA is related to time needed for wax to melt and CAA to dissolve in the absorption media. The release rate (K) was significantly reduced (by 10 folds) upon wax coating. This was probably as a result of the conversion of the pure amorphous absorbable form of the drug to the crystalline form during coating process.



## **5.5 COATED CAA WITH SA AND G**

### **5.5.1 Materials and methods**

The following materials ( mentioned under sections 5.2.1 and 5.4.1 ) were used to prepare wax coated CAA with SA and G:

Cefuroxime axetil amorphous (CAA)	: 500 gm
Stearic acid (SA)	: 250 gm
Gelucire 39/01 (G)	: 150 gm
2-Propanol (IPA), (extra pure)	: 2900 ml

#### **5.5.1.1 Method of coating**

The coating solution was prepared by dissolving SA and G in IPA with the aid of gentle heating. CAA was then coated with the coating solution prepared, using Niro Aeromatic Multi Processor (MP1) at exhaust air temp of 14°C–18°C. Coating was continued with frequent sampling to test the taste masking achieved with time during coating. Approximately all coating solution was consumed to achieve good masking of the bitter taste. The coated particles were passed gently through sieve 0.20 mm.

#### **5.5.1.2 HPLC testing of coated particles**

HPLC assay method mentioned in chapter 2, section 2.9.2.1 was utilised for analyses of 5 different samples from the coated powder to determine the content and homogeneity of CA. Powder quantities analysed were equivalent to the weight needed for the sample preparation in the HPLC method.

#### **5.5.1.3 Particle size distribution of coated particles**

Wax coated CAA particles with SA and G were tested for particle size distribution using the laser particle size analyses method mentioned under chapter 2, section 2.3.2.

#### **5.5.1.4 DSC of coated particles**

Wax coated CAA particles with SA and G were analysed by DSC using the method described under chapter 2, section 2.1.2, after being gently crushed using a mortar and a pestle.

### 5.5.1.5 *In vitro* gut absorption testing of coated particles

Wax coated CAA particles with SA and G were tested for intestinal absorption as was described under chapter 2, section 2.8.2.2. Samples of the test were analysed as was described under 2.9.2.3.

## 5.5.2 Results and discussions

### 5.5.2.1 HPLC analyses

The homogeneity results of CA in coated CAA particles with SA and G, were 52.0-59.0 mg% CA. This indicated good homogeneity ( $\pm 10\%$ ). Around 45% wax coating was needed to provide the required bitter taste masking of CAA.

### 5.5.2.2 Particle size analyses

Results of particle size distribution of CAA coated particles with SA and G are shown in Figure 5.4.

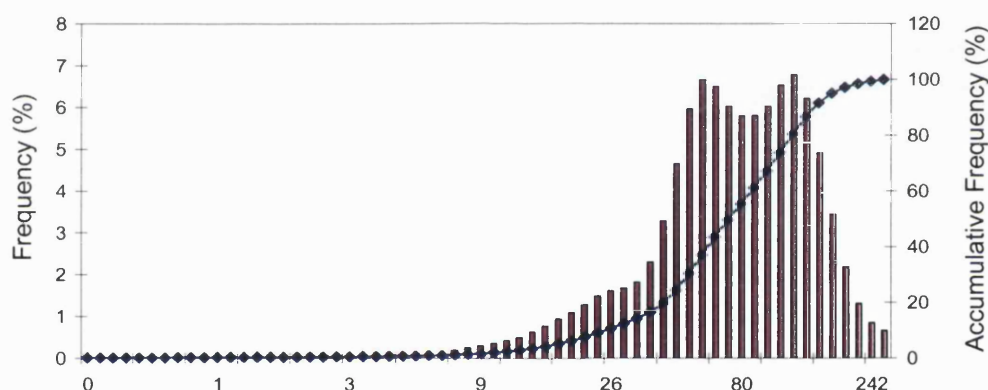


Figure 5.4: Log-normal particle size distribution of coated CAA with SA and G

The geometric mean diameter (median diameter) of CAA coated with SA and G was 76  $\mu\text{m}$ .

Then the geometric standard deviation of the particle size distribution was calculated according to equations 3.1 and 3.2 mentioned in chapter 3. Results were as follows:

$$\sigma_g = \frac{d_{50}}{d_{15.78}} = \frac{75.99 \mu\text{m}}{37.49 \mu\text{m}} = 2.0$$

and

$$\sigma_g = \frac{d_{84.13}}{d_{50}} = \frac{140.13 \mu\text{m}}{75.99 \mu\text{m}} = 1.84$$

It was noticed that smaller particles were obtained after coating CAA with SA and G than that with SA alone ( $d_{50} = 107 \mu\text{m}$ ). This can be related to the fact that G enhances the wax coat properties and reduces the agglomerate formation during coating of CAA powder. The particle size could be fitted to a log-normal distribution.

### 5.5.2.3 DSC measurement

The DSC thermogram of CAA coated with SA and G, presented in Figure 5.5, showed four endothermic peaks, two of them for the melting of SA and G at  $56.6^\circ\text{C}$   $36.7^\circ\text{C}$  respectively. The third peak is for melting of the high melting temperature CAC polymorph at  $177.2^\circ\text{C}$ , while the fourth is thought to be a peak of another crystalline polymorph of CAC at  $122.3^\circ\text{C}$ .

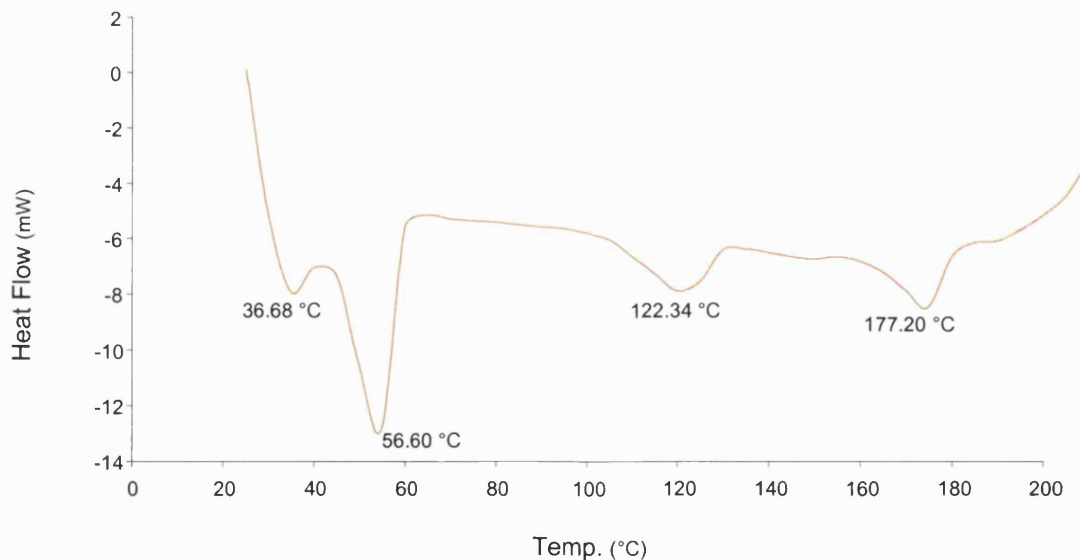


Figure 5.5: DSC thermogram of coated CAA with SA and G, at heating rate  $25^\circ\text{C}/\text{min}$

This indicated that coating of CAA with SA and G, converted the pure CAA to CAC polymorphs of melting peaks at  $122.0^\circ\text{C}$  and  $177.0^\circ\text{C}$ , respectively. This can be

attributed to the heat generated from the friction of the fluidized particles during coating process which would plasticize CAA and enhance crystallisation. It may also be related to the possible dissolution of CAA in IPA and subsequent recrystallisation on the surface of the particles exposed to coating solution.

The reason here of obtaining a polymorph at a lower temperature (122°C) than that obtained with coating with SA alone (153°C), can be related to the presence of G. The latter may have modified the recrystallisation conditions of CAA on the particles surface during coating, thus leading to such a lower melting temperature polymorph.

#### 5.5.2.4 *In vitro* gut intestinal absorption

Results of *In vitro* gut C release from coated CAA with SA and G are shown in Table 5.5 and Figure 5.6.

Time (min)	Average % C release ( $\pm$ SD)
15	0.14 $\pm$ 0.03
30	0.39 $\pm$ 0.10
45	0.89 $\pm$ 0.27
60	1.52 $\pm$ 0.77
75	2.52 $\pm$ 0.80
90	3.40 $\pm$ 1.07
105	4.57 $\pm$ 1.50
120	5.84 $\pm$ 1.70

Table 5.6: *In vitro* gut C% release from CAA coated with SA and G, n=3.

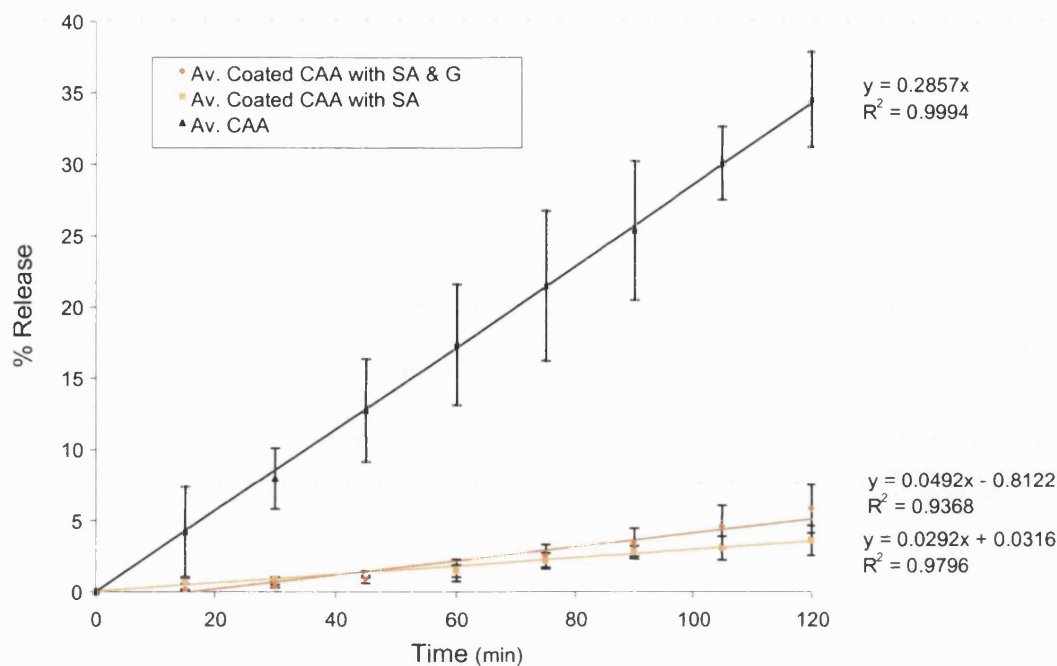


Figure 5.6: *In vitro* gut release of C from CAA coated with SA and G, n=3.

As shown in Figure 5.6, a linear zero order release rate of C from coated CAA was shown. The lag time noticed for wax coated particles was related to the time needed for the wax to melt and the material to dissolve prior to absorption. It is clear that coating of CAA with SA and G showed a 70% increase in CA intestinal absorption rate (K) compared to that obtained from coating with SA alone, both rates were significantly lower than that from uncoated CAA ( by 6 folds for the former, and 10 folds for the latter).

The above results indicated that despite G reduced the melting point of SA ,as was shown under section 5.2, it did not significantly enhance the intestinal absorption rate of CA from wax coated CAA. However, since it provided a flexible coating process, and because of its known effect on preventing oxidation of the wax coating, G was included in further coating studies on CA.

## **5.6 COATED CADC WITH WAX**

It was noticed in previous sections that the absorption rate of CA was significantly reduced upon coating.

The section below illustrates the effect of wax coating on the intestinal absorption rate of CA from CADC granules.

### **5.6.1 Materials and methods**

CADC in 500 gm quantity, prepared as mentioned in chapter 4, section 4.2.2.5 was wax coated with SA and G in the following quantities:

Stearic Acid (SA)	: 250 gm
Gelucire 39/01 (G)	: 150 gm
2-Propanol	: 2900 gm

#### **5.6.1.1 Methods of coating**

The same coating procedure described under section 5.5.1.1 was applied to coat CADC granules. Coated particles were gently passed through 0.2 mm sieve.

#### **5.6.1.2 HPLC testing of coated particles**

HPLC assay method described under chapter 2, section 2.9.2.1 was applied on 5 samples to determine the content and homogeneity of the active material in CADC coated particles with SA and G. Content of CA was tested on powder quantities equivalent to weight needed for the sample preparation in the HPLC method.

#### **5.6.1.3 Particle size distribution of coated powder**

Wax coated CADC particles with SA and G were tested for particle size distribution using the laser particle size analyses method mentioned under chapter 2, section 2.3.2.

#### **5.6.1.4 DSC testing of coated particles**

Wax coated CADC particles with SA and G were analysed by DSC using the same method described under chapter 2, section 2.1.2, after being gently crushed using a mortar and a pestle.

### 5.6.1.5 Electron microscopy testing of coated particles

Wax coated CADC particles with SA and G were tested for electron microscopy as described under chapter 2, section 2.6.2.

### 5.6.1.6 *In vitro* gut absorption testing of coated particles

Wax coated CADC particles with SA and G were tested for intestinal absorption and analysed as described under chapter 2, sections 2.8.2.2 and 2.9.2.3, respectively.

## 5.6.2 Results and discussions

### 5.6.2.1 HPLC analyses

Homogeneity results of CA in coated CADC granules were 0.35mg – 0.38mg% CA, reflecting good homogeneity ( $\pm 10\%$ ), and showing that approximately 45% wax coating was needed to mask the bitter taste of CA in the CADC granules.

### 5.6.2.2 Particle size analyses

Figure 5.7 shows the particle size distribution results of wax coated CADC granules.

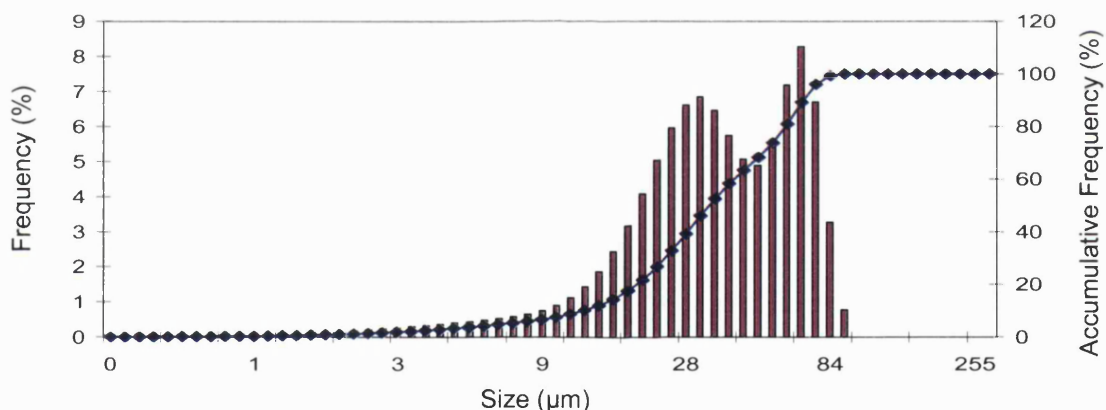


Figure 5.7: Log-normal particle size distribution of the wax coated CADC granules.

The geometric mean diameter (median diameter) of CADC coated granules was 33.25 µm.

Then the geometric standard deviation of the particle size distribution was calculated according to equations 3.1 and 3.2 mentioned in chapter 3. Results were as follows:

$$\sigma_g = \frac{d_{50}}{d_{15.78}} = \frac{33.25 \mu\text{m}}{16.81 \mu\text{m}} = 2.0$$

and

$$\sigma_g = \frac{d_{84.13}}{d_{50}} = \frac{63.04 \mu\text{m}}{33.25 \mu\text{m}} = 1.9$$

The above results showed finer particles of the wax coated CADC than that of the wax coated CAA. This indicated that CADC particles (of bulk density = 0.58 gm/ml) underwent collision during coating in the fluid bed, thus they were crushed down to give finer particles than their original size (90-100 $\mu\text{m}$ ). On the other hand, coated CADC granules didn't agglomerate during coating, as happened with CAA powder. The particle size could be fitted to a log-normal distribution.

### 5.6.2.3 DSC measurements

The DSC thermograms of wax coated CADC compared with the wax coated CAA are shown in Figure 5.8.



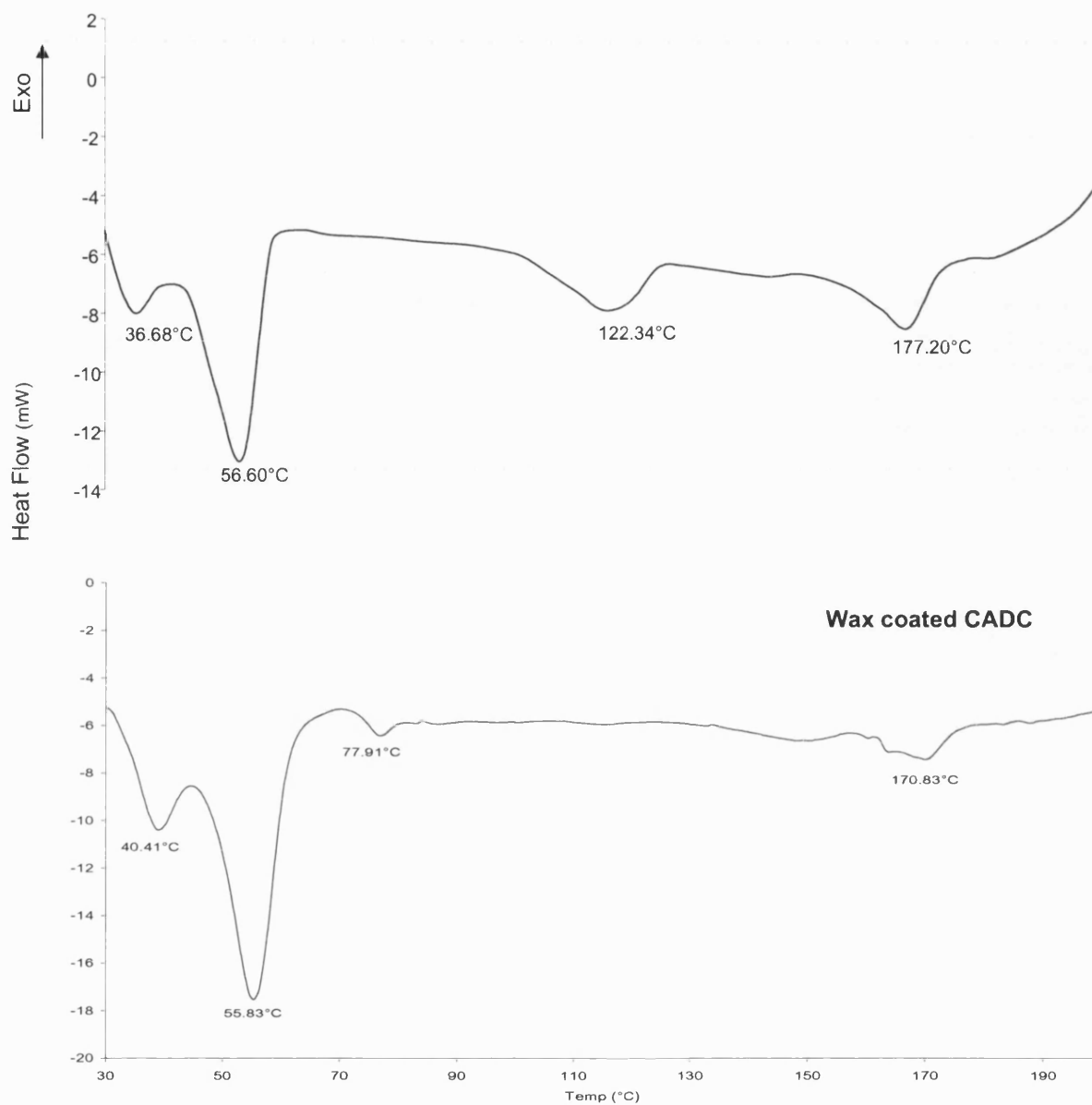


Figure 5.8: DSC thermogram of wax coated CADC, at heating rate 25°C/min.

The thermograms above revealed that there are 4 endothermic peaks for the wax coated CADC, two are for melting of G and SA at 40.4°C and 55.8°C respectively. The other two peaks are characteristic of CA in both its amorphous form CAA having a  $T_g$  at 74°C overlapping a relaxation peak, and the crystalline polymorph having the melting peak at 170.8°C.

The DSC measurements indicated that wax coating of CADC led to a partial transformation of CAA to the crystalline polymorph of the high melting temperature (174.0°C), no other forms were generated. This was different than what was obtained from wax coating of CAA, which resulted in complete transformation of the amorphous form to other two crystalline polymorphs of the drug having lower solubility and permeability.

The presence of excipients in the CADC granules was found to protect the amorphous form of CA from complete transformation to other crystalline forms upon coating (reduced the degree of crystallisation). Thus, enhanced to a greater degree the stability of the amorphous form.

#### 5.6.2.4 *In vitro* gut intestinal absorption

Figure 5.9 and Table 5.7 show the results of % C release from the wax coated CADC across the intestinal membrane.

Time (min)	Average % C release ( $\pm$ SD)
15	2.34 $\pm$ 0.50
30	4.58 $\pm$ 1.20
45	7.37 $\pm$ 2.00
60	10.01 $\pm$ 3.10
75	13.77 $\pm$ 4.20
90	16.30 $\pm$ 5.00
105	19.96 $\pm$ 4.72
120	22.86 $\pm$ 5.20

Table 5.7: *In vitro* gut C% release from wax coated CADC, n=3.

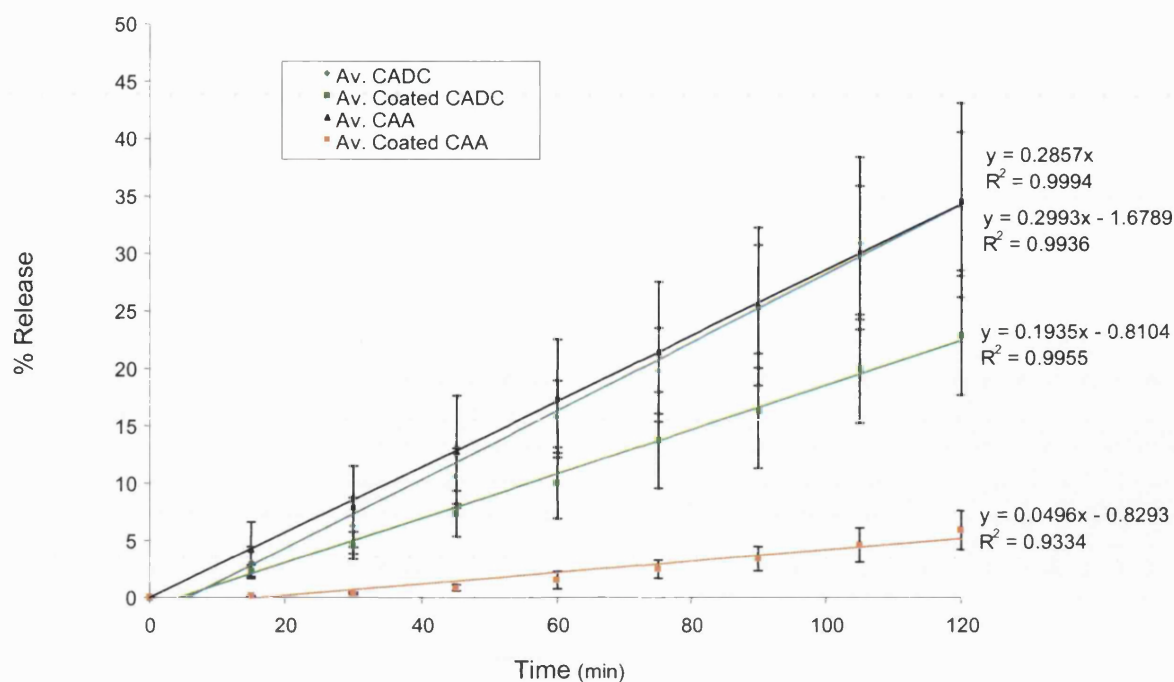


Figure 5.9: *In vitro* gut release of C from CADC wax coated granules, n=3

The above results indicated a linear zero order release rate of C from wax coated CADC. The lag time seen for the wax coated CADC was related to the time needed for the wax coat to melt and the CADC granules to disintegrate before absorption. The rate of CA intestinal absorption (K) from wax coated CADC was 4 folds higher than that from wax coated CAA. Thus, excipients included in CADC granules reduced the effect of wax coating on the absorption rate of CA.

On the other hand, CA absorption rate from CAA was found to be approximately 1.5 folds higher than that from wax coated CADC. Indicating that the wax coating process HAD a negative effect on the release rate of CA, such effect was reduced in the presence of the chosen excipients. Thus Ac-Di-Sol, Aerosil 200, and Pregelatinized starch 1500 mixed and compressed with CAA before wax coating, stabilised ,to a significant degree, the most soluble and permeable amorphous form of CAA, by preventing its complete conversion to other less soluble and permeable forms upon wax coating.

### 5.6.2.5 Electron microscopy of coated particles

The electron microscope images of uncoated CADC, which show rough porous surface of the particles are presented in Figure 5.10.

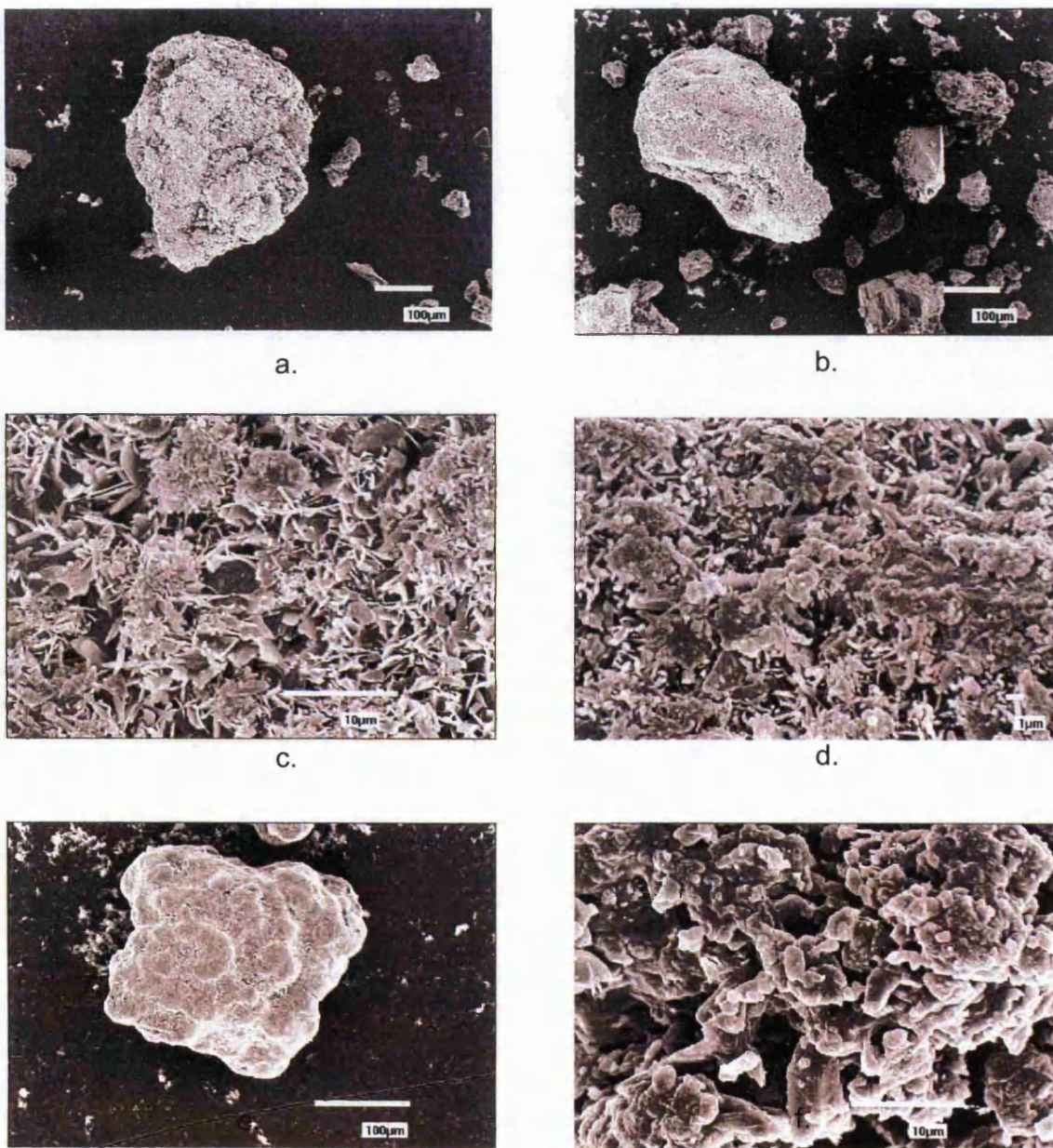
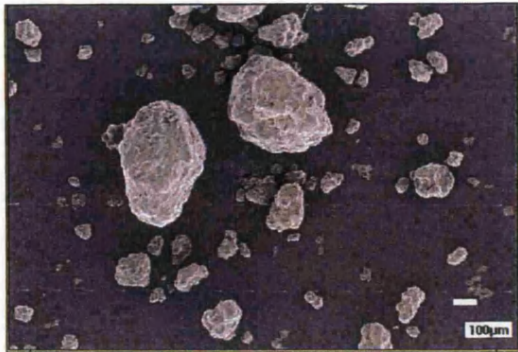


Figure 5.10: Electron microscope images of CADC particles.



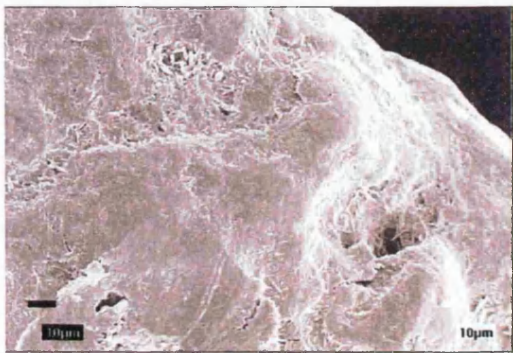
Images of wax coated CAD/C, shown in Figure 5.11, reflect a relatively smooth and less porous surface of the particles, indicating efficient coating.



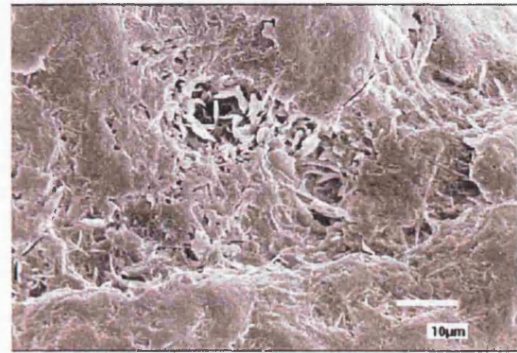
a.



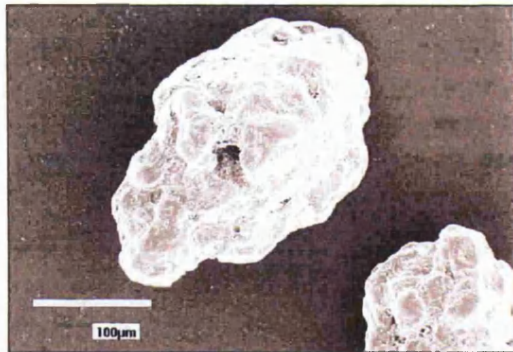
b.



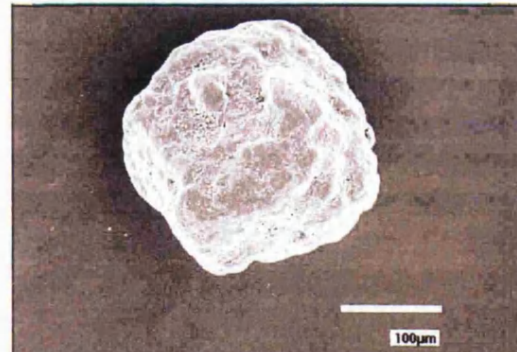
c.



d.



e.



f.

Figure 5.11: Electron microscope images of wax coated CAD/C

## **5.7 COATED CAA MIXTURE WITH EXCIPIENTS**

In previous sections, it was shown that the presence of any and/or all of the excipients Ac-Di-Sol, Starch 1500 and Aerosil 200 mixed and/or compressed with CAA stabilised the amorphous form of the drug. Thus, retaining its intestinal rate of absorption. To determine whether the effect of these excipients is only obtained when in direct contact with CAA in the core or also if surrounding the coated CAA particles, wax coated CAA particles were mixed with the same excipients in the same ratios found in the CADC granules, and then tested.

### **5.7.1 Materials and methods**

Wax coated CAA (55 gm) prepared as mentioned under section 5.5, was mixed with the following excipients (mentioned in Table 4.1, chapter 4), at the amounts shown below:

Ac-Di-Sol	: 5 gm
Starch 1500	: 9 gm
Aerosil 200	: 1 gm

#### **5.7.1.1 Mixture preparation**

The mixture was prepared by gentle mixing of the wax coated particles with the excipients at the quantities mentioned above.

#### **5.7.1.2 HPLC assay testing**

HPLC method described under chapter 2, section 2.9.2.1 was applied to determine the content and homogeneity of CA in the mixed wax coated CAA particles with the excipients. Five samples were analysed using a powder quantity equivalent to the weight needed for sample preparation in the HPLC method.

#### **5.7.1.3 *In vitro* gut absorption**

Wax coated CAA mixture with excipients was tested for intestinal absorption as mentioned under chapter 2, section 2.8.2.2. HPLC analyses of the samples was done as was mentioned under chapter 2, section 2.9.2.3.

## 5.7.2 Results and discussions

### 5.7.2.1 HPLC analyses

The homogeneity results of coated CAA in the mixture were 41.5gm – 45.0gm% CA, indicating good distribution of CAA wax coated particles in the mixture ( $\pm 10\%$ ).

### 5.7.2.2 *In vitro* gut intestinal absorption testing

Table 5.8 and Figure 5.12 show the results of the *in vitro* gut C release from the mixture of wax coated CAA with excipients.

Time (min)	Average % C release ( $\pm$ SD)
15	0.67 $\pm$ 0.20
30	0.53 $\pm$ 0.15
45	1.16 $\pm$ 0.40
60	1.91 $\pm$ 0.53
75	2.74 $\pm$ 0.23
90	3.76 $\pm$ 0.67
105	4.92 $\pm$ 0.75
120	6.09 $\pm$ 1.07

Table 5.8: *In vitro* gut C% release from wax coated CAA mixture with excipients, n=3.

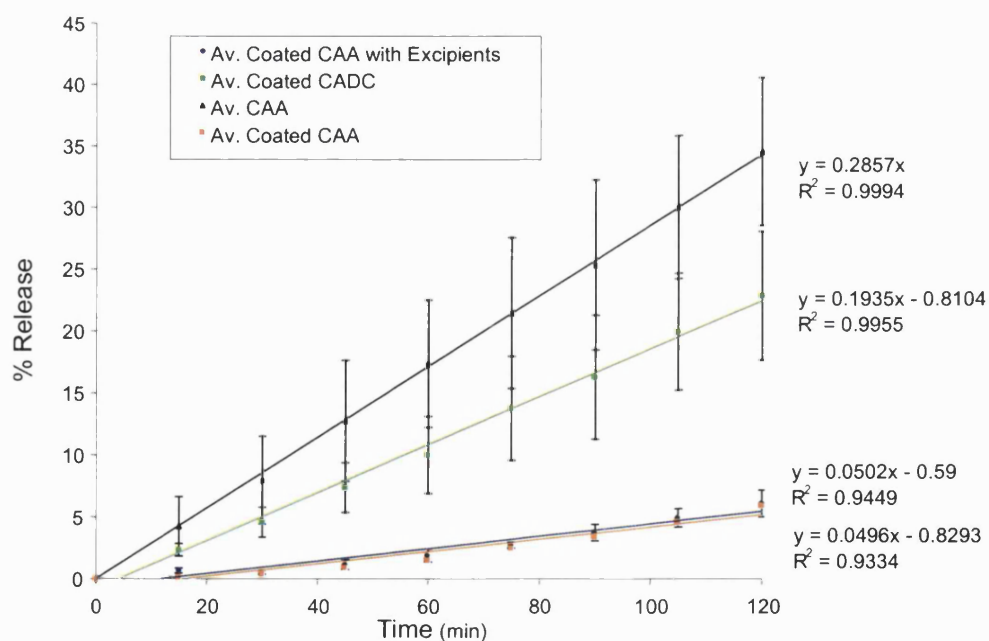


Figure 5.12: *In vitro* gut release of C from coated CAA mixture with excipients, n=3.

The above figure showed a linear zero order release of C form coated CAA mixed with the excipients. Its release rate (K) was found similar to that of wax coated CAA. This indicated that the excipients did not enhance the absorption rate of CA from wax coated CAA, and that they were needed in direct contact with CAA to stabilise the drug.

Stabilisation was achieved by prevention of CAA transformation to other poorly soluble forms of the drug that were generated during coating process. Once CAA had been coated and the formation of less soluble and permeable forms of CA occurred, the excipients would have no enhancement effect on the absorption rate of the drug.

## **5.8 CONCLUSIONS**

Cefuroxime axetil amorphous (CAA) is not stable under wax coating, which is needed to mask its very bitter taste when formulated in the dry suspension dosage form.

Stearic acid is the most common wax used for coating of CAA powder and proved to be physically and chemically compatible with it.

It was found, however, that the wax coating process of CAA led to the transformation of the amorphous form to the less soluble and permeable crystalline polymorphs. This led to a significant decrease in CA absorption via the intestine.

It was also shown that the rate of absorption of CA from wax coated CADG granules was significantly higher than that from wax coated CAA. This may be related to the fact that the excipients (Ac-Di-Sol, Starch 1500, and Aerosil 200), available in the granules stabilised, to a larger degree, the amorphous form of the drug in the core. The protection of the drug from direct heat and frictional effects maintained up to 70% of the original absorption rate of the amorphous form.



## CHAPTER 6

### COMPARISON BETWEEN WAX COATED CADC AND COMMERCIALLY AVAILABLE WAX COATED POWDER FOR SUSPENSION

#### 6.1 INTRODUCTION

Cefuroxime axetil dry suspension is widely prescribed by physicians for children having bacterial infections. Zinnat<sup>®</sup> is a commercially available product, which contains wax coated CAA to mask the very bitter taste of the active material.

In this chapter, the effect of wax coating on CAA in two preparations was studied, these are the wax coated CADC granules and Zinnat<sup>®</sup>, both formulated in the dry suspension form.

#### 6.2 MATERIALS AND METHODS

Coated CADC prepared in the dry suspension form, using the materials shown in Table 6.1, and Zinnat<sup>®</sup> dry suspension batch no. CO63339 were tested at 125 mg cefuroxime/5ml dose, after 4-6 months of manufacturing.

No.	Material Name	Batch No.	Source	Qty/Bottle (gm)
1.	Wax coated CADC granules	prepared as mentioned under chapter 5, section 5.6.1.1	--	4.1
2.	Sucrose	10872	Andenex-Chemie	40.0
3.	Sodium saccharine	S46386065493CS	Fabric	0.05
4.	Xanthan Gum	1175/01	Jungbunzlaver	0.01
5.	Titanium Dioxide	0206061606	Ellies & Everard	0.025
6.	Tutti Frutti	51624	Dragoco	0.10
7.	Lemon Flavour	605238	Dragoco	0.15

Table 6.1: Composition of wax coated CADC dry suspension, batch No. 101003 (1000 bottles).

### **6.2.1 Preparation of coated CADC dry suspension**

Wax coated CADC granules were gently passed through sieve 0.2 mm. Using the HPLC method mentioned in chapter 2, section 2.9.2.1, assay was done for the coated granules to determine the content of the active material. Materials no. 2, 3, 4 & 5 (Table 6.1) were then mixed with the coated granules for 5 minutes, using the tumbler mixer. Finally, materials no. 6 & 7 were added and mixed for 3 minutes. Powder was then filled in bottles at the weight  $44.5 \pm 2.0$  gm/bottle. For reconstitution, 25 ml cold water were added to each bottle to give a final volume of 50 ml.

### **6.2.2 Comparison tests between Zinnat<sup>®</sup> and wax coated CADC**

The following comparison tests were done for the two preparations, Zinnat<sup>®</sup> and wax coated CADC dry suspensions.

#### **6.2.2.1 DSC testing**

As Zinnat<sup>®</sup> suspension contains excipients other than wax coated CAA, and in order to separate the coated particles from these, contents of three bottles were passed through a set of sieves in the range of 0.1–0.7mm, on a vibratory sieve shaker. All fine particles of the suspension passed through the sieves except large coated particles which were retained on top of the 0.7 mm sieve, as off-white large particles.

These particles were then collected, placed on a filter paper connected to a suction set and washed thoroughly with water to remove the sugar. Vacuum was applied to remove all water traces, and particles were then dried using a vacuum dryer for 10 minutes.

Coated particles were then gently crushed using a mortar and a pestle, and were analysed using the DSC method described in chapter 2, section 2.1.2. Results were compared to those of wax coated CADC.

#### **6.2.2.2 *In vitro* gut absorption testing**

*In vitro* gut absorption was studied for both wax coated CADC and Zinnat<sup>®</sup> wax coated CAA, as mentioned in chapter 2, section 2.8.2.2. Obtained samples were analysed as mentioned in chapter 2, section 2.9.2.3.

### 6.2.2.3 Pilot bioequivalence study for wax coated CADC against Zinnat®

This study was conducted in accordance with the “Declaration of Helsinki” related to conducting bioequivalence studies on humans. The study compared the relative bioequivalence of two products (a Test versus a Reference) containing CA.

The Test product, coated CADC in suspension was compared to a Reference product Zinnat® suspension (Glaxo, UK), both at 250 mg C dose. The study was based on a two phased crossover schemed design, carried out on 3 healthy male volunteers whose ages range between 18–45 years. The administered dose was a single dose of 250mg C, and a one-week wash out interval was allowed between the two phases of the study. Sixteen blood samples were withdrawn at 0 (pre-dose) and at 0.25, 0.50, 0.75, 1.00, 1.25, 1.50, 1.75, 2.00, 2.50, 3.00, 4.00, 5.00, 6.00, 7.00 and 8.00 hours post-dose.

Blood samples were analysed for cefuroxime concentrations using the HPLC assay method developed by Wood et al (2001). The bioequivalence of both products was assessed by comparing the pharmacokinetic parameters derived from the cefuroxime plasma concentration time profiles  $t_{max}$ ,  $C_{max}$ ,  $K_e$ ,  $t^{1/2e}$ ,  $AUC_{0 \rightarrow t}$  and  $AUC_{0 \rightarrow \infty}$ . The Test and Reference products were to be considered bioequivalent if the 90% confidence limits of the geometric mean of the log transformed ratios of Test product relative to the Reference, for the values  $AUC_{0 \rightarrow t}$ ,  $AUC_{0 \rightarrow \infty}$  and  $C_{max}$ , were included within the bioequivalence range of 80-125%.

## 6.3 RESULTS AND DISCUSSIONS

### 6.3.1 DSC measurements

Figure 6.1 shows the DSC thermogram of wax coated CAA in Zinnat®, it revealed 2 endothermic peaks, one for melting of stearic acid at 52.5°C and the other for melting of the CAC polymorph at 185.2°C.

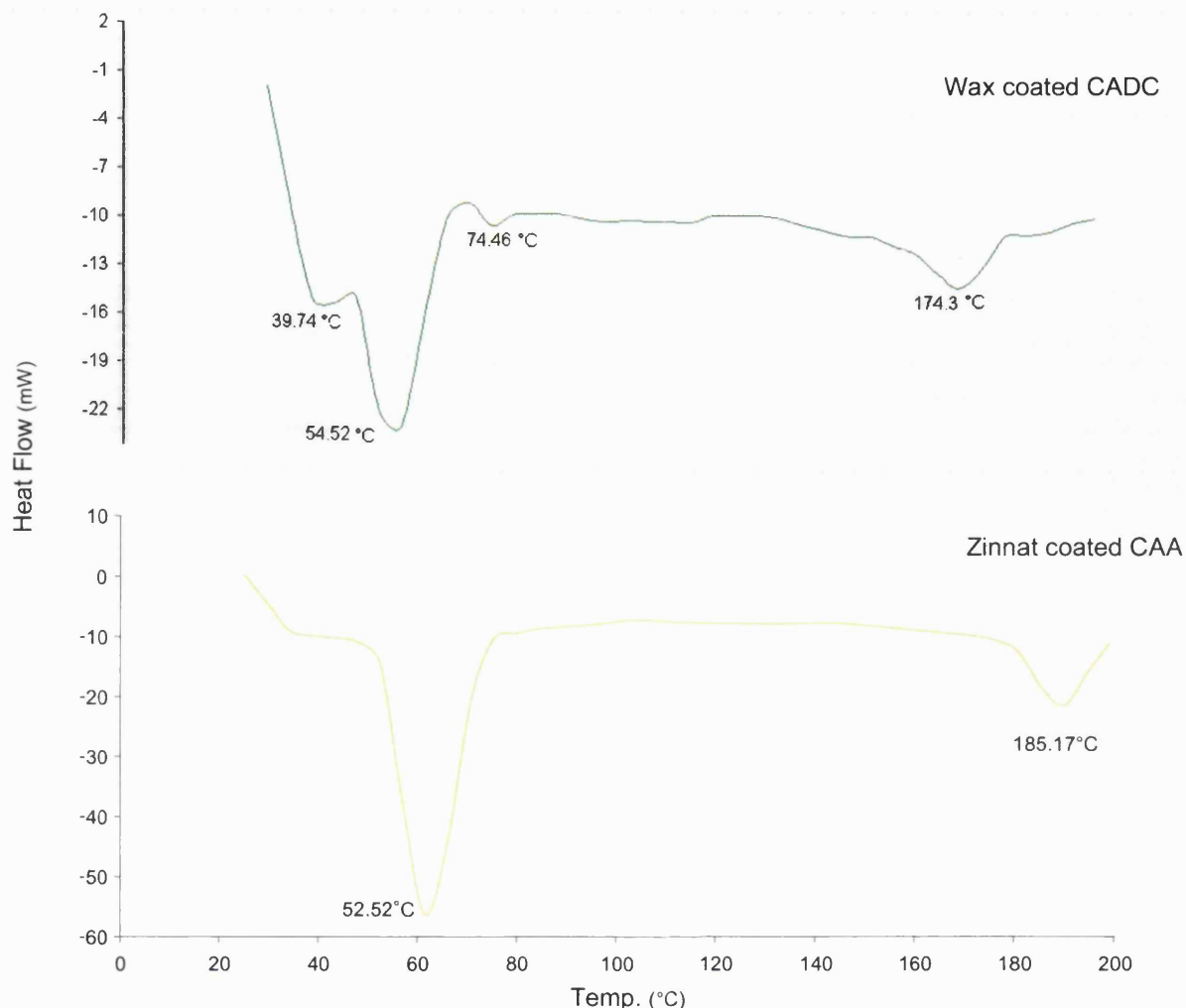


Figure 6.1: DSC thermogram of wax coated CAA in Zinnat<sup>®</sup> compared to that of wax coated CADC, at heating rate 25°C/min

The above DSC thermograms show that CAA in Zinnat<sup>®</sup> was totally transformed to CAC upon wax coating. While in CADC wax coated particles, only partial transformation of CAA to CAC occurred. This is related to stabilisation of CAA in the CADC granules core by the excipients present in there.

### 6.3.2 *In vitro* gut intestinal absorption results

Table 6.2 and Figure 6.2 show the *in vitro* gut absorption results of wax coated CAA in Zinnat<sup>®</sup>, presented as %C release across the intestinal membrane.

Time (min)	15	30	45	60	75	90	105	120
Trial								
%C release from Zinnat <sup>®</sup>	1.11	2.39	3.76	5.55	7.34	8.78	11.16	12.42
SD	0.30	0.21	0.37	1.25	2.50	2.70	3.70	2.50

Table 6.2: *In vitro* gut C% release from wax coated CAA in Zinnat<sup>®</sup>, n=3.

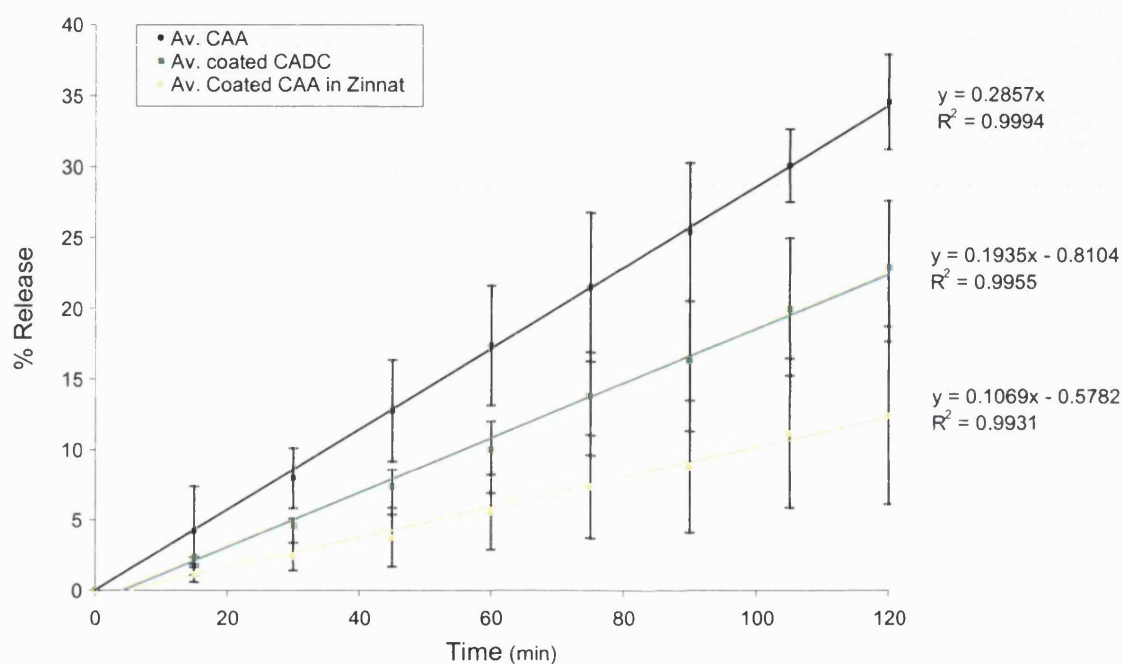


Figure 6.2: *In vitro* gut release of C from Zinnat<sup>®</sup>, n=3.

Figure 6.2 show the linear zero order release rate of C from Zinnat<sup>®</sup> wax coated CAA. The lag time in release is related to time needed for the wax to melt and CA to dissolve before absorption starts.

The above results indicated that the rate of intestinal absorption of CA from wax coated CADC is approximately double that from the wax coated CAA in Zinnat<sup>®</sup>. This is related to the presence of excipients in the CADC granules which stabilised the amorphous form of the drug during wax coating. In Zinnat<sup>®</sup>, CAA is completely transformed to CAC, leading to 60% reduction in the absorption rate of CAA.

### 6.3.3 Pilot bioequivalence study

Mean plasma concentrations and bioavailability data analyses for a single 250mg C dose of coated CADC suspension and Zinnat<sup>®</sup> suspension are presented in Tables 6.3, 6.4, 6.5 and 6.6 and in Figures 6.3 and 6.4.

Project Name : Analyses of cefuroxime in Plasma															
Study No.: CEFU-ADV-S1000/91									No. of Volunteers:3						
Time (h)															
	0.25	0.50	0.75	1.00	1.25	1.50	1.75	2.00	2.50	3.00	4.00	5.00	6.00	7.00	8.00
Vol. #	Concentration (µg/ml)														
1(I)A	0.00	0.18	0.55	1.06	1.54	2.17	2.67	2.70	2.48	1.97	1.06	0.56	0.32	0.17	0.10
1(II)B	0.00	0.20	0.79	1.46	1.69	1.97	1.88	1.70	1.64	1.28	0.85	0.54	0.25	0.12	0.00
2(I)A	0.29	1.13	1.72	2.03	1.97	1.82	1.69	1.50	1.39	1.70	1.02	0.64	0.25	0.13	0.00
2 (II)B	0.23	0.87	1.08	0.97	0.94	0.80	0.75	0.96	1.62	1.58	0.93	0.47	0.24	0.15	0.11
3(I)A	0.29	0.79	1.19	1.25	1.28	1.38	1.69	1.95	2.82	2.23	1.42	0.79	0.33	0.33	0.24
3(II)B	0.34	0.69	0.86	0.81	1.10	1.21	1.61	1.87	1.80	1.49	0.85	0.72	0.38	0.29	0.21

Table 6.3: Mean plasma concentrations of C from Zinnat<sup>®</sup> and wax coated CADC dry suspension.

A: Test formulation, wax coated CADC

B: Reference formulation Zinnat<sup>®</sup>

I : Phase I

II: Phase II

Subject No.	$C_{max}$		
	Zinnat <sup>®</sup>	Coated (CADC) (T)	(T/R)
1	1.97	2.7	137.06
2	1.62	2.03	125.31
3	1.87	2.82	150.80
n	3	3	3
Mean	1.82	2.52	137.72
SD	0.18	0.43	12.76

Table 6.4: Ratio analyses of untransformed data of cefuroxime for  $C_{max}$ .

Subject No.	$AUC_{0 \rightarrow t}$		
	Zinnat <sup>®</sup>	Coated (CADC) (T)	(T/R)
1	6.14	7.96	129.56
2	5.61	7.17	127.81
3	6.72	8.77	130.55
n	3	3	3
Mean	6.16	7.97	129.31
SD	0.56	0.80	1.39

Table 6.5: Ratio analyses of untransformed data of cefuroxime for  $AUC_{0 \rightarrow t}$ .

Subject No.	$AUC_{0 \rightarrow \infty}$		
	Zinnat <sup>®</sup>	Coated (CADC) (T)	(T/R)
1	6.30	8.13	129.04
2	5.85	7.35	125.73
3	7.30	9.45	129.57
n	3	3	3
Mean	6.48	8.31	128.11
SD	0.74	1.06	2.08

Table 6.6: Ratio analyses of untransformed data of cefuroxime for  $AUC_{0 \rightarrow \infty}$ .

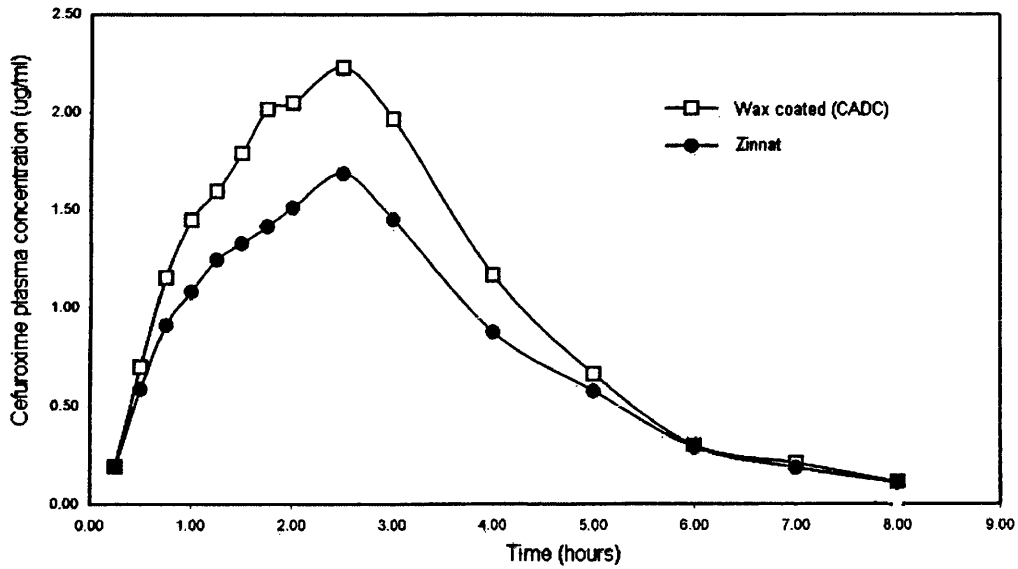


Figure 6.3: Semilogarithmic plot of plasma C concentrations after a single dose (250mg cefuroxime/5ml). (Pilot bioequivalence results of Zinnat<sup>®</sup> versus CADC dry suspension).

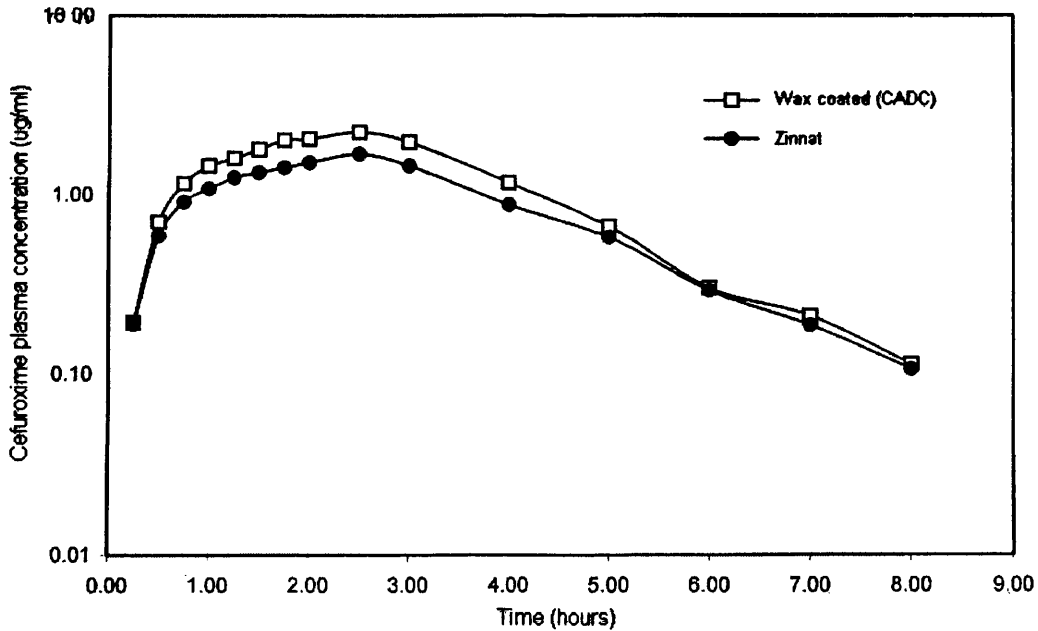


Figure 6.4: Linear plot of plasma C concentrations after a single dose (250mg cefuroxime/5ml). (Pilot bioequivalence results of Zinnat<sup>®</sup> versus CADC dry suspension).



Data points were connected with each other graphically, they do not represent any modeling to an equation.

In the above figures and tables, it was shown that coated CADC is super equivalent to coated CAA in Zinnat<sup>®</sup> with ratios for  $AUC_{0 \rightarrow \infty}$ ,  $AUC_{0 \rightarrow t}$ , and  $C_{max}$  (former to later) of 126%, 128% and 137%, respectively. All values were above the regulatory harmonized stated level for bioequivalence of 80% – 125%.

Bioequivalence results confirmed those obtained from the *in vitro* intestinal absorption, of that excipients in CADC granules stabilised the amorphous form of the drug, and prevented its complete transformation to other less soluble and absorbable forms of the drug. Thus, better bioavailability of CA from wax coated CADC was obtained compared to that from Zinnat<sup>®</sup>.

#### **6.4 CONCLUSIONS**

CAA instability under wax coating was relevant in both Zinnat<sup>®</sup> and wax coated CADC. The presence of excipients in CADC granules stabilised the amorphous form of the drug and prevented its complete transformation to CAC upon coating. Thus, they maintained 70% of the CAA intestinal absorption and provided better bioavailability of the drug from wax coated CADC compared to that from Zinnat<sup>®</sup>.

## CHAPTER 7

### SUMMARY, GENERAL CONCLUSIONS AND FUTURE WORK

#### 7.1 SUMMARY

Pharmaceutical materials which exist in different polymorphic forms exhibit different chemical and physical properties. Of the most important properties that are affected by polymorphism are dissolution, intestinal absorption, and stability (Hancock et al, 1997).

Different methods had been previously applied to obtain and stabilise the most soluble and absorbable, (usually the amorphous), form of a drug, some of which had been discussed in chapter 1. In this study, a simple method was applied to stabilise the amorphous form of cefuroxime axetil (CA).

It was chosen as a model drug because CA dosage forms (tablets, 250 and 500 mg and dry suspension 125 and 250 mg/5ml) are widely prescribed for the treatment of upper and lower respiratory tract as well as urinary tract infections. This is despite of the very bitter taste of CA, which had been wax coated in dry suspension formulations available in the market. In tablets, film coating was done to overcome this problem (James et al, 1989).

The official compendia (Eur. Ph, USP and BP) current monographs of CA allows for the use of both the crystalline and amorphous materials, without specifying a criteria for identification, (e.g. melting point). It has only been mentioned that when either form is used to prepare the drug product (tablets), it should meet the dissolution requirement of > 60% after 15 min and > 75% after 45 minutes.

In this study DSC, MTDSC, XRPD and DVS were used for testing the different polymorphic forms of CA. Results of testing indicated that CA exists in an amorphous form (CAA) with a  $T_g$  at 74°C, and in a crystalline form (CAC), commercialized as a mixture of two polymorphs, having melting peaks at about 130°C and 180°C respectively. It is expected that the crystalline form is either prepared in this way to allow for better dissolution and intestinal permeability of the

resulting mixture, or that it is the applied purification and the crystallisation conditions followed that unintentionally yield such a mixture.

The XRPD testing of CAA revealed broad diffuse peaks, while the CAC diffractogram showed sharp diffraction peaks associated with a highly crystalline material.

The DVS analyses of CAA indicated a limited water uptake (2%) after exposure to high relative humidity conditions (90%RH), close to that of CAC, with no evidence of crystallisation in the range 10 – 90%RH. Its sorption and desorption isotherms were super-imposed, with a faster water expel upon drying than the water uptake during the sorption cycle. Thus, the thermogravimetric analyses of CAA indicated a more stable amorphous material than those known in pharmaceutical applications.

It was noticed that the  $T_g$  of CAA was shifted to lower temperatures with increasing water content in the sample (upon exposure to humid conditions). This indicated that water absorbed by the amorphous material caused plasticization, and shifting of the  $T_g$  to lower temperatures. Both thermal and gravimetric (DVS) analyses showed a limited water uptake of this form (~2%) with a limited effect presented by shifting in the  $T_g$  value to lower temperature. This indicated a better stability of the amorphous CA compared to other pharmaceutical amorphous systems upon exposure to different storage conditions.

When dissolution and *in vitro* intestinal absorption rates were tested, CAA gave higher results compared to CAC. This is despite the fact that the latter was introduced in the study at smaller particle size. This indicated that CA form affects its absorption rate more significantly than its particle size.

Upon compression CAA underwent partial transformation to CAC. Differential scanning calorimetry was found the only technique among others (XRPD and DVS) that detected the presence of CAC in compressed CAA material at the 15% w/w level. Furthermore, it was also found that the DSC technique could detect down to 1% w/w concentration of CAC in a mixture with CAA.

It was not mentioned in the literature the application of any of the XRPD and DVS techniques in the detection of a crystalline content in an amorphous material. On the contrary, the amorphous content in a crystalline drug was reported to be effectively measured using the XRPD at 5-10% w/w (Gerhardt et al, 1994), and the DVS at 0.5% w/w concentrations (Buckton et al, 1995-b).

Compression of CAA resulted in partial crystallisation, which led to a significant reduction in intestinal absorption (by 30%), and dissolution rates. This was related to heat and pressure generated upon compression. They enhanced plasticization of the amorphous material, reduced its  $T_g$  to that of the experimental conditions, and consequently induced crystallisation.

It was found in this study that some excipients can protect the amorphous CA from such effect. Hence mixing and compacting CAA with any or all of the chosen excipients (Ac-Di-Sol, Starch 1500, and Aerosil 200) at their optimum ratios, inhibited its crystallisation.

Good dissolution rates were obtained from the compressed CAA mixtures with excipients (> 80% after 15 min, and > 90% after 45 min). On the other hand, the CAA original absorption rate was maintained.

Choosing these excipients was based on the idea of using polymers of high molecular weights, which may form hydrogen bonding with CA (Ac-Di-Sol, Starch 1500), and/or an amorphous material which has a high  $T_g$  (Aerosil 200). The polymeric excipients chosen were found able to stabilise CAA under the experimental conditions applied, possibly by linking the CA molecular motions to those of the polymers, thus inhibiting its crystallisation. On the other hand, the high  $T_g$  of Aerosil 200 also formed a barrier against CAA crystallisation.

It should also be mentioned that the physical properties of these excipients (poor compressibility and high surface area) might have played a role in protecting CAA from pressure and heat generated during compression.

Effect of wax coating on CAA was also investigated. Thus, the compressed CAA mixture with all the chosen excipients (CADC) was ,further, coated with wax and

tested for changes in physical properties. Results were compared to those of wax coated CAA (prepared), and with the commercially available wax coated CAA in the market (Zinnat<sup>®</sup> dry suspension).

Testing of the prepared wax coated CAA particles revealed complete transformation to other crystalline polymorphs which showed significant reduction in CAA intestinal absorption. For Zinnat<sup>®</sup> wax coated CAA particles, only the crystalline polymorph of the high melting point had been detected, its intestinal absorption rate comprised only 35% of that of CAA. Wax coating of CADC particles led only to a partial crystallisation of CAA, retaining 70% of the original absorption rate of the amorphous drug.

The above mentioned results were also confirmed when a pilot-bioequivalence study was conducted for wax coated CADC against Zinnat<sup>®</sup> in the dry suspension form. The study was conducted on 3 volunteers at the dose of 250 mg cefuroxime / 5 ml. Values of around 130% for  $C_{max}$  and AUC for CADC were obtained compared to Zinnat, indicating higher bioequivalence of the former. This was related to the stabilisation effect of the excipients on the amorphous drug in CADC.

## **7.2 GENERAL CONCLUSION**

Despite the fact that the amorphous form of the drug lack the stability of the crystalline, still the former (of better dissolution and higher bioavailability) can be used in drug formulations and can be further stabilised. Stabilisation can be achieved by different means.

Mixing of CAA with polymeric, high molecular weight excipients and/or amorphous materials having high  $T_g$  values, was found to achieve CAA stabilisation against process conditions. Excipients chosen for this study were able to protect it from crystallisation during compression and coating.

Regarding techniques that can be used in detecting the low crystalline content in the amorphous drug (CAA), it was found that DSC was more sensitive than XRPD and DVS, the well known techniques for detection of low amorphous content in a crystalline material.

## **7.3 FUTURE WORK**

Future work will include isolation and testing of all possible polymorphs of CA, as well as, determination of the factors and conditions that yield each form, either during the purification of the raw material, or during processing of the finished product in its different dosage forms.

More attention will be paid to the separation of the different crystalline polymorphs, for the purpose to characterise them and to study their physical properties.

On the other hand, screening of other excipients will be done to find other stabilisers, which will help in better understanding of other possible stabilisation mechanisms.

It will also be taken into consideration, the screening of other active materials for the purpose to find candidates that have similar stability to that of CAA, to be used in the pharmaceutical preparations.

## REFERENCES

- Agarwal R., Mittal R., Singh A. (2000) "Studies of ion-exchange resin complex of chloroquine phosphate", *Drug Development and Industrial Pharmacy* ,26 (7): 773 – 776.
- Ahlneck C., Zografu G. (1990). "The molecular basis of moisture effects on the physical and chemical stability of drugs in the solid state", *International Journal of Pharmaceutics*, Volume 62, Issues 2-3, 87-95.
- Aiden M., Wulff M., Herdinius S. (1995) "Influence of selected variables on heat of fusion determinations by oscillating differential scanning calorimetry", *Thermochimica Acta*, 265, 89–102.
- Allegra J. R., Hawley S. A. (1972), "Attenuation of sound in suspensions and emulsions : Theory and experiments", *Journal of the acoustical society of America*, 51(5): 1545– 1564.
- Allen T. (1992) "Particle size measurement" 4<sup>th</sup> ed. Chapman and Hall.
- Amidon G. E., Houghton M.E., (1995) "The effect of moisture on the mechanical and powder flow properties of microcrystalline cellulose", *Pharmaceutical Research* ,12(6): 923 – 929.
- Amidon G.L., Lennernas H., Shah V.P., Crison J.R. (1995) "A theoretical basis for a biopharmaceutic drug classification: the correlation of in vitro drug product dissolution and in vivo bioavailability", *Pharmaceutical Research*, 12 : 413-420.
- Amidon P. J., Sinko and Fleisher D. (1988) "Estimating human oral fraction dose absorbed: a correlation using rat intestinal membrane permeability for passive and carrier mediated compounds", *Pharmaceutical Research*, 5 : 651 – 657.
- Angberg M. Nystrom (1988), "Evaluation of heat conduction microcalorimetry in pharmaceutical stability", *Acta pharm suec.* 25(6) : 307 – 320.
- Angell C. A. (1988) "Structural instability and relaxation in liquid and glassy phases near the fragile liquid limit", *J. Non. Cryst Sol* 102 : 205 – 221.
- Angell C. A. (1995) "The old problems of glass and the glass transition, and the many new twists", *Proc Natl Acad Sci U S A.* 18;92(15) : 6675 – 6682.
- Artursson P. and Karlsson J. (1991) "Correlation between oral drug absorption in humans and apparent drug permeability coefficient in human intestinal epithelial Caco2 cells", *Biochem Biophys Res. Comm.* 175: 880 – 885.
- Aso Y., Yoshioka S., Otsuka T., Kojima S. (1995), "The physical stability of amorphous Nifedipine by isothermal microcalorimetry", *Chem. Pharm Bull.* 43: 300 – 303.
- Authier A. (2001) "Dynamical theory of X-ray diffraction", *International union of crystallography, monographs on crystallography.*
- Bakan J. A., Powell T. C., Szotak P. S. (1992) "Recent advances using micro-encapsulation for taste masking of bitter drugs", *CRS press: chapter 7*, 149 – 156.
- Balaguer N. R., Nacher A., Casabo V. (1997), "Nonlinear intestinal absorption kinetics of Cefuroxime Axetil in rats", *Antimicrobial agents and chemotherapy.* 445 – 448.
- Balaguer N. R., Nacher A., Casabo V.G. (2002) "Intestinal transport of Cefuroxime Axetil in rats, absorption and hydrolysis processes", *International Journal of Pharmaceutics*, 234 : 101 – 111.

- Banakar U. V. (1992) "Pharmaceutical dissolution testing", Marcel Dekker. PP 19 – 51.
- Barnes A. F., Hardy M. J., Lever T. J. (1993). "A review of the applications of thermal methods within the pharmaceutical industry", *J. Therm. Anal.* 40: 499–509.
- Barrett (1997) "Stereo selective absorption and hydrolysis of Cefuroxime Axetil diastereomers using the Caco2 cell monolayer model", *Eur. J. DMP.* (22) 4: 409 – 413.
- Barnett International (2002) "Proceedings of Practical Strategies for Predicting, Identifying, and Controlling Polymorphism Crystallisation", Philadelphia P.A. June.
- Barth H. G. (1984) "Modern methods of particle size analyses", Wiley inter science, New York.
- Barthe L., Woodley J., Houin G. (1999), "Gastrointestinal absorption of drugs: Methods and studies", *Fundamental and clinical pharmacology.* 13: 154 – 168.
- Beckers Cj, Veringa Hj, (1982) "Particle size measurement", *Powder technology.* 60: 245 – 248.
- Beekmans L. G. M., Van der Meer D. W., Vancso G. J. (2002) "Crystal melting and its kinetics on polyethylene oxide by in situ atomic force microscopy", *Polymer.* 43: 1887 – 1895.
- Belu A. M., Martyn C. Davies J. Mike Newton and Nikin Patel (2000) "TOF-SIMS characterisation and imaging of controlled-released drug delivery systems", *Analytical Chemistry* 72: 5625 – 5638.
- Berard V., Lesniewska E., Andres C., Pertuy D., Laroche C., Pourcelot Y. (2002) "Dry powder inhaler : Influence of humidity on topology and adhesion studied by AFM", *International Journal of Pharmaceutics*, 232: 213 – 224.
- Berggren J., Frenning G., Alderborn G. (2004) "Compression behaviour and Tablet forming ability of spray dried amorphous composite particles", *Eur. J. Pharm Sci.* 22: 191 – 200.
- Bernstein J. (1987) "Conformational polymorphism", G. R. Desiraju, *Organic Solid State Chemistry*, Elsevier, Amsterdam.
- Birnbaumer L., Abramowitz, Brown A. M. (1990) "Receptor-effectors coupling by G proteins", *Biochem Biophys Acta.* 1031: 163 – 224.
- Blaisdell P. E. D. (2001) "Twenty-First Century Pharmaceutical Development", Interpharm Press. Englewood, CO.
- Blume, Cheryl D., Bonner, Paul H. (1983) "Antihypertensive diuretic, combination composition and associated method", US patent no. 4,444,769.
- Blundell S., Woodley J. f., Ulbrich K., (1993) "Uptake and transfer of soluble polymers across the small intestine" *Proceeding Int. Symp controlled release of bioactive materials.* 20: 320 – 329.
- Bodor, Nicolaes (1977) "Prodrug forms of digoxin and method of preparing and using same", US patent no. 4,021,546.
- Bodor, Nicholas S., Sloan, Kenneth B. (1984) "Prodrugs of 6-mercaptopurine and therapeutic compositions and methods employing them" US patent no. 4,443,435.
- Bogdanovic G. (2002) "Surface interactions and adsorbate structures: An atomic force microscopy study", Doctoral Thesis Institute of Surface Chemistry. Royal Institute of Technology. Stockholm.



- Boller A., Jin Y., Wunderlich B. (1994) "Heat capacity measurement by modulated DSC at constant temperature", *J. Therm. Anal.* 42: 307 – 330.
- Boller A., Schick C., Wunderlich B. (1995) "Modulated Differential Scanning Calorimetry in the glass transition region", *Thermochimica Acta*, 266: 97 – 111.
- Boller A., Okazaki I., Wunderlich B. (1996) "Modulated differential scanning calorimetry in the glass transition region—Part III—Evaluation of polystyrene and polyethylene terephthalate", *Thermochimica Acta*, 284: 1 – 19.
- Bond L., Allen S., Davies M. C., Roberts C. J., Shivji A. P., Tendler S. J. B., Williams P. M., Zhang J. X. (2002) "Differential scanning calorimetry and scanning thermal microscopy analyses of pharmaceutical materials", *International Journal of Pharmaceutics*, 243: 71 – 82.
- Botzolakis J. E., Augsburgertl (1988) "Disintegrating agents in hard gelatine capsules", *Drug Development and Industrial Pharmacy*, 14: 29 – 41.
- Breslin P. A. S., Beauchamp G. K. (1997) "Suppression of Bitterness by Sodium: Implications for Flavor Enhancement. In I. Glenn Roy (ed), *Modifying Bitterness: Mechanism, Ingredients and Applications*", Technomic. 179 – 214.
- Brickel, Rolf, Gruber, Peter (1984) "Dipyridamole-containing pharmaceutical form", US patent no. 4,427,648.
- Bridges J. (1980) "Uptake of macromolecules by rat small intestine *in vitro*", PhD thesis, Keele University.
- Brittain H. (1999) "Methods for the characterisation of polymorphs and solvates". In *Polymorphism in Pharmaceutical Solids*. Marcel Dekker. Inc., New York, pp. 227-278.
- Brokovec M., Behrens S. H. (2000), "Influence of the secondary interaction energy minimum on the early stages of colloidal aggregation" *J. Colloid Intert. Sci.* 225: 460 – 465.
- Broman E., Khoo C., Taylor LS. (2001) "A comparison of alternative polymer excipients and processing methods for making solid dispersions of a poorly water soluble drug". *International Journal of Pharmaceutics*, 222(1) :139 – 151.
- Brown (1998) "Handbook of thermal methods of analyses and calorimetry", Elsevier science. 260 – 299 and 348.
- Brown W. (1993) "Dynamic light scattering: The methods and some applications" Oxford university Press, Oxford.
- Buckton G., Darcy Pan Mackellar A. J. (1995-a) "The use of isothermal microcalorimetry in the study of small degree of amorphous content of powders", *International Journal of Pharmaceutics*, 117: 253 – 256.
- Buckton G., Darcy P. (1995-b) "The use of gravimetric studies to study the degree of crystallinity of predominantly crystalline powder", *International Journal of Pharmaceutics*, 123: 265 – 271.
- Buckton G., Darcy P., Greenleaf D. (1995-c) "The use of isothermal microcalorimetry in the study of changes in crystallinity of spray dried salbutamol sulphate" *International Journal of Pharmaceutics*, 116: 113 – 118.
- Buckton G., Daracy P. (1996) "Water mobility in amorphous lactose below and close to glass transition temperature", *International Journal of Pharmaceutics*, 136: 141 – 146.

- Buckton G., Yonemochi E. (1998-a) "Use of Near Infra-red spectroscopy to detect changes in the amorphous and crystalline lactose", *International Journal of Pharmaceutics*, 168: 23 – 28.
- Buckton G., Darcy P. (1998-b) "Crystallisation of bulk samples of partially amorphous spray dried lactose", *Pharm Dev. Technol.* 3(4): 503 – 507.
- Buckton G., Patricia D. (1999) "Assessment of disorder in crystalline powders – a review of analytical techniques and their application", *International Journal of Pharmaceutics*. 179: 141 – 158.
- Burger A., Ramberger R. (1979) "On the polymorphism of pharmaceuticals and other molecular crystals, Theory of thermodynamic Rules", *Mikrochimica Acta.* 2, 259 – 316.
- Bustin O., Descamps M. (1999) "Slow structural relaxation of glass forming maltitol by modulated DSC Calorimetry", *J. Chem. Phys.* 110 (22) : 10982–10992.
- Byrn S. R., Pfeiffer R. R., Stowell J. G. (1982) "Solid-State Chemistry of Drugs", 2<sup>nd</sup> Edition. Academic press: New York
- Byrn S. R., Pfeiffer R. R., and Stowell J. G. (1995) "Solubility and dissolution testing", *Solid state chemistry of drugs*, 2<sup>nd</sup> edition, Academic Press : 91 – 101.
- Cadwallader D. E., (1971) "Biopharmaceutics and Drug Interactions", Roche Laboratories, Nutley, NJ. P.53.
- Campbell J., Chantrell L. J., and Eastmond R. (1987) "Purification and partial characterisation of rat intestinal Cefuroxime Axetil esterase", *Biochem. Pharmacol.* 36: 2317 – 2324.
- Carli, Fabio (1985) "Pharmaceutical composition", US patent no. 4,639,370.
- Carpenter J. F. (1997) "Interactions of stabilisers with proteins during freezing and drying", in Cleland L. J., Langer R., ACS Symposium Series 567, Formulation and delivery of proteins and peptides, ACS, Washington, DC, pp. 134 – 147.
- Carretero Riuz. P., Nacher A., Merino M. (2000) "Pharmacokinetics and absolute bioavailability of oral Cefuroxime Axetil in the rat", *International Journal of Pharmaceutics*, 202: 89 – 96.
- Carstensen J. T., Morris T. (1993) "Chemical stability of indomethacin in the solid amorphous and molten states", *J. Pharm. Sci.* 82(6):657-659.
- Chapman S. K. (1986) "Working with a scanning electron microscopy", Lodge mark press.
- Chescoe D., Goodhew P. J. (1990) "The operation of transmission and scanning electron microscopes", Royal microscopical society, Oxford University.
- Chew N. Y, Chan H.K. (1999) "Influence of particle size, air flow, and inhaler device on the dispersion of mannitol powders as aerosols", *Pharmaceutical Research*, 1999 16(7):1098-1103.
- Chiou W. L., Smith L. D (1971) "Solid dispersion approach to the formulation of organic liquid drugs using polyethylene glycol 6000 as a carrier", *J. Pharm. Sci.* 60(1):125-127.
- Chowhan Z. T. and Amaro A. A. (1977) "Everted rat intestinal sacs as an *in vitro* model for assessing absorptivity of new drugs", *J. Pharm Sci.* 66 : 1249 – 1253.
- Christopher G. (1997) "X-ray diffraction and Bragg equation", *J. Chem. Edu.* 7(4) : 192 – 195.
- Coleman N. J., Craig D. Q. M. (1996) "Modulated temperature differential scanning calorimetry : a novel approach to pharmaceutical thermal analyses", *International Journal of Pharmaceutics*, 135 : 13 – 29.

- Columbano A, Buckton G, Wikeley P. A. (2002) "Study of the crystallisation of amorphous salbutamol sulphate using water vapour sorption and near infrared spectroscopy", *International Journal of Pharmaceutics*, 237 (1-2) :171 -178.
- Conradi R. A., Wilkinson K. f., Rush B. D. (1993) "*In vitro* / *In vivo* models for peptide oral absorption : comparison of Caco2 cell permeability with rat intestinal absorption of rennin inhibitory peptides". *Pharmaceutical Research*, 10 : 1790 – 1792.
- Cooper J. (1998) "Particle size analyses the laser diffraction technique", *Materials world*. 6(1) : 5 – 7.
- Corrigan D. O., Corrigan O. I., Healy A.M. (2004) "Predicting the physical state of spray dried composites: salbutamol sulphate/lactose and salbutamol sulphate / polyethylene glycol co-spray dried systems". *International Journal of pharmaceutics* 273 (1-2):171-182.
- Craig D. Q. M., Royall P. G. (1998) "The use of modulated temperature DSC for the study of pharmaceutical systems: Potential uses and limitations", *Pharmaceutical Research*, 18(8), 1152– 1153.
- Craig D. Q. M., Royall P. G., Kett V. L., Hopton M. L. (1999-a) "The relevance of the amorphous state to pharmaceutical dosage forms: glassy drugs and freeze dried systems", *International Journal of Pharmaceutics*, 179: 179 – 207.
- Craig D., Feely L., Hill V. (1999-b) "The effects of experimental parameters and calibration on MTDSC data", *International Journal of Pharmaceutics*, 192: 21 – 32.
- Craig D. Q. M., McPhillips H., Royall P., Hill V. L. (1999-c) "Characterisation of the glass transition behavior of HPMC using modulated differential scanning calorimetry". *International Journal of Pharmaceutics*, 180: 83 – 90.
- Craig D. Q., He R. (2001) "An investigation into the thermal behaviour of an amorphous drug using low frequency dielectric spectroscopy and modulated temperature differential scanning calorimetry", *J. Pharm. Pharmacol.* 53(1):41 – 48.
- Craig D. Q. M., Kett V. L., Andrews C. S., Royall P. G. (2002-a) "Pharmaceutical applications of micro-thermal analyses", *J. Pharm. Sci.* 91: 201 – 1213.
- Craig D. Q. M. (2002-b) "Novel approaches to thermal analyses – possibilities and challenges". *American Pharmaceutical Review*: spring 1 – 5.
- Crang R. R., Klomparens K. L. (1988), "Artefacts in biological electron microscopy", Plenum press.
- Creswell, Ronald M., Holstius, Elvina "Method and preparation for increasing bioavailability of digoxin", US patent no. 4,088,750.
- Crisp H. A., Clayton (1985), US patent no. 4,562,181 Glaxo Group Ltd.
- Crisp H. A., Clayton J. C., Elliott L. G. (1991), United States patent 5,013,833. Glaxo Group Ltd.
- Crisp H. A., Clayton J., Elliott L. G. Wilson M. E. (1989), US Patent no. 4,820, 833, Glaxo Group Ltd.
- Crowe J. H. Carpenter J. F. Crowe L. M. (1998) "The role of verification in anhydrobiosis", *Annu. Rev. Physiol.* 60: 73 – 103.

- Cser F., Rasoul F., Kosior E. (1997) "Modulated differential scanning calorimetry – The effect of experimental variables", *J. Therm. Anal.* 50 (5-6), 727-744.
- Cullmann W. (1995) "Clinical pharmacokinetics of oral cephalosporins", *Antibiot. Chemother.* 47: 72 – 109.
- Cuna M., Lorenzo M. L., Vila-Jato J. L. (1996) "Enteric Cellulosic microspheres for taste masking of Cefuroxime Axetil stability and in vitro release behaviour", *Acta Technol Vol VII* , No. 3.
- Cuna M., Vila-Jato J. L., Torres D., Alonso M. J. Lorenzo-Lamosa M. L. (1997-a) "Development of a microencapsulated form of Cefuroxime Axetil using pH-sensitive acrylic polymers", *J. Microencapsul.* 14(5): 607-616.
- Cuna M., M. L. Lorenzo-Lamosa, J. L. Vila-Jato, D. Torres, M. J. Alonso (1997-b) "pH-Dependent Cellulosic Microspheres Containing Cefuroxime Axetil: Stability and In Vitro Release Behavior", *Drug Development and Industrial Pharmacy*, 23(3): 259-265.
- Dagan R., Shvartzman P., Liss Z. (1994) "Variation in acceptance of common oral antibiotic suspensions". *Pediatr Infect Dis J.* 13(8):686-690.
- Danesh A., Chen X. Y., Davies M. C., Roberts C. J., Sanders G. H. W., Tendler S. J. B, Williams P. M., Wilkins M. J. (2000) "The discrimination of drug polymorphic forms from single crystals using atomic force microscopy". *Pharmaceutical Research* , 17: 887 – 890.
- Dantzig A. H., Duckworth D. C. and Tabas L. B. (1994) "Transport mechanisms responsible for the absorption of Loracarbef, Cefuroxime and Cefuroxime Axetil into human intestinal Caco2 cells. *Biochim Biophys Acta.* 1191 (1) : 7 – 13.
- Davis G. R., Santa Ana, Morawski S. G. (1982) "Permeability characteristics of human jejunum, ileum, proximal colon and distal colon, Results of potential difference measurements and unidirectional fluxes", *Gastroenterology.* 83: 844 – 850.
- De Sommers K., Van Wyk M., Moncrieff J. (1984) "Influence of food and reduced gastric acidity on the bioavailability of bacampicillin and Cefuroxime Axetil", *Br. J. Clin. Pharm.* 18, 535 – 539.
- Debenedetti P. B. (1996) "Metastable liquids: Concepts and principles", Princeton, NJ: Princeton University Press.
- Deutsch D. S, Jamshed A. (1990-a), United States Patent no. 4,865,851 "Pharmaceutical composition".
- Deutsch D. S., Jamshed A. (1990-b) "Pharmaceutical Compositions", US Patent No. 4,897,270.
- Dhanaraju M. D., Kumaran K. S., Baskaran T. (1998) "Enhancement of bioavailability of griseofluvin by its complexation with Beta cyclodextrin drug", *Drug Development and Industrial Pharmacy.* 24(6): 583–587.
- Donn K. H., James N. C. and Powell R. (1994) "Bioavailability of Cefuroxime Axetil Formulation", *Journal of Pharmaceutical Science.* 83 (6) : 842 – 844.
- Dressman J. B., Amidon G. L., Reppas. C (1998) "Dissolution testing as a prognostic tool for oral drug absorption: Immediate release dosage forms", *Pharmaceutical Research.* 15: 11 – 22.

- Duddu S. P., Sokoloski T. D. (1995) "Dielectric analyses in the characterisation of amorphous pharmaceutical solids. 1. Molecular mobility in poly (vinylpyrrolidone)-water systems in the glassy state", *J. Pharm Sci.* 84(6):773-776.
- Duddu S. P., Dal Monte P. R. (1997) "Effect of glass transition temperature on the stability of lyophilized formulations containing a chimeric therapeutic monoclonal antibody", *Pharmaceutical Research.* 14(5): 591 – 595.
- Elamin A. A., Ahlneck C., Sebhatu T. (1994) "Effect of moisture sorption on Tableting characteristics of spray dried (15% amorphous) lactose", *Pharmaceutical Research*, 11(9):1233 – 1238.
- Elfarra, Adnan (1992) "Prodrugs of 6-mercaptopurine and 6-thioguanine" US patent no. 5,120,740.
- Elliott S. R. (1990) "Physics of amorphous materials", 2<sup>nd</sup> ed. Essex: Longman Scientific and Technical.
- Erko A., Aristov V. (1996) "Diffraction X-ray optics", Institute of physics publishing.
- Erlandsson R., Apell P. (2000) "Progress in scanning probe microscopy: high resolution force microscopy and spectroscopy", *Current Science.* 78: 1445-1457.
- Espitalier F., Biscans B., Authelin J. R., Laguerie C. (1997-a) "Modelling of the Mechanism of Formation of Spherical Grains Obtained by the Quasi-Emulsion Crystallisation Process", *Trans. Chem. E.* 75(A2), 257-267.
- Espitalier F., Biscans B., Laguerie C. (1997-b) "Particle Design Part A: Nucleation Kinetics of Ketoprofen", *Chemical Engineering Journal.* 68: 95-102.
- Everhart T. E., Hayes T. L. (1972) "The scanning electron microscope", *Sci Am.* 226 (1): 55 – 69.
- Fabre H., Ibork H., Lerner D. A. (1994) "Photoisomerization kinetics of Cefuroxime Axetil and related compounds", *J. Pharm. Sci.* 83(4): 553- 558.
- Fagerholm U., Johansson M., Lennernas H. (1996) "Comparison between permeability coefficients in rat and human jejunum", *Pharmaceutical Research*, 13(9): 1336 – 1342.
- Fares H. M., Zatz J. L. (1995) "Measurement of drug release from topical gels using two types of apparatus", *Pharm. Technol.* 19(1): 52 – 58.
- Feeley J. C. P., York B. S., Sumbly and Dicks H. (1998) "Determination of surface properties and flow characteristics of salbutamol sulphate, before and after micronisation", *International Journal of Pharmaceutics*, 172: 89 -96.
- Fevotte G., Calas J., Puel F., Hoff C. (2004) "Applications of NIR spectroscopy to monitoring and analyzing the solid state during industrial crystallisation processes", *International Journal of Pharmaceutics.* 273 (1-2): 159 – 169.
- Finn A., Straugun A., Meyer M., Chubb J. (1987) "Effect of dose and food on the bioavailability of Cefuroxime Axetil", *Biopharm. Drug Dispos.* 8, 519 – 526.
- Fitzpatrick S., Ellis R. (1995) "Comparison of particle sizing methods". <http://www.Cpsinstruments.com/Tech library/ documents. Html>.

- Ford J. L. (1999) "Thermal analyses of hydroxypropylmethylcellulose and methylcellulose: powders, gels and matrix Tablets". *International Journal of Pharmaceutics*, 179(2): 209-228. Review.
- Forster A., Hempenstall J., Rades T. (2001) "Characterisation of glass solutions of poorly water-soluble drugs produced by melt extrusion with hydrophilic amorphous polymers". *J. Pharm. Pharmacol.* 53(3): 303 – 315.
- Friend D. R. (1992) "Polyacrylate Resin Microcapsules for Taste-Masking of Antibiotics", *Journal of Micro-encapsulation* 9(4), 469-480.
- Fukumori Y., Hideki Ichikawa, Yumiko Yamaoka, Eiichi Akaho, Yoshikazu Takeuchi, Tomoaki Fukuda, Ryuichi Kanamori, Yoshifumi Osako (1991) "Microgranulation and Encapsulation of Pulverized Pharmaceutical Powders with Ethyl Cellulose by the Wurster Process", *Chem. Pharm. Bull.* 39(7), 1806-1812.
- Fukuoka E., Makita M., Yamamura S. (1989) "Glassy state of pharmaceuticals, III thermal properties and stability of glassy pharmaceuticals and their binary glass systems", *Chem. Pharm. Bull.* 37: 1047 – 1050.
- Gaßmann M. List A., Schweitzer, Sucker H. (1994) "Hydrosols Alternatives for the parenteral application of poorly water soluble drugs", *Eur. J. Pharm. Biopharm.* 40c: 64 – 72.
- Galia E., Nicolaides E., Horter D., Lobenberg R. (1998) "Evaluation of various dissolution media for predicting *in vivo* performance of class I and II drugs". *Pharmaceutical Research*, 15: 698 – 705.
- Gallagher P. (1997) "Thermoanalytical Instrumentation, techniques and methodology", 2<sup>nd</sup> edition.
- Garcia Villaluenga J. P., Seoane B., Compan V., Diaz Calleja R. (1997) "Thermomechanical and diffusive studies in films prepared from copolymers of ethylene-1-octene subject to longitudinal and transversal induced stretching", *Polymer.* 38: 3827 – 3836.
- Gennari Fedrico (1987) "Carnitine salts particularly suitable for oral use", US patent 4,673,534.
- Gerhardt S. A. (1993) "Role of water in the solid state properties of crystalline and amorphous sugars", Ph.D. Thesis, University of Wisconsin – Madison.
- Gerhardt S. A., Ahlneck C., Zografu G. (1994) "Assessment of disorder in crystalline solids", *International Journal of Pharmaceutics*, 101: 237 – 247.
- Gerhardt S. A., Stowell J. G., Byrn S. R. (1995) "Hydration and dehydration of crystalline and amorphous forms of raffinose", *J. Pharm. Sci.* 84: 318 – 323.
- Gibbs B. F., Kermasha S., Alli I., Mulligan C. N. (1999) "Encapsulation in the food industry: a review", *Int. J. Food Sci. Nutr.* 50(3): 213 – 224.
- Gill P. S., Sauerbrunn S. R., Reading M. (1993) "Modulated differential scanning calorimetry", *J. Therm. Anal.* 40: 931– 939.
- Ginsburg C. M., McCracken G. H., Petruska M., Olson K. (1985) "Pharmacokinetics and bactericidal activity of Cefuroxime Axetil", *Antimicrob. Agents Chemother.* 28 (4), 504–507.
- Giron Daniele (1998) "Contribution of thermal methods and related techniques to the rational development of pharmaceuticals-part 1", *PSTT Vol. 1, 5* : 191 – 199.

- Gissinger D., Stamm (1980) "A comparative evaluation of the properties of some Tablets disintegrants", *Drug Development and Industrial Pharmacy*, 6: 511 – 536.
- Gordon R., Middleton R., Nesbitt R., Fawzi M. (1986) "A Unique Application and Characterisation of Eudragit E30D Film Coatings in Sustained Release Formulations", *International Journal of Pharmaceutics*, 31(43-54).
- Gorman E. A., Rhodes C. T., Rudnic E. M. (1982) "An evaluation of croscarmellose as a Tablet disintegrant in direct compression systems", *Drug Development and Industrial Pharmacy*, 8: 397 – 410.
- Gouesbet G., Grehan (1988) "Optical particle sizing: Theory and practice", Plenum pub corp, New York.
- Grant D. J. W. (1999), "Theory and origin of polymorphism", H. G. Brittain (ed), *Polymorphism in pharmaceutical solids*. Marcel Dekker Inc. New York, PP: 1 – 34.
- Guinier A. (1994) "X-ray diffraction, in crystals, imperfect crystals and amorphous bodies", Dover Publications.
- Guk H. J., Jin Hy, Ji Hy (2002), "Preparation of amorphous form of Cefuroxime Axetil using supercritical fluid processing", *Scientific Paper*.
- Haines P. J. (1995) "Thermal methods of analyses, principles, applications and problems", Blackie Academic professional. 15 – 76.
- Hancock B. C., Zografi G. (1994) "The relation ship between the glass transition temperature and the water content of amorphous pharmaceutical solids". *Pharmaceutical Research*, 11, 471 – 477.
- Hancock B. C., Shamblin S. L., Zografi G. (1995) "Molecular mobility of amorphous pharmaceutical solids below their glass transition temperatures". *Pharmaceutical Research*. 12: 799 –806.
- Hancock B.C., Zografi G. (1997) "Characteristics and significance of the amorphous state in pharmaceutical systems". *J. Pharm. Sci.* 86:1-12.
- Handa V. K., Tyagi O. D., Ray V. K. (2002), United States patent no. 6,384,213. application no. 574311, Ranbaxy Ltd.
- Hanss J. David (2001) "Lipid-based systems for oral drug delivery: Enhancing the bioavailability of poorly water soluble drugs" *American Pharmaceutical Review*. 1-7.
- Harris D.C. (1995) "Quantitative chemical analyses", 4<sup>th</sup> ed., Freeman and company, New York.
- Hasan O. S. "Effect of Solvent Composition on the Spherical Crystallisation of Salicylic Acid", *Doctoral Dissertation*, Rutgers, the State University
- Hatley R. H. M., Blair J. A. (1999) "Stabilisation and delivery of labile materials by amorphous carbohydrates and their derivatives", *Mol. J., Catalysis B: Enzymatic* 7: 11 – 19.
- Heidemann D. R., Jarosz P. J. (1991) "Preformulation studies involving moisture uptake in solid dosage forms" *Pharmaceutical Research*, 8(3): 292 – 297.
- Her L. M., Nail S. L. (1994) "Measurement of glass transition temperatures of freeze-concentrated solutes by differential scanning calorimetry", *Pharmaceutical Research*, 11(1):54 – 59.

- Heywood V. E. (1971) "Scanning electron microscopy". Academic press.
- Hikima T., Hanaya M., Oguni M., (1999) "Microscopic observation of a peculiar crystallisation in the glass transition region and beta-process as potentially controlling the growth rate in triphenylethylene", *J. Mol. Structure.* 479, 245 – 250.
- Hill V. L., Craig D. Q. M., Feely L. C. (1998) "Characterisation of spray-dried lactose using modulated differential scanning calorimetry", *International Journal of Pharmaceutics*, 161, 95–107.
- Hino T. (2001) "Assessment of Nicotinamide Polymorphs by Differential Scanning Calorimetry", *Thermochimica Acta*, 374: 85 – 92.
- Hiroshi Matoba, Shinji Ohmori, Hiroyoshi Koyama, Toshio Kashihara (1994) "Taste-Masked Solid Preparation and its Production", European Patent Application 0622083A1.
- Hogan Sarah E., Buckton G. (2000) "The application of near infrared spectroscopy and dynamic vapor sorption to quantify low amorphous content of crystalline lactose", *Pharmaceutical Research*, 18(1): 112 – 116.
- Hohng, Hemminger W., Flammersheim H. J. (1996) "Differential scanning calorimetry". Springer-Verlag. Berlin Heidelberg.
- Holt D. E., Louvios J., Hurley R. (1990) "A high performance liquid chromatography system for the simultaneous assay of some antibiotics commonly found in combination in clinical samples", *J. Antimicrob chemother.* 26(1) : 107 – 115.
- Holt K., Rajendro K. Khankari (2000) "Taste-Masking Rapid Release Coating System", WO 00/30617.
- Hourston D. J., Song M., Pollock H. M., Hammiche A. (1995) "Application of modulated temperature differential scanning calorimetry to a range of problems in polymer science". *Proc. 24<sup>th</sup> NATAS Conf.*, 109–114.
- Irshaid Ym, Rawashdeh N. M., Zghol F., (1995) "Comparative pharmacokinetics of two brands of Cefuroxime following a single intramuscular injection", *Int. J. Clin Pharmacol Ther.* 33 (5): 285 – 293.
- Izzard M. J., Ablett S., Lillford P. J., Hill V. L., Groves I. F. (1996) "A modulated differential scanning calorimetric study: glass transition occurring in sucrose solutions", *J. Therm. Anal.* 47, 1407–1418.
- Jacobs C. O. Kayser, Muller R.H. (2000) "Nanosuspensions as a new approach for the formulation for the poorly soluble drug tarazepide", *International Journal of Pharmaceutics*, 196: 161 – 164.
- James M. B., Elliott L. G. (1989) United States Patent no. 4,865,851, Glaxo group Ltd.
- James R. W. (1982) "The optical principles of diffraction of x-ray", OX Bow press Woodbridge CT.
- Jenkins R., Snyder R. L. (1996) "Introduction to X-Ray powder Diffractometry", Vol. 138, Wiley-Interscience, New York 378, 355-556 and 371.
- Jilla venkatesa J., Kelly S. J. (2002) "Some issues in particle size and size distribution characterisation of powders", *American Pharmaceutical Review.* 98 – 105.



- Jin Y., Boller A., Wunderlich B., (1993) "Heat capacity measurement by modulated DSC at constant temperature", Proc. 22<sup>nd</sup> NATAS Conf., Denver, CO. p. 59–64.
- Jolley J. E. (1970) "Microstructure of photographic gelatine binders", Photogr Sci Eng. 14: 169 – 177.
- Joshi V. S. Dwivedi, Ward G. H. (2002) "Increase in the specific surface area of budesonide during storage postmicronization", Pharmaceutical Research, 19: 7 – 12.
- Junginger H. E., Meeting report (2003), workshop on "Hands on dissolution and bioequivalence", Dissolution Technologies. 10(2): 17, 19.
- Kararli T. T. (1995) "Comparison of the gastrointestinal anatomy, physiology and biochemistry of humans and commonly used laboratory animals", Biopharmaceutics and drug disposition. 16: 351 – 380.
- Kasapis S, Mitchell JR. "Definition of the rheological glass transition temperature in association with the concept of iso-free-volume", Int. J. Biol. Macromol. 2001 Dec 10; 29(4-5) :315-21.
- Katsurugi Yoshihisa, Kurihara Kenzo (1997) "Specific Inhibitor for Bitter Taste", In I. Glenn Roy, Modifying Bitterness: Mechanism, Ingredients and Applications, Technomic. 255 - 284.
- Kaushal A. M., Gupta P., Bansal A. K. (2004) "Amorphous drug delivery systems: molecular aspects, design, and performance", Crit Rev Ther Drug Carrier Syst. 21(3):133 -193.
- Kauzman W. (1948) "The nature of the glassy state and the behaviour of liquids at low temperatures", Chem Rev. 43: 219 – 256.
- Kawashima Y., Takeuchi H., Niwa T., Hino T., Yamakoshi M., Kihara K. (1989) "Preparation of spherically agglomerated crystals of an antibacterial drug for direct Tableting by a novel spherical crystallisation technique", Congr. Int. Technol. Pharm. 3: 228-34.
- Kawashima Y., Morishima K., Takeuchi H., Niwa T., Hino T. (1991) "Crystal design for direct Tableting and coating by the spherical crystallisation technique", AIChE Symp. Ser. 87(284), 26-32.
- Kawashima Y., Takeuchi H., Yamamoto H., Hino T., Sakai Y. (1998) "Preparation of spherically granulated crystals of waxy drug (tocopherol nicotinate) for direct Tableting by spherical crystallisation technique", World Congr. Part. Technol. 3, 1121-1130.
- Kawashima Y. (2001) "Nanoparticulate systems for improved drug delivery", Adv. Drug Deliv. Rev. 47: 1-2.
- Kawata, Hiroitsu, Ohmura (1983) "Nefidipine containing solid preparation composition", US patent no. 4,412,986.
- Kenkins R., Snyder R. L. (1996) "Introduction to X-ray powder diffractometry", Wiley.
- Kerc J., Srcic S., Kenz Z., and Sencar P., Bozic (1999) "Micronization of drugs supercritical carbon dioxide", International Journal of Pharmaceutics, 182: 33 – 39.
- Khattab I., Menon A., Sakr A. (1993) "Effect of mode of incorporation of disintegrants on the characteristics of fluid bed wet granulated Tables", J. Pharm. Pharmacol. 45: 687 – 691.
- Kibbe A. H. (2000) "Handbook of Pharmaceutical Excipients", third edition.

- Kim A. I., Akers M. J., Nail S. L (1998) "The physical state of mannitol after freeze drying: effects of mannitol concentration, freezing rate, and a noncrystallising cosolute", J. Pharm. Sci. 87: 931 – 935.
- Kim D. C, Burton P. S., Borchardt R. T. (1993) "A correlation between the permeability characteristics of a series of peptides using an *in vitro* cell culture model Caco2 and those using an *in situ* perfused rat ileum model of the intestinal mucosa", Pharmaceutical Research, 10: 1710 – 1714.
- Klaus, Hofheinz W., Laneury J. (1998) "Stability of cephalosporin prodrug esters in human intestinal juice: Implications for oral bioavailability", Antimicrobial agents and chemotherapy. 42(10): 2602 – 2606.
- Klug H. P., Alexander L. E (1974) "X-ray diffraction procedures", 2<sup>nd</sup> ed. Wiley.
- Kontny M. J. (1985) "Water vapour sorption studies on solid surfaces", Ph.D. Thesis, University of Wisconsin – Madison.
- Koot M. J., derberg I. J., Stuurman R. M. (1992) "High pressure liquid chromatographic analyses of the serum concentration of Cefuroxime after an intravenous bolus injection of Cefuroxime in patients with a Coronary artery by pass grafting", Pharm. Week bl. Sci. 14(6): 360 – 364.
- Kremminger P. (2003) EC Patent No. VS2003161888 Glaxo Group Ltd.
- Kron Dahl E., Orzechowski A., Ekstrom G., Lennernas H. (1997) "Rat jejunal permeability and metabolism of mu-selective tetrapeptides in gastrointestinal fluids from humans and rats", Pharmaceutical Research, 14(12):1780 -1785.
- Lai M. C, Topp E. M. (1999) "Solid state chemical stability of proteins and peptides", J. Pharm. Sci. 88: 489 – 500.
- Lande M. B., Priver N. A., Zeidel M. L. (1994) "Determinants of apical membrane permeabilities of barrier epithelia", Am J Physiol. 267(2 Pt 1):C367 – 374.
- Lande M. B., Donovan J. M., Zeidel M. L. (1995) "The relationship between membrane fluidity and permeabilities to water, solutes, ammonia, and protons", J. Gen Physiol. 106(1) : 67 – 84.
- Langguth P., Breves G., Stockli A., Merkle H. P., Wolfram S. "Colonic absorption and bioavailability of the pentapeptide metkephamid in the rat", Pharmaceutical Research, 11(11):1640 – 1645.
- Leason, Luis J. (1988) "Enhanced absorption of psychoactive 2-anil-pyrazolo quinolines as a solid molecular dispersion in polyvinyl pyrrolidone", US patent 4,758,427.
- Lennernas H., Ahrenstedt O., Hallgren R., Knutson L., Ryde M., Paalzow L. K. (1992) "Regional jejunal perfusion, a new *in vivo* approach to study oral drug absorption in man", Pharmaceutical Research, 9(10): 1243 – 1251.
- Lennernas H. (1995-a) "Does fluid flow across the intestinal mucosa affect quantitative oral drug absorption? Is it time for a reevaluation?" Pharmaceutical Research, 12(11):1573 – 1582. Review.

- Lennernas H., Fagerholm U., Raab Y., Gerdin B., Hallgren R. (1995-b) "Regional rectal perfusion: a new in vivo approach to study rectal drug absorption in man", *Pharmaceutical Research*, 12(3): 426 – 432.
- Lennerans H. (1998) "Human intestinal permeability", *J. Pharm. Sci.*, 87 (4): 403 – 410.
- Lerk C. F., Bolhiuos G. K., Smederma S. S. (1977) "interaction of lubricants and colloidal silica during mixing with excipients I: its effect on Tableting", *Pharm. Acta. Dev.* 52: 33 – 39.
- Levine H., Slade L. (1988) "Water as a plasticizer: Physico-chemical aspects of low moisture polymeric systems", *Water Sci. Rev.* 3: 79 – 185.
- Levine R. R., McNarry W. f., Blanc R. (1970) "Histological reevaluation of everted gut technique for studying intestinal absorption", *Eur. J. Pharm.* 9: 211 – 219.
- Lieberman H. (2003) "Advances in X-ray powder diffraction, Micro diffraction and high through put investigations", *American Pharmaceutical Review.* 57 – 60.
- Louey M. D., Mulvaney P., Stewart P. J. (2001) "Characterisation of adhesional properties of lactose carriers using atomic force microscopy", *J. Pharm. Biomed. Anal* 25: 559 – 567.
- Lusting C., Lennholm H., Iversen T., Nystrom C. (1997) "Assessment of degree of disorder in lactose by solid-state NMR and isothermal microcalorimetry", *Pharmaceutical Research*, 14: 196 – 202.
- Lyman C. E., Newburyl D. E. (1990) "Scanning electron microscopy, X-Ray microanalyses and analytical microscopy". Plenum publish
- Macedo R. O. (2001) "Thermal analyses techniques", *Journal of thermal analyses and calorimetry.* 751 – 756.
- Mackin L. S., Sartnurak. I., Thomas, Moore S. (2002) "The impact of low levels of amorphous material (< 5%) on the blending characteristics of a direct compression formulation", *International Journal of Pharmaceutics*, 231: 213 – 226.
- Mahesh V. Patel, Feng-Jing Chen (2003) "Solid Carriers for improved delivery of hydrophobic active ingredient in pharmaceutical compositions", US Patent 6,569,463 B2.
- Mahlin Denny, Berggren Jonas, Alderborn Goran, Seven angstrom (2004) "Moisture induced surface crystallisation of spray dried lactose particles studied by Atomic Force Microscopy", *J. Pharm. Sci.* 93: 29 – 37.
- Margolskee R. F. (1993) "The biochemistry and molecular biology of taste transduction", *Curr. Opini. Neurobiol.* 3: 526 – 531.
- Martin, Frederick, Tsuk (1982) "Therapeutic compositions with enhanced bioavailability", US patent no. 4,344,934.
- Mauger J. W. (1996) "Physico-chemical and fluid mechanical factors related to dissolution testing", *Dissolution Technologies.* 3(1): 7 -11.
- Mauger J., Ballard J., Brockson R. (2003) "Intrinsic dissolution performance testing of the USP dissolution apparatus 2 (Rotating Paddle) proof of principle", *Dissolution Technologies.* 8: 27 – 32.
- Mauger, John, Robinson, Dennis H. (1998) "Coating technology for taste masking orally administered bitter drugs", US patent no. 5,728,403.

- Mc Cram N. G., Buckley C. P., Bucknall C. B. (1998) "Principles of polymer engineering", New York, Oxford University Press.
- Mc Kenna G. B. (1989) "In Comprehensive Polymer Science", Booth C., Price C., Pergamon press. New York, 311 – 362.
- Mc Laughlin S. K., McKinnon P. J., Margolskee R. F. (1992) "Gustducin is a taste-cell-specific G protein closely related to the transducins", *Nature*. 357:563-569.
- Mc Laughlin S. K., Ruiz-Avila L., Wildman D., McKinnon P. J., Robichon A., Spickofsky N., Margolskee R. F. (1995) "Coupling of bitter receptor to phosphodiesterase through transducin in taste receptor cells". *Nature* 376:80-84.
- Mc Lean A. J. et al. (1978) "Food, splanchnic blood flow, and bioavailability of drugs subject to first-pass metabolism", *Clin. Pharmacol. Ther.* 24:5-10
- Ming D., Ninomiya Y., Margolskee R. F. (1999) "Blocking taste receptor activation of gustducin inhibits gustatory responses to bitter compounds", *Proc Natl Acad Sci USA*. 96(17):9903-9908
- Mishima O. (2004) "The glass-to-liquid transition of the emulsified high-density amorphous ice made by pressure-induced amorphization", *J. Chem. Phys.* 15; 121(7): 3161 - 3164.
- Mitchell S. A., Reynolds T. D., Dasbach T. P. (2003) "A compaction process to enhance dissolution of poorly water soluble drugs using HPMC". *International Journal of Pharmaceutics*, 250: 3 – 11.
- Mitrevej K. T., Augsburger L. L. (1982) "Adhesion of Tablets in a rotary Tablet press", *Drug Development and Industrial Pharmacy* , 8: 237 – 282.
- Miyazaki T., Yoshioka S., Aso Y., Kojima S. (2004) "Ability of polyvinylpyrrolidone and polyacrylic acid to inhibit the crystallisation of amorphous acetaminophen", *J. Pharm. Sci.* 93(11): 2710 – 2717.
- Mohanty (1982) "Electron microscopy for Biologists", Springfield, Ill: Thomas Chapter 17.
- Moloyama, Shimesu, Sato, Satoshi, (1988) "Pharmaceutical composition of cyclandelate having a high degree of bioavailability", US patent no. 4,751,241.
- Morishita Masataka, Inaba, Yoshihito, Fukushima, (1973) "Process for encapsulation of medicaments", US Patent No. 3,960,757.
- Mosher G., Mullen V. (1991), United States patent no. 5,063,224 Eli Lilly.
- Mosher L., McBee J., Shaw D. B. (1992) "Esterase activity toward the diastereomers of Cefuroxime Axetil in the rat and dog", *Pharmaceutical Research*, 9:687-689.
- Moynihan C. T., Lee S. K., Tatsumisago M., Minami T. (1996) "Estimation of activation energies for structural relaxation and viscous flow from DTA and DSC experiments", *Thermochimica Acta*, 280: 153 – 162.
- Mukherjig Goel S., Arora K. (2003) "Taste masked compositions", US Patent no. 6,565,877B1. Ranbaxy Ltd.
- Muller R. H., Peters K., Becker R., Kruss B. (1996) "Nanosuspensions for the i.v. administration of poorly soluble drugs stability during sterilization and long term storage", *Proc. Intern. Symp. Control Rel. Bioact Mater.* 22: 574 – 575.

- Muller R. H. C. Jacobs, Kayser O. (2001) "Nanosuspensions as particulate drug formulations in therapy. Rationale for development and what we can expect for the future", *Adv. Drug del. Rev.* 47: 2 – 19.
- Mullin J. W. (1993) "Crystallisation", 3<sup>rd</sup> edition. Butter Worth-Heimann, Boston
- Mullin J. W. (1998) "Some historical notes on industrial crystallisation". In *International Symposium on Industrial Crystallisation*. N. Kubota (Ed.), Tokyo, 17-18 September, 57-66.
- Mura P., Faucci M. T., Parrini P. L., Furlanetto S., Pinzauti S. (1999) "Influence of the preparation method on the physico-chemical properties of ketoprofen-cyclodextrin binary systems", *International Journal of Pharmaceutics*. 179(1): 117 – 128.
- Murase N., Abe S., Takahashi H., Katagiri C., Kikegawa T. (2004) "Two-dimensional diffraction study of ice crystallisation in polymer gels", *Cryo Letters*. 25(3):227 – 234.
- Ndesendo V. M. K., Meixner W., Korsatko W., Korsatko-Wabnegg B. (1996) "Micro-encapsulation of chloroquine diphosphate by Eudragit RS100", *Journal of Micro-encapsulation*. 13(1): 1 – 8.
- Nielsen J. A., Mc Morrow D. (2001) "Elements of modern X-ray physics", John Wiley and sons.
- O'Neil M. H. (2003) "The polymorph life cycle", *Pharm. Tech.* 44 – 58.
- Oksanen C. A., Zografi G. (1990) "The relationship between the glass transition temperature and water vapour absorption by PVP", *Pharmaceutical Research*, 7(6) 654 – 657.
- Oksanen C. A. Zografi G. (1993) "Molecular mobility in mixtures of absorbed water and solid poly (vinylpyrrolidone)", *Pharmaceutical Research*, 10, 791 – 799.
- Oszczapowicz I., Malafiej E., Szelachowska M. (1995) "Esters of Cephalosporins – Part II: Differences in the properties of various forms of the 1-acetoxyethyl ester of Cefuroxime", *Acta Pol Pharm*, Vol. 52, No. 5: 397 – 401.
- Pacha J. (2000) "Development of intestinal transport function in mammals", *Physiological Reviews*. 80: 1633 – 1667.
- Pade V., stavchansky S. (1998) "Link between drug absorption solubility and permeability measurements in Caco2 cells", *J. Pharm Sci*, 87: 1064 – 1607.
- Paradisis, George N. (1988) "Sachet drug delivery system", US patent no. 9,764,375.
- Parrott E. L., Comminution J., Swarbrick, Boylan J. C. (1990) "Encyclopaedia of Pharmaceutical Technology", Vol. 3, Marcel Decker Inc. New York, 101 -121.
- Pereira R., Sienkiewicz G., Rudnic E. M., Lausier J. M., Rhodes C. T. (1997) "Spheronization of theophylline-Avicel combinations using a fluidized-bed roto-granulation technique", *Drug Development and Industrial Pharmacy*, 23(2), 173-182.
- Phillip J. Percel, Gopi M. Venkatesh and Krishna S. Vishnupad (2001) "Functional Coating of Linezolid Microcapsules for Taste-masking and Associated Formulation for Oral Administration", WO 01/52848.
- Physicians Desk reference, PDR (1995).
- Pich C. H., Moest T. (1986) "Process for the Preparation of Solid Pharmaceutical Products", USA 4,632,843.

- Pikal M. J., Lukes A. L., Lang J. E., Gaines K. (1978) "Quantitative crystallinity determination for  $\beta$ -Lactam antibiotics by solution calorimetry: Correlations with stability", J. Pharm. Sci. 67, 767-773.
- Pikal M. J. (1993) "Freeze drying of proteins", Chemical Society, Washington.
- Pikal M. J (1994) "Freeze drying of proteins: process, formulation and stability", L. J. Cleland, R. Langer, ACS Symposium Series 567", Formulation and Delivery of Proteins and Peptides, ACS, Washington, DC, 20 – 133.
- Plumb J. A., Burston D., Baker T. (1987) "A comparison of the structural integrity of several commonly used preparations of rat small intestine *in vitro*", Clin. Sci. 73: 53 – 59.
- Posanski Ulrich, Ramsch Klaus-Dieter (1985) "Composition containing Nifedipine and Beta-blocker", EPO patent 165450.
- Price Robert, Young Paul M. (2004) "Visualization of the crystallisation of lactose from the amorphous state", J. Pharm. Sci. 93: 155 – 164.
- Puddipenddi M., Sokolosk T. D., Duddu S. P., Carsionesen J. T. (1996) "Quantitative characterisation of adsorption isotherms using isothermal microcalorimetry", J. Pharm. Sci. 85: 381 – 386.
- Rame A., (2002) "Basic principles of particle size analyses" Technical paper, Malvern instruments limited.
- Ramos J. J., Taveira-Marques R., Diogo H. P. (2004) "Estimation of the fragility index of indomethacin by DSC using the heating and cooling rate dependency of the glass transition", J. Pharm. Sci. 93(6):1503 – 1507.
- Reading M., (1993-a) "Modulated differential scanning calorimetry – a new way forward in materials characterisation", Trends Polym. Sci. 8: 248–253.
- Reading M., Elliott D., Hill V. L. (1993-b) "MDSC, a new approach to the calorimetric investigation of physical and chemical transitions", J. Therm. Anal. 40: 949–955.
- Reading M., Luget A., Wilson R. (1994) "Modulated differential scanning calorimetry", Thermochemica Acta, 238: 295 – 307.
- Reimer (1985) "Scanning electron microscopy physics of image formulation and microanalyses". Springer, Verlag.
- Reo et al (1999), US Patent no. 5,891,476 application no. 995, 466.
- Reo P. J., Fredrickson J. K. (2002) "Taste masking science and technology applied to compacted oral solid dosage forms", American Pharmaceutical Review, Autumn : 1-10.
- Repta A. J. (1987) "Rectally absorbable form of L-Dopa", US patent 4,771,073.
- Richard Frank Tester and John Karkalas, (1999) "Orally Administrable Compositions Comprising Cation Cross-Linked Polysaccharide and a Polymer Digestible in the Lower Gastrointestinal Tract", WO 99/53902.
- Richter W. F., Chong Y. H., Stella V. J. (1990), "On the mechanism of isomerization of cephalosporin esters", J. Pharm. Sci. 79:185 – 186.
- Ridgway E., Stewart K., Rai G., Kelsey M. C., Bielawska C. (1991) "The pharmacokinetics of Cefuroxime Axetil in the sick elderly patient", J. Antimicrob Chemother. 27(5): 663 – 668.

- Roberts R. J., Rowe R.C., York P. (1994) "The relationship between hardness of organic solids and their molecular structure", *J. Mater. Sci.* 29: 2289 – 2296.
- Robinson J. R. (1993) "Recent advantages in formulation of poorly absorbed drugs. In current status on targeted drug delivery to the gastrointestinal tract", *Capsugel Library*, pp. 59-63.
- Robson H. J., Craig D. Q. Deutsch D. (1999) "An investigation into the release of Cefuroxime Axetil from taste masked stearic acid microspheres", Part 1 "The influence of the dissolution medium on the drug release profile and the physical integrity of the microspheres", *International Journal of Pharmaceutics*, 190 (2): 183-192.
- Robson H., Craig D. Q. M., Deutsch D. (2000-a) "Development of a microencapsulated form of Cefuroxime Axetil using pH-sensitive acrylic polymer", *International Journal of Pharmaceutics*, 201: 211-219.
- Robson H., Craig D. Q. M., Deutsch D. (2000-b) "An investigation into the release of Cefuroxime Axetil from taste – Masked stearic acid microspheres. Part II the effect of buffer composition on drug release", *International Journal of Pharmaceutics*, 195: 137 – 145.
- Robson H., Craig D. Q. M., Deutsch D. (2000-c) "An investigation into the release of Cefuroxime Axetil from taste – Masked stearic acid microspheres. Part III the use of DSC and HSDSC as means of characterising the interaction of the microspheres with buffered media", *International Journal of Pharmaceutics*, 201(2): 211 – 219.
- Rohrs B. (2001) "Dissolution method development for poorly soluble compounds", *Dissolution Technologies*. 8(3) 1 – 5.
- Rosseel M. T., Peleman R., Hoorebeke H., (1997) "Measurement of Cefuroxime in human bronchoalveolar lavage fluid by high performance liquid chromatography after solid phase extraction", *J. Chromato. B. Biomed Sci Appl.* 689(2): 438 – 441.
- Rowland R. N., Woodley J. F. (1981) "Uptake of free and liposome – entrapped horse radish peroxidase by rat intestinal sacs in vitro *FEBS letters*", 123: 41 – 44.
- Roy G. (1994) "Taste-Masking in Oral Pharmaceuticals", *Pharmaceutical Technology* 18, 84, 86, 88, 90, 92, 94, 96-99.
- Roy G. (1997) "General Ingredient or Process Approaches to Bitterness Inhibition and Reduction in Oral Pharmaceuticals", I. Glenn Roy, *Modifying Bitterness: Mechanism, Ingredients and Applications* (Chapter 13), Technomic. 285 - 320.
- Roy S., Alexander K., Riga A. (2003) "A statistical Approach for the evaluation of parameter affecting preformulation studies of pharmaceuticals by DSC", *American Pharmaceutical Review*. August 1 - 6.
- Royall P. G., Craig D. Q., Doherty C. (1999) "Characterisation of moisture uptake effects on the glass transitional behaviour of an amorphous drug using modulated temperature DSC", *International Journal of Pharmaceutics*. 192(1): 39 – 46.
- Royall P. G., Kett V. L., Andrews C. S., Craig D. Q. M. (2001) "Identification of crystalline and amorphous regions in low molecular weight materials using microthermal analyses", *J. Phys. Chem. B* 105: 7021 – 7026.

- Saab A. N., Dittert L. W., Hussain A. A. (1988) "Isomerization of cephalosporin esters: implications for the prodrug ester approach to enhancing the oral bioavailabilities of cephalosporins", *J. Pharm. Sci.* 77: 906-907.
- Saklatvala R., Royall P., Craig D. (1999) "The detection of amorphous material in a nominally crystalline drug using modulated temperature DSC – a case study", *International Journal of Pharmaceutics*. 192: 55 – 62.
- Salvetti G., Tognoni E., Tombari E., Johari G.P. (1996) "Excess energy of polymorphic states or glass over the crystal state by heat of solution measurement", *Thermochimica Acta*, 285: 243-252.
- Sanders G. H., Roberts C. J., Danesh A., Murray A. J., Price D. M., Davies M. C., Tendler S. J. B, Wilkins M. J. (2000) "Discrimination of polymorphic forms of a drug product by localized thermal analyses", *Journal of Microscopy*. 198(2): 77-81.
- Sanjuan M., Casabo V., Nacher a. (2002) "Intestinal transport of CA in rats: absorption and hydrolysis processes", *International Journal of Pharmaceutics*. 234: 101 – 111.
- Sanz E. (2003), EC Patent no. GR 2002100506, Glaxo Group Ltd.
- Sasinowska-Motył M., Wisniewska I., Gumutka W., Oszczapowicz I., Szelachowska M., Interewicz B. (1995) "Esters of chephalosporins Part I: Permeability". *Acta Pol Pharm*, 52: 391.
- Sauerbrunn S. R., Crowe, B.S., Reading M. (1992). Proc. 21<sup>st</sup> NATAS Conf., Atlanta, GA, Sept. 13–16, 1992, pp. 137–144.
- Sauerbrunn S. R., Thomas L. (1995). Determination of initial crystallinity in polymers by modulated differential scanning calorimetry, *Am. Lab.* 19–22.
- Schawe J. E. K. (1995-a) "A comparison of different evaluation methods in modulated temperature DSC", *Thermochimica Acta*, 260: 1–16.
- Schawe J. E. K. (1995-b) "Principles for the interpretation of modulated temperature DSC measurements. Part 1. Glass transition", *Thermochimica Acta*, 261: 183 -194.
- Schawe J. E. K. (1996-a) "Modulated temperature DSC measurements: the influence of the experimental conditions", *Thermochimica Acta*, 271: 127–140.
- Schawe J. E. K. (1996-b) "Investigations of the glass transitions of organic and inorganic substances, DSC and temperature- modulated DSC", *J. Therm. Anal.* 47: 475 – 484.
- Schimpf M. E., Caldwell K., Giddings J. C. (2000) "Field flow fractionation Handbook", Wiley – Interscience. New York.
- Schreck D. W. and Vary J. E. (1984) "Mechanism by which hydralazine increases propranolol bioavailability", *Clin. Pharmacol. Ther.* 35: 447 – 453.
- Sepaniak M. J., De Jesus M. A., Giesfeldt S. G. (2003) "Advances in surface enhanced Raman spectroscopy for pharmaceutical analyses", *American Pharmaceutical Review*. Spring, 1-12.
- Serajuddin A. T, Dannenfelser R. M., He H., Joshi Y., Bateman S. (2004) "Development of clinical dosage forms for a poorly water soluble drug I: application of polyethylene glycol-polysorbate 80 solid dispersion carrier system", *J. Pharm. Sci.* 93(5):1165 – 1175.
- Seyer J. J., Luner P. E., Kemper M. S. (2000) "Application of diffuse reflectance near-infrared spectroscopy for determination of crystallinity", *J. Pharm. Sci.* 89(10):1305-1316.



- Shakesheff K. M., Davies M. C., Roberts C. J., Tendler S. J. B., Williams P. M. (1996) "The role of scanning probe microscopy in drug delivery research", *Crit. Rev. Ther. Drug.* 13: 225 – 256.
- Shalaev E. Y., Franks F. (1995) "Structural glass transition and thermo-physical processes in amorphous carbohydrates and their supercritical solutions", *J. Chem. Soc. Faraday Trans.* 91: 1511-1517.
- Shalaev E. Y., Lu Q., Shalaeva M., Zografi G. (2000) "Acid catalyzed inversion of sucrose in the amorphous state at very low levels of residual water", *Pharmaceutical Research*, 17: 366 – 370.
- Shalaev E. M., Zografi G. (2002) "The effect of disorder on the chemical reactivity of an organic solid, tetraglycine methyl ester: change of the reaction mechanism", *J. Pharm. Sci.* 91: 584 – 593.
- Shamblin S. L., Huang E. Y., Zografi G. (1996) "The effects of colyophilized polymeric additives on the glass transition temperature and crystallisation of amorphous sucrose", *J. Thermal Anal.* 47: 1567 – 1579.
- Shamblin S. L., Zografi G. (1998) "Enthalpy relaxation in binary amorphous mixtures containing sucrose", *Pharmaceutical Research*, 15: 1828 – 1834.
- Shamblin S. L., Hancock B. C., Dupuis Y., Pikal M. J. (2000) "Interpretation of relaxation time constants for amorphous pharmaceutical systems", *J. Pharm. Sci.* 89: 417–427.
- Shangraw R. F., Wallace J. W., Bowers F. M. (1981) "Morphology and functionality in Tablet excipients for direct compression", *Pharm. Technol.* 5(10): 44 – 60.
- Sheridan P. L., Buckton G., Storey D. E. (1995) "Development of a flow microcalorimetry method for the assessment of the surface properties of powders", *Pharmaceutical Research*, 12: 1025 – 1030.
- Sherman (2002), US Patent no. 6, 485,744, Bernard Charles.
- Shimano K., Kondo O., Miwa A., Higashi Y., Koyama I., Yoshida T., Ito Y., Hirose J., Goto S. (1995) "Evaluation of Uniform-sized Microcapsules using a vibration-nozzle method", *Drug Development and Industrial Pharmacy*, 21(3): 331-347.
- Shirai Y., Kiyomi Sogo, Kazumitsu Yamamoto, Kenji Kojima, Hiroshi Fujioka, Hirokazu Makita and Yasuhiko Nakamura (1993) "A Novel Fine Granule System for Masking Bitter Taste", *Biological and Pharmaceutical Bulletin.* 16(2): 172-177.
- Sindel U., Zimmermann I. (2001) "Measurement of interaction forces between individual powder particles using an atomic force microscope", *Powder Technol.* 117: 247 – 254.
- Sinko C. M., Yee A. F., Amidon G. L. (1991) "Prediction of physical aging in controlled-release coatings: the application of the relaxation coupling model to glassy cellulose acetate", *Pharmaceutical Research*, 8(6):698 – 705.
- Skoog D. A., West D. M., Holler F. J. (1994) "Analytical Chemistry in introduction", saunders College Publishing, 6<sup>th</sup> ed. Philadelphia.
- Sokoloski T. D., Ostovic J. R. (1997) "Characterisation of the physical and chemical interaction of a freeze dried peptide with water using isothermal microcalorimetry", *J. Pharm. Pharmacol.* 49 (4): 32 – 35.

- Somani J. K., Bhushen I., Sen H. (2001), US patent 6,323,193 B1, Application no.: 091642,402. Ranbaxy laborations Ltd.
- Somani J. K., Sethi S., Tyagi O. D. (2003), US patent 6,534,494 B1. Application no. 091673,922. Ranbaxy Laboratories Ltd.
- Sparks R. E., Norbert S. Mason (1987) "Method for coating particles or liquid droplets", US patent 4,675,140.
- Sparks R. E., Irwin C. Jacobs, Norbert S. Mason (1999) "Micro-encapsulation", Drug Manufacturing Technology. Ser. 3: 177-222.
- Spockel O. L., Parpaitrakul W. (1990) "A comparison of micro-encapsulation by various emulsion techniques". International Journal of Pharmaceutics. (58): 123 – 127.
- Sridhar, Stephen R. Anderson, Paul A. Meenan, Pascal H. Toma, (2000) "Crystallisation challenges in drug development: Scale-up from laboratory to pilot plant and beyond", Current Opinions in Drug Discovery and Development. 3(6): 723-733.
- Stewart B. H., Chan O. H., Reyner E. (1995) "Comparison of intestinal permeabilities determined in multiple *In vitro* and *In situ* methods: Relationship to absorption in humans", Pharmaceutical Research, 12(5): 693 – 699.
- Stoeckel K., Hayton W. L., Edwards D. J. (1995) "Clinical pharmacokinetics of oral cephalosporins", Antibiot. Chemother. 47:34-71.
- Stoeckel K., Harell M., Dan M. (1996) "Penetration of cefetamet pivoxil and Cefuroxime Axetil into the maxillary sinus mucosa at steady state", Antimicrob Agents Chemother. 40(3): 780 – 783.
- Stoeckel K., Hofheinz W., Laneury J. P., Duchene P., Shedlofsky S., Blouin R. A. (1998) "Stability of cephalosporin prodrug esters in human intestinal juice: implications for oral bioavailability", Antimicrob Agents Chemother. 42(10): 2602 – 2606.
- Struik L. C. E. (1978) "Physical aging in amorphous polymer and other materials", New York Elsevier.
- Styvistsk J. P. (1991) "Principles, methods and application of particle size analyses", Cambridge University press. New York.
- Sun W. Q., Davidson P., Chan H. S. O. (1998) "Protein stability in the amorphous carbohydrate matrix: relevance to anhydrobiosis", Biochim. Biophys. Acta. 1425: 245 – 254.
- Sun Y., David C. Watt, Atul J. Shukla and Chang Rong-Kun (1998) "Pharmaceutical approaches of taste-masking in liquid dosage forms", American Pharmaceutical Review, 2(3), 7,9-10,12-14,16.
- Takeuchi H., Yasuji T., Yamamoto H., Kawashima Y. (2000) "Temperature and moisture induced crystallisation of amorphous lactose in composite particles with sodium alginate prepared by spray drying", Pharm Dev Technol. 5: 355 – 363.
- Taylor L. S., Zografi G. (1997) "Spectroscopic characterisation of interactions between PVP and indomethacin in amorphous molecular dispersions", Pharmaceutical Research, 14(12): 1691 - 1698.

- Taylor LS, Langkilde FW, Zografi G. (2001) "Fourier transform Raman spectroscopic study of the interaction of water vapor with amorphous polymers", *J. Pharm Sci.* 90(7): 888 - 901.
- Ther L., Winne D. (1971) "Drug absorption", *Annu. Rev. Pharmacol.* 11: 57 – 70.
- Thomas J. (1992) "Influence of D-glucose induced water absorption on rat jejunal uptake of two passively absorbed drugs", *J. Pharm. Sci.* 81: 21 – 25.
- Thompson K. C., Draper J. P., Kaufman M. J., Brenner G. S. (1994) "Characterisation of the crystallinity of drugs: a case study", *Pharmaceutical Research*, 11: 1362 – 1365.
- Ticehurst M. D., Rowe R.C., York P. (1994) "Determination of the surface properties of two batches of Salbutamol Sulphate by inverse gas chromatography", *International Journal of Pharmaceutics*, 111: 241 – 249.
- Tomasi C., Mustarelli P., Hawkins N. A., Hill V. (1996) "Characterisation of amorphous materials by modulated differential scanning calorimetry", *Thermochemica Acta*, 278: 9–18.
- Trojak A., Kocevar K., Musevic I., Srcic S. (2001) "Investigation of the felodipine glassy state by atomic force microscopy", *International Journal of Pharmaceutics*, 218: 145 – 151.
- Tsuji A., Yamana T. (1974) "Kinetic approach to the development in beta-lactam antibiotics. II. Prodrug. (I). Simultaneous determination of hetacillin and ampicillin, and its application to the stability of hetacillin in aqueous solutions", *Chem Pharm Bull.* 22(10): 2434 - 2443.
- Turnbull D., Cohen M. H. (1961) "Free-volume model of the amorphous phase: Glass transition", *J. Chem. Phys.* 34: 120 – 125.
- Turnbull D. (1986) "Undercooled alloy phases". *War 17 rendale, PA: Metallurgical Soc*, pp 3-22.
- Tyle P., Cary Kuenn, Lauri Geier, Paul Jarosz (1990) "Effect of Size, Shape and Hardness of particles in suspension on oral palatability", *Drug Development and Industrial Pharmacy*, 16(8): 1339-1364.
- USP 24 (2000) "Scanning Electron Microscopy", General Chapter 1181, 2125-2128.
- Van de Mooter G., Augustijns P., Kinget R. (1999) "Stability prediction of amorphous benzodiazepines by calculation of the mean relaxation time constant using the Williams-Watts decay function", *Eur. J. Pharm. Biopharm.* 48:43 – 48.
- Varma-Nair M., Wunderlich B. (1996) "Non isothermal heat capacities and chemical reactions using modulated DSC", *J. Therm. Anal.* 46: 879 – 892.
- Veigas T. X., Curatella R. U., Brinker G. (2001) "Measurement of intrinsic drug dissolution using two types of apparatus", *Pharm. Tech.* 25(6): 44 – 53.
- Verdonck E., Schaap K., Thomas L. C. (1999) "A discussion of the principles and applications of Modulated Temperature DSC (MTDSC)", *International Journal of Pharmaceutics.* 192(1): 3 – 20.
- Vrentas J. S. (1993) "The use of solution theories for predicting water vapour absorption by amorphous pharmaceutical solids", *Pharmaceutical Research*, 10(9): 1262 – 1267.
- Wang L. H., Chowhan Z. T. (1990) "Drug excipient interactions resulting from powder mixing V: role of sodium lauryl sulphate", *International Journal of Pharmaceutics*, 60: 61 – 78.
- Ward G. H., Shultz R. K. (1995) "Process induced crystallinity changes in albutamol sulphate and its effect on powder physical stability", *Pharmaceutical Research*, 12 (5) : 773 – 779.

- Warren B. T. (1990) "X-ray diffraction", General publishing company.
- Watt I. M. (1997) "The principles and practice of electron microscopy". Cambridge University.
- Welling P. G. (1984) "Interactions affecting drug absorption", *Clinical Pharmacokinetics*. 9: 404 – 434.
- Weuts I., Kempen D., Six K., Peeters J., Verreck G., Brewster M., Van den Mooter G. (2003) "Evaluation of different calorimetric methods to determine the glass transition temperature and molecular mobility below T<sub>g</sub> for amorphous drugs", *International Journal of Pharmaceutics*, 259 (1-2):17 - 25.
- Wikman A. Karlsson J., Carlstedt I. and Artursson P. (1993) "A drug absorption model based on the mucus layer producing human intestinal goblet cell line HT29 – H" , *Pharmaceutical Research*, 10: 843 – 852.
- Wilding I. R., Kenyon C. J., Hooper G. (2000) "Gastrointestinal spread of oral prolonged release mesalazine microgranules dosed as either Tablets or sachet", *Alimentary pharmacology and therapeutics*. 14: 163 – 169.
- William G., Watts D. C. (1970) "Non Symmetrical dielectric relaxation behaviour arising from a simple empirical decay function", *Trans Faraday Soc*. 66: 80 - 85.
- William H., Murray M. C., Firestone (1992) "Bioavailability enhancers", US patent 5,126,348.
- Wilson H. Decamp (2000) "The impact of polymorphism on drug development, A regulator's view point", *American Pharmaceutical Review*. 1122 – 1131.
- Wilson T. H., Iseman G. (1954) "The use of sacs of avverted small intestine for the study of the transference of substances from the mucosal to the serosal surface", *J. Physiol*. 123: 116 – 125.
- Winne D. (1979) "Rat jejunum perfused *in situ*: effect of perfusion rate and intra luminal radius on absorption rate and effective unstirred layer thickness", *Archives of pharmacology*. 307: 265 – 274.
- Wissing S., Craig D. Q. M., Barker S. A., Moore W. D. (2000) "An investigation into the use of step wise isothermal high sensitivity DSC as a means of detecting drug excipient incompatibility", *International Journal of Pharmaceutics*, 199: 141 – 150.
- Woo J. S., Chang H. C. (2000), US Patent no. 6,107,290 application no. 091397,745. Hammi Pharma Co.Ltd.
- Wood G. C., Ling R. M., Herring L. V. (2001) "Pharmacokinetics of Cefuroxime Axetil Oral Suspension in Elderly volunteers", *J. Inform Pharmacol*. 95: 100 – 103.
- Worthington, Mettler Toledo (1999) "Thermal analyses of pharmaceuticals", *Collected Applications*, pp : 4,22, 26, 29, and 32.
- Yamamoto K., Nakano M., Arita T., Nakai Y. (1974) "Dissolution rate and bioavailability of griseofulvin from a ground mixture with microcrystalline cellulose", *J. Pharmacokinetic Biopharm*. 2(6):487 - 493.
- Yamamoto K., Nakano M., Arita T., Takayama Y., Nakai Y. (1976) "Dissolution behaviour and bioavailability of phenytoin from a ground mixture with microcrystalline cellulose", *J. Pharm. Sci*. 65(10): 1484 - 1488.

- Yoshida, Tsunemasa, Toshio (1986) "Composition for curing respiratory diseases", US patent no. 4,571,334.
- Yoshioka M., Hancock B. C., Zografi G. (1994) "Crystallisation of indomethacin from the amorphous state below and above its glass transition temperature", *J. Pharm. Sci.* 83: 1700 - 1705.
- Yoshioka M., Hancock B. C., Zografi G. (1995) "Inhibition of indomethacin crystallisation in PVP coprecipitate", *J. Pharm. Sci.* 84: 983 – 986.
- Yu L. X., Amidon G. L. (1999) "Analytical Solutions to Mass Transfer", G. L. Amidon, P. I. Lee, and E. M. Topp (eds.) *Transport Processes in Pharmaceutical Systems*. Marcel Dekker. Inc. p. 23-54.
- Yu L. X. (2001) "Amorphous pharmaceutical solids: Preparation, characterisation and stabilisation", *Adv Drug Del Rev.* 48: 27 - 42.
- Yu L. X., Amidon G. L., Polli J. E., Zhao H., Mehta M., Conner D. P., Shah V. P., Lesko L. J., Chen M. L., Lee V. H. L., Hussain A. S. (2002) "Biopharmaceutics Classification system: The scientific basis for bio-waiver extension", *Pharmaceutical Research*, 19: 921 – 925.
- Zachariasen (1997) "Theory of X-ray diffraction in crystals", Dover.
- Zenoni M., Leone M., Cattaneo A. (1997) US Patent no. 5,677,443, Application no. 664, 552 Acs Dobfar.
- Zhou D., Zhang G. G., Law D., Grant D. J., Schmitt E. A. (2002) "Physical stability of amorphous pharmaceuticals: Importance of configurational thermodynamic quantities and molecular mobility", *J. Pharm Sci.* 91(8):1863-72.
- Zografi G., Hancock B. C. (1994) "In Topics in pharmaceutical sciences 1993", proceedings international congress on pharmaceutical sciences FIP, Crommelin D.J.A. Midha. K. K., Nagi T. (Eds.) Medpharm scientific, Stuttgart, Germany. 405 – 419.
- Zografi George, Matsumoto Takahiro (1999) "Physical properties of solid molecular dispersions of indomethacin with polyvinylpyrrolidone and polyvinylpyrrolidone-co-vinyl-acetate in relation to indomethacin crystallisation", *Pharmaceutical Research* 16. (11) : 1722 - 1728.
- Zografi G., Shamblin S. L. (1999) "The effects of absorbed water on the properties of amorphous mixtures containing sucrose", *Pharmaceutical Research*. 16(7): 1119 – 1124.
- Zworykin K., Hiller J., Synder R. L. (1942) *ASTM Bull*, 15.